Charles University

Faculty of Science

Plant Anatomy and Physiology

Interaction of Plant Protein Complex Exocyst with Proteins Involved in Plant Immunity

PhD Thesis

Mgr. Jitka Ortmannová

Supervisor:

Doc. RNDr. Viktor Žárský, PhD

Consultants:

Tamara Pečenková, PhD

Ing. Martin Potocký, PhD

Declaration

I declare that this work is the result of my own research except as cited in the references. The thesis has not been accepted for any degree and is not currently submitted in the candidature of any other degree.

I understand that my results relate to the rights and obligations of the Act No. 121/2000 Coll., the Copyright Act, as amended, in particular the fact that Charles University in Prague has the right to conclude a licence agreement on the use of this work as a school work pursuant to Section 60 paragraph 1 of the Copyright Act.

In Prague, 3th of April in 2018 Jitka Ortmannová

Prohlášení

Prohlašuji, že tato práce je výsledkem experimentů, které jsem vykonala samostatně či ve spolupráci s kolegy, kteří jsou rovněž uvedeni jako spoluautoři na předložených publikacích. Dále prohlašuji, že všechny použité informační zdroje jsou citovány v textu a jsou řádně uvedeny v seznamu literatury. Podaná práce nebyla dříve ani souběžně použita k získání jakéhokoliv titulu v ČR či v zahraničí.

Chápu, že má práce podléhá právům a povinnostem dle zákona č. 121/2000 Sb., autorského zákona, ve znění pozdějších předpisů. Jsem srozumněna s tím, že Univerzita Karlova v Praze může uzavřít licenční smlouvu o užívání této práce jako školní práce podle § 60 odst. 1 autorského zákona.

V Praze, 3. dubna 2018 Jitka Ortmannová

Acknowledgement

On the first place, I would like to acknowledge Kurt and my family, especially my mother who supported me and kept asking when I finish my studies and start a real job. It always reminded me that science is neither obligatory nor traditional profession. It was the great honour for me to be Viktor's student and as well Tamara's, thank you. I am grateful for the opportunity to work at the IEB AS CR with the best OCD boss Martin Potocký, the cloning master Přemysl Pejchar, the beer lover Roman Pleskot, the best colleague in the world Nemanja Vukašinović, Lukáš Synek, Denisa Oulehlová, Jana Šťovíčková, Hana Soukupová, Anamika Rawat, Lucie Brejšková, Edita Drdová, Klára Aldorfová, Andrea Potocká, Martin Janda and Lucie Trdá. I will always remind the endless scientific (mostly) discussions with the Kulich's Family, thank you, Katarina and Ivan. At last, but not at least, the most about files organisation and material sharing I have learned from my friend and colleague Emily Larson.

Abstract

Plants have an artillery to defend themselves. The plant surface is protected by water-resistant cuticle and mechanically strong cell wall. Then each plant cell has tools to recognize and to answer to a pathogen threat. In an extreme case, the answer is programmed cell death. Plant immunity is a complex process integrating these passive and active mechanisms in an effort to overstay a pathogen attack. When the plant cell is attacked by a pathogen, the metabolic resources are redirected towards immunity reaction which results in growth restriction. Both the immunity reaction and the growth are dependent on the efficient polarized secretion of various cargoes.

Exocyst complex mediates tethering of a secretory vesicle with a target membrane and SNARE complex orchestrates the subsequent steps of vesicle docking and fusion. Exocyst and SNAREs are regulated by various proteins. In my work, I focused on identifying the exocyst interaction partners in plant immunity. In cooperation with my colleagues, we found the direct association between Qa-SNARE SYP121 involved in plant penetration resistance and EXO70B2 exocyst subunit. Moreover, we confirmed the relevance of their interaction for the formation of epidermal defensive structures, papillae and haustorial encasements in plant defence against non-adapted powdery mildew fungi. We wanted to further inspect if the exocyst-SNARE interaction could have an impact on the exocyst complex general function in secretion. We performed the membrane-bound mbSUS interaction assay between several exocyst subunits and SNAREs. We have demonstrated that more subunits of the exocyst complex have the ability to interact with several SNAREs, both in yeast and plant models. We have described an amplified growth phenotype in the double mutant for the EXO70A1 exocyst subunit and the VAMP721 R-SNARE protein. This additive defect, in our view, reflects the importance of the interaction between the two complexes in plant growth. We conducted a broad proteomic analysis where we identified proteins bound to all eight subunits of the exocyst complex, including EXO70A1, and also to the EXO70B1 and EXO70B2 isoforms. The additional set of co-immunoprecipitation along with the LC/MS/MS analysis shows the SYP121/VAMP721 is the most prominent interactor shared between the entire exocyst, while other SNAREs were less common. However, we also detected other SNARE proteins involved, for example, in the secretory pathway leading from the Golgi apparatus to the vacuole. We described the importance of secretion for growth response on the phenomenon of fast root hair growth reaction after contact with plant-specific bacteria. We identified the secretory pathway

and ethylene signalling as the major players in the rapid root growth inhibition and root hairs growth stimulation upon the bacteria treatment.

Taken together, we brought the evidence about exocyst and SNAREs interaction in plant defence and regular growth.

Souhrn

Rostlina je sesilní organismus, proto je vybavena odolným povrchem v podobě buněčné stěny překryté ještě voděodpudivou kutikulou, který působí jako pasivní mechanická bariéra proti napadání různorodými škůdci. Rostlina se však dokáže také aktivně bránit a pomocí senzorických a sekrečních drah vnímat a dále odpovídat na případný útok. Mezní obrannou reakcí každé buňky je indukovaná buněčná smrt. Rostlinná imunita je souborem těchto obranných mechanismů, které spojuje ve snaze zabránit infekci. Napadení patogenem většinou provází dočasné zastavení růstu a přesměrování metabolických i sekrečních drah na obranu. Sekreční dráhy rostlinné buňky a jejich regulace jsou tedy nezbytné pro růst i obranyschopnost.

Proteinový komplex exocyst poutá sekretorické váčky k cílové membráně a hraje tak významnou úlohu v polarizaci sekreční dráhy. Po upoutání váčku exocystem dochází k energeticky náročné fúzi membrán, kterou řídí komplex SNARE. Během své práce jsem se zaměřila na identifikaci interakčních partnerů komplexu exocyst, kteří jsou zapojeni do rostlinné imunity. Ve spolupráci s kolegy jsem popsala přímou interakci podjednotek EXO70B2 komplexu exocyst a SYP121 komplexu SNARE. Dle našich výsledků oba komplexy spolupracují v sekretorické dráze, která je zapojena do obrany rostlin vůči průniku hub způsobujících padlí, respektive do tvorby epidermálních obranných struktur, papil a haustoriálních obalů. Dále jsme prokázali, že schopnost interakce se SNARE proteiny má většina podjednotek komplexu exocyst, shodně v kvasinkovém i rostlinném modelu. Popsali jsme zesílený růstový defekt u dvojitého mutanta pro EXO70A1 podjednotku exocystu a VAMP721 protein komplexu SNARE. Tento prohloubený defekt podle nás ukazuje důležitost vzájemné interakce mezi oběma komplexy při růstu a vývoji rostliny. Ve snaze lépe popsat interakční partnery exocystu jsme provedli širokou proteomickou analýzu, kde jsme identifikovali proteiny vázané na všech osm základních podjednotek komplexu exocyst a EXO70B1 i EXO70B2. Potvrdili jsme, že SNARE komplex SYP121/VAMP721 je jedním z výrazných interaktorů exocystu. Odhalili jsme ale i další SNARE proteiny zapojené například do sekretorické dráhy vedoucí z Golgiho aparátu do vakuoly. Dále jsme našli několik nových interaktorů exocystu, mezi nimi např. proteinové kinázy sedící na plazmatické membráně, proteiny modifikující buněčnou stěnu či signalizační kaskády rostlinné buňky. V neposlední řadě jsme popsali vliv sekretorické dráhy na rychlou růstovou odpověď kořenových vlásků a hlavního kořene u *Arabidopsis*, konkrétně stimulaci kořenových vlásků a inhibici hlavního kořene po ošetření patogenními bakteriemi. Tuto reakci jsme ztotožnili s reakcí na bakterie

podporující růst a povrdili, že kromě funkční sekretorické dráhy je k ní zapotřebí signální dráha rostlinného hormonu ethylenu.

Práce posouvá dosavadní poznání o vlivu sekretorické dráhy na imunitní i růstové odpovědi rostliny a ukazuje nový vztah mezi komplexy exocyst a SNARE v sekretorické dráze rostlin. Provedené experimenty ukazují, že komplex exocyst je schopen přímo interagovat se SNARE proteiny a může tak usnadňovat membránovou fúzi či skládání SNARE komplexu.

Table of Contents

1. Introduction

1.1. Plant immunity

During the evolution, plants had to learn how to face variable microbial pathogens, such as fungi, oomycetes, bacteria and viruses. To accomplish their lifecycle, these pathogens use three major types of infection strategies: biotrophy, necrotrophy and hemibiotrophy. Biotrophic microbes colonize host cells in order to draw the nutrients of it, frequently they manipulate host metabolism in their profit and try to mask their presence to avoid plant cell reaction and keep it alive (Xin et al. 2016). Necrotrophic microbes kill host cells and feed on nutrients from the dead tissue (Schouten et al. 2008). The third category of microbes combines two previous strategies, the hemibiotrophic microbes acts on the edge of infection as biotrophs till the certain point of conversion when they switch to the necrotrophs strategy (Vargas et al. 2012; Chowdhury et al. 2017).

The first plant barrier for microbial pathogens entry is constituted by plant surface, the hydrophobic wax and cutin cuticle layer and mechanical as well chemical resistant cell wall (CW) (Bacete et al. 2018). Pathogens exploit every possible way to colonize their host, nevertheless, there are preferred methods of the entry. Bacteria and viruses use either pre-existing openings, as stomata and hydathodes, or a wound (caused by mechanical injury or insect) to colonize plants. Usually, bacteria stays in the apoplastic fluid, where they proliferate and communicate with host cells through their secretion system. Viruses are obligate cell inhabitant and thus their delivery relies on a wound or on the injection through a vector organism (insect, nematodes, fungi). Fungal and oomycetes pathogens develop specialized invasive structure, called appressorium (Fig. 1), for the direct penetration of plant surface barriers and cell colonization (Hacquard et al. 2017a; Bacete et al. 2018).

Fungal/oomycetes spore germinates with primary hyphae, which may evoke a reaction of a host cell, but usually doesn't progress in growth, and the major invasive thread is secondary hyphae - the germ tube (Fig. 1). The germ tube breaks plant cell surface with a pressure developed by the appressorium (Fig. 1) and with help of secreted cell-wall degradation enzymes (King et al. 2011; Silva 2013). As the tip of germ tube is undergoing the transition from the melanised and high turgor capable appressorium, through the penetration pore attached in cuticle, to penetration peg, the actual penetration structure, the fungus probably sense the actual barriers and reacts on the actual need of enzyme set, such as cutinases, cellulases, pectinases and proteases (King et al. 2011). Thus in order to successfully penetrate

plant cell surface, fungal pathogens deploy the secretory system, as well recycling. Also, the role of functional autophagy pathway has been described as a crucial for fungal penetration (Kershaw & Talbot 2009).

The first active barrier against penetration deposited by a plant cell beneath the contact site with a pathogen is called defensive papilla (Fig. 1). The papilla is a dome-shaped apposition full of CW components, antimicrobial molecules, reactive oxygen specious (ROS), secondary metabolites, which strengthens the CW. Into this focused place secretory vesicles and multivesicular bodies (MVB) brings material such as, callose synthases, ABC transporters, plant inhibitors of CW degradation enzymes, phytoalexins, defensins, lignins precursors, arabinoxylans, cellulose synthases and many others remain to be identified (Aist 1977; Meyer et al. 2009; Böhlenius et al. 2010; Micali et al. 2011; Chowdhury et al. 2014). In order to build up the effective papilla, two factors seem to be crucial, the precise timing of pathogen recognition and fast efficient polarize secretion. The slowdown in either recognition or secretion may cause the delay in deposition or lower output of defensive compounds in papilla, what results in an increase in penetration incidence (Assaad 2004; Ellinger et al. 2013; Chowdhury et al. 2016).

Successfully penetrated biotrophic fungal pathogens establish their settlement with the feeding structure called haustorium. To keep continuity with the germ tube, the haustorium growths through penetration peg but stays excluded from the cell cytoplasm via specialized extrahaustorial membrane (EHM) (Gil & Gay 1977; Manners 1989; Micali et al. 2011). The EHM represents semipermeable interfacial layer, where the fungal effectors and plant R proteins may lend and influence each other metabolism and where the soaking of nutrient via fungus occurs (Koh et al. 2005; Micali et al. 2011). The collar or alternatively neckband structure of the host cell may isolate the apoplast from the leaking of nutrients from the extrahaustorial matrix – the space between haustorial CW and EHM (Heat et al. 1976; Gil & Gay 1977). Moreover, the entire haustorium can be seal by plant cell in an encasement in order to stop fungal growth (Fig 1) (Gil & Gay 1977). The origin of EHM remains elusive, although it was suggested it is synthesized *de novo* (Koh et al. 2005; Micali et al. 2011; Berkey et al. 2017). The experimental isolation of *Golovinomyces orontii* (*Gvo*) haustorium revealed the similar composition of papilla, collar and encasement (see further) mostly filled with the exosomes of variable sizes, callose and CW components (Koh et al. 2005; Meyer et al. 2009; Micali et al. 2011). On the other hand, the EHM lacks classical CW and PM proteins, such as H^+ATPase, SYP121 (Koh et al. 2005; Micali et al. 2011). The R proteins of RPW8.2/1 family

targets the EHM and mediates ROS dependent HR, but they are excluded from papilla or collar (Wang et al. 2007; Wang et al. 2009). Two AtHR1 and AtHR3 homologous proteins to RPW8 exhibits PM but also EHM localization (Berkey et al. 2017). Using these proteins and plasmolysis experiments, it has been shown that the conventional secretory pathway is important for papillae biogenesis, but not for the EHM formation (Berkey et al. 2017). The role of unconventional secretion pathway in the EHM biogenesis supports also the localization of plant-specific RABF1/ARA6 and RABF2b/ARA7 into the EHM surrounding adapted fungal or oomycete pathogens (Inada et al. 2016). Another candidate for the EHM membrane source is ER, which has been found in close proximity to a haustorium. Indeed, the ER shares lipid and protein components with the EHM (Leckie et al. 1995; Berkey et al. 2017; Kwaaitaal et al. 2017). Intriguingly, both vesicle associated membrane proteins VAMP721/722 have been indicated as important for EHM protein RPW8.2 delivery (H. Kim et al. 2014). However composition of PM differs from EHM, other PM-associated proteins REMORIN1.3 and R protein AVRblb2 have been found sitting on the EHM surrounding oomycete haustorium (Bozkurt et al. 2014). Also, the plasmodesmata specific protein PDLP1 is targeted to the EHM in *Arabidopsis* under the oomycete attack (Caillaud et al. 2014). Importantly, the taken observations may be influenced by different experimental setting, especially the localization studies and the functional status of unencased haustoria may be crucial for EHM composition.

Plant cell actively seals the haustorium in an encasement (Fig. 1), the bulb shape defensive structure of similar composition as the papilla, which surrounds the EHM. Based on many observations, plant cell tries to enclose and divide the current PM membrane from the EHM in the place of fungal penetration with the neckband/collar structure to stop a possible drift of nutrients away or simply held the turgor (Bracker & Littlefield 1973; Green et al. 1995). Out of the collar, which is surrounded by PM, plant cell built gradually the encasement up (Bracker & Littlefield 1973). The building is driven by secretion of vesicles and MVB until enclosing, although the papilla poses the same composition as collar and encasement, this secretory pathway shows striking differences from the GNOM mediated SYP121 driven secretion to papillae (Nielsen et al. 2012; Nielsen et al. 2017). The encasement formation process has been compared with the cell-plate development, where the majority of a material present in a cell is redirected to the one place (Kwaaitaal et al. 2017). Nevertheless, the process of encasement formation and its regulation remains poorly explored.

Figure 1

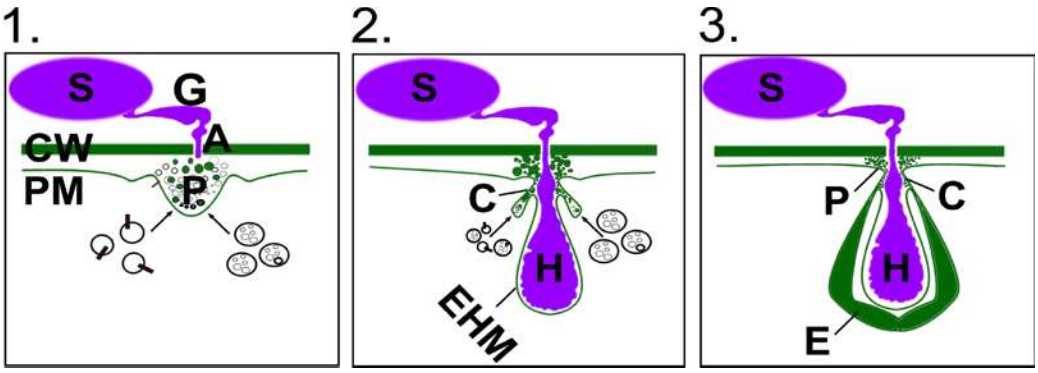

Schematic model of biotrophic fungus development after landing on an epidermal plant cell. 1) The spore (S) germinates and creates the germ tube (G), which develops the appressorium (A). The plant cell reacts with the formation of a cell wall (CW) plug – the papilla (P) surrounded by the plasma membrane (PM). 2) The fungus penetrates the cell wall and creates a feeding structure – the haustorium (H) surrounded by a specialized extra-haustorial membrane (EHM). 3) The plant cell fights back with deposition of an encasement (E) and seals the haustorium in it.

Fungal/oomycete spore development may be influenced by a various condition such as light, humidity, temperature, pH and nutrient availability (sugars, amino acids, minerals) (Talley et al. 2002; Imada et al. 2014; Turgeman et al. 2016; Gordon 2017), as well by the presence of antimicrobial compounds dependent on plant species, development and metabolism state of the individual plant. In addition, the plant surface used to be colonized by beneficial microbes, which can positively influence plant health or even prime innate immunity mechanisms (Fig. 2) and therefore its worth to count it as an additional layer of protection (Hacquard et al. 2017; Peer & van Peer 1991). The set of plant barriers and tools protecting it before a pathogen intersection and becoming the host for a pathogen is also called non-host resistance. The phenomenon of non-host resistance explains why the majority of plant species is resistant to a broad range of pathogens. Non-host resistance integrates the constitutive barriers and as well induced defence components, also called innate immunity. The innate immunity is an ancestral mechanism which involves microbial recognition, signal transduction, transcriptional reprogramming and cell death, and its evolution involves the continuing arm-race between a plant and a pathogen (Maekawa et al. 2011).

Conceptually the innate immunity operates in two modules, according to the type of molecules recognized by its receptor proteins. The molecules associated with microbiota presence, pathogen activity or self-cell activity directed against microbes are named as microbe/pathogen/danger associated molecular patterns MAMPs/PAMPs/DAMPs. The basal

immunity layer that is triggered by MAMPs/PAMPs/DAMPs recognition via PM-bound pattern recognition receptors PRRs is called pattern-triggered immunity (PTI). MAMPs usually represent set of non-self molecules for hosts, which are common for a microbe body, e.c. flagellin and chitin, or for microbial activity, e.c. CW degradation fragments. The PTI defence signalling goes through a membrane or cytoplasmic receptor-like kinases RLKs and MAPK cascades to the nucleus and results in changes in gene activity (Fig. 2). Some pathogens developed strategy how to manipulate the PTI system via secretion of specialized molecules - the effectors (Kleemann et al. 2012). The *Pseudomonas syringae* pv. *tomato* (*Pst*) secretes the effector protein HopM1 to degrade the immunity protein AtMIN7 and suppress PTI (Nomura et al. 2006). For such a case, the effector-triggered immunity (ETI) recognizes effector molecules through mostly cytoplasmic and specialized nucleotide-binding leucine-rich repeat NLR receptors, coded by genes of resistance (R). In the case of AtMIN7, the ETI activation stops AtMIN7 degradation and stabilizes its pool against HopM1 (Nomura et al. 2011). Thus ETI overcomes pathogenic suppression of PTI and re-establishes plant resistance (Chisholm et al. 2006). The microbial effectors recognized with R proteins become the proteins of avirulence (Avr; Jones & Dangl 2006). The R gene family was highly multiplied during the plant evolution as a consequence of the molecular arms race between plant immune system and pathogen effectors (leading to the generation of multiple Avr proteins). After its activation, the PTI and ETI immunity modules lead to fast immune response. Importantly, both the PTI and the ETI share the common responses such as ROS production, gene and protein activity modulation, callose secretion and eventually programmed cell death (Jones & Dangl 2006).

Figure 2

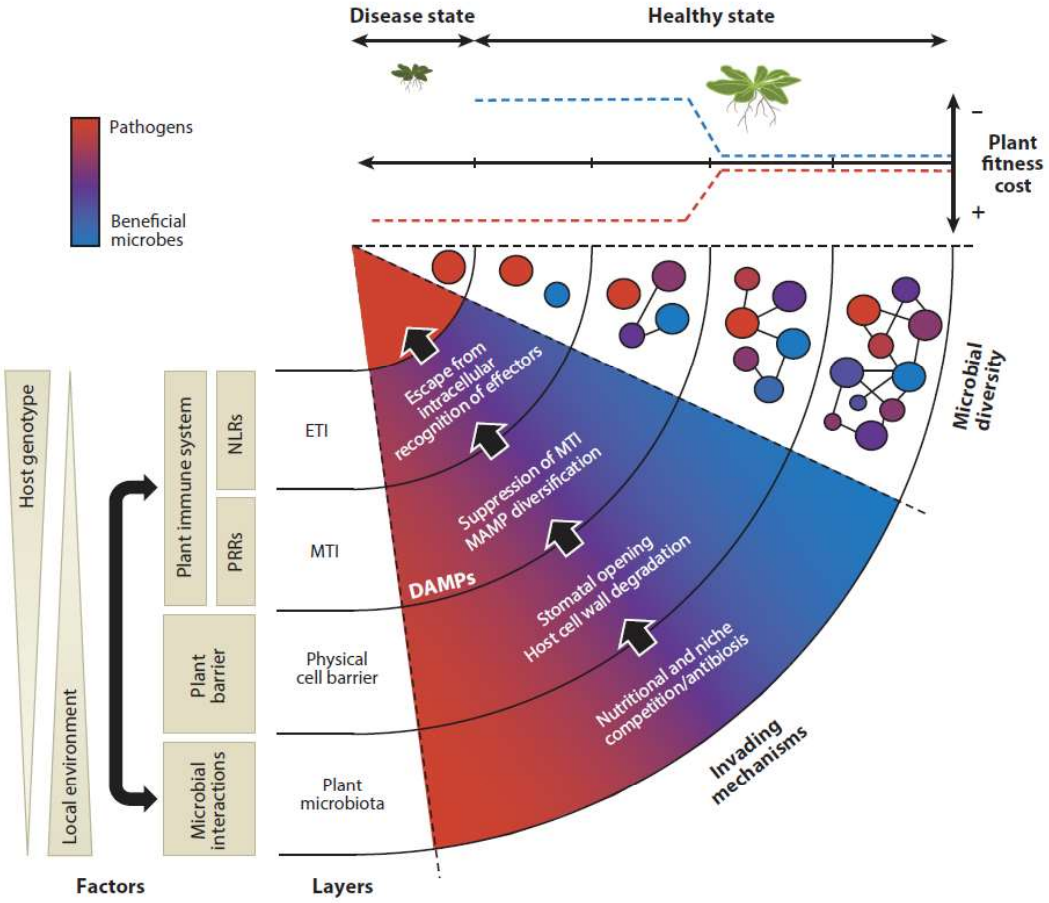

Plant immunity is a multi-layered complex of defence mechanisms. Four layers of immune mechanisms act to reduce microbial threat on plant tissue. The first protective layer is mediated by the microbiota acting as a biological and environmental restriction for pathogens invading plant surface. The surface microbiota creates nutritional competition and antibiotics niche. The invaders that evolved cooperative/competitive mechanisms to overcome the beneficial microbiota must then overcome the epidermal cell barriers via secretion of cuticle and cell-wall degrading enzymes, the formation of appressorium (turgor pressure) or effectors for stomata reopening (coronatine). The first active immune layer PTI is triggered by sensing the MAMPS by pattern recognition receptors PRRs. Importantly both the beneficial and pathogenic microbes overcome the PTI through MAMPs modification or the secretion of effectors. However, the contrasting outcome on plant fitness implies different selective pressure on the immune system. Therefore the second induced layer ETI involves NLR protein receptors that specifically detect the acting of pathogen effectors. Overcoming of all barriers by a microbe leads to the disease state. Adapted from (Hacquard et al. 2017).

In addition, plant innate immunity responses are regulated by three major hormone signalling pathways, including salicylic acid (SA), jasmonic acid (JA) and ethylene (ET; White

1979; Penninckx et al. 1998; Thomma et al. 1999). While JA and ET work mostly synergistically and their signalling requires immunity responses against necrotrophs, SA functions in response to biotrophs and often antagonistically to JA/ET pathway (Y. Kim et al. 2014; Sato et al. 2010). In addition, JA is essential in signalling of immunity against herbivores. Pathogens exploit the opposing role of SA vs. JA/ET in immunity. The hemibiotrophic bacterial pathogen *Pst* strain DC3000 injects in cells a specific toxin coronatine, which actually mimics bioactive conjugate molecule of JA, thus activates JA/ET pathway, what inhibits the SA accumulation and promotes stomata opening (Zheng et al. 2012). The concept of antagonism between plant hormones has been used several years, however, the complexity and overlaps between individual hormone sectors in plant immune system are more complicated (Fig. 3; Tsuda et al. 2009). The work with multiple mutants has shown different behaviour of hormone signalling sectors in PTI and ETI responses. The synergistic relationships were found between hormone pathways in PTI, while the compensatory relationships dominate in ETI (Tsuda et al. 2009). Along with the SA, JA and ET hormone sub-sectors, the immunity response is controlled by the major immunity regulator PAD4, from phytoalexin-deficient 4 (Tsuda et al. 2009, Kim et al. 2014). The PAD4 belongs to a phospholipase protein family, accumulates after SA treatment and in positive feedback stimulate SA dependent defence responses (Jirage et al. 2009). The four sectors create a robust network for the final output response to a pathogen attack (Kim et al. 2014).

Figure 3

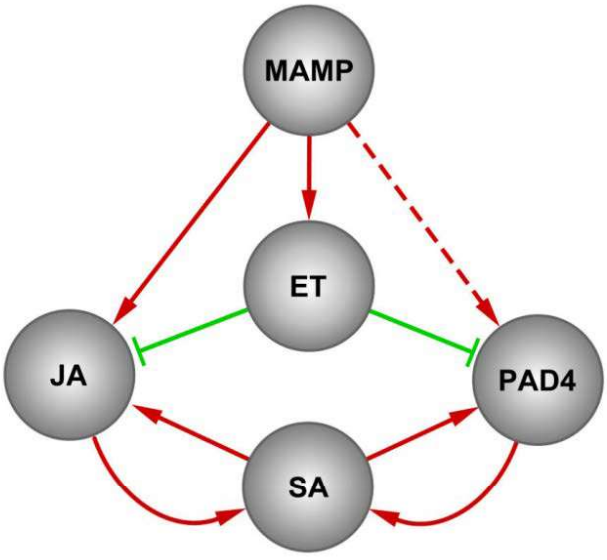

The PTI signalling network model between four sectors of JA, ET, PAD4 and SA activated by a MAMP. Directional links in red and green represent the parameters activation and inhibition, respectively (Y. Kim et al. 2014).

1.2. The membrane trafficking in plant immunity

One of the basic features of eukaryotic cell is existence of an endomembrane system, the spatial sequestration of synthetic processes and precise regulation of material transfer in the cell. For its optimal functioning, the endomembrane system deploys two major trafficking pathways (1) the endocytic pathway driven by internalization of PM-associated cargoes for intracellular sorting, recycling or degradation, and (2) the secretory pathway mediated via membrane trafficking of proteins synthesized in ER to their final destination such as PM or vacuole (Inada & Ueda 2014; Žárský et al. 2009). The membrane trafficking is a highly dynamic system which allows each cell to efficiently react on various environmental conditions such as microbe threat and thus plays major role in response to pathogen attack (Watanabe et al. 2013; Beck et al. 2012). The importance of these two pathways in plant immunity is projected in the fact that both of them serve as a common target for various pathogen effectors (Chaparro-Garcia et al. 2015; Bartetzko et al. 2009; Nomura et al. 2006). A vesicle, the functional unit of the membrane trafficking, undergoes several transitions as budding from the donor membrane, subsequent movement along the cytoskeleton, towards the final tethering, docking and fusion with the target membrane (Inada & Ueda 2014). Each of these steps is regulated by its own protein machinery, which is also the common target for pathogens.

1.2.1. The membrane budding

The membrane-deforming proteins such as ADP ribosylation factors ARFs (Lundmark et al. 2008) or coat protein complexes - clathrin, COPI and COPII, regulate the initiation of membrane budding (Dacks & Robinson 2017).

In plants, the clathrin mediates vesicle budding from PM (endocytosis) and Trans Golgi Network (TGN). To bend a membrane, the clathrin coat requires adaptor protein, such as AP1 – 3 (Hinrichsen al. 2006). The AP2 function comprises the recognition of a cargo and the composition of a membrane domain, specifically the domain rich for phospholipid phosphatidylinositol 4,5 - bisphosphate (PI(4,5)P2; Hinrichsen et al. 2006). Based on these requirements and clathrin monomer flexibility, it has been proposed that clathrin itself is insufficient to bend a membrane into a bud (Nossal 2001). In plants, clathrin-mediated endocytosis is a major regulator of early immune responses and is required for the

internalization and signalling of PRRs, such as FLS2 - flagellin receptor, EF - elongation factor receptor, PEPR1 - danger peptide receptor, and Cf-4 - Avr4 receptor (Postma et al. 2016; Mbengue et al. 2016; Ortiz-Morea et al. 2016). Without its ligand flagellin, the FLS2 constitutively cycles in a BFA-sensitive manner between the PM and early endosome (Beck et al. 2012). BFA is the fungal toxin which inhibits several ARF-GEFs and blocks endosome recycling (Mansour et al. 1999; Renault et al. 2003). Surprisingly, the ligand bound FLS2 internalization runs in BFA-insensitive manner. The FLS2 endocytosis is essential for signal transduction, but if its ubiquitinated the internalization leads to its degradation in the vacuole and signal quenching (Geldner & Robatzek 2008). Plant pathogen *Pst* DC3000 uses its effector AvrPtoB for PM-localized FLS2 ubiquitination to evade its own recognition (Göhre et al. 2008). Unlike the situation with bacterial effectors injection through type III secretion system, the mechanism of fungal proteins entry into a plant cell remains poorly understood. One of the possible mechanisms may be the receptor-mediated endocytosis of toxins. Toxins are bacterial or fungal effector proteins secreted into the apoplast such as ToxA of *Pyrenophora f. sp. triticirepentis* (Manning et al. 2008; Kale & Tyler 2011).

The COPI drives a retrograde transport from cis-Golgi cisternae back to ER. The budding requires the COPI coat proteins, ARF and a cargo tail, but there is no need for special lipid composition (Bremser et al. 1999). Similarly, COPII runs the anterograde transport from ER to cis-Golgi, and the energy for membrane budding is provided by the associate small GTPase Sar1 (Barlowe & Schekman 1993; Matsuoka et al. 1998).

The special modes of membrane remodelling and budding are guided by the two antagonistic protein complexes operating on the same compartment, the endosomal sorting complex required for transport (ESCRT) and the retromer. The ESCRT bends the phosphatidylinositol 3-phosphate (PI(3)P) rich late endosome/TGN membrane away from the cytoplasm and thus initiates the development of MVBs before targeting and fusion with a lytic vacuole (Cui et al. 2016). The PI(3)-kinase VPS34 synthesizes the PI(3)P and its enrichment on the endosome membrane initiate binding of FYVE domain-containing proteins (Hurley & Hanson 2010). The FYVE is the major domain of ESCRT-0 complex, which further binds ubiquitin rich cargoes aimed for degradation. The ESCRT-0 initiates binding of ESCRT-I, -II and -III. The ESCRT-I and -II bends membrane into buds or tubules, whereas the ESCRT-III closes the bud and executes its scission (Hurley & Hanson 2010). The retromer complex components are also targeted to a cargo on TGN/MVB, but instead of its internalization, they are involved in its recycling (Seaman 2012). The late endosome/TGN/MVB degradation

pathway ensures proper receptor turnover but could also work as a prevention of PRRs over-activation (Spallek et al. 2013; Smith et al. 2014; Mbengue et al. 2016).

The membrane composition, especially the phosphoinositide species content, usually serve as domains or endomembrane trafficking pathway markers (Cui et al. 2016; Noack & Jaillais 2017). In a plant cell, the PI(3)P decorates the membrane of late endosomes/MVB/vacuole and autophagosomes, the components of degradation and recycling pathway (Simon et al. 2014). Intriguingly, it has been shown that fungal pathogen *Phytophtora* may use an extracellular PI(3)P to enter the host plant cell (Kale et al. 2010; Lu et al. 2013). Thus, specific lipid composition might be relevant for the host resistance and pathogen virulence. On the other hand, the PI(4,5)P and PI(4)P define the TGN/EE/PM secretory pathway. The phosphoinositide can cascade from one species to another and thus change the membrane identity, morphology and regulate the membrane trafficking (Noack & Jaillais 2017). Indeed, the precise membrane phosphoinositides patterning may affect the associated proteins and thus repolarize the trafficking pathway into a particular domain (Sekeres et al. 2015). It has been suggested that the FLS2 receptor-rich domain spatial separation could influence its signalling specificity from BRI1 (Bücherl et al. 2017). Amongst many others, the localization of a vesicle tethering complex exocyst involved in polarized secretion has been found to be dependent on the phosphoinositide membrane composition (Pleskot et al. 2015; Bloch et al. 2016).

1.2.2. The membrane tethering/docking/fusion

The transport of various cargoes toward the PM (exocytosis) is crucial for the membrane and CW biogenesis. It is also essential for the cell-to-cell communication, reaction to different abiotic stresses and defence against pathogen and insect attack. The need for precise spatiotemporal cargo delivery during the plant life with constant exposure of the sessile body to changeable environmental conditions possibly resulted in the massive amplification of the regulatory genes required for the exocytosis. The main regulator of vesicle tethering towards PM is the effector of Rab GTPases - the exocyst complex. Subsequently, the vesicular docking and fusion are controlled by the SNAp REceptor (soluble N-ethylmaleimide sensitive factor attachment protein receptor) (SNARE) complex.

Figure 4

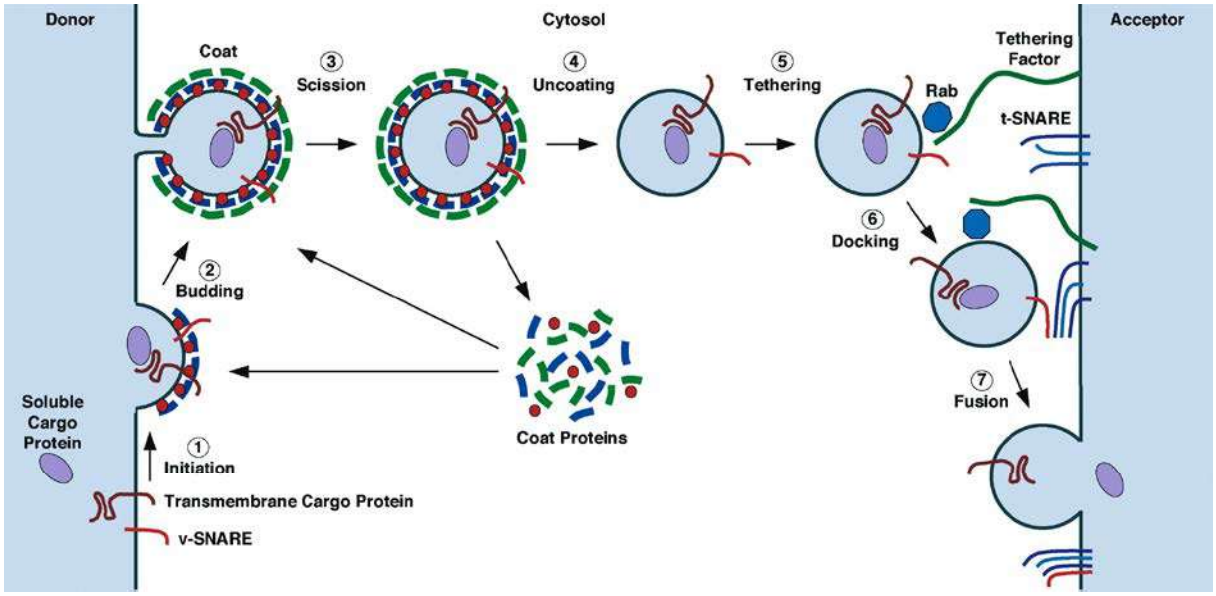

Steps of vesicle budding and fusion. (1) Initiation of coat assembly. The membrane-proximal coat components (blue) are recruited to the donor compartment by binding to a membrane-associated GTPase (red) and/or to a specific phosphoinositide. Transmembrane cargo proteins and SNAREs begin to gather at the assembling coat. (2) Budding. The membrane-distal coat components (green) are added and polymerized. Cargo becomes concentrated and membrane curvature increases. (3) Scission. The neck between the vesicle and the donor compartment is severed either by direct action of the coat or by accessory proteins. (4) Uncoating. The vesicle loses its coat due to various events including inactivation of the small GTPase, phosphoinositide hydrolysis, and the action of uncoating enzymes. Cytosolic coat proteins are then recycled. (5) Tethering. The "naked" vesicle moves to the acceptor compartment, possibly guided by the cytoskeleton and becomes tethered to the acceptor compartment by the combination of a GTP bound Rab and a tethering factor. (6) Docking. The v- and t-SNAREs assemble into a four-helix bundle. (7) This "*trans*-SNARE complex" promotes membranes fusion. Cargo is transferred to the acceptor compartment, and the SNAREs are recycled. (Bonifacino & Glick 2004)

1.2.2.1. Exocyst complex

The evolutionarily conserved exocyst complex, which belongs to multisubunit tethering complexes (MTCs), consists of eight subunits: Sec3, Sec5, Sec6, Sec8, Sec10, Sec15, Exo70 and Exo84 (TerBush 1995; TerBush et al. 1996). Originally exocyst was found in yeast *S. cerevisiae*, where it mediates targeting of Golgi derived secretory vesicles to PM. The exocyst complex holds the two membranes in proximity so that SNARE proteins can interact and execute membrane fusion (Bonifacino & Glick 2004). The question of SNARE regulation via exocyst has been studied in yeasts and comes predominantly from their structure - the exocyst subunits are characterized by CATCHR (complexes associated with tethering containing

helical rod) protein structure. In opisthokonts, all members of the CATCHR protein family directly interact with specific SNARE partners (Vukašinović & Žárský 2016). The Sec6 ability to interact with SM protein Munc18/Sec1, another SNARE regulator, in yeast and plants supports the role of the exocyst complex in the regulation of the SNARE complex assembly. Recently, the first functional direct interaction was revealed between the exocyst Sec6 subunit and cytoplasmic Qbc-SNARE Sec9 as a binary Sec9-Sso1 and ternary Sec9-Sso1-Snc2/1 complex that directly facilitates exocytosis in yeast (Dubuke et al. 2015). The exocyst can function as an opener of closed Qa-SNARE Sso1, as was proposed on the bases of its structural similarities with the Munc13 protein (Li et al. 2011). Indeed, Sec3 interacts with Qa-SNARE Sso2p catalyzing the binary SNARE assembly prior a fusion (Yue et al. 2017). The understanding of vesicle tethering, docking and fusion are still in its infancy, mainly for incomplete knowledge about the exocyst complex assembly and exocyst/SNARE cooperation.

The most recent studies brought a new view of exocyst assembly and function. In yeasts, when one of the subunits was removed, the complex was divided into two stable modules (Heider et al. 2016; Mei et al. 2018). The one half is composed of Sec3-Sec5-Sec6-Sec8 subunits and the other half from Sec10-Sec15-Exo70-Exo84. Interestingly loss of Sec3, previously reckoned as PM landmark along with Exo70, caused only minor destabilization of the complex (Heider et al. 2016). Moreover, the exocyst stability was not interrupted by the loss of any tested partner, such as Rab GTPase Sec4 or SNARE Sec9. It has been concluded, out of these observations that the exocyst mediates vesicle tethering as the fully assembled holocomplex (Fig. 5) (Heider et al. 2016; Mei et al. 2018). The high-resolution cryo-electron microscopic study supports the stable exocyst model and provides a detailed view on assembled exocyst (Heider et al. 2016; Mei et al. 2018). The working model of the stable exocyst complex, although with a flexible motility around the core, in membrane fusion was shown also in living cells (Picco et al. 2017). The authors compare its structure to open hand, where each subunit contributes to a core by one end, while the second end is exposed as a finger to a surrounding cytoplasm and possibly available for another interaction partner (Fig. 5). Interestingly, the most buried subunits in the complex structure and less accessible for interaction partners were Sec5 and Exo84 subunits (Picco et al. 2017). This model could explain why all of the exocyst subunits are critical for exocyst function. Nevertheless, the unique position within the exocyst has PH domain containing Sec3, which is at the same time the largest subunit. Sec3 bends around the exocyst structure with its flexible C-term domain and serves as a landmark in sites of the exocyst assembly (Mei et al. 2016, Liu et al. 2018). Thus, the remarkable structural

flexibility supports Sec3 as the last assembled subunit of the exocyst complex and more relevant for the proper positioning than the other core subunits (Heider et al. 2016; Mei et al. 2018). The landmark function of Sec3 has been further supported by experiments in yeasts in which Sec3 was fused to mitochondria resident protein Tom20, and consequently, the secretory pathway was redirected to mitochondria (Luo et al. 2014; Heider et al. 2016). Furthermore, this redirecting required the exocyst core binding domain of Sec3 in yeast (Mei et al. 2018). The original model of exocyst complex split between PM associated landmarks Sec3 with Exo70 on one side, and vesicle-associated core of Sec5, Sec6, Sec8, Sec10, Sec15, Exo84 on the other side, has been weaken. Although, the recent study has been showing that the Sec3 and Exo70, when expressed in fusion with transmembrane anchor, are exclusively capable of functioning on PM (Liu et al. 2018). However, these results do not challenge the existence of the holocomplex, but show the exocyst complex work at the PM exclusively. On the bases of this recent evidence, it may be concluded that the exocyst complex performs its PM function as the holocomplex and via the Sec3 and Exo70 subunits (Luo et al. 2014; Heider et al. 2016; Mei et al. 2018; Liu et al. 2018). The hypothetical exocyst subcomplexes may occur in the cytoplasm still, although in minority, and it is still not clear whether they might have other functions there.

Figure 5

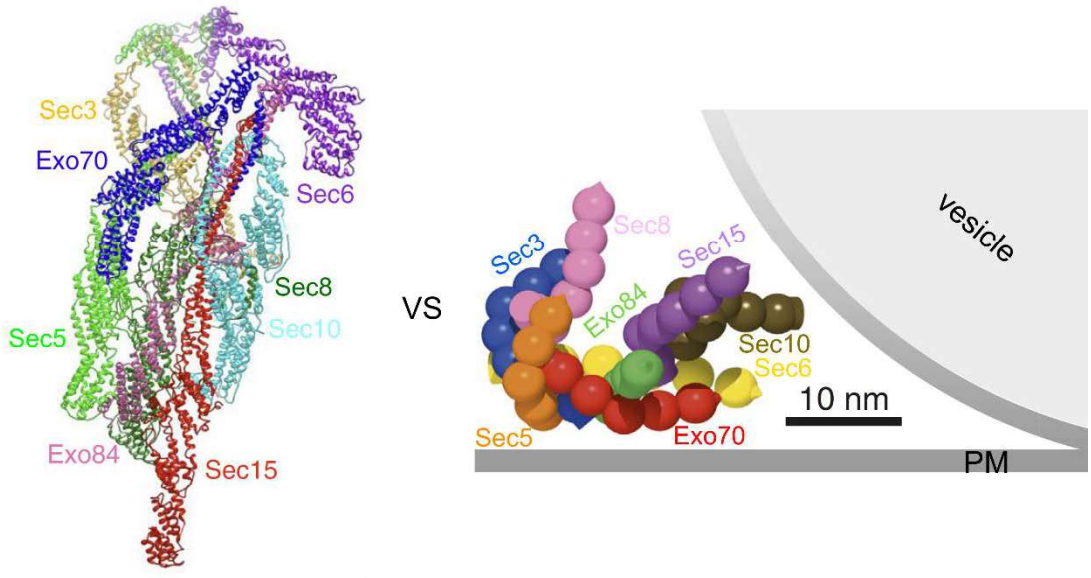

Comparison of two yeast holocomplex exocyst models. On the left: the structure identified with cryo-electron microscopy and chemical crosslinking. Sec6 purple, Sec10 turquoise, EXO84 pink. (Mei et al. 2018). On the right: the structure identified with the 3D integrative approach of high-resolution fluorescence microscopy in vivo. (Picco et al. 2017).

The importance of the plant exocyst in polarized exocytosis is manifested in the lethality of exocyst mutants (Friedrich et al. 1997; Hála et al. 2008). In plants, the exocyst subunits underwent a massive multiplication, especially the EXO70 subunit (Eliáš et al. 2003; Cvrčková et al. 2012). In *Arabidopsis*, several studies showed the canonical function of exocyst in polarized secretion in pollen germination, pollen tube and root hair growth, cell division, tracheary element development, seed coat deposition, trichome CW maturation, meristem and stigma function (Cole et al. 2005; Synek et al. 2006; Hála et al. 2008; Fendrych et al. 2010; Kulich et al. 2010; Fendrych et al. 2013; Drdová et al. 2013; Žárský et al. 2013; Rybak et al. 2014; Kulich et al. 2015; Sekereš et al. 2017; Vukašinović et al. 2017; Li et al. 2017; Kulich et al. 2018) . Although the role of SEC3 and EXO70 as the landmarks is still unresolved in plants, there is growing evidence supporting the exocyst independent functions of some exocyst subunit paralogues (Sekereš et al. 2017; Synek et al. 2017). In agreement with yeast data, AtSEC3a mediates in a PI(4,5)P2-dependent manner the direction of a CW material secretion and pollen tube growth (Bloch et al. 2016). The two SEC3 isoforms, AtSEC3a and AtSEC3b differ in their tissue or developmental specific expression, even though AtSEC3a is expressed also in sporophyte (Winter et al. 2007; Sekereš et al. 2017). In case of EXO70, which possess 23 paralogues in *Arabidopsis*, the EXO70A1 isoform is able to bind the PM possibly through its BAR-like C-terminus (Fendrych et al. 2013; Pleskot et al. 2015; Kalmbach et al. 2017). Nevertheless, tobacco EXO70 isoforms, when expressed in pollen tubes, show a striking difference between paralogues in localization and ability to bind a membrane (Sekereš et al. 2017). Several AtEXO70 isoforms, when overexpressed, exhibit a formation of an exocyst positive membrane compartments found also in the apoplast, named EXPO, which doesn't require the involvement of other exocyst complex subunits (Wang et al. 2010). The EXO70C2 subunit has also unique features - it neither interacts nor colocalizes with other members of the exocyst complex and functions possibly as the exocyst independent regulator of pollen tube growth (Synek et al. 2017). The AtEXO70B1 mediates the Golgi independent autophagy transport to the vacuole and is capable to interact with several exocyst subunits previously described to be employed in mammals-related autophagy (Bodemann et al. 2011; Kulich et al. 2013). Moreover, the autophagy-dependent early senescence phenotype of *exo70B1* and development phenotype of dwarfish *exo70A1* were fully additive, what suggests the existence of more exocyst variants in cells or subcomplexes (Kulich et al. 2013).

Since the first revelation of the exocyst role in plant immunity, evidences supporting its function in both PTI and ETI are increasing. First, the role of EXO70B2 and EXO70H1 in

defence against *Psm* and non-host pathogen *Blumeria graminis f. sp. hordei* (*Bgh*) has been shown. The LOF mutants in *EXO70B2* are more sensitive to *Psm* and they have disrupted development of defensive papillae against *Bgh* (Pečenková et al. 2011). Interestingly, the double mutant *exo70A1/exo70B2* showed an additive phenotype in papillae deformation (Žárský et al. 2013). It has been shown that the *exo70B2* mutants are less sensitive to various MAMPs and more susceptible towards *Pst*, *Pst*DC3000 and *Hyalonoperenospora arabidopsis* (*Hpa*; Stegmann et al. 2012; Stegmann et al. 2013). The EXO70B2 undergoes constitutive negative regulation via PUB22 ubiquitination, which is enhanced upon flg22 treatment in protoplasts (Stegmann et al. 2012). Thus, it has been proposed that the EXO70B2 works as the positive regulator of PTI (Stegmann et al. 2012). The post-translational regulation via PUB18 ubiquitination regulates also its closest homolog the EXO70B1, whose mutant generally exhibits elevated resistance against various pathogens such as *Pst* DC3000, *Hpa*, *Gvo* (Stegmann et al. 2013; Zhao et al. 2015; Seo et al. 2016). The resistance of the *exo70B1* mutant has two speculative explanations: EXO70B1 is a target of pathogen effectors and its integrity is control by NLR-like disease resistance protein TN2 (Zhao et al. 2015; Sabol et al. 2017), or the EXO70B1 drives the selective autophagy of pathogen effectors or activated receptors as TN2 (Pečenková et al. 2016). However, the mutant *exo70B1* exhibits age and SA dependent spontaneous cell death phenotype (Kulich et al. 2013) which has to be taken in evaluation of its resistance. Intriguingly, the EXO70B1 is attracted on PM by Rpm1 interacting protein (RIN4). The RIN4 serves as the integrator of PTI and ETI and is cleaved upon *Pst* DC3000 attack. Its cleavage triggers the hypersensitive PCD through RPS2 R protein, which could be activated in *exo70B1* (Sabol et al. 2017). Intriguingly, the double mutants *exo70B1/exo70B2* did not show the additive phenotype and rather partially complement each other (Stegmann et al. 2013). It remains elusive, what causes the functional difference between two homologues EXO70B1 and EXO70B2, especially because the duplication event leading to rising of two EXO70Bs seems to be unique for *Brassicaceae* (Cvrčková et al. 2012; Sekereš et al. 2017). The structures of proteins show only minor differences, what supports the ability of both EXO70Bs to interact with proteins, such as RIN4, SNAP33 (Pečenková et al. 2011; Zhao et al. 2015; Sabol et al. 2017). Thus, rather than structural motifs, the differential expression or co-expression and posttranslational regulation may cause the different phenotypes and non-redundant functioning of EXO70Bs in *Arabidopsis*. This supports analysis of a regulon involved in the antifungal immunity - while the EXO70B2 is co-expressed with the MLO2, SYP121 and PEN2/PEN3 defensive pathways, the EXO70B1 pairs only with SYP121

pathogen expression regulon in *Arabidopsis* (Humphry et al. 2010). It has been shown lately, that the exocyst core subunit SEC5a is required for immunity dependent callose deposition and PR1 secretion in *N. benthamiana*, and that it is a target for oomycete effector (Du et al. 2015). Subsequently, the new study has shown similar secretory defects for more exocyst subunits transiently silenced in *N. benthamiana* (Du et al. 2018). That would point to the general positive function of the exocyst in innate immunity. Remarkably, the rice OsSEC3A as the member of exocyst complex mediates negative regulation of immunity associated PCD. Although the mutant *Ossec3a* resembles the PAD4 dependent lesions mimic phenotype of *Atexo70B1*, it doesn't exhibit an increase SA level without a treatment (Ma et al. 2018). Nevertheless, it has never been conclusively explained whether the plant exocyst tethering complexes may play a role in the regulation of the SNARE complex assembly and SNARE driven membrane fusion and whether their roles should be studied as a one hierarchical membrane fusion regulatory module.

1.2.2.2. The SNARE complex

SNARE complex formation occurs when the four SNARE helixes carried either with three or four SNARE proteins meet in the proximity of the target membrane. The t-SNARE (target) protein usually contains single SNARE helix domain and is anchored through the transmembrane-domain to the membrane. The SNARE domains are orthologous to synaptic syntaxin and contain the conserved Glutamine (Q in one-letter code) residue, therefore are called Qa-SNARE (Fasshauer et al. 1998). Except for the SNARE domain, the Qa-SNAREs has Habc domain connected through linker with the SNARE helix (Fig. 6; Fernandez et al. 1998). This domain holds SNARE in their closed conformation before a helper protein from SM, NSF ATPase or its cofactor SNAP family open it and allow the SNARE partners to bind into a binary or ternary SNARE complex (Fig. 6; Demircioglu et al. 2014; Schwartz et al. 2017). The v-SNARE or vesicle-associated partners of Qa-SNAREs have only a single SNARE domain connected via a short linker domain with the transmembrane domain, which means that they are permanently open and active (Siddiqui et al. 2007). These v-SNAREs, also referred as vesicle-associated membrane proteins VAMPs in plants, contain the conserved arginine residue (Fig. 6), therefore are named also R-SNAREs (Fasshauer et al. 1998). The third and fourth SNARE helices are carried by Qb-, Qc- or Qbc-SNAREs, which also have the glutamine residue, but they are usually cytoplasmic or lipid-anchored and closely related to synaptic soluble NSF attachment proteins SNAPs (Söllner 2002; Karnik et al. 2017). The SNAP25 is

Qbc-SNARE, which has a palmitoylated linker connecting the two SNARE domains. The fully formed ternary SNARE complex assembles from four parallel SNARE core helices provided by one copy of each Qa-, Qb-, Qc-, R-SNAREs (Fig. 6), which follows through their zippering towards the C terminal membrane anchor and allows membrane fusion (Fasshauer et al. 1998; Sutton et al. 1998; Karnik et al. 2017). The resulted cis-SNARE complex, sitting on the same membrane has to be untangled with an active help of NSF and SNAP proteins. The Qa-SNARE stays where it is until its recycled, the Qbc-SNARE dissociates and the R-SNARE has to be recycled from the target membrane by endocytosis (Jahn & Fasshauer 2012). Despite the elegance of the zippering model, the dynamic and specificity of SNARE complex assembly remain unclear (Weber et al. 1998). *In vitro* experiments following the SNARE assembly have shown that the individual SNAREs are promiscuous and even compete with each other thus blocking the natural SNARE complex assembly. On that account, the surrounding conditions such as membrane composition, helper proteins presence, ATP and Ca^{+2} the membrane fusion, are essential for smooth membrane fusion and regulation of membranes fusion specificity (Honigmann et al. 2013; Laufman et al. 2013; Demircioglu et al. 2014; Li et al. 2016).

Figure 6

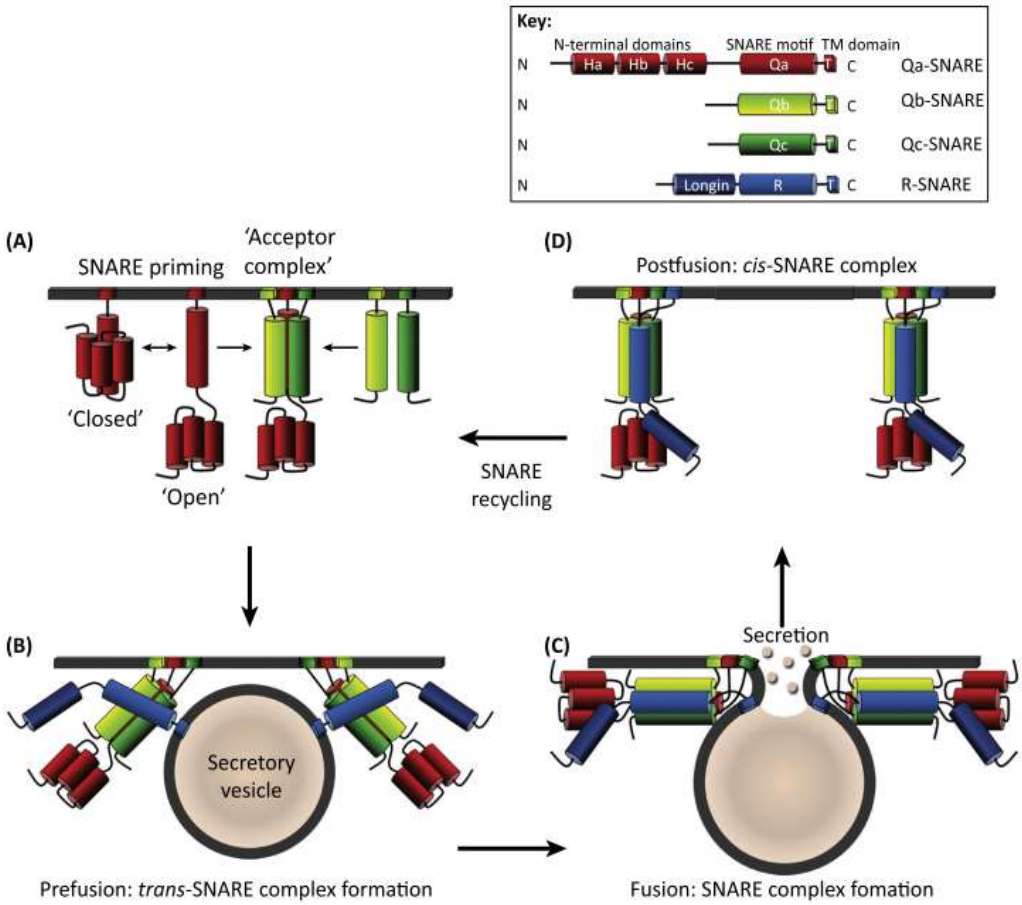

The SNARE complex assembly. SNARE assemble a tetrameric coiled-coil around a central core of three glutamine Qa-, Qb-, Qc- and one arginine R- residues to draw vesicle and target membranes together for fusion. In some cases, the Qb- and Qc- resides on the same polypeptide, as is the case for SNAP33. Binding of membrane and vesicle localized SNAREs in a cognate SNARE complex involves priming of the Qa- SNARE on the target membrane. A) The Qa- SNARE transits from its closed to open conformation through the unfurling of the Habc-domain, which exposes the Qa- domain to its binding with Qb- and Qc- SNAREs. The Qa-, Qb-, Qc- domains form the acceptor complex, which is available for binding with R-SNARE. B) Formation of trans-SNARE complex following the four SNARE domains binding draws the vesicle and target membrane for fusion. C) The membrane fusion leads to the release of secretory cargo and movement of the SNARE complex to the same membrane, the cis-SNARE complex. D) Following the vesicular fusion, cis-SNARE complex disassembly allows for recycling of the SNARE proteins and sustained secretory traffic. Key: TM transmembrane domain. (Karnik et al. 2017).

In *Arabidopsis*, SNARE proteins are encoded by 54 genes, covering all steps of conventional endomembrane trafficking pathway (Sanderfoot et al. 2000; Sanderfoot et al. 2001). Out of them, eighteen SNAREs are involved in transport towards PM (Uemura et al.

2004). Although some of them exhibit partial redundancy in developmental processes, the unique Qa-SNAREs functional specificity was found in *Arabidopsis* (Sanderfoot et al. 2001; Reichardt et al. 2011). The known example is Qa-SNARE SYP121, named also PEN1 (penetration 1), which was found together with non-SNARE related PEN2 and PEN3 in a screen for mutants with abolished penetration resistance against *Bgh* (Collins et al. 2003). The SYP121/PEN1 recruits SNAP33/VAMP721/722 SNARE partners in defensive secretion manner, while the second pathway relies on PEN3 dependent transport of PEN2 products (Stein et al. 2006; Kwon et al. 2008). The PEN3 belong to the pleiotropic drug-resistant ABC transporters and one of its substrates is the product of peroxisome and mitochondria-associated B-thioglucoside glucohydrolase PEN2, which synthesizes indole glucosinolates (Bednarek & Osbourn 2009; Lu et al. 2015). SYP121 role in penetration resistance against powdery mildew fungi has been shown in monocots and dicots, therefore it is an evolutionarily conserved function in plants (Collins et al. 2003). The usually stable PM-localized SYP121 undergoes massive recycling upon fungal treatment and accumulates beneath the contact sites (Assaad et al. 2004). The GFP-SYP121 marks also the internal apoplastic space of papilla, probably because of MVB degradation pathway redirection into the attack site, since this localization does not have any impact on its function in defence (Nielsen et al. 2012; Nielsen & Thordal-Christensen 2013). Interestingly GFP-SYP121 works as a reliable marker of exosomes, paramural space of papillae and encasement (Hansen & Nielsen 2017; Regente et al. 2017; Rutter & Innes 2017). The disruption of SYP121 abolishes the precise timing of callose secretion into the defensive papillae (Nielsen et al. 2012). The GFP-SYP121 localizes into the encasement together with tagged SNAP33 and PEN3 but does not have an impact on its development, thus other SNAREs are suggested to be important in secretory pathway targeting haustorial encasement (Meyer et al. 2009; Nielsen et al. 2017). Since the two close homologues, VAMP721 and VAMP722 are the major PM R-SNAREs in *Arabidopsis*, they may be part of more than one SNARE complex. Indeed, it has been shown that contrary to SYP121, VAMP721/722 play a role in R protein secretion to EHM (H. Kim et al. 2014). The involvement of TGN localized Qa-SNAREs SYP42/43 in penetration resistance to non-adapted *Ep* has been described, thus confirming the role of the secretory pathway in defence (Uemura et al. 2012). According to the transcriptional analysis, we can expect the connection with plant defence for more SNARE complexes, further supported by the ability of VAMP721 to interact with SYP121/122/132, SYP41/42/43, SYP22 (Fujiwara et al. 2014).

1.2.3. The autophagy

Autophagy is an evolutionary conserved catabolic process which allows regulated sequestration of various cargo such as damaged organelles, aggregated proteins or metabolic thresh. The autophagy is a unique system of degradation and recycling mediated through prominent membrane modulation, enclosures and trafficking. It has been very well studied in yeast and animal models, however, in recent years, the knowledge on plant autophagy has been increasing as well (Enrique Gomez et al. 2018; Wang et al. 2017)

The autophagy deploys formation of PI(3)P rich double membrane structure, the autophagosome. The site of an autophagosome initiation is named phagophore assembly site (PAS; Xie & Klionsky 2007). The machinery of autophagy-related proteins (ATG) regulates spatiotemporally the process of autophagosome assembly at PAS. The ATGs workflow at PAS still undergoes intensive investigation. On the ER surface, the ATG5 decorates an ATG8 positive cistern of phagophore, which subsequently grows through a planar structure into a cup shape, where the ring-like structure of ATG5 holds the phagophore until it is sealed probably by ATG1/13 complex (Suttangkakul et al. 2011; Le Bars et al. 2014). Interestingly the ATG5 ring has been found almost exclusively on the flat surface of ER (Le Bars et al. 2014). This connection may be explained by anticipated membrane tethering function of ATG5 or taking ER as a membrane source for phagophore assembly (Le Bars et al. 2014). Intriguingly, the transmembrane ATG9 plays an essential role for the direct outgrowth of autophagosome from ER (Zhuang et al. 2017). Thus ER serves as one source of membrane for autophagosome. Nevertheless, it has been suggested that various membranes may serve as the source for PAS. Importantly, the SH3P2 protein facilitates an existing membrane nucleation via binding to PI3P, PI3Kinase and ATG8 (Zhuang et al. 2013). The SH3P2 bends a membrane through it's BAR domain, thus may serve as a membrane curvature promoter and mediates formation of so-called omegasomes, structures resemble the Greek letter omega (Axe et al. 2008; Zhuang et al. 2013). The other membrane-associated protein EXO70B1, the isoform of EXO70 subunit of the exocyst complex, regulates also the autophagosome delivery into a vacuole in Golgi independent manner (Kulich et al. 2013). Moreover, the ATG8 interacting motifs were identified in other subunits of the exocyst (Cvrčková & Žárský 2013). The endosome-associated ESCRT complex participates also on the autophagosome targeting to the vacuole, where it cooperates again with the SH3P2 (Gao et al. 2015). Besides it, the ESCRT subunit CHMP1 mediates the autophagosome loading (Spitzer et al. 2015). The retromer impairment influences the endosome sorting and vacuole targeting, similarly to ESCRT, and impairs

autophagy (Munch et al. 2015). Also, the standard trafficking machinery participants such as RabG3b GTPases and VTI12 R-SNARE regulate the autophagy (Surpin et al. 2003; Kwon et al. 2013). While basal level of non-selective autophagy executes cellular homeostasis, the developmental and stress conditions deploy elevated selective autophagy (Hofius et al. 2009). In theory, the selective autophagy mediates cargo-specific degradation via a receptor recognition. This feature may be part of plant innate immunity. The specialized sequestration of viral proteins by NBR1 protein via autophagy has been shown, but the mechanism of receptor specificity remains to be explored (Hafrén et al. 2017).

Although autophagy mostly serves as a prosurvival and anti-senescence mechanism, it also may initiate or execute PCD (Hackenberg et al. 2013). The RabG3b induces the autophagy-related HR-like PCD but doesn't influence the basal resistance (Kwon et al. 2013). Contrary, the RabG3b mediated autophagy suppresses a spread of uncontrolled vacuolar death, necrosis (Kwon et al. 2013). Local activation of HR-like PCD is the common response in plant innate immunity, therefore its activation became a target of microbe colonization strategy. Currently, the data according to a pathogen life-strategy support a role of autophagy in both, pro-survival mechanism of the PCD spread inhibition and pro-death role in PCD activation (Üstün et al. 2017).

The role of trafficking system and exocyst in the autophagy pathway and its connection with plant immunity is introduced further (PAPER No. 1).

2. Questions and aims of the thesis

The overall aim of my thesis was to uncover new aspects of the role of the exocyst complex in plant response to the microbes and answer these questions.

What are the main components in the rapid root hair growth response after the contact with bacteria?

Plant penetration resistance relies on the fast development of defensive structures, the papillae and haustorial encasements. Does the exocyst contribute to their formation?

Callose is the prominent component of the defensive structures. Does the exocyst specifically regulates its deposition in defence reaction?

The SNARE complex SYP121/VAMP721/722/SNAP33 regulates secretory pathway in growth and defence. Does the exocyst cooperate in the similar secretory pathway as the SNARE complex and what is their relationship?

Are there other exocyst interactors connected with plant immunity?

3. Results

Obtained data are presented in three research papers PAPER No. 2, 3, 4 and one scientific view serves as the extension of introduction part and discussion PAPER No. 1. More experiments were done in case of PAPER No. 3 and are added as the Addition to PEPER No. 3.

3.1. PAPER No. 1

Title: Constitutive Negative Regulation of R Proteins in Arabidopsis also via Autophagy Related Pathway?

Authors: TamaraPečenková, Peter Sabol, Ivan Kulich, Jitka Ortmannová and Viktor Žárský

Summary: Even though resistance (R) genes are among the most studied components of the plant immunity, there remain still a lot of aspects to be explained about the regulation of their function. Many gain-of-function mutants of R genes and loss-of-function of their regulators often demonstrate up-regulated defence responses in combination with dwarf stature and/or spontaneous leaf lesions formation. For most of these mutants, phenotypes are a consequence of an ectopic activation of R genes. Based on the compilation and comparison of published results in this field, we have concluded that the constitutively activated defence phenotypes recurrently arise by disruption of tight, constitutive and multilevel negative control of some of the R proteins that might involve also their targeting to the autophagy pathway. This mode of R protein regulation is supported also by protein-protein interactions listed in available databases, as well as *in silico* search for autophagy machinery interacting motifs. The suggested model could resolve some explanatory discrepancies found in the studies of the immune responses of autophagy mutants

My contribution: I dealt with the membrane trafficking and R protein targeting chapter. I contributed to the problems connected with the SNARE proteins, the searching for dwarfed mutants showing accelerated cell death, and added my comments to the fruitful discussion about the conclusive model of possible R proteins targeting.

frontiers in Plant Science

HYPOTHESIS AND THEORY
published: 04 March 2016
doi: 10.3389/fpls.2016.00260

Constitutive Negative Regulation of R Proteins in *Arabidopsis* also via Autophagy Related Pathway?

Tamara Pečenková[1,2], Peter Sabol[2], Ivan Kulich[2], Jitka Ortmannová[1,2] and Viktor Žárský[1,2]*

[1] Laboratory of Cell Biology, Institute of Experimental Botany, Academy of Sciences of Czech Republic, Prague, Czech Republic, [2] Laboratory of Cell Morphogenesis, Department of Experimental Plant Biology, Faculty of Science, Charles University in Prague, Prague, Czech Republic

Even though resistance (R) genes are among the most studied components of the plant immunity, there remain still a lot of aspects to be explained about the regulation of their function. Many gain-of-function mutants of R genes and loss-of-function of their regulators often demonstrate up-regulated defense responses in combination with dwarf stature and/or spontaneous leaf lesions formation. For most of these mutants, phenotypes are a consequence of an ectopic activation of R genes. Based on the compilation and comparison of published results in this field, we have concluded that the constitutively activated defense phenotypes recurrently arise by disruption of tight, constitutive and multilevel negative control of some of R proteins that might involve also their targeting to the autophagy pathway. This mode of R protein regulation is supported also by protein–protein interactions listed in available databases, as well as *in silico* search for autophagy machinery interacting motifs. The suggested model could resolve some explanatory discrepancies found in the studies of the immunity responses of autophagy mutants.

Keywords: resistance, autophagy, R, Avr, ETI, dwarf, lesions, exocyst

OPEN ACCESS

Edited by:
Pietro Daniele Spanu, Imperial College London, UK

Reviewed by:
Mario Serrano, Universidad Nacional Autónoma de México, Mexico
Tolga Osman Bozkurt, Imperial College London, UK

****Correspondence:***
Tamara Pečenková
pecenkova@ueb.cas.cz

Specialty section:
This article was submitted to Plant Biotic Interactions, a section of the journal Frontiers in Plant Science

Received: *25 November 2015*
Accepted: *18 February 2016*
Published: *04 March 2016*

Citation:
Pečenková T, Sabol P, Kulich I, Ortmannová J and Žárský V (2016) Constitutive Negative Regulation of R Proteins in Arabidopsis also via Autophagy Related Pathway? Front. Plant Sci. 7:260. doi: 10.3389/fpls.2016.00260

INTRODUCTION

There are several approaches how to study and classify the plant immunity related events, and the most widespread is division of the plant immunity into two modes – a pathogen-associated molecular patterns (PAMPs) triggered immunity (PTI), which is triggered usually by recognition of structural components of pathogen on the surface of the host cell, and effector triggered immunity (ETI; Jones and Dangl, 2006). These two defense modes employ basically the same means, but PTI is more general and mild, while ETI is much stronger and more efficient. ETI is triggered by the direct or indirect interaction between a specific disease resistance (R) protein and a corresponding avirulence (Avr) protein of pathogen and is accompanied by a number of changes within the plant – production of reactive oxygen species (ROS) by an oxidative burst, accumulation of the salicylic acid (SA), and the transcriptional activation of genes involved in defense response, that lead to a possible final stage – localized programmed cell death called the hypersensitive response (HR; Pontier et al., 1998; review in McDowell and Woffenden, 2003; Vlot et al., 2008).

Disease resistance (R) genes are central components of the plant immune response. All R proteins contain at least some of basic motifs – either Toll/interleukin-1 receptor (TIR) or coiled-coil (CC) structure on the N terminal part, nucleotide-binding site (NBS), leucine-rich repeat

(LRR), protein kinase and transmembrane domains (review by Martin, 1999; Liu et al., 2007). There are 145 putative genes encoding a product with a TIR domain and 51 with CC domain predicted in the *Arabidopsis thaliana* Col-0 genome (Meyers et al., 2003; Jacob et al., 2013). Majority encode proteins with TIR, NBS, and LRR domains, making the TNL group; some genes encode proteins with TIR and NBS domains but no LRR domain (TN genes) and some encode proteins with a TIR domain only (TX genes; Meyers et al., 2003; Nandety et al., 2013). Besides CC-NBS-LRR containing proteins which make CNL group, there are also four proteins that have NBS motifs similar to CNLs, but lack a CC motif (Meyers et al., 2003).

There are several important molecules involved in signaling downstream the successful R-Avr recognition – ENHANCED DISEASE SENSITIVITY 1 (EDS1), PHYTOALEXIN DEFICIENT 4 (PAD4), NON-RACE SPECIFIC DISEASE RESISTANCE 1 (NDR1) and SENESCENCE ASSOCIATED GENE 101 (SAG101), which are essential for the accomplishment of HR and for the accumulation of the SA. EDS1, PAD4 and SAG101 are involved in transferring signals mainly from TNL proteins, while CNL pathway mostly relies on signaling through NDR1 (Century et al., 1997; Feys et al., 2001; He and Gan, 2002; Wagner et al., 2013).

In *Arabidopsis* mutants in genes coding for R and R-associated proteins, along with defense related deviations, two other most frequent phenotypes are a dwarf stature and a spontaneous HR lesion formation; many times present even simultaneously (**Table 1**). Rarely, a lethal phenotype occurs as well, even though no developmental function for these genes has been found so far. We could notice that for most of the R genes mutants, described phenotypes are a consequence of their activation, in some cases even a gain of function mutations (GOF). Based on the comparison of different studies of plant immunity, our hypothesis aims to suggest a model in which the hyper immune phenotypes arise as a result of disruption of tight, multistep and constitutive negative control of R proteins that possibly involves also their inactivation by the autophagy pathway.

OF DWARFS AND LESIONS

It was shown that mutants with over activated R protein dependent defense response develop mostly two phenotypes – dwarfism and/or necrotic leaf lesions (reviewed e.g., in Lorrain et al., 2003 and Janda and Ruelland, 2014). For instance, in plants overexpressing a CNL gene *ACTIVATED DISEASE RESISTANCE 1* (*ADR1*), a constitutive defense response and a dwarf phenotype were found (Grant et al., 2003). A TNL protein SUPPRESSOR OF NPR1 CONSTITUTIVE 1 (SNC1) was found to be overactive in the *bonzai1-1* (*bon1-1*) mutant which also shows a constitutive defense response and reduced plant size (Yang and Hua, 2004). Along with *bon1*, several other autoimmune dwarf mutations were found to be suppressed by mutation of SNC1 locus; namely in *BON1-ASSOCIATED PROTEIN* (*bap1*), *BAK1-INTERACTING RECEPTOR-LIKE KINASE 1* (*bir1*), *SUPPRESSOR OF RPS4-RLD 1* (*srfr1*), *CONSTITUTIVE EXPRESSER OF PATHOGENESIS-RELATED GENE* (*cpr1*) and *MITOGEN-ACTIVATED PROTEIN KINASE 1* (*mpk1*; review in Gou and Hua, 2012). Plants overexpressing a TIR-X gene At2g32140 show also dwarf phenotype and activated expression of defense-related genes (Kato et al., 2014). This phenotype was dependent on EDS1, PAD4, and partially dependent on SALICYLIC ACID INDUCTION DEFICIENT 2 (SID2).

HR-like spontaneous leaf necrotic lesions were found to be even more frequently associated with the mutations in R genes and constitutively activated immunity. For instance, a GOF mutant in TNL RPP4 locus called *chilling sensitive 2* (*chs2*) shows lesions in the low temperature conditions (Huang et al., 2010). GOF *Arabidopsis* mutant in the other *CHS* gene, *chs3-1,* which encodes an unconventional disease resistance (R) protein belonging to the TIR-NB-LRR class with a zinc-binding LIM domain (Lin-11, Isl-1 and Mec-3 domains) at the carboxyl terminus, shows arrested growth, chlorosis and constitutively activated defence responses at 16°C (Yang et al., 2010). A mutant in TNL gene *ssi4* develops chlorotic lesions which can be suppressed by high humidity (Shirano et al., 2002; Zhou et al., 2004). In addition, there are several examples of mutants with spontaneous lesions induction which are suppressed by mutations in loci encoding R proteins of CNL type – *ACTIVATED DISEASE RESISTANCE 1* – *adr1*, *adr1-l1* and *adr1-l2* suppress *LESION SIMULATING DISEASE 1* (*lsd1*) by down regulating SA signaling (Bonardi et al., 2011; Roberts et al., 2013). Likewise, when a putative TNL encoded by *LAZARUS 5* (*LAZ5*) gene is mutated, *accelerated cell death 11* (*acd11*) lesion phenotype can be suppressed (Palma et al., 2010). It was also shown, that in the absence of the copine-like proteins BON1 and BON3 function, several R-like genes of the TNL/TN type were found to trigger lesion cell death (LCD; Li et al., 2009). Mutation in *SUPPRESSOR OF MKK1 MKK2 2* (*summ2*) which encodes putative NB-LRR, suppresses lesions formation and dwarfism of mutants of MAP kinase pathway *mkk1/mkk2 and mpk4* (Kong et al., 2012).

There are genes coding for other defense related components that when mutated trigger the same constitutive immunity activation and dwarf or/and lesion mimic phenotypes – e.g., *CONSTITUTIVE EXPRESSOR OF PATHOGENESIS-RELATED GENE 1* (*CPR1*), *SUPPRESSOR OF SALICYLIC ACID INSENSITIVITY OF NPR1-5* 2 (*SSI2*), *DEFENSE NO DEATH* 1 (*DND1*), TYPE III *PHOSPHATIDYLINOSITOL-4-KINASES* β*1*β*2* (*PI4KIII*β1β2) (Bowling et al., 1994; Yu et al., 1998; Zhang et al., 2003; Sekine et al., 2004; Gou et al., 2012; Sasek et al., 2014). As a regular aspect of these mutants' phenotype deviations, hyper accumulation of SA was observed.

LETHALITY OF THE HUB

Overactive immunity can disturb plant growth and fitness, and in an extreme case, this can be deleterious. Unexpectedly, an embryo lethal phenotype was found for LOF mutation of a defense related gene *RPM1-INTERACTING PROTEIN 4* (*RIN4*). Being evolutionarily conserved protein in plants, RIN4 is targeted to the plasma membrane by C-terminal acylation, and is required for the activation of a CNL *RESISTANCE TO*

TABLE 1 | List of *Arabidopsis* mutants related to R proteins hyper activity causing dwarf and lesion mimic phenotypes.

Gene	Name	Function category	Related mutant phenotypes	Reference
acd11	*accelerated cell death 11*	Sphingosine transfer protein	Lesions	Brodersen et al., 2002
adr1	*activated disease resistance 1*	CNL	Lesions suppression, dwarf oe	Grant et al., 2003
adr1-l1	*activated disease resistance 1-like 1*	CNL	Lesions suppression, dwarf oe	Collier et al., 2011
adr1-l2	*activated disease resistance 1-like 2*	CNL	Lesions suppression	Bonardi et al., 2011
atg5	*autophagy related gene 5*	Autophagy, ubiquitin ligase	Early senescence	Thompson et al., 2005
atg6	*autophagy related gene 6/Beclin1*	Autophagy activation	Pollen-lethality	Fujiki et al., 2007
atg7	*autophagy related gene 7*	Autophagy, ubiquitin activating enzyme	Defense-related	Doelling et al., 2002
atg8	*autophagy related gene 8*	Ubiquitin-like protein, cargo recruitment	/	Ketelaar et al., 2004
bak1	*brassinosteroid-insensitive associated 1*	Receptor-like protein kinase	Semidwarf	Li et al., 2002
bap1	*bon1-associated protein*	Calcium-dependent phospholipid-binding	/	Hua et al., 2001
bir1	*bak1-interacting receptor-like kinase 1*	Receptor-like protein kinase	Dwarf	Gao et al., 2009
bon1	*bonzai1*	Copine-like, membrane trafficking	Dwarf	Hua et al., 2001
bon2	*bonzai2*	Copine-like, membrane trafficking	Dwarf	Yang et al., 2006
bon3	*bonzai3*	Copine-like, membrane trafficking	Dwarf	Yang et al., 2006
chs2	*chilling-sensitive 2*	TNL	Lesions	Huang et al., 2010
chs3	*chilling-sensitive 3*	TNL	Lesions	Yang et al., 2010
cpr1	*constitutive expresser of pathogenesis-related gene*	F-box protein	Dwarf	Gou et al., 2012
dnd1	*defense no death 1*	Cyclic nucleotide-gated ion channel	Dwarf	Yu et al., 1998
eds1	*enhanced disease sensitivity 1*	R related signaling	Lesions suppression	Rogers and Ausubel, 1997
exo70A1	*exo70A1*	Membrane trafficking	Dwarf	Synek et al., 2006
exo70B1	*exo70B1*	Membrane trafficking	Lesions	Kulich et al., 2013
fls2	*flagellin-sensitive 2*	Receptor-like protein kinase	Defense related	Gomez-Gomez and Boller, 2000
laz4	*lazarus 4*	Membrane trafficking	Lesion suppression	Munch et al., 2015
laz5	*lazarus 5*	R protein	Lesions suppression	Palma et al., 2010
lsd1	*lesion simulating disease 1*	Cell death related	Lesions	Kliebenstein et al., 1999
mkk1/mkk2	*mitogen-activated protein kinase kinase kinase 1/2*	Signaling	Dwarf, lesions	Qiu et al., 2008
mpk1	*mitogen-activated protein kinase 1*	Signaling	Dwarf	Bartels et al., 2009
mpk4	*mitogen-activated protein kinase 4*	Signaling	Dwarf, lesions	Petersen et al., 2000
ndr1	*non-race specific disease resistance 1*	R related signaling	Lesions suppression	Century et al., 1995
pad4	*phytoalexin deficient 4*	R related signaling	Lesions suppression	Jirage et al., 1999
rar1	*required for mlo12 resistance 1*	R related signaling	Lesions suppression	Azevedo et al., 2002
rin4	*rpm1-interacting protein 4*	Immunity related	Embryo lethal	Mackey et al., 2002
rpm1	*resistance to p. syringae pv maculicola 1*	R protein	Defense related	Debener et al., 1991
rps2	*pesistant to p. syringae 2*	R protein	Defene related	Yu et al., 1993
sag101	*senescence associated gene 101*	R related signaling	/	Feys et al., 2005
sgt1b	*suppressor of g-two allele of skp1*	R related signaling	Lesions suppression	Azevedo et al., 2002
sid2	*salicylic acid insensitive 2*	SA synthesis	Defense related	Nawrath and Metraux, 1999
slh1	*sensitive to low humidity 1*	R protein	Lesions	Noutoshi et al., 2005
snc1	*suppressor of npr1 constitutive 1*	R protein	Dwarfism suppression	Li et al., 2010
srfr1	*suppressor of rps4-rld 1*	Tetratricopeptide repeat domain containing	Dwarf	Kim et al., 2010
ssi2	*suppressor of SA insensitivity of npr1-5 2*	Stearoyl-ACP desaturase	Dwarf, lesions	Sekine et al., 2004

(Continued)

TABLE 1 | Continued

Gene	Name	Function category	Related mutant phenotypes	Reference
ssi4	*Suppressor of SA insensitivity of npr1-5 4*	R protein	Dwarf	Shirano et al., 2002
summ2	*Suppressor of mkk1 mkk2 2*	R protein	Dwarfism and lesions suppression	Zhang et al., 2012
syp121/syp122	*Syntaxin 121/syntaxin 122*	Membrane trafficking	Dwarf, lesions	Zhang et al., 2008
syp23	*Syntaxin 23*	Membrane trafficking	Semi-dwarf	Ohtomo et al., 2005
syp31	*Syntaxin 31*	Membrane trafficking	/	Chatre et al., 2009
TN2	*TIR-NBS 2*	R protein	Lesions suppression	Zhao et al., 2015
TX At2g32140	/	R protein	Dwarf	Kato et al., 2014

PSEUDOMONAS SYRINGAE PV. MACULICOLA 1 (RPM1; Kim et al., 2005; Takemoto and Jones, 2005). RIN4 is phosphorylated upon infection with *P. syringae* expressing either AvrB or AvrRpm1 (Mackey et al., 2002). RIN4 is also involved in the activation of another CNL type R protein *RESISTANCE TO P. SYRINGAE 2* (RPS2) by putative Cys protease AvrRpt2 of *P. syringae*, which causes posttranscriptional cleavage and disappearance of RIN4 and this is required for full RPS2 activation (Axtell and Staskawicz, 2003; Mackey et al., 2003). Interestingly, in coimmunoprecipitation experiments, RIN4 was found to associate with RPM1, RPS2 as well as with pathogen recognition receptor (PRR) FLAGELLIN-SENSITIVE 2 (FLS2), creating thus a physical link between PTI and ETI (Qi et al., 2011). The *rin4* null mutation lethality is rescued in a *rin4rps2* double mutant, indicating that RIN4 negatively regulates inappropriate activation of RPS2 (Mackey et al., 2003). In addition, fragments of RIN4, including those produced by AvrRpt2, each containing a nitrate-induced (NOI) domain specific for plants, suppress PTI, also in the *rpm1/rps2/rin4* mutant background, and activate a cell death response in the wild type (Afzal et al., 2011).

MEMBRANE TRAFFICKING AND THE R PROTEINS-DEPENDENT IMMUNITY

Surprisingly, several basic regulators expected to function in the endomembrane trafficking and membrane fusion events, such as SNARE and exocyst proteins, might be also connected to the regulation of activity of R proteins. For instance, the dwarf and lesion-mimic double mutant of plasma membrane syntaxins SYP121 and SYP122 constitutively expresses the SA signaling pathway- as well as other known pathogen-responsive genes (Zhang et al., 2008). The same study shows that based on the suppressor mutant analysis of *syp121 syp122*, PAD4 is of key importance for the lesion development. Mutant alleles of signaling mediators of both TNL and CNL-type resistances *EDS1*, *NDR1*, *REQUIRED FOR MLO12 RESISTANCE 1* (*RAR1*) and *SUPPRESSOR OF G-TWO ALLELE OF SKP1* (*SGT1b*) partially rescued the lesion-mimic phenotype. Interestingly, the double mutant was crossed to the autophagy *atg7* mutant, however, as there was no effect of this mutation on the appearance of lesions, authors concluded that the autophagy does not play a role in this process (Azevedo et al., 2002; Zhang et al., 2008).

Recently, *exo70B1* loss-of-function mutant was found to develop spontaneous leaf lesions, over-express defense responses genes and show enhanced resistance to fungal, oomycete and bacterial pathogens (Kulich et al., 2013; Stegmann et al., 2013). Unexpectedly, its function is not related to the secretion of secretory vesicles to the plasma membrane; instead, EXO70B1 positive compartments were found to end in the central vacuole and to co-localize with autophagosomal marker ATG8f. In a screen for mutants that suppress *exo70B1* phenotype, nine alleles of TIR-NBS2 (TN2) were identified, suggesting that loss-of-function of EXO70B1 leads to activation of this TN protein (Zhao et al., 2015). It was also shown that TN2 interacts with EXO70B1 in yeast and *in planta*. However, it is not known whether TN2 directly monitors EXO70B1 integrity (as proposed by Zhao et al., 2015) or whether EXO70B1 is only required for autophagic transport to the vacuole and subsequent degradation of TN2. EXO70B1-mediated autophagy-related transport to the vacuole might be participating in TN2 degradation. Both scenarios would explain the observed phenotype.

Additionally, recent work confirmed the importance of membrane trafficking in the plant cell death lesion suppression – *lazarus 4* (*laz4*) was found to be mutated in one of three *VACUOLAR PROTEIN SORTING 35* (*VPS35*) genes which code for a subunit of the retromer complex functioning in endosomal protein sorting and vacuolar trafficking – esp. of retrograde retrieval of vacuolar sorting receptors. These results also showed that the retromer deficiency impairs endosomal sorting of immune components and targeting of vacuolar cargo (Munch et al., 2015).

Interestingly, the endosomal compartment may be as well the site of R-Avr proteins interaction – potato R3A and *Phytophtora infestans* effector AVR3a interact and relocalize from the cytoplasm to endocytotic compartment from where they turn on HR signaling (Engelhardt et al., 2012).

Even though it was not described for plants so far, we can expect that the both endosomes and autophagy related membrane trafficking will provide pathogens an opportunity to manipulate both for the purposes of more successful infection. Such an example was recently described for human epithelium-*Salmonella* interaction – at early stages of *S. typhimurium* infection, autophagy is used to seal endosomal membranes damaged by *Salmonella* secretion system during host cell invasion, but later it is also necessary for the further progression of *Salmonella* infection (Kreibich et al., 2015).

FROM AUTOPHAGY TO IMMUNITY

Autophagy is a bulk degradation by which cell/organism recycles nutrients, deals with stress, clears off dysfunctional organelles, aggregates etc. (Levine and Klionsky, 2004). Several types of autophagy have been reported, including macroautophagy, which is present in many organisms including fungi, animals and plants. This process relies on the concerted action of autophagy-related (*ATG*) genes encoded proteins to form first phagophore, to promote phagophore enclosure into autophagosome, and to deliver autophagosomes to the vacuole or lysosomes to release the autophagic bodies for eventual breakdown (Li and Vierstra, 2012; Reggiori and Klionsky, 2013).

When *Arabidopsis* mutants are disrupted in *ATG* genes represented by single loci, they grow normally under non-stress conditions, but are hypersensitive to nitrogen and carbon starvation (Doelling et al., 2002; Hanaoka et al., 2002; Yoshimoto et al., 2004; Thompson et al., 2005). However, unlike other non-plant organisms, *Arabidopsis* has nine *ATG8* and two *ATG12* gene isoforms, which makes the study of their role more difficult and suggests that the autophagic process in plants is more complicated than in other organisms. Some of its complexity is reflected in the role of autophagy in plant immunity.

The importance of autophagy in the plant immunity was first demonstrated in Liu et al. (2005) – it was found that the autophagy was required to restrict the spread of plant HR cell death. The activation of hypersensitive cell death via the R gene RPM1 upon infection with bacteria also led to cell death beyond the borders of the infection site in plants silenced for *atg6/Beclin1* (Patel and Dinesh-Kumar, 2008). It was concluded that autophagy prevents unrestricted HR cell death and that functions as a pro-survival pathway in plant–pathogen interactions. All of these observations and conclusions were based on experimenting with older *Arabidopsis* plants and on tissues surrounding the actual infection sites, a few days after local infection.

However, a pro-death function of autophagy during HR cell death was reported as well (Hofius et al., 2009). Autophagy was found to be triggered by some, but not all types of R proteins in the infected tissue and its surroundings. HR cell death triggered by R proteins RPS4, RPP1 and RPM1 was significantly suppressed in *atg* (autophagy) mutants; especially the first two of them which signal through EDS1 signaling component. In this case, cell death was monitored in the actual infection site, in the range of hours after inoculation (Hofius et al., 2009).

Yoshimoto et al. (2009), found no deviations in RPM1-triggered cell death beyond the initial infection site in younger atg mutants. However, in older *atg* mutants such as *atg5*, they observed lesions in non-infected tissues 6–9 days after infection. Interestingly, these effects were suppressed by removal of the SA and by mutations in SA signaling hub "non-expressor of *PR* genes" – NPR1. The authors proposed that autophagy negatively regulates the cell death by controlling NPR1-dependent SA signaling. In contrast to younger leaves, older *atg* mutant leaves contain higher levels of toxic metabolites, disrupted organelles and oxidized proteins which contribute to the cell death spread (Yoshimoto et al., 2009). This could be as well explained as a combination of effects of different sets of genes involved in the adult plant resistance and ineffective autophagy (Carviel et al., 2009). Scientists tried to explain and integrate these conflicting results obtained from studies on HR lesions of *atg* mutants. Zhou et al. (2014) propose that autophagy suppresses SA and ROS signaling amplification loop that leads to cell death, while in the resistance to necrotrophic pathogens it promotes JA signaling. Consistently, a recent hypothesis suggests that SA is not only an autophagy inducer, but also a cargo for autophagy-related ER to vacuole membrane transport and catabolism (Kulich and Zarsky, 2014). Recently, a model was worked out in which the autophagy is both initiator and executioner of cell death and is placed downstream of the R protein activation, and supposed to help the cell to deal with the ER stress provoked by a heavy load with pathogenesis related proteins (PRs, review in Minina et al., 2014).

CONCLUSION AND PERSPECTIVES

Here we show that most of the observed defects in *Arabidopsis* R protein regulator mutants are a direct or indirect consequence of non-pathogen related ectopic R protein activation. It thus seems conceivable that the plant constantly down regulates R protein function, and when this constitutive negative regulation is disturbed, the R proteins are activated and spontaneously signal the non-existent pathogen attack. Based on the example of *rin4* mutant lethality we could speculate, that, similarly to other organisms, the proper function of the negative control might be set already in the earliest stages of development. The plant innate immunity has to be kept as low as possible when it is not necessary in order to prevent high energy costs of defense, and yet in the state of alertness which will allow its fast, in fact instantaneous, activation. We believe that the best way to achieve this is to keep these components (i.e., in our case R genes) transcribed and translated on a sufficient basic level, but to keep their function tightly under negative control which will prevent undesired overactive autoimmunity. How could be this achieved? There are many examples of negative controls involved at various stages of defense that include ubiquitination and proteolysis, phosphorylation of proteins, as well as redox dependent changes in protein multimerization and localization (e.g., Trujillo et al., 2008; Anderson et al., 2011; Vogelmann et al., 2012). We suggest that one of the mechanisms to achieve this is also targeting of defense machinery components – here especially R proteins – to the autophagy pathway for degradation (**Figure 1**). Once the R protein is recruited by autophagy machinery into the autophagosome, it might share the destiny of other autophagic cargos – transport to the vacuole and degradation. We speculate that along with proteins the autophagy related degradation process might destroy also other molecules including signaling relevant molecules as ROS or SA. After the interaction of R protein with its counterpart Avr, R protein is protected against this autophagy-dependent degradation and can interact with downstream components and trigger ETI. This model may be valid also for indirect R-Avr interactions; e.g., the proposed R protein guard function (reviewed e. g. in Spoel and Dong, 2012)

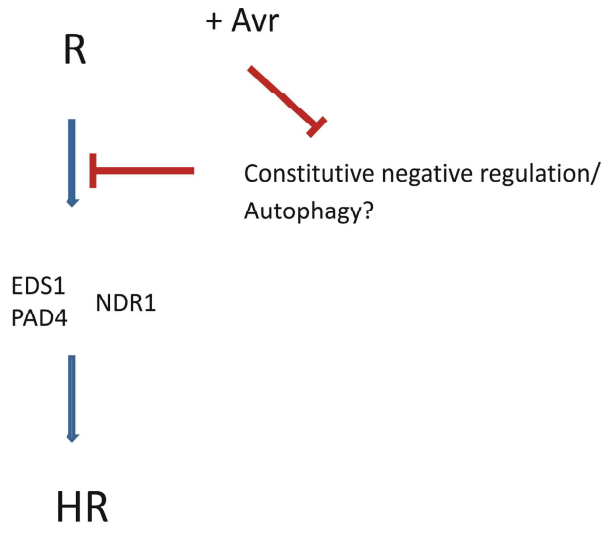

FIGURE 1 | The plant constitutively negatively regulates R protein function. The interaction R-Avr serves mainly to release this negative regulation. The important component of negative regulation is autophagy; when it is non-efficient, R proteins spontaneously over activate defense responses.

could be based on the avoidance of this negative regulation after the recognition of the changed status of the guardee. It should be stressed that we certainly expect other ways of regulations of R proteins to exist, such as a switch from inactive to active state of R protein upon Avr recognition, as well as other ways of negative regulation.

Based on our hypothesis one would expect that autophagy mutants should copy the phenotype of *exo70B1* mutant, having at least some R proteins constitutively activated. While some of the mutants in the autophagy pathway indeed show similar phenotypic deviations (e.g., early senescence and yellowing, sensitivity to starvation, as well as SA hyperaccumulation in *atg2* and *atg5* mutants; Yoshimoto et al., 2009; Wang et al., 2011), others seem to display only early senescence phenotype and cell death phenotypes only after starvation induction (like *atg7* mutant). It also seems that some subunits of autophagy machinery might be more important for the negative regulation of the immunity, while others, e.g., ATG7 and ATG9, in the execution of HR (Hofius et al., 2009; Minina et al., 2014). It should be, however, noted that autophagy proteins (and EXO70B1) have been also implicated in diverse cellular processes independently of their roles in autophagy.

We also expect that, pathogen effectors might have evolved to manipulate and hijack this negative regulation and worsen the plant defense – recently, a *Phytophtora infestans* effector PexRD54 has been shown to outcompete the autophagy cargo receptor Joka and enhance virulence of this pathogen. Interestingly, PexRD54 does this probably through the activation of selective autophagy. Joka could participate in the removal of plant or pathogen molecules that negatively affect host defenses. As authors of the study speculate, PexRD54 would thus counteract the positive role of Joka2-mediated selective autophagy in pathogen defense. An alternative, but not exclusive explanation based on our hypothesis would be that PexRD54 at the same time stimulates the selective autophagy of R proteins capable of detecting it and thus promotes pathogen virulence (Dagdas et al., 2016). Already the report of Engelhardt et al. (2012) demonstrated the capability of cytoplasmic R protein to be recruited to endomembranes, but not for degradation, rather for the purpose of activation. However, this is not exclusive with our model – the interaction of R3A and Avr3A might release the negative regulation of R3A and switch on the HR. This interaction is obviously indirect and requires an intermediate connected to ARA6/ARA7 marked endosomes. It is possible that this activation evolved from the mechanisms of negative regulation. More information on R3A and Avr3A interactors could help to solve this ambivalent situation.

We found an indirect support for our hypothesis in the autopagy-related events described for mammalian cells – it is known from experiments performed on HeLa cells that endocytosed plasma membrane contributes to ATG12–ATG5-ATG16L1-positive/ATG8-negative phagophore precursor vesicles by both clathrin-dependent and -independent routes (Moreau and Rubinsztein, 2012). The subsequent maturation of these small phagophore precursors into phagophores (ATG12–ATG5-ATG16L1-positive/ATG8-positive) is assisted by SNARE-mediated homotypic fusion that increases their size. Additionally, *Arabidopsis* BON1/2/3 belong to copine proteins, a family of ubiquitous Ca(2+)-dependent, phospholipid-binding proteins that are known to be involved in animal membrane trafficking events (Tomsig and Creutz, 2002), and in *Dictyostelium* localize to plasma membrane, contractile vacuoles, organelles of the endolysosomal pathway, and phagosomes (Damer et al., 2005). Therefore, besides confirmed role of EXO70B1 in autophagy and regulation of TN2 activity, very probably SNARE and BON proteins could implement similar role in autophagy-related membrane targeting and membrane fusion events leading to the negative control of R proteins.

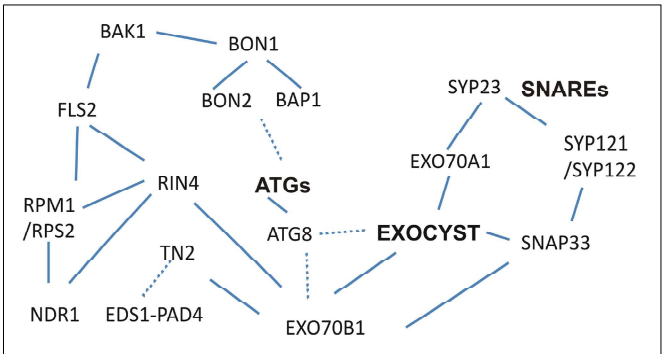

FIGURE 2 | Interactions of PTI, ETI and ATG related proteins with SNAREs and exocyst. The RIN4 interacts with PTI receptor FLS2 and associated proteins, which further interact with BON1, BON2 and BAP. Additionally, RIN4 and related R-proteins may be in the same complex. R proteins and autophagy functions are connected by exocyst and SNARE interactions. (Experimentally confirmed interactions are visualized with lines, non-confirmed with dashed lines).

We found further support for this hypothesis in the connection between assumed autophagy regulating proteins and R proteins, as well as other key molecules of the both PTI and ETI immune response, in the web of protein-protein interactions that are available in Biogrid and PPIN databases (Stark et al., 2006; Mukhtar et al., 2011; **Figure 2**; **Table 1**). The components of PAMP-sensing complexes interact with RIN4, which further interacts with R proteins. Mainly through mediating kinase BAK1, they are connected and interact as well with BON1, BON2 and BAP. RIN4 interacts with R proteins as well as with EXO70B1 (Afzal et al., 2013). Besides its capability to interact with other exocyst and SNARE proteins, EXO70B1, together with 20 other paralogs of *Arabidopsis* EXO70 exocyst subunits, possess ATG8 interacting motives, which indicates that the autophagy machinery and exocyst complex functions are multiply connected (Cvrčková and Zárský, 2013; Tzfadia and Galili, 2013; Sabol et al., in preparation). Thus, in the vicinity of plasma membrane, and depending on membrane trafficking which involves SNARE, exocyst and autophagy complex proteins, a tight control of R protein activation allows the immunity to be kept low but in a constant alert.

Recently, a role for EXO70F3 of *Oryza sativa* in immunity against *Magnaporthe oryzae* was found – OsEXO70F3 appears to play a crucial role in immunity triggered by Pii, suggesting a role for this EXO70 paralog as a decoy or helper in Pii/Avr-Pii interaction (Fujisaki et al., 2015). It may be true that pathogen effectors target these and other exocyst subunits in order to suppress defense, however, we don't consider it to be mutually exclusive with our hypothesis.

Our model could help to better understand and reconcile conflicting aspects of autophagy in the plant immunity (Teh and Hofius, 2014): in the infection sites, R-Avr recognition prevents R protein targeting to inactivation/destruction pathway and triggers the ETI, and with the increased distance from the infection site, declining concentration of Avr protein allows the autophagy to overtake again a control over R protein. In *atg* mutants, the existing constitutive immunity activation results in spontaneous HR lesions formation; but after the pathogen attack, in the case of younger leaves, in addition to R protein deregulation, R is further activated by Avr recognition, which makes cells more resistant and lesions smaller. Or, under conditions with additional stresses, as in the case also of older leaves, because of coincidence between consequences of ineffective autophagy of *atg* mutants and Avr-enhanced over activation of R proteins, less Avr is needed for HR threshold to be crossed and lesions spread farther.

Our model's aim is to focus on one aspect only – a possibility of a negative regulation of some NLRs/innate immunity related proteins by autophagy in plants. However, there are many difficulties that will have to be overcome in order to confirm its validity. Part of difficulties is coming from the complexity of autophagy machinery and a large number of ATG proteins that have also been implicated in diverse cellular processes independently of their roles in autophagy. Autophagy machinery is also difficult to study separately from other endomembrane compartments, especially by using pharmacological treatments. For instance, wortmannin, which is often used for these purposes, is rather pleiotropic drug – dependent on cell type and concentration it affects different types of phosphoinositide kinases, having thus multiple interference with endomembrane dynamics.

To conclude, plants have mechanisms to downregulate R proteins function, and when they are attacked by an appropriate Avr carrying pathogen, the R proteins are stabilized, activating defense responses. This would also mean that R proteins are capable of immunity activation without Avr and that the interaction R-Avr serves mainly to release R proteins negative regulation. The disturbance of the basic autophagy machinery has pleiotropic effects on many plant functions including development and is influenced by growth conditions, abiotic stresses and senescence, hence it is very difficult to study effects of *atg* mutants that would concern specifically defense responses. We believe that in the near future, R proteins studies will bring more information on the regulation of their activity including proteins that target them for the suggested autophagy destruction.

AUTHOR CONTRIBUTIONS

TP did a compilation of data on R-related dwarf and lesion mimic mutants and most of the writing; PS did the RIN4-related data mining and text editing; IK explained the connection to autophagy; JO delt with membrane traficking chapter; VZ did the most of text editing and integrating as well as the finalization of the manuscript.

FUNDING

This work was supported by The Czech Science Foundation project No. GA15-14886S. The part of the VZ income is covered by Ministry of Education, Youth and Sports project NPU LO1417.

ACKNOWLEDGMENT

Authors would like to thank Lucie Trdá and Martin Janda for the critical reading of the manuscript.

REFERENCES

Afzal, A. J., da Cunha, L., and Mackey, D. (2011). Separable fragments and membrane tethering of *Arabidopsis* RIN4 regulate its suppression of PAMP-triggered immunity. *Plant Cell* 23, 3798–3811. doi: 10.1105/tpc.111.088708

Afzal, A. J., Kim, J. H., and Mackey, D. (2013). The role of NOI-domain containing proteins in plant immune signaling. *BMC Genomics* 14:327. doi: 10.1186/1471-2164-14-327

Anderson, J. C., Bartels, S., Gonzalez Besteiro, M. A., Shahollari, B., Ulm, R., and Peck, S. C. (2011). *Arabidopsis* MAP Kinase Phosphatase 1 (AtMKP1)

negatively regulates MPK6-mediated PAMP responses and resistance against bacteria. *Plant J.* 67, 258–268. doi: 10.1111/j.1365-313X.2011.04588.x

Axtell, M. J., and Staskawicz, B. J. (2003). Initiation of RPS2-specified disease resistance in *Arabidopsis* is coupled to the AvrRpt2-directed elimination of RIN4. *Cell* 112, 369–377. doi: 10.1016/S0092-8674(03)00036-9

Azevedo, C., Sadanandom, A., Kitagawa, K., Freialdenhoven, A., Shirasu, K., and Schulze-Lefert, P. (2002). The RAR1 interactor SGT1, an essential component of R gene-triggered disease resistance. *Science* 295, 2073–2076. doi: 10.1126/science.1067554

Bartels, S., Anderson, J. C., Gonzalez Besteiro, M. A., Carreri, A., Hirt, H., Buchala, A., et al. (2009). MAP kinase phosphatase1 and protein tyrosine phosphatase1 are repressors of salicylic acid synthesis and SNC1-mediated responses in *Arabidopsis*. *Plant Cell* 21, 2884–2897. doi: 10.1105/tpc.109.067678

Bonardi, V., Tang, S., Stallmann, A., Roberts, M., Cherkis, K., and Dangl, J. L. (2011). Expanded functions for a family of plant intracellular immune receptors beyond specific recognition of pathogen effectors. *Proc. Natl. Acad. Sci. U.S.A.* 108, 16463–16468. doi: 10.1073/pnas.1113726108

Bowling, S. A., Guo, A., Cao, H., Gordon, A. S., Klessig, D. F., and Dong, X. (1994). A mutation in *Arabidopsis* that leads to constitutive expression of systemic acquired resistance. *Plant Cell* 6, 1845–1857. doi: 10.1105/tpc.6.12.1845

Brodersen, P., Petersen, M., Pike, H. M., Olszak, B., Skov, S., Odum, N., et al. (2002). Knockout of *Arabidopsis* accelerated-cell-death11 encoding a sphingosine transfer protein causes activation of programmed cell death and defense. *Genes Dev.* 16, 490–502. doi: 10.1101/gad.218202

Carviel, J. L., Al-Daoud, F., Neumann, M., Mohammad, A., Provart, N. J., Moeder, W., et al. (2009). Forward and reverse genetics to identify genes involved in the age-related resistance response in *Arabidopsis thaliana*. *Mol. Plant Pathol.* 10, 621–634. doi: 10.1111/j.1364-3703.2009.00557.x

Century, K. S., Holub, E. B., and Staskawicz, B. J. (1995). NDR1, a locus of *Arabidopsis thaliana* that is required for disease resistance to both a bacterial and a fungal pathogen. *Proc. Natl. Acad. Sci. U.S.A.* 92, 6597–6601. doi: 10.1073/pnas.92.14.6597

Century, K. S., Shapiro, A. D., Repetti, P. P., Dahlbeck, D., Holub, E., and Staskawicz, B. J. (1997). NDR1, a pathogen-induced component required for *Arabidopsis* disease resistance. *Science* 278, 1963–1965. doi: 10.1126/science.278.5345.1963

Chatre, L., Wattelet-Boyer, V., Melser, S., Maneta-Peyret, L., Brandizzi, F., and Moreau, P. (2009). A novel di-acidic motif facilitates ER export of the syntaxin SYP31. *J. Exp. Bot.* 60, 3157–3165. doi: 10.1093/jxb/erp155

Collier, S. M., Hamel, L. P., and Moffett, P. (2011). Cell death mediated by the N-terminal domains of a unique and highly conserved class of NB-LRR protein. *Mol. Plant Microbe Interact.* 24, 918–931. doi: 10.1094/MPMI-03-11-0050

Cvrčková, F., and Zárský, V. (2013). Old AIMs of the exocyst: evidence for an ancestral association of exocyst subunits with autophagy-associated Atg8 proteins. *Plant Signal. Behav.* 8, e27099. doi: 10.4161/psb.27099

Dagdas, Y. F., Belhaj, K., Maqbool, A., Chaparro-Garcia, A., Pandey, P., Petre, B., et al. (2016). An effector of the Irish potato famine pathogen antagonizes a host autophagy cargo receptor. *Elife* 5, e10856. doi: 10.7554/eLife.10856

Damer, C. K., Bayeva, M., Hahn, E. S., Rivera, J., and Socec, C. I. (2005). Copine A, a calcium-dependent membrane-binding protein, transiently localizes to the plasma membrane and intracellular vacuoles in *Dictyostelium*. *BMC Cell Biol.* 6:46. doi: 10.1186/1471-2121-6-46

Debener, T., Lehnackers, H., Arnold, M., and Dangl, J. L. (1991). Identification and molecular mapping of a single *Arabidopsis thaliana* locus determining resistance to a phytopathogenic *Pseudomonas syringae* isolate. *Plant J.* 1, 289–302. doi: 10.1046/j.1365-313X.1991.t01-7-00999.x

Doelling, J. H., Walker, J. M., Friedman, E. M., Thompson, A. R., and Vierstra, R. D. (2002). The APG8/12-activating enzyme APG7 is required for proper nutrient recycling and senescence in *Arabidopsis thaliana*. *J. Biol. Chem.* 277, 33105–33114. doi: 10.1074/jbc.M204630200

Engelhardt, S., Boevink, P. C., Armstrong, M. R., Ramos, M. B., Hein, I., and Birch, P. R. (2012). Relocalization of late blight resistance protein R3a to endosomal compartments is associated with effector recognition and required for the immune response. *Plant Cell* 24, 5142–5158. doi: 10.1105/tpc.112.104992

Feys, B. J., Moisan, L. J., Newman, M. A., and Parker, J. E. (2001). Direct interaction between the *Arabidopsis* disease resistance signaling proteins, EDS1 and PAD4. *EMBO J.* 20, 5400–5411. doi: 10.1093/emboj/20.19.5400

Feys, B. J., Wiermer, M., Bhat, R. A., Moisan, L. J., Medina-Escobar, N., Neu, C., et al. (2005). *Arabidopsis* SENESCENCE-ASSOCIATED GENE101 stabilizes and signals within an ENHANCED DISEASE SUSCEPTIBILITY1 complex in plant innate immunity. *Plant Cell* 17, 2601–2613. doi: 10.1105/tpc.105.033910

Fujiki, Y., Yoshimoto, K., and Ohsumi, Y. (2007). An *Arabidopsis* homolog of yeast ATG6/VPS30 is essential for pollen germination. *Plant Physiol.* 143, 1132–1139. doi: 10.1104/pp.106.093864

Fujisaki, K., Abe, Y., Ito, A., Saitoh, H., Yoshida, K., Kanzaki, H., et al. (2015). Rice Exo70 interacts with a fungal effector, AVR-Pii, and is required for AVR-Pii-triggered immunity. *Plant J.* 83, 875–887. doi: 10.1111/tpj.12934

Gao, M., Wang, X., Wang, D., Xu, F., Ding, X., Zhang, Z., et al. (2009). Regulation of cell death and innate immunity by two receptor-like kinases in *Arabidopsis*. *Cell Host Microbe* 6, 34–44. doi: 10.1016/j.chom.2009.05.019

Gomez-Gomez, L., and Boller, T. (2000). FLS2: an LRR receptor-like kinase involved in the perception of the bacterial elicitor flagellin in *Arabidopsis*. *Mol. Cell* 5, 1003–1011. doi: 10.1016/S1097-2765(00)80265-8

Gou, M., and Hua, J. (2012). Complex regulation of an R gene SNC1 revealed by auto-immune mutants. *Plant Signal. Behav.* 7, 213–216. doi: 10.4161/psb.18884

Gou, M., Shi, Z., Zhu, Y., Bao, Z., Wang, G., and Hua, J. (2012). The F-box protein CPR1/CPR30 negatively regulates R protein SNC1 accumulation. *Plant J.* 69, 411–420. doi: 10.1111/j.1365-313X.2011.04799.x

Grant, J. J., Chini, A., Basu, D., and Loake, G. J. (2003). Targeted activation tagging of the *Arabidopsis* NBS-LRR gene, ADR1, conveys resistance to virulent pathogens. *Mol. Plant Microbe Interact.* 16, 669–680. doi: 10.1094/MPMI.2003.16.8.669

Hanaoka, H., Noda, T., Shirano, Y., Kato, T., Hayashi, H., Shibata, D., et al. (2002). Leaf senescence and starvation-induced chlorosis are accelerated by the disruption of an *Arabidopsis* autophagy gene. *Plant Physiol.* 129, 1181–1193. doi: 10.1104/pp.011024

He, Y., and Gan, S. (2002). A gene encoding an acyl hydrolase is involved in leaf senescence in *Arabidopsis*. *Plant Cell* 14, 805–815. doi: 10.1105/tpc.010422

Hofius, D., Schultz-Larsen, T., Joensen, J., Tsitsigiannis, D. I., Petersen, N. H., Mattsson, O., et al. (2009). Autophagic components contribute to hypersensitive cell death in *Arabidopsis*. *Cell* 137, 773–783. doi: 10.1016/j.cell.2009.02.036

Hua, J., Grisafi, P., Cheng, S. H., and Fink, G. R. (2001). Plant growth homeostasis is controlled by the *Arabidopsis* BON1 and BAP1 genes. *Genes Dev.* 15, 2263–2272. doi: 10.1101/gad.918101

Huang, X., Li, J., Bao, F., Zhang, X., and Yang, S. (2010). A gain-of-function mutation in the *Arabidopsis* disease resistance gene RPP4 confers sensitivity to low temperature. *Plant Physiol.* 154, 796–809. doi: 10.1104/pp.110.157610

Jacob, F., Vernaldi, S., and Maekawa, T. (2013). Evolution and conservation of plant NLR functions. *Front. Immunol.* 4:297. doi: 10.3389/fimmu.2013.00297

Janda, M., and Ruelland, E. (2014). Magical mystery tour: salicylic acid signaling. *Environ. Exp. Bot.* 114, 117–128. doi: 10.1016/j.envexpbot.2014.07.003

Jirage, D., Tootle, T. L., Reuber, T. L., Frost, L. N., Feys, B. J., Parker, J. E., et al. (1999). *Arabidopsis thaliana* PAD4 encodes a lipase-like gene that is important for salicylic acid signaling. *Proc. Natl. Acad. Sci. U.S.A.* 96, 13583–13588. doi: 10.1073/pnas.96.23.13583

Jones, J. D., and Dangl, J. L. (2006). The plant immune system. *Nature* 444, 323–329. doi: 10.1038/nature05286

Kato, H., Saito, T., Ito, H., Komeda, Y., and Kato, A. (2014). Overexpression of the TIR-X gene results in a dwarf phenotype and activation of defense-related gene expression in *Arabidopsis thaliana*. *J. Plant Physiol.* 171, 382–388. doi: 10.1016/j.jplph.2013.12.002

Ketelaar, T., Voss, C., Dimmock, S. A., Thumm, M., and Hussey, P. J. (2004). *Arabidopsis* homologues of the autophagy protein Atg8 are a novel family of microtubule binding proteins. *FEBS Lett.* 567, 302–306. doi: 10.1016/j.febslet.2004.04.088

Kim, H. S., Desveaux, D., Singer, A. U., Patel, P., Sondek, J., and Dangl, J. L. (2005). The *Pseudomonas syringae* effector AvrRpt2 cleaves its C-terminally acylated target, RIN4, from *Arabidopsis* membranes to block RPM1 activation. *Proc. Natl. Acad. Sci. U.S.A.* 102, 6496–6501. doi: 10.1073/pnas.0500792102

Kim, S. H., Gao, F., Bhattacharjee, S., Adiasor, J. A., Nam, J. C., and Gassmann, W. (2010). The *Arabidopsis* resistance-like gene SNC1 is activated by mutations in SRFR1 and contributes to resistance to the bacterial effector AvrRps4. *PLoS Pathog.* 6:e1001172. doi: 10.1371/journal.ppat.1001172

Kliebenstein, D. J., Dietrich, R. A., Martin, A. C., Last, R. L., and Dangl, J. L. (1999). LSD1 regulates salicylic acid induction of copper zinc superoxide

dismutase in *Arabidopsis thaliana*. *Mol. Plant Microbe Interact.* 12, 1022–1026. doi: 10.1094/MPMI.1999.12.11.1022

Kong, Q., Qu, N., Gao, M., Zhang, Z., Ding, X., Yang, F., et al. (2012). The MEKK1-MKK1/MKK2-MPK4 kinase cascade negatively regulates immunity mediated by a mitogen-activated protein kinase kinase kinase in *Arabidopsis*. *Plant Cell* 24, 2225–2236. doi: 10.1105/tpc.112.097253

Kreibich, S., Emmenlauer, M., Fredlund, J., Ramo, P., Munz, C., Dehio, C., et al. (2015). Autophagy proteins promote repair of endosomal membranes damaged by the *Salmonella* type three secretion system 1. *Cell Host Microbe* 18, 527–537. doi: 10.1016/j.chom.2015.10.015

Kulich, I., Pecenkova, T., Sekeres, J., Smetana, O., Fendrych, M., Foissner, I., et al. (2013). *Arabidopsis* exocyst subcomplex containing subunit EXO70B1 is involved in autophagy-related transport to the vacuole. *Traffic* 14, 1155–1165. doi: 10.1111/tra.12101

Kulich, I., and Zarsky, V. (2014). Autophagy-related direct membrane import from ER/cytoplasm into the vacuole or apoplast: a hidden gateway also for secondary metabolites and phytohormones? *Int. J. Mol. Sci.* 15, 7462–7474. doi: 10.3390/ijms15057462

Levine, B., and Klionsky, D. J. (2004). Development by self-digestion: molecular mechanisms and biological functions of autophagy. *Dev. Cell* 6, 463–477. doi: 10.1016/S1534-5807(04)00099-1

Li, F., and Vierstra, R. D. (2012). Regulator and substrate: dual roles for the ATG1-ATG13 kinase complex during autophagic recycling in *Arabidopsis*. *Autophagy* 8, 982–984. doi: 10.4161/auto.20240

Li, J., Wen, J., Lease, K. A., Doke, J. T., Tax, F. E., and Walker, J. C. (2002). BAK1, an *Arabidopsis* LRR receptor-like protein kinase, interacts with BRI1 and modulates brassinosteroid signaling. *Cell* 110, 213–222. doi: 10.1016/S0092-8674(02)00812-7

Li, Y., Pennington, B. O., and Hua, J. (2009). Multiple R-like genes are negatively regulated by BON1 and BON3 in *Arabidopsis*. *Mol. Plant Microbe Interact.* 22, 840–848. doi: 10.1094/MPMI-22-7-0840

Li, Y., Tessaro, M. J., Li, X., and Zhang, Y. (2010). Regulation of the expression of plant resistance gene SNC1 by a protein with a conserved BAT2 domain. *Plant Physiol.* 153, 1425–1434. doi: 10.1104/pp.110.156240

Liu, J., Liu, X., Dai, L., and Wang, G. (2007). Recent progress in elucidating the structure, function and evolution of disease resistance genes in plants. *J. Genet. Genomics* 34, 765–776. doi: 10.1016/S1673-8527(07)60087-3

Liu, Y., Schiff, M., Czymmek, K., Talloczy, Z., Levine, B., and Dinesh-Kumar, S. P. (2005). Autophagy regulates programmed cell death during the plant innate immune response. *Cell* 121, 567–577. doi: 10.1016/j.cell.2005.03.007

Lorrain, S., Vailleau, F., Balague, C., and Roby, D. (2003). Lesion mimic mutants: keys for deciphering cell death and defense pathways in plants? *Trends Plant Sci.* 8, 263–271. doi: 10.1016/S1360-1385(03)00108-0

Mackey, D., Belkhadir, Y., Alonso, J. M., Ecker, J. R., and Dangl, J. L. (2003). *Arabidopsis* RIN4 is a target of the type III virulence effector AvrRpt2 and modulates RPS2-mediated resistance. *Cell* 112, 379–389. doi: 10.1016/S0092-8674(03)00040-0

Mackey, D., Holt, B. F. III, Wiig, A., and Dangl, J. L. (2002). RIN4 interacts with *Pseudomonas syringae* type III effector molecules and is required for RPM1-mediated resistance in *Arabidopsis*. *Cell* 108, 743–754. doi: 10.1016/S0092-8674(02)00661-X

Martin, G. B. (1999). Functional analysis of plant disease resistance genes and their downstream effectors. *Curr. Opin. Plant Biol.* 2, 273–279. doi: 10.1016/S1369-5266(99)80049-1

McDowell, J. M., and Woffenden, B. J. (2003). Plant disease resistance genes: recent insights and potential applications. *Trends Biotechnol.* 21, 178–183. doi: 10.1016/S0167-7799(03)00053-2

Meyers, B. C., Kozik, A., Griego, A., Kuang, H., and Michelmore, R. W. (2003). Genome-wide analysis of NBS-LRR-encoding genes in *Arabidopsis*. *Plant Cell* 15, 809–834. doi: 10.1105/tpc.009308

Minina, E. A., Bozhkov, P. V., and Hofius, D. (2014). Autophagy as initiator or executioner of cell death. *Trends Plant Sci.* 19, 692–697. doi: 10.1016/j.tplants.2014.07.007

Moreau, K., and Rubinsztein, D. C. (2012). The plasma membrane as a control center for autophagy. *Autophagy* 8, 861–863. doi: 10.4161/auto.20060

Mukhtar, M. S., Carvunis, A. R., Dreze, M., Epple, P., Steinbrenner, J., Moore, J., et al. (2011). Independently evolved virulence effectors converge onto hubs in a plant immune system network. *Science* 333, 596–601. doi: 10.1126/science.1203659

Munch, D., Teh, O. K., Malinovsky, F. G., Liu, Q., Vetukuri, R. R., El Kasmi, F., et al. (2015). Retromer contributes to immunity-associated cell death in *Arabidopsis*. *Plant Cell* 27, 463–479. doi: 10.1105/tpc.114.132043

Nandety, R. S., Caplan, J. L., Cavanaugh, K., Perroud, B., Wroblewski, T., Michelmore, R. W., et al. (2013). The role of TIR-NBS and TIR-X proteins in plant basal defense responses. *Plant Physiol.* 162, 1459–1472. doi: 10.1104/pp.113.219162

Nawrath, C., and Metraux, J. P. (1999). Salicylic acid induction-deficient mutants of *Arabidopsis* express PR-2 and PR-5 and accumulate high levels of camalexin after pathogen inoculation. *Plant Cell* 11, 1393–1404. doi: 10.2307/3870970

Noutoshi, Y., Ito, T., Seki, M., Nakashita, H., Yoshida, S., Marco, Y., et al. (2005). A single amino acid insertion in the WRKY domain of the *Arabidopsis* TIR-NBS-LRR-WRKY-type disease resistance protein SLH1 (sensitive to low humidity 1) causes activation of defense responses and hypersensitive cell death. *Plant J.* 43, 873–888. doi: 10.1111/j.1365-313X.2005.02500.x

Ohtomo, I., Ueda, H., Shimada, T., Nishiyama, C., Komoto, Y., Hara-Nishimura, I., et al. (2005). Identification of an allele of VAM3/SYP22 that confers a semi-dwarf phenotype in *Arabidopsis thaliana*. *Plant Cell Physiol.* 46, 1358–1365. doi: 10.1093/pcp/pci146

Palma, K., Thorgrimsen, S., Malinovsky, F. G., Fiil, B. K., Nielsen, H. B., Brodersen, P., et al. (2010). Autoimmunity in *Arabidopsis* acd11 is mediated by epigenetic regulation of an immune receptor. *PLoS Pathog.* 6:e1001137. doi: 10.1371/journal.ppat.1001137

Patel, S., and Dinesh-Kumar, S. P. (2008). *Arabidopsis* ATG6 is required to limit the pathogen-associated cell death response. *Autophagy* 4, 20–27. doi: 10.4161/auto.5056

Petersen, M., Brodersen, P., Naested, H., Andreasson, E., Lindhart, U., Johansen, B., et al. (2000). *Arabidopsis* map kinase 4 negatively regulates systemic acquired resistance. *Cell* 103, 1111–1120. doi: 10.1016/S0092-8674(00)00213-0

Pontier, D., Balague, C., and Roby, D. (1998). The hypersensitive response. A programmed cell death associated with plant resistance. *C. R. Acad. Sci. III* 321, 721–734. doi: 10.1016/S0764-4469(98)80013-9

Qi, Y., Tsuda, K., Glazebrook, J., and Katagiri, F. (2011). Physical association of pattern-triggered immunity (PTI) and effector-triggered immunity (ETI) immune receptors in *Arabidopsis*. *Mol. Plant Pathol.* 12, 702–708. doi: 10.1111/j.1364-3703.2010.00704.x

Qiu, J. L., Zhou, L., Yun, B. W., Nielsen, H. B., Fiil, B. K., Petersen, K., et al. (2008). *Arabidopsis* mitogen-activated protein kinase kinases MKK1 and MKK2 have overlapping functions in defense signaling mediated by MEKK1, MPK4, and MKS1. *Plant Physiol.* 148, 212–222. doi: 10.1104/pp.108.120006

Reggiori, F., and Klionsky, D. J. (2013). Autophagic processes in yeast: mechanism, machinery and regulation. *Genetics* 194, 341–361. doi: 10.1534/genetics.112.149013

Roberts, M., Tang, S., Stallmann, A., Dangl, J. L., and Bonardi, V. (2013). Genetic requirements for signaling from an autoactive plant NB-LRR intracellular innate immune receptor. *PLoS Genet.* 9:e1003465. doi: 10.1371/journal.pgen.1003465

Rogers, E. E., and Ausubel, F. M. (1997). *Arabidopsis* enhanced disease susceptibility mutants exhibit enhanced susceptibility to several bacterial pathogens and alterations in PR-1 gene expression. *Plant Cell* 9, 305–316. doi: 10.1105/tpc.9.3.305

Sasek, V., Janda, M., Delage, E., Puyaubert, J., Guivarc'h, A., Lopez Maseda, E., et al. (2014). Constitutive salicylic acid accumulation in pi4kIIIbeta1beta2 *Arabidopsis* plants stunts rosette but not root growth. *New Phytol.* 203, 805–816. doi: 10.1111/nph.12822

Sekine, K. T., Nandi, A., Ishihara, T., Hase, S., Ikegami, M., Shah, J., et al. (2004). Enhanced resistance to *Cucumber mosaic* virus in the *Arabidopsis thaliana* ssi2 mutant is mediated via an SA-independent mechanism. *Mol. Plant Microbe Interact.* 17, 623–632. doi: 10.1094/MPMI.2004.17.6.623

Shirano, Y., Kachroo, P., Shah, J., and Klessig, D. F. (2002). A gain-of-function mutation in an *Arabidopsis* Toll Interleukin1 receptor-nucleotide binding site-leucine-rich repeat type R gene triggers defense responses and results in enhanced disease resistance. *Plant Cell* 14, 3149–3162. doi: 10.1105/tpc.005348

Spoel, S. H., and Dong, X. (2012). How do plants achieve immunity? Defence without specialized immune cells. *Nat. Rev. Immunol.* 12, 89–100. doi: 10.1038/nri3141

Stark, C., Breitkreutz, B. J., Reguly, T., Boucher, L., Breitkreutz, A., and Tyers, M. (2006). BioGRID: a general repository for interaction datasets. *Nucleic Acids Res.* 34, D535–D539. doi: 10.1093/nar/gkj109

Stegmann, M., Anderson, R. G., Westphal, L., Rosahl, S., McDowell, J. M., and Trujillo, M. (2013). The exocyst subunit Exo70B1 is involved in the immune response of *Arabidopsis thaliana* to different pathogens and cell death. *Plant Signal. Behav.* 8, e27421. doi: 10.4161/psb.27421

Synek, L., Schlager, N., Elias, M., Quentin, M., Hauser, M. T., and Zarsky, V. (2006). AtEXO70A1, a member of a family of putative exocyst subunits specifically expanded in land plants, is important for polar growth and plant development. *Plant J.* 48, 54–72. doi: 10.1111/j.1365-313X.2006.02854.x

Takemoto, D., and Jones, D. A. (2005). Membrane release and destabilization of *Arabidopsis* RIN4 following cleavage by *Pseudomonas syringae* AvrRpt2. *Mol. Plant Microbe Interact.* 18, 1258–1268. doi: 10.1094/MPMI-18-1258

Teh, O. K., and Hofius, D. (2014). Membrane trafficking and autophagy in pathogen-triggered cell death and immunity. *J. Exp. Bot.* 65, 1297–1312. doi: 10.1093/jxb/ert441

Thompson, A. R., Doelling, J. H., Suttangkakul, A., and Vierstra, R. D. (2005). Autophagic nutrient recycling in *Arabidopsis* directed by the ATG8 and ATG12 conjugation pathways. *Plant Physiol.* 138, 2097–2110. doi: 10.1104/pp.105.060673

Tomsig, J. L., and Creutz, C. E. (2002). Copines: a ubiquitous family of Ca(2+)-dependent phospholipid-binding proteins. *Cell. Mol. Life Sci.* 59, 1467–1477. doi: 10.1007/s00018-002-8522-7

Trujillo, M., Ichimura, K., Casais, C., and Shirasu, K. (2008). Negative regulation of PAMP-triggered immunity by an E3 ubiquitin ligase triplet in *Arabidopsis*. *Curr. Biol.* 18, 1396–1401. doi: 10.1016/j.cub.2008.07.085

Tzfadia, O., and Galili, G. (2013). The *Arabidopsis* exocyst subcomplex subunits involved in a golgi-independent transport into the vacuole possess consensus autophagy-associated atg8 interacting motifs. *Plant Signal. Behav.* 8, e26732-1–e26732-3. doi: 10.4161/psb.26732

Vlot, A. C., Liu, P. P., Cameron, R. K., Park, S. W., Yang, Y., Kumar, D., et al. (2008). Identification of likely orthologs of tobacco salicylic acid-binding protein 2 and their role in systemic acquired resistance in *Arabidopsis thaliana*. *Plant J.* 56, 445–456. doi: 10.1111/j.1365-313X.2008.03618.x

Vogelmann, K., Drechsel, G., Bergler, J., Subert, C., Philippar, K., Soll, J., et al. (2012). Early senescence and cell death in *Arabidopsis* saul1 mutants involves the PAD4-dependent salicylic acid pathway. *Plant Physiol.* 159, 1477–1487. doi: 10.1104/pp.112.196220

Wagner, S., Stuttmann, J., Rietz, S., Guerois, R., Brunstein, E., Bautor, J., et al. (2013). Structural basis for signaling by exclusive EDS1 heteromeric complexes with SAG101 or PAD4 in plant innate immunity. *Cell Host Microbe* 14, 619–630. doi: 10.1016/j.chom.2013.11.006

Wang, Y., Nishimura, M. T., Zhao, T., and Tang, D. (2011). ATG2, an autophagy-related protein, negatively affects powdery mildew resistance and mildew-induced cell death in *Arabidopsis*. *Plant J.* 68, 74–87. doi: 10.1111/j.1365-313X.2011.04669.x

Yang, H., Shi, Y., Liu, J., Guo, L., Zhang, X., and Yang, S. (2010). A mutant CHS3 protein with TIR-NB-LRR-LIM domains modulates growth, cell death and freezing tolerance in a temperature-dependent manner in *Arabidopsis*. *Plant J.* 63, 283–296. doi: 10.1111/j.1365-313X.2010.04241.x

Yang, S., and Hua, J. (2004). A haplotype-specific Resistance gene regulated by BONZAI1 mediates temperature-dependent growth control in *Arabidopsis*. *Plant Cell* 16, 1060–1071. doi: 10.1105/tpc.020479

Yang, S., Yang, H., Grisafi, P., Sanchatjate, S., Fink, G. R., Sun, Q., et al. (2006). The BON/CPN gene family represses cell death and promotes cell growth in *Arabidopsis*. *Plant J.* 45, 166–179. doi: 10.1111/j.1365-313X.2005.02585.x

Yoshimoto, K., Hanaoka, H., Sato, S., Kato, T., Tabata, S., Noda, T., et al. (2004). Processing of ATG8s, ubiquitin-like proteins, and their deconjugation by ATG4s are essential for plant autophagy. *Plant Cell* 16, 2967–2983. doi: 10.1105/tpc.104.025395

Yoshimoto, K., Jikumaru, Y., Kamiya, Y., Kusano, M., Consonni, C., Panstruga, R., et al. (2009). Autophagy negatively regulates cell death by controlling NPR1-dependent salicylic acid signaling during senescence and the innate immune response in *Arabidopsis*. *Plant Cell* 21, 2914–2927. doi: 10.1105/tpc.109.068635

Yu, G. L., Katagiri, F., and Ausubel, F. M. (1993). *Arabidopsis* mutations at the RPS2 locus result in loss of resistance to *Pseudomonas syringae* strains expressing the avirulence gene avrRpt2. *Mol. Plant Microbe Interact.* 6, 434–443. doi: 10.1094/MPMI-6-434

Yu, I. C., Parker, J., and Bent, A. F. (1998). Gene-for-gene disease resistance without the hypersensitive response in *Arabidopsis* dnd1 mutant. *Proc. Natl. Acad. Sci. U.S.A.* 95, 7819–7824. doi: 10.1073/pnas.95.13.7819

Zhang, Y., Goritschnig, S., Dong, X., and Li, X. (2003). A gain-of-function mutation in a plant disease resistance gene leads to constitutive activation of downstream signal transduction pathways in suppressor of npr1-1, constitutive 1. *Plant Cell* 15, 2636–2646. doi: 10.1105/tpc.015842

Zhang, Z., Lenk, A., Andersson, M. X., Gjetting, T., Pedersen, C., Nielsen, M. E., et al. (2008). A lesion-mimic syntaxin double mutant in *Arabidopsis* reveals novel complexity of pathogen defense signaling. *Mol. Plant* 1, 510–527. doi: 10.1093/mp/ssn011

Zhang, Z., Wu, Y., Gao, M., Zhang, J., Kong, Q., Liu, Y., et al. (2012). Disruption of PAMP-induced MAP kinase cascade by a *Pseudomonas syringae* effector activates plant immunity mediated by the NB-LRR protein SUMM2. *Cell Host Microbe* 11, 253–263. doi: 10.1016/j.chom.2012.01.015

Zhao, T., Rui, L., Li, J., Nishimura, M. T., Vogel, J. P., Liu, N., et al. (2015). A truncated NLR protein, TIR-NBS2, is required for activated defense responses in the exo70B1 mutant. *PLoS Genet.* 11:e1004945. doi: 10.1371/journal.pgen.1004945

Zhou, F., Menke, F. L., Yoshioka, K., Moder, W., Shirano, Y., and Klessig, D. F. (2004). High humidity suppresses ssi4-mediated cell death and disease resistance upstream of MAP kinase activation, H2O2 production and defense gene expression. *Plant J.* 39, 920–932. doi: 10.1111/j.1365-313X.2004.02180.x

Zhou, J., Yu, J. Q., and Chen, Z. (2014). The perplexing role of autophagy in plant innate immune responses. *Mol. Plant Pathol.* 15, 637–645. doi: 10.1111/mpp.12118

Conflict of Interest Statement: The authors declare that the research was conducted in the absence of any commercial or financial relationships that could be construed as a potential conflict of interest.

The reviewer TOB and handling Editor declared their shared affiliation, and the handling Editor states that the process nevertheless met the standards of a fair and objective review

3.2. PAPER No. 2

Title: Early Arabidopsis root hair growth stimulation by pathogenic strains of *Pseudomonas syringae*

Authors: Tamara Pečenková, Martin Janda, Jitka Ortmannová, Vladimíra Hajná, Zuzana Stehlíková and Viktor Žárský

Summary:

Background and Aims Selected beneficial Pseudomonas spp. strains have the ability to influence root architecture in *Arabidopsis thaliana* by inhibiting primary root elongation and promoting lateral root and root hair formation. A crucial role for auxin in this long-term (1week), long-distance plant-microbe interaction has been demonstrated.

Methods *Arabidopsis* seedlings were cultivated in vitro on vertical plates and inoculated with pathogenic strains *Pseudomonas syringae pv. maculicola* (*Psm*) and *P. syringae pv. tomato* DC3000 (*Pst*), as well as *Agrobacterium tumefaciens* (*Atu*) and *Escherichia coli* (*Eco*). Root hair lengths were measured after 24 and 48h of direct exposure to each bacterial strain. Several *Arabidopsis* mutants with impaired responses to pathogens, impaired ethylene perception and defects in the exocyst vesicle tethering complex that is involved in secretion were also analysed.

Key Results *Arabidopsis* seedling roots infected with *Psm* or *Pst* responded similarly to when infected with plant growth-promoting rhizobacteria; root hair growth was stimulated and primary root growth was inhibited. Another plant- and soil-adapted bacteria induced similar root hair responses. The most compromised root hair growth stimulation response was found for the knockout mutants *exo70A1* and *ein2*. The single immune pathways dependent on salicylic acid, jasmonic acid and PAD4 are not directly involved in root hair growth stimulation; however, in the mutual cross-talk with ethylene, they indirectly modify the extent of the stimulation of root hair growth. The Flg22 peptide does not initiate root hair stimulation as intact bacteria do, but pretreatment with Flg22 prior to *Psm* inoculation abolished root hair growth stimulation in an FLS2 receptor kinase-dependent manner. These early response phenomena are not associated with changes in auxin levels, as monitored with the pDR5::GUS auxin reporter.

Conclusions Early stimulation of root hair growth is an effect of an unidentified component of living plant pathogenic bacteria. The root hair growth response is triggered in the range of hours after bacterial contact with roots and can be modulated by FLS2 signalling. Bacterial

stimulation of root hair growth requires functional ethylene signalling and an efficient exocyst-dependent secretory machinery.

My contribution: I performed part of the original experiments with the *Psm* inoculation and root hair and main root lengths measurement. I helped with the subsequent evaluation and analysis of experimental results and participated in the final text work and graphical scheme creation.

Annals of Botany Page 1 of 10
doi:10.1093/aob/mcx073, available online at https://academic.oup.com/aob

ANNALS OF BOTANY
Founded 1887

Early *Arabidopsis* root hair growth stimulation by pathogenic strains of *Pseudomonas syringae*

Tamara Pečenková[1,2]*†, Martin Janda[3,5†], Jitka Ortmannová[1,2], Vladimíra Hajná[4,5], Zuzana Stehlíková[3,5] and Viktor Žárský[1,2]

[1]Laboratory of Cell Biology, Institute of Experimental Botany, Czech Academy of Sciences, Rozvojova 263, 165 02, Prague 6, Czech Republic, [2]Laboratory of Cell Morphogenesis, Department of Experimental Plant Biology, Faculty of Science, Charles University in Prague, Vinicna 5, 128 44 Prague 2, Czech Republic, [3]Laboratory of Pathological Plant Physiology, [4]Laboratory of Signal Transduction, Institute of Experimental Botany, Czech Academy of Sciences, Rozvojova 263, 165 02 Prague 6, Czech Republic, [5]Laboratory of Plant Biochemistry, Department of Biochemistry and Microbiology, University of Chemistry and Technology Prague, Technicka 5, 166 28 Prague 6, Czech Republic
**For correspondence. E-mail pecenkova@ueb.cas.cz*
[†]These authors contributed equally.

Received: 9 November 2016 Returned for revision: 20 April 2017 Editorial decision: 25 April 2017 Accepted: 16 May 2017

• **Background and Aims** Selected beneficial *Pseudomonas* spp. strains have the ability to influence root architecture in *Arabidopsis thaliana* by inhibiting primary root elongation and promoting lateral root and root hair formation. A crucial role for auxin in this long-term (1 week), long-distance plant–microbe interaction has been demonstrated.
• **Methods** *Arabidopsis* seedlings were cultivated *in vitro* on vertical plates and inoculated with pathogenic strains *Pseudomonas syringae* pv. *maculicola* (Psm) and *P. syringae* pv. *tomato DC3000* (Pst), as well as *Agrobacterium tumefaciens* (Atu) and *Escherichia coli* (Eco). Root hair lengths were measured after 24 and 48 h of direct exposure to each bacterial strain. Several *Arabidopsis* mutants with impaired responses to pathogens, impaired ethylene perception and defects in the exocyst vesicle tethering complex that is involved in secretion were also analysed.
• **Key Results** Arabidopsis seedling roots infected with Psm or Pst responded similarly to when infected with plant growth-promoting rhizobacteria; root hair growth was stimulated and primary root growth was inhibited. Other plant- and soil-adapted bacteria induced similar root hair responses. The most compromised root hair growth stimulation response was found for the knockout mutants *exo70A1* and *ein2*. The single immune pathways dependent on salicylic acid, jasmonic acid and PAD4 are not directly involved in root hair growth stimulation; however, in the mutual cross-talk with ethylene, they indirectly modify the extent of the stimulation of root hair growth. The Flg22 peptide does not initiate root hair stimulation as intact bacteria do, but pretreatment with Flg22 prior to Psm inoculation abolished root hair growth stimulation in an FLS2 receptor kinase-dependent manner. These early response phenomena are not associated with changes in auxin levels, as monitored with the pDR5::GUS auxin reporter.
• **Conclusions** Early stimulation of root hair growth is an effect of an unidentified component of living plant pathogenic bacteria. The root hair growth response is triggered in the range of hours after bacterial contact with roots and can be modulated by FLS2 signalling. Bacterial stimulation of root hair growth requires functional ethylene signalling and an efficient exocyst-dependent secretory machinery.

Key words: Root hair, *Arabidopsis*, *Pseudomonas*, exocyst, Flg22, vesicle trafficking, *dde2*/*ein2*/*pad4*/*sid2*.

INTRODUCTION

Plants are in contact during their life cycle with both beneficial and harmful bacteria. It is thus of key importance for a plant to distinguish between such bacteria and react accordingly. Some beneficial bacteria, so-called plant growth-promoting rhizobacteria (PGPR), may stimulate plant growth (Kremer *et al*., 1990; Lugtenberg and Kamilova, 2009). Recently, the ability of selected beneficial *Pseudomonas* spp. strains to influence root architecture in *Arabidopsis thaliana* by inhibiting primary root elongation and promoting lateral root and root hair formation was reported, with the role of auxin in this long-term (1 week) and long-distance interaction clearly demonstrated (Rudrappa and Bais, 2008; Zamioudis *et al*., 2013). In addition, auxin-independent root architecture modifications caused by bacteria have been found, with bacterial quorum-sensing signalling N-acyl-homoserine lactones (AHLs) found to affect primary root growth, lateral root formation and root hair development (Ortíz-Castro *et al*., 2008).

Evidence that plants initially respond similarly to both PGPR and pathogenic bacteria has emerged in recent years (van Loon *et al*., 2008; reviewed by Zamioudis and Pieterse, 2012). In agreement with this, one of the most studied pathogen/microbe associated molecular patterns (P/MAMPs), the conserved peptide Flg22 derived originally from *Pseudomonas aeruginosa* flagellar protein, has also been shown to induce inhibition of primary root growth just as observed with PGPRs (Gómez-Gómez *et al*., 1999; Millet *et al*., 2010). Flg22 is recognized by the plant cell via the plant pathogen recognition receptor kinase FLS2 (FLAGELLIN SENSITIVE 2) and the co-receptor BAK1

(BRI1-ASSOCIATED KINASE 1). The activated FLS2 switches on a signalling cascade leading to activation of the transcription of defence genes and production of reactive-oxygen species (ROS) and salicylic acid (SA) which also function as signalling molecules (Chinchilla *et al.*, 2007; Beck *et al.*, 2012). SA is involved in the plant immune response alongside jasmonic acid (JA), ethylene (ET) and the protein PHYTOALEXIN DEFICIENT 4 (PAD4) (Tsuda *et al.*, 2009, Kim *et al.* 2014). The SA-dependent transcriptional activation relies on NPR1 (NONEXPRESSOR OF PATHOGENESIS-RELATED GENES 1), a transcriptional co-activator that is relocated from the cytoplasm to the nucleus (Kinkema *et al.*, 2000). One of the major outcomes of this gene activation is a modification of cell walls and the extracellular space. This is supported by efficient targeted secretion, which depends upon correct tethering and fusion of vesicles to the target plasma membrane. These processes are mediated, amongst others, by the exocyst and SNARE (soluble N-ethylmaleimide-sensitive fusion attachment protein receptors) protein complexes (Rothman and Warren, 1994; TerBush *et al.*, 1996; Dörmann *et al.*, 2014).

The exocyst, a secretory vesicle-tethering protein complex, was first discovered in yeast and animals, but in recent years it has also been found to function as a complex in plants (Guo *et al.*, 1999; Hsu *et al.*, 2004; Hála *et al.*, 2008; Zárský *et al.*, 2009, 2013; Kulich *et al.*, 2013). The *Arabidopsis exo70A1* mutant, as well as the maize *sec3* mutant (roothairless1 – *rth1*) fails to properly elongate root hairs (Wen *et al.*, 2005; Synek *et al.*, 2006). The exocyst has also been found to be important for efficient plant defence against several pathogens (Pečenková *et al.*, 2011; Stegmann *et al.*, 2012; Du *et al.*, 2015).

Whilst biotic interactions and plant defence reactions have been mostly studied in above-ground plant tissues, specific PAMP perception has also been identified in root tissues in *Arabidopsis* (Millet *et al.*, 2010). When the transcriptional activation of reporter genes and callose deposition were monitored in roots after treatment with different PAMPs, including Flg22, strong tissue-specific upregulation of defence-related responses was triggered (Millet *et al.*, 2010). These responses were ET- but not SA- or JA-signalling dependent. The sensitivity of roots to Flg22 may be explained by the fact that Flg22, as well as other elicitors, are derived from highly conserved bacterial components that are present in both phylosphere and soil.

The function and morphology of root hairs in relation to the acquisition of water and nutrients have been well studied. Tanaka *et al.* (2014) demonstrated that root hairs play significant roles in: the absorption of water, phosphorus, iron, calcium, zinc, copper and potassium; in the secretion of acid phosphatase, malate and citrate; and in penetration of the primary roots into gels. Root hairs have been found to be induced and their lengths more elongated under different nutrient deficiencies (phosphorus, potassium, magnesium, iron and manganese) (Bates and Lynch, 1996; Schikora and Schmidt, 2001; Yang *et al.*, 2008; Jung *et al.*, 2009; Niu *et al.*, 2014). Although the role of root hairs in interactions with nitrogen-fixing bacteria has been investigated, little attention has been given to their role during plant–pathogen interactions.

This study of the response of *Arabidopsis* seedlings to the attack by the pathogenic bacteria *Pseudomonas syringae* pv. *maculicola* (Psm) and *Pseudomonas syringae* pv. *tomato DC3000* (Pst) revealed, in *in vitro* cultivated seedlings, primary root growth inhibition together with stimulation of rapid root hair growth. A detailed investigation of this observed behaviour was conducted by examining plant responses and the activity of an auxin-responsive promoter. Several *Arabidopsis* mutants were employed, comprising exocyst mutants, and a whole set of *dde2/ein2/pad4/sid2* single to quadruple mutants. We show that the stimulation of root hair growth is triggered in a range of hours after contact of bacteria with roots, is dependent on unknown component(s) of living bacteria other than those described so far, and that the stimulation can be modified by FLS2 signalling. We also show that correct functioning of the EIN2 ET signal transducer and the exocyst complex play important roles in this stimulation of root hair growth. This appears to be in contrast to SA/JA/PAD4. Although in mutual cross-talk these pathways indirectly modify the outcome, independently they do not influence this plant response.

MATERIAL AND METHODS

Plant material

The *A. thaliana* T-DNA insertional mutant lines that were used in this study comprised: N8844 (At5g03280, *ein2*), SALK_122399 (At3g25070), *npr1-1* [donated by Saskia van Wees (Utrecht University; Cao *et al.*, 1994)] and SALK_014826 (At5g03540, *exo70A1*) and set of the mutants connected with the quadruple mutant (*dde2-2/ein2-1/pad4-1/sid2-2*), triple mutants (*dde2-2/ein2-1/pad4-1*, *dde2-2/ein2-1/sid2-2*, *dde2-2/pad4-1/sid2-2* and *ein2-1/pad4-1/sid2-2*), double mutants (*dde2-2/ein2-1*, *dde2-2/pad4-1*, *dde2-2/sid2-2*, *ein2-1/pad4-1*, *ein2-1/sid2-2* and *pad4-1/sid2-2*) and single mutants (*dde2-2*, *ein2-1*, *pad4-1* and *sid2-2*) all donated by Dr Kenichi Tsuda (Max Planck Institute of Plant Breeding Research in Cologne; Tsuda *et al.*, 2009).

For experiments with Psm, seeds were surface sterilized and plated on half strength Murashige and Skoog medium (1/2 MS), 1·6 % plant agar. Germinated plants were propagated *in vitro* for 7 d on vertical plates. In addition, the GUS gene under the control of the DR5 promoter carrying line was used to check for changes in the expression of auxin-related genes (Ulmasov *et al.*, 1997). For experiments with Pst, seeds were surface sterilized and plated on 1/2 MS containing 1% sucrose (pH 5·7 adjusted with KOH) and 1·2 % plant agar. The plants were propagated *in vitro* for 4 d on Petri dishes (diameter 6 cm) vertically. The cultivation conditions were 16/8 h light/dark at 21–22 °C.

Inoculation of plant material with bacteria

For inoculation with *P. syringe* pv. *maculicola* strain 795 (Psm; Dong *et al.*, 1991), bacteria were prepared as described by Katagiri *et al.* (2002). Briefly, freshly inoculated plates (2–3 d old; Luria–Bertani medium with 25 mg L^{-1} streptomycin) were used to prepare liquid overnight culture (40 mL), without streptomycin, with incubation at 28 °C on an orbital shaker at 130 r.p.m. Bacteria were centrifuged at 1500 *g* for 10 min and the pellet was resuspended in dH_2O and diluted to an OD_{600} of 0·3 (10^8 CFU mL^{-1}). Approximately 10-µL droplets were

applied to cover root tips within the elongation and differentiation zone. As a mock control, dH_2O was applied in the same manner and, 48 h later, the root growth and architecture was inspected. Experiments with other bacteria, namely, Atu – *Agrobacterium tumefaciens* GV3101, Eco – *Escherichia coli* DH5a, Psp – *Pseudomonas savastanoi* pv. *phaseolicola* and Pst – *Pseudomonas syringae* pv. *tomato DC3000*, were performed as described for experiments with Psm.

For experiments involving inoculation with Pst (Xin and He, 2013), bacteria were incubated overnight on plates (King's B medium with 50 mg L^{-1} rifampicin) and inoculum removed from the plate and diluted to an OD_{600}= of 0·01 in MS/2 + 1 % sucrose (pH 5·7 adjusted with KOH). Seedlings were flooded with 3 mL of the bacterial solution and the plates were placed in horizontal position for 24 h.

Flg22 treatment

Flg22 is a 22-amino-acid peptide derived from *P. aeruginosa* flagellin, a structural protein that forms the major portion of flagellar filaments (QRLSTGSRINSAKDDAAGLQIA, synthesized by Vidia, Vestec, Czech Republic). The peptide was diluted in dH_2O to a final concentration 10 μM and applied in 10-μL drops to cover the root tips of approx. 1-week-old seedlings and then left for 48 h until evaluation. The peptide was applied at a concentration 10 times higher than usually employed for such treatments, given the potential diffusion of the peptide from the roots on the agar plate.

BFA treatment

For measurement of root hair lengths, the 4-d-old seedlings were flooded with a Pst solution containing 0·1% DMSO or 50 μM brefeldin A (BFA) for 24 h.

Histochemical GUS staining procedure

After the treatment (including a mock to serve as a control), whole seedlings were submerged for 3 h at 37 °C in a solution consisting of 25 mM sodium phosphate buffer (pH 7·0), 10 mM EDTA, 2 mM X-gluc, 0·5 mM ferricyanide and 0·5 mM ferrocyanide. The GUS staining solution was replaced with 70 % ethanol to bleach the tissues, and the seedlings roots were then examined.

Microscopic examination of inoculated roots

The plant responses to pathogens were monitored by microscopy and documented by photography. Microscopic analysis was performed using an Olympus BX51 microscope with attached DP50 camera (Olympus; Psm) or Zeiss AxioImager ApoTome2 microscope (Pst). In the Psm experiments, five plants were analysed for each genotype and photographed. Root hair lengths were determined for the first 20 root hairs starting from the root tip for each plant; for statistical analysis, the 40 longest root hairs for each line were used. In addition, root hairs were also observed under a confocal microscope (Zeiss LSM Duo510) 20 min after staining with the membrane dye FM 4-64. For the Pst experiments, at least 10 seedlings were analysed for each variant. After Pst inoculation, five root hairs were measured, beginning approx. 1 mm from the site of root hair initiation. The distance of the first root hairs from the root cap was also analysed.

Statistical evaluation

Image processing software was employed for image data quantification. Roots and root hair sizes were analysed using AnalySIS (Soft Imaging System GmbH, Germany) or ImageJ (Schneider *et al.*, 2012) software. The numerical data obtained were processed using Microsoft Excel. To determine statistical significance, Student's *t*-test and ANOVA tests were conducted either using Excel or on-line calculators (http://in-silico.net, and http://statpages.info/anova1sm.html). *P*-values of less than 0·05 indicated a significant difference among the various groups. For multiple-comparison experiments, the Tukey Honestly Significant Difference (HSD) *post hoc* test was used.

RESULTS

Early stimulation of root hair growth by bacteria in Arabidopsis *WT and selected mutants*

When roots of *Arabidopsis* seedlings were exposed to direct contact with the plant pathogenic bacterium Psm, a rapid modification of root architecture was observed. One unexpected but significant change involved root hair growth within 48 h of exposure to Psm. We quantified root hair growth using 1-week-old seedlings grown on vertical plates and inoculated either with mock (sterile deionized water) or with Psm. Psm-treated root hairs were approx. 3·3 times longer than those of mock-treated plants (Fig. 1A). As expected, we also found that primary root growth was inhibited; the ratio of Psm-treated to mock-treated average root lengths of wild type (WT) Col-0 was approx. 0·82. A small but significant difference in root hair density between Psm- and mock-treated plants was also observed, with average values, respectively, of 37±8 and 29±6 root hairs per 1 mm region closest to the root tip. The inhibition of root growth may be a consequence of the reduced length of the elongation/differentiation zone, while the size of the meristematic zone remained unchanged (Supplementary Data, Fig. S1).

Next we analysed these root growth responses to Psm using three types of mutants: a line carrying a mutation in the gene responsible for SA-dependent activation of pathogenesis-related genes (*npr1-1*); a well-studied mutant affected in ET perception, *ein2* (Guzmán and Ecker, 1990; Rahman *et al.*, 2002); and a line carrying a mutation in a gene encoding the exocyst vesicle-tethering complex, *exo70A1*. Both *ein2* and *exo70A1*, when cultivated under the described conditions without bacterial treatment, produce fewer and shorter root hairs than the wild type plant. In addition, along with Col-0, we also studied the Wassilewskija (Ws-4) ecotype, which is a natural mutant in the bacterial flagellin receptor FLS2 (with a STOP codon in the kinase domain; Gómez-Gómez *et al.*, 1999; Zipfel *et al.*, 2004).

Average root hair lengths differed significantly after 48 h of treatments (two to three times) between the mock- and bacteria-treated plants for all tested lines (Fig. 1B). As root hair

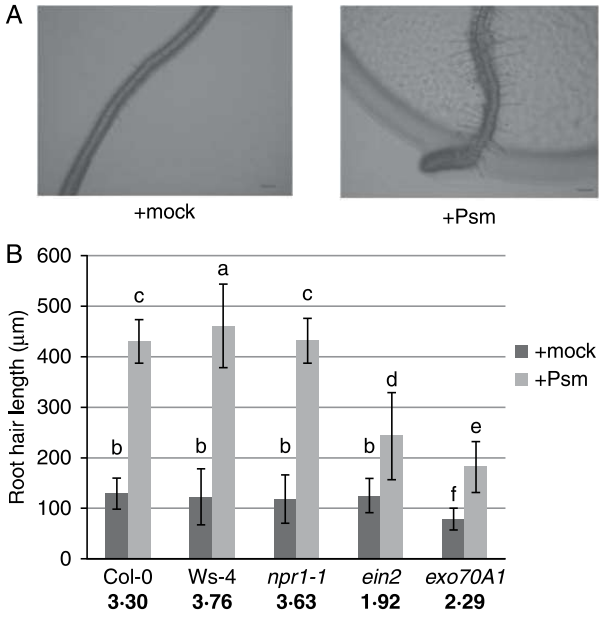

FIG. 1. Stimulation of root hair growth 48 h post-inoculation with Psm. (A) Appearance of root hairs after mock and Psm treatment (scale bar=200 µm). (B) Length of root hairs of mock- (dark grey) and Psm-treated (light grey) seedlings for different mutant lines. Ratios calculated for Psm vs. mock-treated seedlings are shown in bold for each mutant line under the respective columns in the graph. Different letters indicate significant differences in length ($P<0{\cdot}05$).

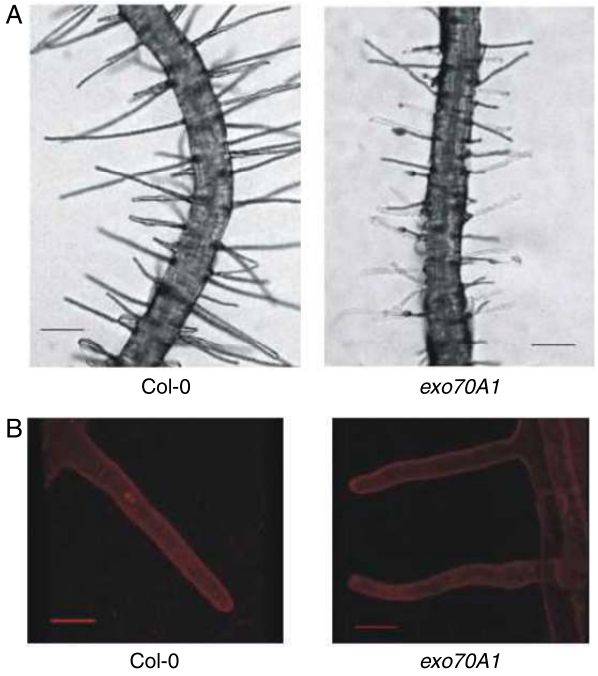

FIG. 2. Appearance of the *exo70A1* root hairs stimulated by Psm, in comparison with WT root hairs. (A) Optical microscopy (scale bar=200 µm). (B) Confocal images taken after staining of the plasma membrane with FM4-64 dye (scale bar=20 µm).

lengths in the mock treatment varied across mutant lines, we calculated the ratio of the root hair lengths from bacteria-treated versus mock-treated plants, for each of the lines, and compared this to the ratio calculated for the wild type. The most prominent differences were found for the *exo70A1* and *ein2* mutants, which had shorter root hairs than Col-0. For each of the mutant lines, deviations from the Col-0 ratio were found to be statistically significant, with the exception of *npr1-1*.

Exocyst functioning is important for stimulation of root hair growth, possibly due to an enhanced requirement for exocytosis in root hair elongation. Root hairs of mutant *exo70A1* after exposure to bacteria were not only shorter, but also appeared with a severely distorted wavy shape (Fig. 2A). Although these root hairs were further examined using confocal microscopy after staining with FM-dye (Fig. 2B), no difference in endomembrane structures between the mutant and the WT was found after stimulation of root hair growth by Psm.

We also quantified changes in primary root growth after the application of bacteria. Average primary root lengths for all tested lines after 48 h are shown in Supplementary Data Fig. S2. The strongest deviation from the WT response of growth inhibition of primary roots was found in the *npr1-1* mutant, which showed weaker inhibition. The *exo70A1* also showed lower inhibition of root growth after pathogen treatment compared to WT plants. Primary root lengths were found to be significantly different between mock- and bacteria-treated seedlings; however, differences in lengths between the WT and each mutant line (with the exception of Ws-4) within a given treatment were not statistically significant.

Continuous root tip imaging was used to observe the sequence of events after contact between the seedling roots and Psm. We found that stimulation of root hair growth and inhibition of root growth were noticeable 8 or 10 h post-inoculation (hpi), respectively, while a more detailed time-course analysis revealed that root hair growth may be stimulated by 4 hpi (Fig. 3, Supplementary Data Figs S3 and S7).

Flg22 pretreatment suppresses stimulation of root hair growth by Psm

To test whether the observed pathogen-induced stimulation of root hair growth could be triggered or affected by the Flg22 peptide, we treated seedling roots with 10 µM Flg22 alone or with 10 µM Flg22 12 h prior to inoculation with Psm. Treatment with Flg22 alone failed to induce enhanced root hair growth, while primary root growth inhibition was observed as previously reported (Bauer *et al.*, 2001). Pretreatment of Col-0 with Flg22 led to moderated stimulation of root hair growth and the difference compared to growth in Psm-treated Col-0 was significant. However, these results differed significantly from those found for Ws-4. In the case of Ws-4, an FLS2 null mutant, pretreatment had no impact on root hair and primary root growth (Fig. 4, Supplementary Data Fig. S4).

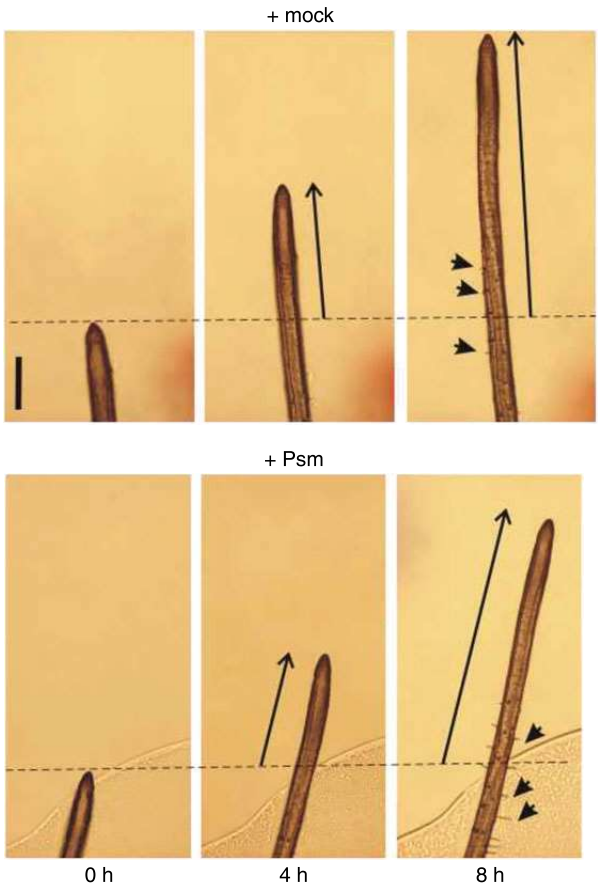

FIG. 3. Continuous root tip imaging after the Psm treatment, in comparison with mock-treated roots. The primary root growth from 0 to 4 and 8 h are marked with arrows; some of the root hairs appearing and growing in this time range and region are indicated as well (marked with arrowheads; scale bar=0·2 mm).

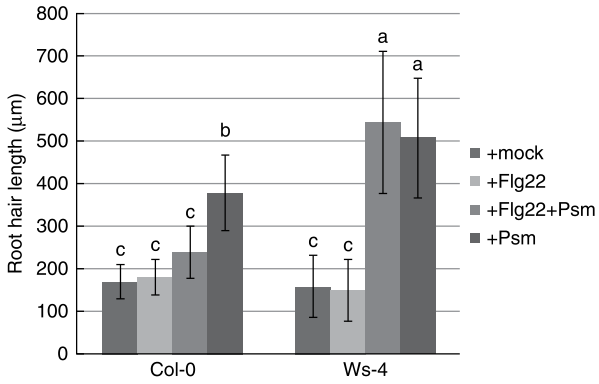

FIG. 4. Stimulation of root hair growth by Psm after pretreatment with the Flg22 peptide. Seedling roots were treated with 10 µM Flg22 alone, or with 10 µM Flg22 followed by Psm inoculation 12 h later. Mock and Psm inoculations were used as negative and positive controls, respectively. Pretreatment of Col-0 with Flg22 moderates stimulation of root hair growth, while in Ws-4, the pretreatment had no effect. Different letters indicate significant differences ($P<0·05$).

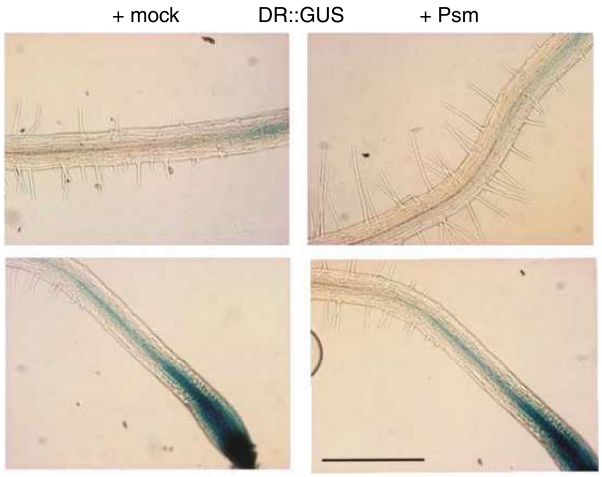

FIG. 5. GUS assay on seedlings carrying pDR5::GUS and inoculated with Psm. There was no detectable upregulation of the auxin responsive reporter expression after Psm inoculation (scale bar=0·5 mm).

Activity of an auxin-responsive promoter in the root tip was not affected early after the contact with bacteria

We examined whether auxin is involved in early stimulation of root hair growth, as it is involved in long-term stimulation (Zamioudis *et al.*, 2013). Using the GUS assay in seedlings carrying the auxin-sensitive pDR5::GUS reporter (Ulmasov *et al.*, 1997) and inoculation with Psm, no upregulation of the auxin-responsive reporter was observed within the time frame of our experiments (Fig. 5). This result indicates that these early root reactions are possibly regulated by different mechanisms to those described by Zamioudis *et al.* (2013), in which the bacteria were placed 5 cm from younger seedlings and the effects were quantified after a much longer period of exposure (8 d).

Testing with other bacteria and treatments for stimulation of root hair growth

To examine whether the root responses described above are specific to particular bacterial species, we performed the same test with Col-0 *Arabidopsis* plants and four other bacteria species: *Agrobacterium tumefaciens* GV3101 (Atu), *Escherichia coli* DH5α (Eco), *P. syringae* pv. *tomato DC3000* (Pst) and *Pseudomonas savastanoi* pv. *phaseolicula* CCM 2861 (Psp). Exposure to Atu resulted in stimulation; the root hairs were twice as long as those exposed to the mock treatment. The reaction to Psp and Pst was comparable to the reaction to Psm: root hairs were approx. 2·5–3 times longer than those in the mock treatment. Exposure to Eco resulted in slight inhibition of root hair growth (Fig. 6). These results suggest that the stimulation of root hair growth is similar for different soil- and plant-adapted bacteria, while the response to animal-adapted *E. coli* is different.

Interestingly, treatment with bacteria inactivated by heat or sonication, with filtrate from the bacterial culture, with supernatant from culture of Psm-infected plants, with elf18, chitin, peptidoglycan, coronatine and root tissue powdered in liquid N_2 [from infected and non-infected seedlings, as a source of

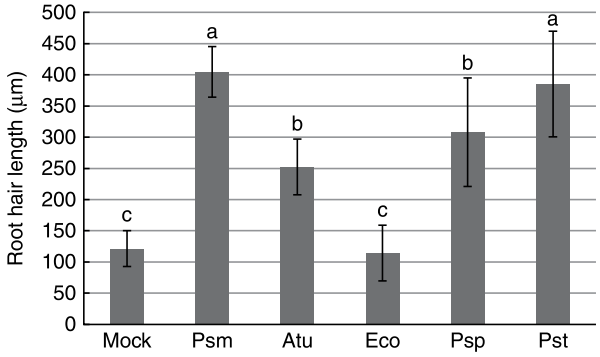

FIG. 6. Stimulation of root hairs growth by Atu, Eco, Psm, Pst and Psp. Root hair growth in Col-0 seedlings treated with bacteria: *Agrobacterium tumefaciens* GV3101 (Atu), *Escherichia coli* DH5α (Eco), *Pseudomonas syringae* pv. *tomato DC3000* (Pst) and *Pseudomonas savastanoi* pv. *phaseolicula* strain CCM 2861 (Psp), in comparison with Psm. All treatments except Eco stimulated root hair growth. Different letters indicate significant differences ($P<0{\cdot}05$).

DAMPs (danger-associated molecular patterns); data not shown] had no effect on root hairs. Additionally, we tested two bacterial quorum-sensing AHLs that were previously shown to enhance root hair lengths, N-decanoyl-HLs, namely C10-HL and oxo-C10-HL (Sigma; Ortíz-Castro *et al.*, 2008). These chemicals failed to stimulate root hair growth, even over a wide range of tested concentrations (data not shown). Thus, only living bacteria at high inocula were capable of provoking stimulation of root hair growth. Interestingly, type 3 secretion system mutants of *Pseudomonas* provoked the same range of root hair growth stimulation as did its WT counterpart (in agreement with Maketon *et al.*, 2012; data not shown).

SA, JA, ET and PAD4 interplay and root hair growth

A mutant impaired in JA, ET and SA signalling pathways and PAD4-dependent immunity, *dde2/ein2/pad4/sid2* (*deps*) was described by Tsuda *et al.* (2009). *Dde2* is a knock-out mutant of the *AOS* (*ALLENE OXIDE SYNTHASE*) gene, which is responsible for the biosynthesis of JA (von Malek *et al.*, 2002). The *sid2* mutant is a knock-out of the *ICS1* (*ISOCHORISMATE SYNTHASE 1*), gene which is a crucial component in the pathway responsible for the biosynthesis of SA after pathogen attack (Wildermuth *et al.*, 2001). Interestingly, the quadruple mutant *deps* has never been used previously to study root responses to pathogenic bacteria. Here, we employed the entire set of mutant combinations related to *deps* and treated them with Pst by the flooding method for 24 h. We examined the stimulation of root hair growth in *Arabidopsis* Col-0 (WT) seedlings after flooding with Pst (OD_{600} of 0·01; Supplementary Data Figs S5, S6 and S8, and Tables S1 and S2). This method was appropriate for analysis of very large numbers of seedlings of all *deps* mutants. We showed that impaired ET signalling is responsible for the shorter root hairs in *deps* (Fig. 7C). Interestingly, SA-, JA- and PAD4-related pathways enhance the effect of impaired ET signalling such that the *ein2* single mutant had the shortest root hairs of all studied mutants (Fig. 7C). The *deps* mutant displayed root hairs almost twice as long as those in *ein2* after Pst stimulation (Fig. 7).

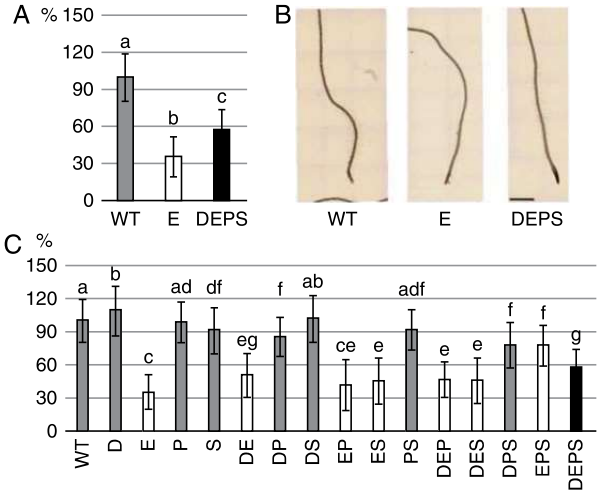

FIG. 7. The influence of SA, JA, ET and PAD4 on root hair growth. Four-day-old seedlings were treated with *P. syringae* pv. *tomato DC3000* and root hair lengths were measured 24 hpi. (A) Lengths of root hairs of selected genotypes – WT, *ein2* (E) and *dde2/ein2/pad4/sid2* (DEPS). (B) Representative images of WT and selected mutants after Pst treatment. Scale bar=1000 µm. (C) Lengths of root hairs of all 'DEPS' collection mutants. D, *dde2*; E, *ein2*; P, *pad4*; S, *sid2*. For A and C, $n = 10$–200 for each genotype. Values represent the mean, and error bars represent s.d. Small letters indicate statistically significant ($P < 0{\cdot}01$) differences between treatments. Root hair lengths are given as %, with value for WT set as 100%.

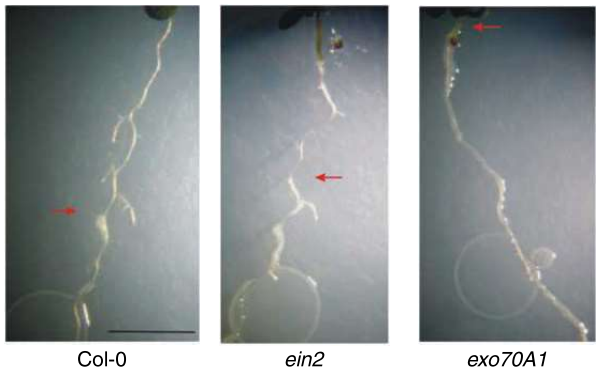

Fig. 8. Psm colonization of roots and growth during prolonged co-cultivation. After 5 d of growth of bacteria on roots, Psm completely colonized only *exo70A1*. The red arrows indicate the uppermost positions on primary roots that were colonized by Psm spreading from the root tip (scale bar=0·5 mm).

Correlation of root hair stimulation with overall growth of bacteria

To understand how the stimulation of root hair growth reflects the ability of a plant to limit the spread of a pathogen, we analysed the spread of the bacteria on the inoculated plants after a further 3 d of exposure. The most remarkable result was found for the *exo70A1* mutant, which, unlike *ein2* and Col-0 WT, displayed roots that were often completely colonized by Psm (Fig. 8). As root hair stimulation is impaired in *exo70A1* and *ein2*, the root hair growth response is not simply correlated with the ability of the plant to limit the growth of bacteria in the rhizosphere.

DISCUSSION

We describe the early growth response of root hairs in *Arabidopsis* to bacterial contact. We found that the general responses of the root and root hairs to pathogenic bacteria resemble previously described reactions to the presence of PGPR microbes – root hair growth is stimulated and primary root growth is inhibited (e.g. López-Bucio *et al*., 2007; reviewed by Vacheron *et al*., 2013).

We show here that stimulation of root hair growth and inhibition of primary root growth begin after the first few hours of direct contact with bacteria. Both these phenomena appear to be initiated simultaneously; however, as Flg22 inhibits primary root growth without stimulating growth of root hairs, we hypothesized that these processes are independent. In contrast to the auxin-dependent long-term (i.e. 1 week) and long-distance responses described by Zamioudis *et al*. (2013), our results suggest no major involvement of auxin signalling during the short time-frame responses studied here. Stimulation of root hair growth with *A. tumefaciens* and *P. savastanoi* provoke similar effects to those produced by Psm and Pst, suggesting that the enhanced root hair growth may be a general response of roots to contact with living plant- and soil-adapted bacteria.

Our results show that functional ET perception is necessary for efficient pathogen-induced stimulation of root hair growth. In addition, vesicle trafficking plays a role in this phenomenon, as seen not only in the example with the *exo70A1* mutant but also in the exocyst subunit mutant *sec8* (Supplementary Data Fig. S8) and in the co-treatment with Pst and BFA, which blocks the stimulation of root hair growth (Supplementary Data Fig. S9). In the *ein2* and *exo70A1* knockout mutants, stimulation of root hair growth is largely compromised compared to the WT, but bacterial growth along the roots of the two mutants differs – bacteria overgrow on *exo70A1* but not on *ein2* seedlings. The *exo70A1* mutant plants display a strong defect in secretion that results in dwarfed plants with smaller cotyledons and delayed lateral roots. Therefore, it is possible that the *exo70A1* mutant plants during co-cultivation with bacteria produce lower levels of defence compounds that limit bacterial growth when compared to WT plants and the mutant lines that do not have a defective growth phenotype. Interestingly, our previous tests with Psm leaf inoculation showed the same level of bacterial growth in leaves of *exo70A1* and WT plants (data not shown). The contrasting results obtained for *exo70A1* clearly indicate that substantially different plant–microbe interaction mechanisms operate in leaves and roots (Balmer and Mauch-Mani, 2013).

The prominent role of EXO70A1 in the bacterial root hair stimulation phenomenon confirms that a secretion/exocytosis mechanism that is supported by the exocyst complex is important for root hair tip growth. The wavy appearance of root hairs of the *exo70A1* mutant after treatment with Psm could reflect inefficient secretion and a deficiency in the mutant's ability to support fast tip growth; unfortunately, the specific mechanism remains unexplained. The wavy root hair phenotype resembles that found in the *Arabidopsis rhd3* (root hair-defective 3) mutant, which carries a mutation in a large GTP binding protein; however, we are currently unable to speculate whether there might be a functional connection between RHD3 and EXO70A1 other than involvement of the both in the endomembrane dynamics (Brands and Ho, 2002; Stefano *et al*., 2012).

In parallel to vesicle trafficking, we focused on the involvement of plant immune signalling pathways in the stimulation of root hair growth. For this we used a quadruple mutant (*deps*) that is impaired in the key SA, JA and ET phytohormonal pathways, as well as in the immune signalling dependent on the PAD4 protein (Tsuda *et al*., 2009; Kim *et al*., 2014). Tsuda *et al*. (2009) have defined the SA, JA, ET and PAD4 pathways as signalling sectors (portions of plant immunity signalling; Tsuda and Katagiri, 2010) and described their roles in PAMP- and effector-triggered immunity. SA signalling is commonly involved in defence responses against biotrophic and hemibiotrophic pathogens (e.g. *P. syringae*), while JA and ET are involved in immune responses to necrotrophic pathogens (Glazebrook, 2005; Pieterse *et al*., 2009). PAD4 forms heterodimers with EDS1 (ENHANCED DISEASE SUSCEPTIBILITY 1) after pathogen attack and triggers the plant immune responses that are mostly connected with induction of the SA signalling pathway, but EDS1/PAD4 may also be involved in SA-independent immune responses (Rietz *et al*., 2011; Janda and Ruelland, 2015; Cui *et al*., 2017). According to the general model of phytohormonal crosstalk in defence responses, JA and ET inhibit SA signalling and vice versa. However, new evidence shows that the relationships between these pathways are much more complicated than previously supposed. Kim *et al*. (2014) proposed a model that shows a synergistic relationship between SA and JA with a positive feedback loop that was further elaborated by the epistatic role of PAD4 over the SA sector (Mine *et al*., 2017).

Using 16 combinatorial genotypes related to the *deps* quadruple mutant we showed that ET is directly responsible for the stimulation of root hair growth after treatment with Psm/Pst, as expected based on the known positive role of ET in root hair cell expansion (Fig. 7; Dolan, 2001). Based on the fact that the *deps* mutant has longer root hairs than the single *ein2* mutant, we concluded that the full inhibitory effect of the *ein2* mutation on root hair growth requires functional JA, PAD4 and SA sectors. Our data support a negative regulatory relationship with ET on the one side, and SA and JA on the other side in the rhizosphere (Figs 7 and 9B). When ET, which is the most important factor for root hair growth enhancement, is non-functional (*ein2*), the unbalanced phytohormonal condition allows the three SA/JA/PAD4 sectors to inhibit root hair growth, which can be explained only by the negative control of ET over these three sectors. However, the JA and PAD4 sectors also have minor and indirect influence in the pathogen induction of root hair growth (Fig. 9A). This is observable on the behaviour of the double *dp* mutant and triple *dps* mutant (both with functional ET signalling) root hairs, which were shorter than WT root hairs, probably due to an overall slower recognition of Pst (Fig. 7). The *dp* and *dps*, but not *ds* and *ps*, mutants have shorter root hairs, which indicates that there might be a cooperation between JA and PAD4 pathways/sectors in root hair growth stimulation. This is also in agreement with the suggested dominant role of the PAD4 sector over the SA sector in immunity (Mine *et al*., 2017; Fig. 7). Interestingly, in the *deps* mutant, the greater distance between the initiation zone of root hairs and

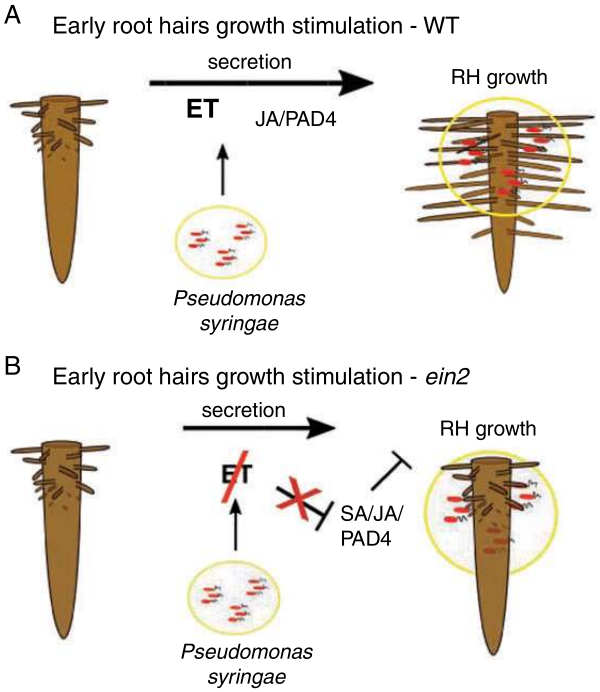

FIG. 9. Model of stimulation of root hair growth by Psm/Pst and role of four phytohormonal/immunity sectors in this model. Ethylene (ET) is of key importance in root hair growth in the developmental context. The other sectors, especially the jasmonic acid (JA) and PAD4 pathways, also have minor and indirect influences on the pathogen-related induction of root hair growth (A). When the most important sector, ethylene signalling, is missing (*ein2*), the phytohormonal misbalance allows salicylic acid (SA)/JA/PAD4 to inhibit root hair growth, which can be explained only by the possible negative control of ethylene over these three sectors (B).

the root tip (Supplementary Data Fig. S6) indicates that traditional immune pathways are involved in the primary root growth inhibition caused by *Pseudomonas*.

The downstream component of the SA signalling pathway, NPR1, is abundantly expressed in roots that are not under any biotic stress (Cao *et al*., 1994; Lamesch *et al*., 2010). However, the lack of NPR1 function did not affect root hair growth in our assays. Additionally, the missing immune receptor FLS2 had no major effect on stimulation of root hair growth in the Ws ecotype. FLS2 was, however, important for the desensitization of plants pretreated with Flg22, as it might have either decreased the sensitivity of plants following bacterial contact through the FLS2 degradation, as reported by Smith *et al.* (2014), or triggered PAMP-triggered immunity, slowing bacterial growth.

While we have identified at least some of the players in this phenomenon in plants, unfortunately we are currently unable to explain the cause of early stimulation of root hair growth by bacteria from the pathogen side, as shown by the list of chemicals and treatments that we tested without a positive result. The most promising candidates tested were AHLs (Ortíz-Castro *et al*., 2008); however, it is possible that because they quickly lose their activity, the effect was insufficient to enhance root hair growth under our experimental conditions. It has been recently shown that pyocyanin, a virulence factor of the plant and animal pathogen *P. aeruginosa*, affects the growth and development of *Arabidopsis* seedlings by inhibiting primary root growth and promoting lateral root and root hair growth without affecting meristem viability or causing cell death (Ortíz-Castro *et al*., 2014). This modulation works independently of auxin, cytokinin and abscisic acid but requires ET signalling (Ortíz-Castro *et al*., 2014). Based on this evidence, we speculate that the plant pathogenic *Pseudomonas* might contain a similar metabolite that could stimulate *Arabidopsis* root hair growth at certain concentrations. Alternatively, the presence of *Pseudomonas* bacteria around the root tips might temporarily change nutrient availability. It has recently been shown that pyoverdine, a siderophore produced by beneficial *Pseudomonas*, not only modulates the availability of soil iron to plants, but also positively regulates the expression of genes related to development and iron acquisition in plants grown under iron-deficient conditions and represses the expression of defence-related genes (Vansuyt *et al*., 2007; Trapet *et al*., 2016). This system demonstrates that there are many levels at which plant hosts and bacteria can influence each other and that plants need to trade-off between defence and growth to preserve their fitness.

To conclude, while the most common plant cell response to pathogens is growth arrest, root hair cells can perform the opposite reaction. Functional ET signalling and efficient exocyst-dependent vesicular trafficking are important for this stimulation of root hair growth. As the presence of high levels of bacteria in a soil patch might signal the proximity of a higher nutrient content, it is also possible that root systems, including root hairs, interpret contact with soil-adapted bacteria as a signal of a putative local nutrient maximum. This phenomenon also reflects the differences in defence strategies between shoots and roots, which warrant further examination of the *Arabidopsis–Pseudomonas* interaction.

SUPPLEMENTARY DATA

Supplementary data are available online at www.aob.oxfordjournals.org and consist of the following. Fig. S1: the root tip zones of mock- and Psm-treated plants. Fig. S2: inhibition of primary root growth 48 h post-inoculation. Fig. S3: time-course experiment of the early effect of Psm treatment on root architecture. Fig. S4: inhibition of primary root growth after pretreatment with the Flg22 peptide. Fig. S5: stimulation of root hair growth by *Pseudomonas syringae* pv. *tomato DC3000* (Pst). Fig. S6: the influence of the *dde2/ein2/pad4/sid2* (DEPS) pathways on root growth. Fig. S7: characterization of the root hair growth induced by Pst over time. Fig. S8: additional set of exocyst *sec8* and *syp122* SNARE mutants. Fig. S9: the effect of brefeldin A on the execution of the root hairs growth stimulation. Table S1: characterization of the stimulation of root hair growth in WT seedlings after Pst flooding. Table S2: lengths of root hairs and primary roots after Pst flooding

ACKNOWLEDGMENTS

This work was supported by the GACR/CSF projects 15-14886S (T.P., J.O., V.Z.), 14-09685S (M.J., V.H., Z.S.) and GA UK project 1102214 (J.O.). T.P. would like to thank Dr

Andrea Genre (University of Turin) for help with root hair microscopy, to collegues Dr Roman Pleskot for help with figure and statistical analysis, Dr Edita Drdová Janková for helpful discussion on *exo70A1* mutant and Michal Kuchar for technical support. M.J., Z.S. and V.H. would like thank to leaders of their laboratories Prof. Olga Valentová, Assoc. Prof. Lenka Burketová and Dr Jan Martinec and to Lucie Lamparová and Petra Konopáčová for their great technical support. We also would like to thank Dr Kenichi Tsuda and Dieter Becker (from Max Planck Institute for Plant Breeding Research, Cologne) who kindly provided seeds of the whole '*deps*' collection and also *P. syringae* pv. *tomato DC3000*. We thank Dr Emily Larson for critical reading of the manuscript and language editing.

LITERATURE CITED

Balmer D, Mauch-Mani B. 2013. More beneath the surface? Root versus shoot antifungal plant defenses. *Frontiers in Plant Science* **4**: 256. doi:10.3389/fpls.2013.00256.

Bates TR, Lynch JP. 1996. Stimulation of root hair elongation in *Arabidopsis thaliana* by low phosphorus availability. *Plant, Cell & Environment* **19**: 529–538.

Bauer Z, Gómez-Gómez L, Boller T, Felix G. 2001. Sensitivity of different ecotypes and mutants of *Arabidopsis thaliana* toward the bacterial elicitor flagellin correlates with the presence of receptor-binding sites. *The Journal of Biological Chemistry* **276**: 45669–45676. doi:10.1074/jbc.M102390200

Beck M, Zhou J, Faulkner C, MacLean D, Robatzek S. 2012. Spatio-temporal cellular dynamics of the *Arabidopsis* flagellin receptor reveal activation status-dependent endosomal sorting. *The Plant Cell* **24**: 4205–4219. doi:10.1105/tpc.112.100263.

Brands A, Ho TD. 2002. Function of a plant stress-induced gene, HVA22. Synthetic enhancement screen with its yeast homolog reveals its role in vesicular traffic. *Plant Physiology* **130**: 1121–1131. doi:10.1104/pp.007716

Cao H, Bowling SA, Gordon AS, Dong X. 1994. Characterization of an *Arabidopsis* mutant that is nonresponsive to inducers of systemic acquired resistance. *The Plant Cell* **6**: 1583–1592. doi:10.1105/tpc.6.11.1583

Chinchilla D, Zipfel C, Robatzek S, *et al.* 2007. A flagellin-induced complex of the receptor FLS2 and BAK1 initiates plant defence. *Nature* **448**: 497–500. doi:10.1038/nature05999

Cui H, Gobbato E, Kracher B, Qiu J, Bautor J, Parker JE. 2017. A core function of EDS1 with PAD4 is to protect the salicylic acid defense sector in *Arabidopsis* immunity. *New Phytologist* **213**: 1802–1817. doi:10.1111/nph.14302.

Dolan L. 2001. The role of ethylene in root hair growth in *Arabidopsis*. *Journal of Plant Nutrition and Soil Science* **164**: 141–145.

Dong X, Mindrinos M, Davis KR, Ausubel FM. 1991. Induction of *Arabidopsis* defense genes by virulent and avirulent *Pseudomonas syringae* strains and by a cloned avirulence gene. *The Plant Cell* **3**: 61–72. doi:10.1105/tpc.3.1.61

Dörmann P, Kim H, Ott T, *et al.* 2014. Cell-autonomous defense, re-organization and trafficking of membranes in plant-microbe interactions. *New Phytologist* **204**: 815–822. doi:10.1111/nph.12978.

Du Y, Mpina MH, Birch PRJ, Bouwmeester K, Govers F. 2015. *Phytophthora infestans* RXLR effector AVR1 interacts with exocyst component Sec5 to manipulate plant immunity. *Plant Physiology* **169**: 1975–1990. doi:10.1104/pp.15.01169

Glazebrook J. 2005. Contrasting mechanisms of defense against biotrophic and necrotrophic pathogens. *Annual Review of Phytopathology* **43**: 205–227. doi:10.1146/annurev.phyto.43.040204.135923

Gómez-Gómez L, Felix G, Boller T. 1999. A single locus determines sensitivity to bacterial flagellin in *Arabidopsis thaliana*. *The Plant Journal* **18**: 277–284.

Guo W, Roth D, Walch-Solimena C, Novick P. 1999. The exocyst is an effector for Sec4p, targeting secretory vesicles to sites of exocytosis. *The EMBO Journal* **18**: 1071–1080. doi:10.1093/emboj/18.4.1071

Guzmán P, Ecker JR. 1990. Exploiting the triple response of *Arabidopsis* to identify ethylene-related mutants. *The Plant Cell* **2**: 513–523. doi:10.1105/tpc.2.6.513

Hála M, Cole R, Synek L, *et al.* 2008. An exocyst complex functions in plant cell growth in *Arabidopsis* and tobacco. *The Plant Cell* **20**: 1330–1345. doi:10.1105/tpc.108.059105

Hsu S-C, TerBush D, Abraham M, Guo W. 2004. The exocyst complex in polarized exocytosis. *International Review of Cytology* **233**: 243–265. doi:10.1016/S0074-7696(04)33006-8

Janda M, Ruelland E. 2015. Magical mystery tour: salicylic acid signaling. *Environmental and Experimental Botany*, **114**:117–128. doi:10.1016/j.envexpbot.2014.07.003

Jung J-Y, Shin R, Schachtman DP. 2009. Ethylene mediates response and tolerance to potassium deprivation in *Arabidopsis*. *The Plant Cell* **21**: 607–621. doi:10.1105/tpc.108.063099

Katagiri F, Thilmony R, He SY. 2002. The *Arabidopsis thaliana-Pseudomonas syringae* interaction. *Arabidopsis Book* **1**: e0039. doi:10.1199/tab.0039

Kim Y, Tsuda K, Igarashi D, *et al.* 2014. Mechanisms underlying robustness and tunability in a plant immune signaling network. *Cell Host & Microbe* **15**: 84–94. doi:10.1016/j.chom.2013.12.002

Kinkema M, Fan W, Dong X. 2000. Nuclear localization of NPR1 is required for activation of PR gene expression. *The Plant Cell* **12**: 2339–2350.

Kremer RJ, Begonia MF, Stanley L, Lanham ET. 1990. Characterization of rhizobacteria associated with weed seedlings. *Applied and Environmental Microbiology* **56**: 1649–1655.

Kulich I, Pečenková T, Sekereš J, *et al.* 2013. *Arabidopsis* exocyst subcomplex containing subunit EXO70B1 is involved in autophagy-related transport to the vacuole. *Traffic* **14**: 1155–1165. doi:10.1111/tra.12101

Lamesch P, Dreher K, Swarbreck D, Sasidharan R, Reiser L, Huala E. 2010. Using the *Arabidopsis* information resource (TAIR) to find information about *Arabidopsis* genes. *Current Protocols in Bioinformatics* Suppl. 30: Chapter 1, Unit1.11. doi:10.1002/0471250953.bi0111s30

López-Bucio J, Campos-Cuevas JC, Hernández-Calderón E, *et al.* 2007. *Bacillus megaterium* rhizobacteria promote growth and alter root-system architecture through an auxin- and ethylene-independent signaling mechanism in *Arabidopsis thaliana*. *Molecular Plant-Microbe Interactions* **20**: 207–217. doi:10.1094/MPMI-20-2-0207

Lugtenberg B, Kamilova F. 2009. Plant-growth-promoting rhizobacteria. *Annual Review of Microbiology* **63**: 541–556. doi:10.1146/annurev.micro.62.081307.162918

Maketon C, Fortuna A, Okubara PA. 2012. Cultivar-dependent transcript accumulation in wheat roots colonized by *Pseudomonas fluorescens* Q8r1-96 wild type and mutant strains. *Biological Control* **60**: 216-224.

Millet YA, Danna CH, Clay NK, *et al.* 2010. Innate immune responses activated in *Arabidopsis* roots by microbe-associated molecular patterns. *The Plant Cell* **22**: 973–990. doi:10.1105/tpc.109.069658

Mine A, Nobori T, Salazar-Rondon MC, *et al.* 2017. An incoherent feed-forward loop mediates robustness and tunability in a plant immune network. *EMBO Reports* **18**: 464–476. doi:10.15252/embr.201643051

Niu Y, Chai R, Liu L, *et al.* 2014. Magnesium availability regulates the development of root hairs in *Arabidopsis thaliana* (L.) Heynh. *Plant, Cell & Environment* **37**: 2795–2813. doi:10.1111/pce.12362

Ortíz-Castro R, Martínez-Trujillo M, López-Bucio J. 2008. N-acyl-L-homoserine lactones: a class of bacterial quorum-sensing signals alter post-embryonic root development in *Arabidopsis thaliana*. *Plant, Cell & Environment* **31**: 1497–1509. doi:10.1111/j.1365-3040.2008.01863.x

Ortíz-Castro R, Pelagio-Flores R, Méndez-Bravo A, Ruiz-Herrera LF, Campos-García J, López-Bucio J. 2014. Pyocyanin, a virulence factor produced by *Pseudomonas aeruginosa*, alters root development through reactive oxygen species and ethylene signaling in *Arabidopsis*. *Molecular Plant-Microbe Interactions* **27**: 364–378. doi:10.1094/MPMI-08-13-0219-R

Pečenková T, Hála M, Kulich I, *et al.* 2011. The role for the exocyst complex subunits Exo70B2 and Exo70H1 in the plant-pathogen interaction. *Journal of Experimental Botany* **62**: 2107–2116. doi:10.1093/jxb/erq402

Pieterse CM, Leon-Reyes A, Van der Ent S, Van Wees SC. 2009. Networking by small-molecule hormones in plant immunity. *Nature Chemical Biology* **5**: 308–16. doi:10.1038/nchembio.164

Rahman A, Hosokawa S, Oono Y, Amakawa T, Goto N, Tsurumi S. 2002. Auxin and ethylene response interactions during *Arabidopsis* root hair development dissected by auxin influx modulators. *Plant Physiology* **130**: 1908–1917. doi:10.1104/pp.010546

Rietz S, Stamm A, Malonek S, *et al.* 2011. Different roles of Enhanced Disease Susceptibility1 (EDS1) bound to and dissociated from Phytoalexin Deficient4 (PAD4) in *Arabidopsis* immunity. *New Phytologist* **191**: 107–119. doi:10.1111/j.1469-8137.2011.03675.x.

Rothman JE, Warren G. 1994. Implications of the SNARE hypothesis for intracellular membrane topology and dynamics. *Current Biology* **4**: 220–233.

Rudrappa T, Bais HP. 2008. Rhizospheric pseudomonads: Friends or foes? *Plant Signaling and Behavior* **3**: 1132–1133.

Schikora A, Schmidt W, 2001. Iron stress-induced changes in root epidermal cell fate are regulated independently from physiological responses to low iron availability. *Plant Physiology* **125**: 1679–1687.

Schneider CA, Rasband WS, Eliceiri KW. 2012. NIH Image to ImageJ: 25 years of image analysis. *Nature Methods* **9**: 671–675.

Smith JM, Salamango DJ, Leslie ME, Collins CA, Heese A. 2014. Sensitivity to Flg22 is modulated by ligand-induced degradation and de novo synthesis of the endogenous flagellin-receptor FLAGELLIN-SENSING2. *Plant Physiology* **164**: 440–454. doi:10.1104/pp.113.229179

Stefano G, Renna L, Moss T, McNew JA, Brandizzi F. 2012. In *Arabidopsis*, the spatial and dynamic organization of the endoplasmic reticulum and Golgi apparatus is influenced by the integrity of the C-terminal domain of RHD3, a non-essential GTPase. *Plant Journal* **69**: 957–966. doi:10.1111/j.1365-313X.2011.04846.x

Stegmann M, Anderson RG, Ichimura K, *et al.* 2012. The ubiquitin ligase PUB22 targets a subunit of the exocyst complex required for PAMP-triggered responses in *Arabidopsis*. *The Plant Cell* **24**: 4703–4716. doi:10.1105/tpc.112.104463

Synek L, Schlager N, Eliás M, Quentin M, Hauser M-T, Zárský V. 2006. AtEXO70A1, a member of a family of putative exocyst subunits specifically expanded in land plants, is important for polar growth and plant development. *Plant Journal* **48**: 54–72. doi:10.1111/j.1365-313X.2006.02854.x

Tanaka N, Kato M, Tomioka R, *et al.* 2014. Characteristics of a root hair-less line of *Arabidopsis thaliana* under physiological stresses. *Journal of Experimental Botany* **65**: 1497–1512. doi:10.1093/jxb/eru014.

TerBush DR, Maurice T, Roth D, Novick P. 1996. The Exocyst is a multiprotein complex required for exocytosis in *Saccharomyces cerevisiae*. *EMBO Journal* **15**: 6483–6494.

Trapet P, Avoscan L, Klinguer A, *et al.* 2016. The *Pseudomonas fluorescens* siderophore pyoverdine weakens *Arabidopsis thaliana* defense in favour of growth in iron-deficient conditions. *Plant Physiology* **171**: 675–693. doi:10.1104/pp.15.01537

Tsuda K, Katagiri F. 2010. Comparing signaling mechanisms engaged in pattern-triggered and effector-triggered immunity. *Current Opinion in Plant Biology* **13**: 459–465. doi:10.1016/j.pbi.2010.04.006.

Tsuda K, Sato M, Stoddard T, Glazebrook J, Katagiri F. 2009. Network properties of robust immunity in plants. *PLoS Genetics* **5**(12), doi:10.1371/journal.pgen.1000772

Ulmasov T, Murfett J, Hagen G, Guilfoyle TJ. 1997. Aux/IAA proteins repress expression of reporter genes containing natural and highly active synthetic auxin response elements. *The Plant Cell* **9**: 1963–1971. doi:10.1105/tpc.9.11.1963

Vacheron J, Desbrosses G, Bouffaud ML, *et al.* 2013. Plant growth-promoting rhizobacteria and root system functioning. *Frontiers in Plant Science* **4**: 356. doi:10.3389/fpls.2013.00356.

van Loon LC, Bakker PAHM, van der Heijdt WHW, Wendehenne D, Pugin A. 2008. Early responses of tobacco suspension cells to rhizobacterial elicitors of induced systemic resistance. *Molecular Plant-Microbe Interactions* **21**: 1609–1621. doi:10.1094/MPMI-21-12-1609

Vansuyt G, Robin A, Briat J-F, Curie C, Lemanceau P. 2007. Iron acquisition from Fe-pyoverdine by *Arabidopsis thaliana*. *Molecular Plant-Microbe Interactions* **20**: 441–447. doi:10.1094/MPMI-20-4-0441

von Malek B, van der Graaff E, Schneitz K, Keller B, 2002. The *Arabidopsis* male-sterile mutant *dde2-2* is defective in the ALLENE OXIDE SYNTHASE gene encoding one of the key enzymes of the jasmonic acid biosynthesis pathway. *Planta* **216**: 187–192. doi:10.1007/s00425-002-0906-2

Wen T-J, Hochholdinger F, Sauer M, Bruce W, Schnable PS. 2005. The roothairless1 gene of maize encodes a homolog of *sec3*, which is involved in polar exocytosis. *Plant Physiology* **138**: 1637–1643. doi:10.1104/pp.105.062174

Wildermuth MC, Dewdney J, Wu G, Ausubel FM, 2001. Isochorismate synthase is required to synthesize salicylic acid for plant defence. *Nature* **414**: 562–565. doi:10.1038/35107108

Xin XF, He SY. 2013. *Pseudomonas syringae* pv. *tomato DC3000*: a model pathogen for probing disease susceptibility and hormone signaling in plants. *Annual Review of Phytopathology* **51**: 473-498. doi:10.1146/annurev-phyto-082712-102321

Yang TJW, Perry PJ, Ciani S, Pandian S, Schmidt W. 2008. Manganese deficiency alters the patterning and development of root hairs in *Arabidopsis*. *Journal of Experimental Botany* **59**: 3453–3464. doi:10.1093/jxb/ern195

Zamioudis C, Pieterse CMJ. 2012. Modulation of host immunity by beneficial microbes. *Molecular Plant-Microbe Interactions* **25**: 139–150. doi:10.1094/MPMI-06-11-0179

Zamioudis C, Mastranesti P, Dhonukshe P, Blilou I, Pieterse CMJ. 2013. Unraveling root developmental programs initiated by beneficial *Pseudomonas* spp. bacteria. *Plant Physiology* **162**: 304–318. doi:10.1104/pp.112.212597

Zárský V, Cvrčková F, Potocký M, Hála M. 2009. Exocytosis and cell polarity in plants – exocyst and recycling domains. *New Phytologist* **183**: 255–272. doi:10.1111/j.1469-8137.2009.02880.x

Zárský V, Kulich I, Fendrych M, Pečenková T. 2013. Exocyst complexes multiple functions in plant cells secretory pathways. *Current Opinion in Plant Biology* **16**: 726–733. doi:10.1016/j.pbi.2013.10.013

Zipfel C, Robatzek S, Navarro L, *et al.* 2004. Bacterial disease resistance in *Arabidopsis* through flagellin perception. *Nature* **428**: 764–767. doi:10.1038/nature02485

Sup. Fig. 1. The root tip zones of mock- and Psm-treated plants. The red signal is FM4-64 dye used to stain and distinguish the meristematic from the elongation and differentiation zones (bar = 100 μm). The mock- versus Psm-treated plant were found to be significant for the elongation and differentiation zones (n=five for each measurement; mz – meristematic zone; ez+dz – elongation and differentiation zone).

Sup. Fig. 2. Inhibition of primary root growth 48 hours post-inoculation. **(A)** Appearance of primary roots after the mock and Psm treatment. **(B)** Lengths of primary roots of mock- (light-grey) and Psm-treated (dark-grey) roots. Ratios of the lengths of Psm-treated vs. mock-treated roots are shown for each line under the respective columns in the graph. n=5-10 for each of lines; different letters indicate significant differences ($p<0.05$)

Sup. Fig. 3. Time-course experiment of early effect of Psm treatment on root architecture**. (A)** The root hair growth stimulation in early time intervals after Psm inoculation. Values that are significantly different ($p<0.05$) between mock- and Psm- treated plants are marked with asterisks. n= 12-15 **(B)** The rate of root growth in early time intervals after Psm inoculation.

Sup. Fig. 4. Inhibition of primary root growth after pretreatment with the Flg22 peptide. Seedlings´ roots were treated with 10 μM Flg22 alone, or with 10 μM Flg22 followed by Psm inoculation 12 hours later. Mock and Psm inoculations were used as negative and positive controls, respectively. Different letters indicate significant differences ($p<0.05$) as determined using ANOVA and post-hoc Tukey's HSD comparisons.

Sup. Fig. 5. Stimulation of the root hairs growth by *Pseudomonas syringae* pv. *tomato DC3000* (Pst). Representative images of the roots of five days old seedlings. Seedlings were flooded for 24h with MS/2 or MS/2 containing Pst (OD600=0.01). The scale bar represents 500 μm.

Sup. Fig. 6 The influence of the DEPS pathways on root growth. The four-days-old seedlings were treated with *P. syringae* pv *tomato* DC3000 for 24h. The distance between the first root hairs and the root cap was analysed in selected genotypes WT, *ein2* (E) and *dde2/ein2/pad4/sid2* (DEPS). Values represent means and the error bars represent the SD. Number of analysed genotypes: WT=176; E=55; DEPS=107. Small letters indicate statistically significant ($P < 0.01$) differences between treatments

Sup. Fig. 7 Characterisation of the root hair growth induced by Pst over time. **(A)** Length of the root hairs of five days old seedlings, stimulated by flooding with *Pseudomonas syringae pv tomato DC3000* (Pst) solution in 10 and 24 hpi. **B)** Distance of the first root hairs from the root cap in 10 and 24 hpi. Seedlings were flooded with pure MS/2 or Pst (OD_{600}=0.01) solution. Values represent means, and error bars represent the SD from n=14 (10h) and n=22 (24h).

Sup. Fig. 8. Additional set of exocyst *sec8* and *syp122* SNARE mutants**. (A)** The graph shows weaker root hair growth stimulation after Psm treatment of root tips of mutants in core exocyst subunit sec8 (*sec8-4*; SALK_118129; Cole *et al.,* 2005) in comparison to the SNARE protein mutant *syp122* (SALK_008617; Assaad *et al*., 2011) and WT (Col0); different letters indicate significant differences ($p<0.05$). **(B)** The percentages of lengths of seedling primary roots occupied by progressing bacterial infection after five days of cocultivation. Graphs show the importance of exocyst subunit SEC8 in the root hair growth reaction; absence of SEC8 results in shorter root hairs after Psm inoculation. Spread of bacteria along the primary root is however not significantly enhanced in this mutant. The SNARE mutant *syp122* has no significantly different root hair response in comparison to the WT, likely because it´s closest homolog, SYP121, can compensate for its loss of function.

Sup. Fig. 9. The effect of brefeldin A on the execution of the root hairs growth stimulation. **(A)** Representative images of roots of five days old *Arabidopsis thaliana* Col-0 seedlings flooded for 24 h with *Pseudomonas syringae* pv *tomato DC3000* (Pst) and in presence of 0.1% DMSO or 50 µM brefeldin A (BFA). The scale bar represents 500 µm. **(B)** Lengths of root hairs (RH) after 24 h exposure to Pst in the presence of 0.1% DMSO or 50 µM BFA. The values represent means, and the error bars represent the SD from n=10. The asterisks indicate significant difference between Pst and Pst+BFA (*** $P<0.001$).

Sup. Table I Characterisation of the stimulation of root hair growth in WT seedlings after Pst-flooding

Sup. Table II Lengths of root hairs and primary roots after Pst-flooding

Table I. Characterisation of the stimulated root hair growth

	MS/2		Pst	
Root hairs	NO	YES	NO	YES
[%]	80.2	19.8	0	100

* for RH induced 0.8 – 1.5 mm from the root cap

Table II. Quantification of Pst-stimulated growth of root hairs and primary roots

	mean	SD
Lengths of root hairs length [µm]*	408.5	79.6
Distance of root hairs from root cap [µm]*	899.9	154.5

* n=205 seedlings.

Supplementary Figure 1

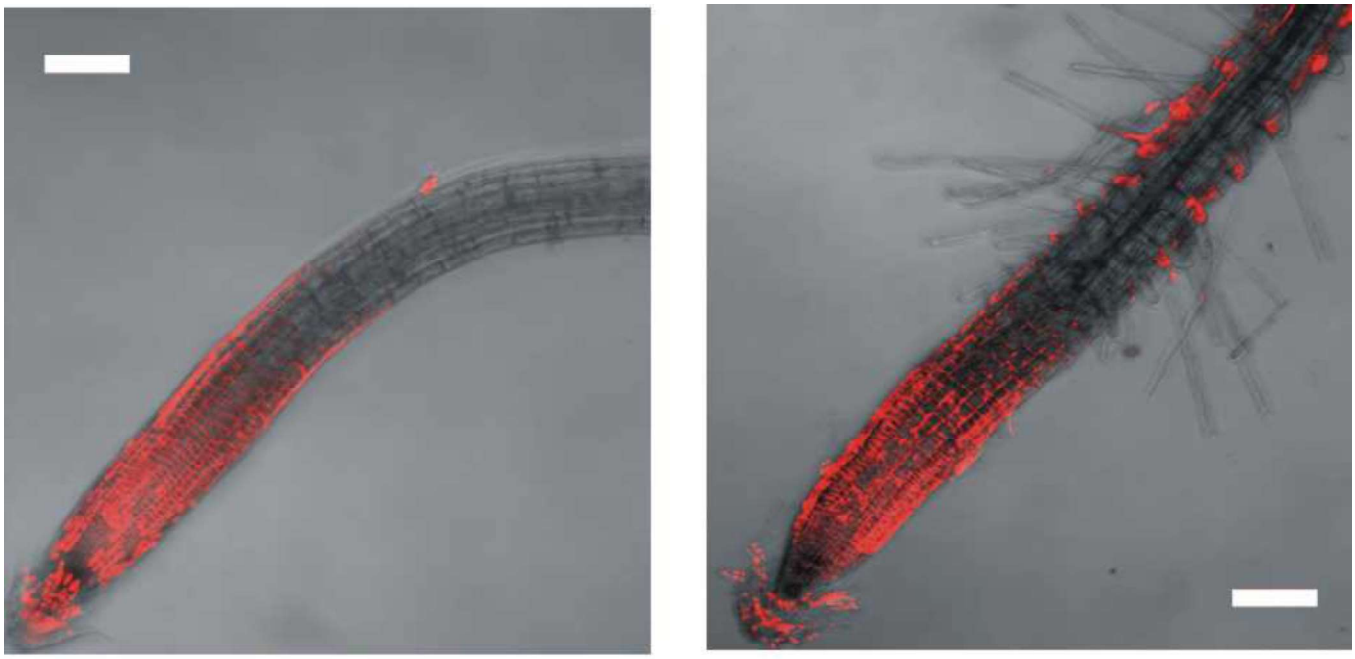

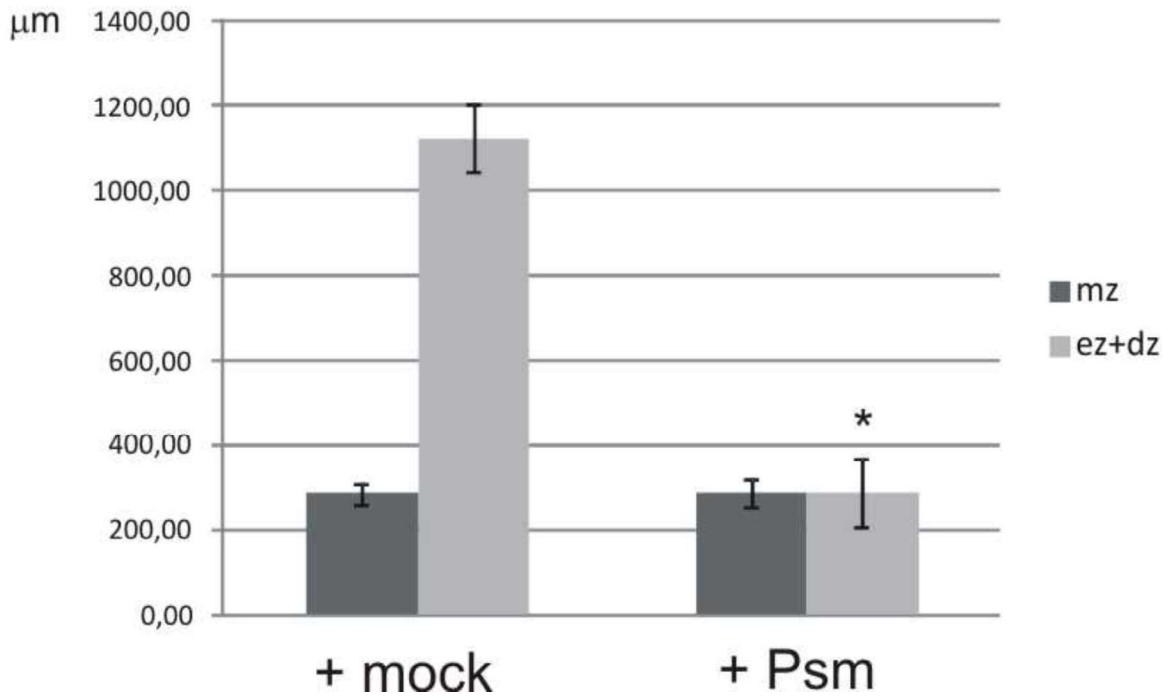

Supplementary Figure 2

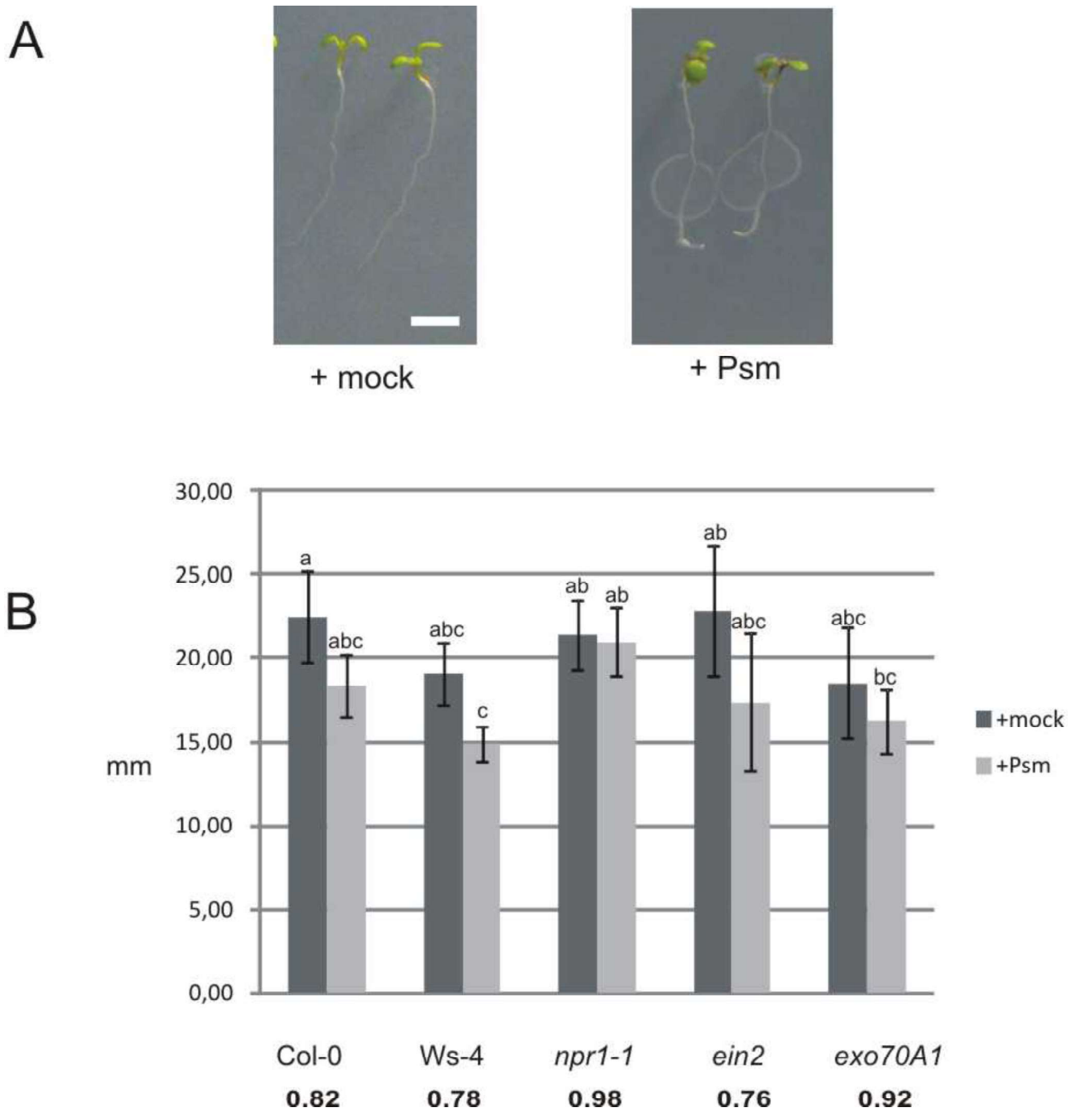

Supplementary Figure 3

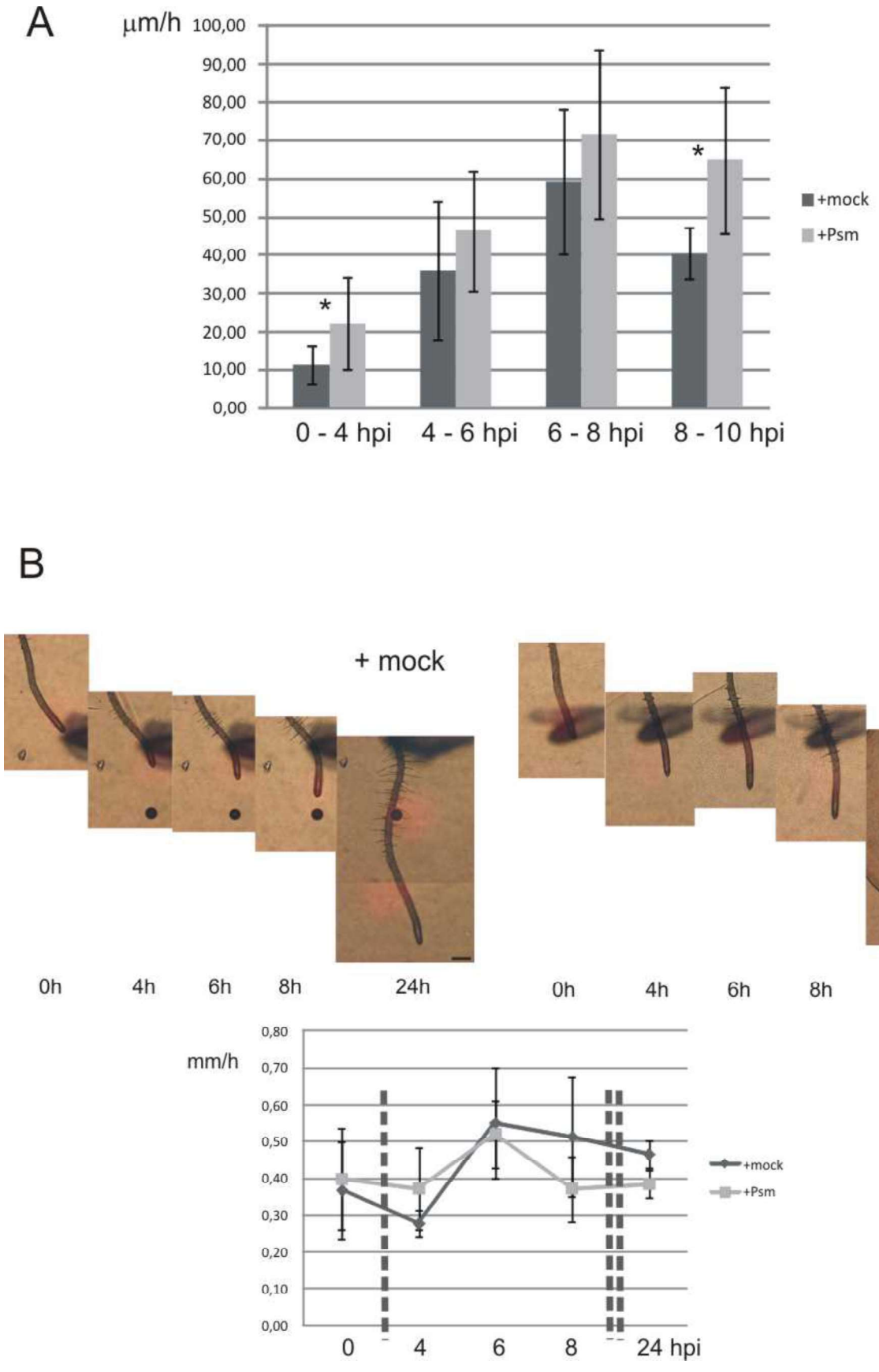

Supplementary Figure 4

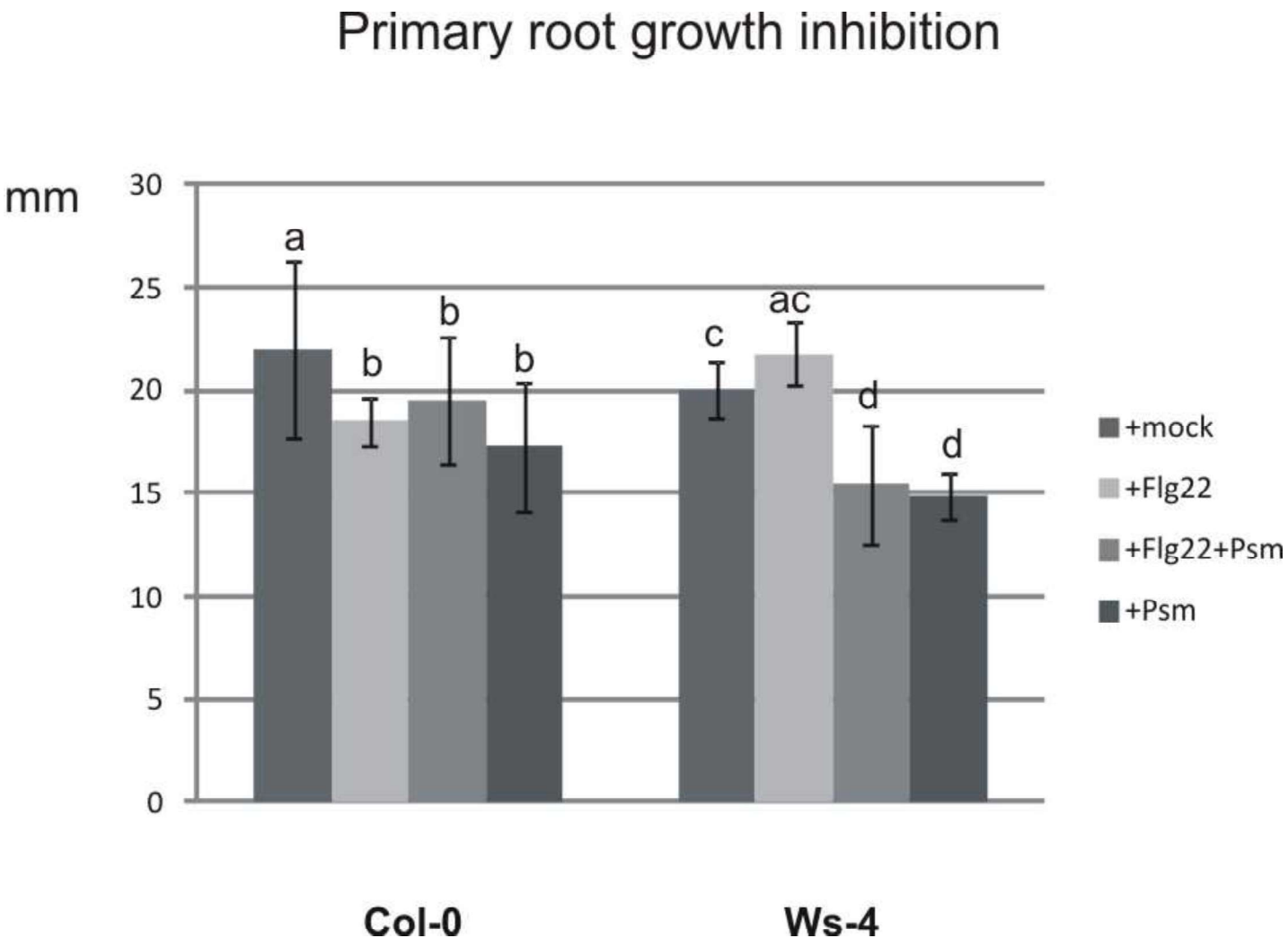

Supplementary Figure 5

Supplementary Figure 6

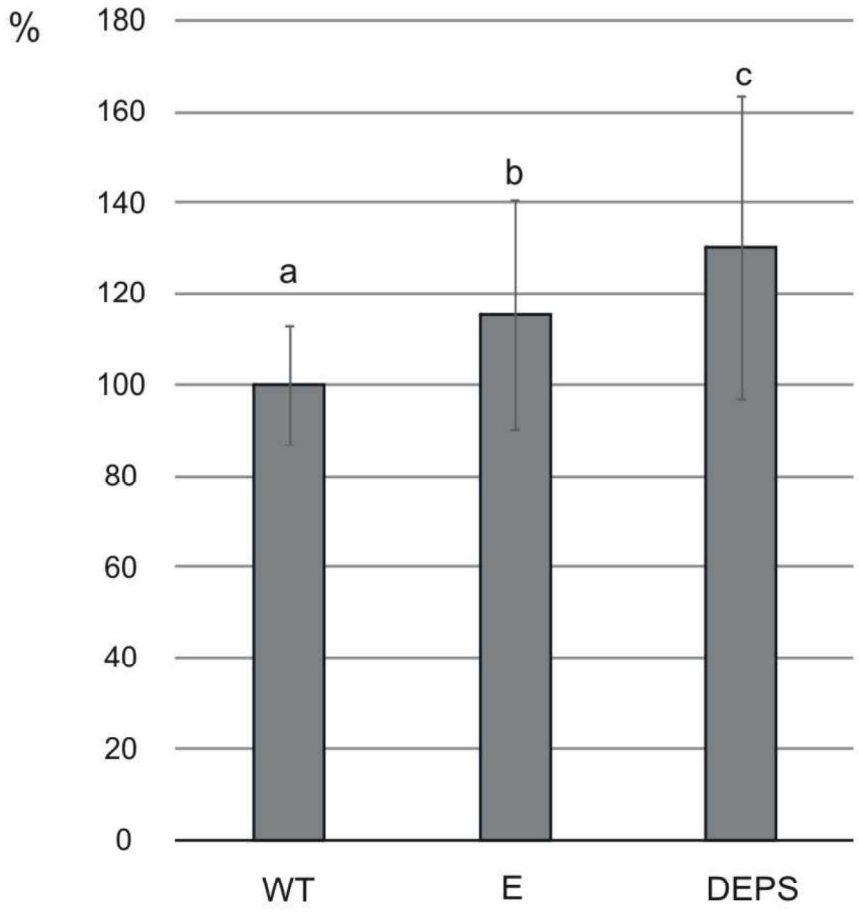

Supplementary Figure 7

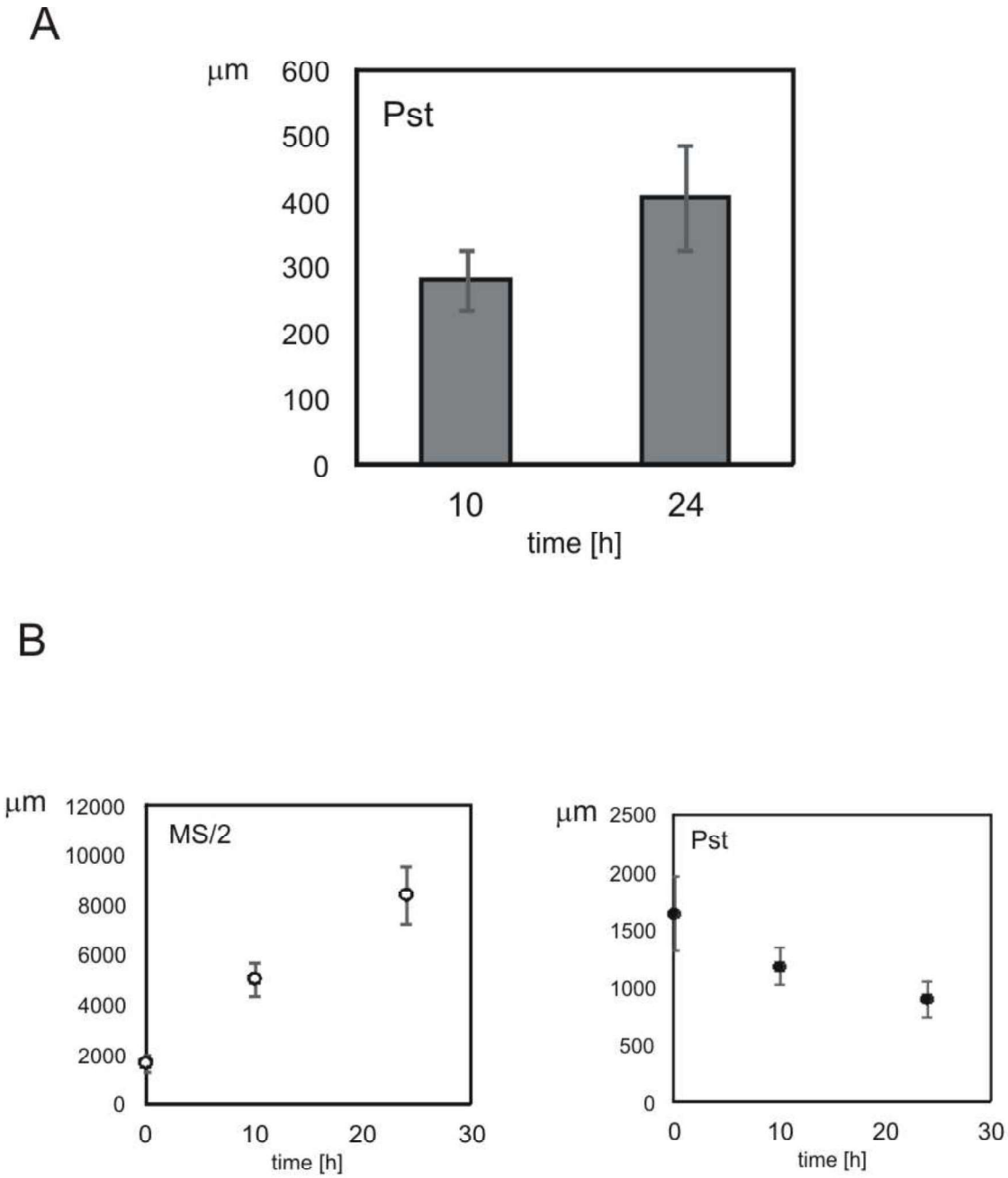

Supplementary Figure 8

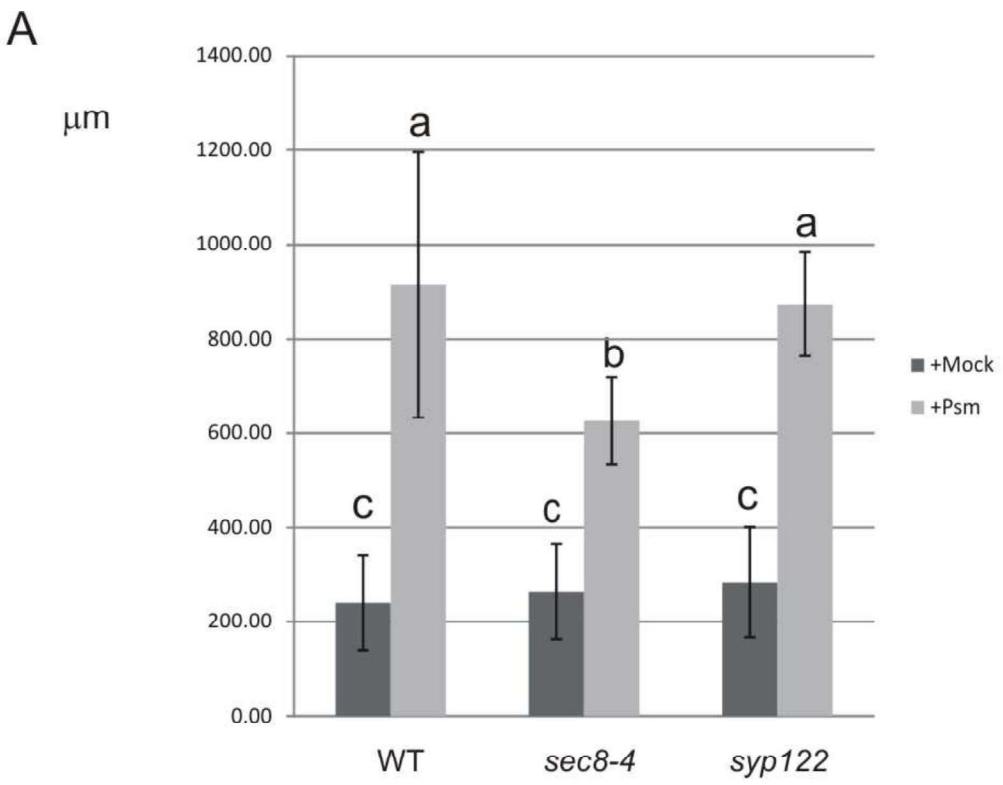

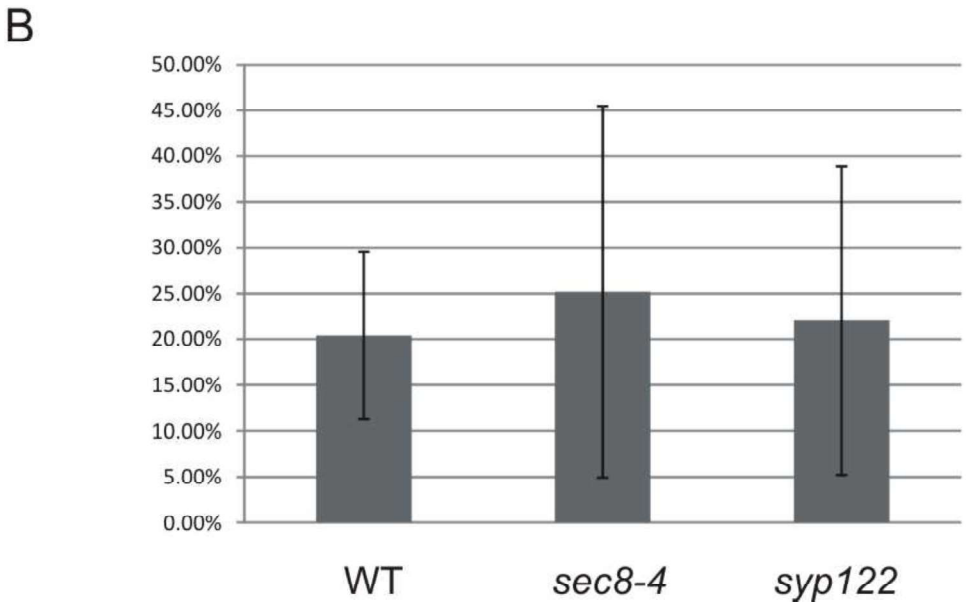

Supplementary Figure 9

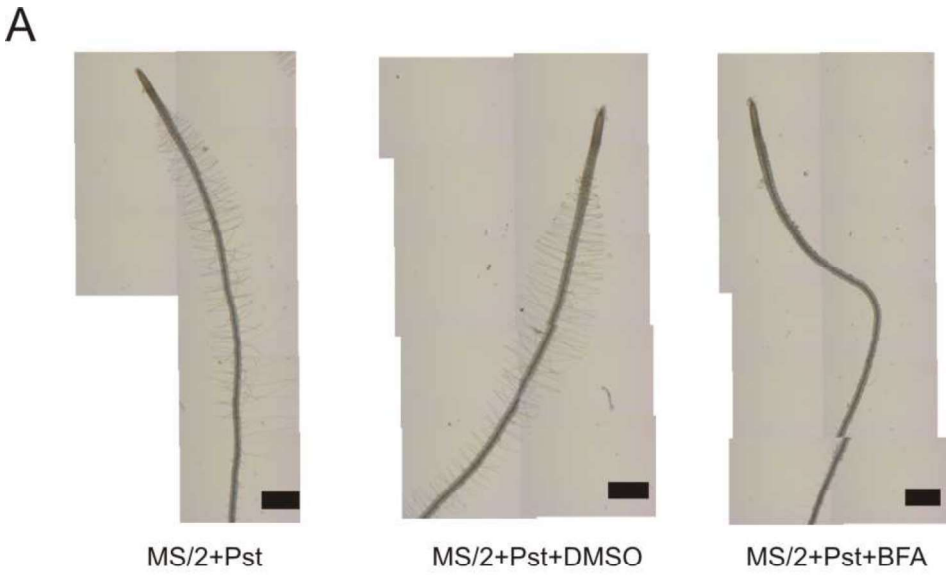

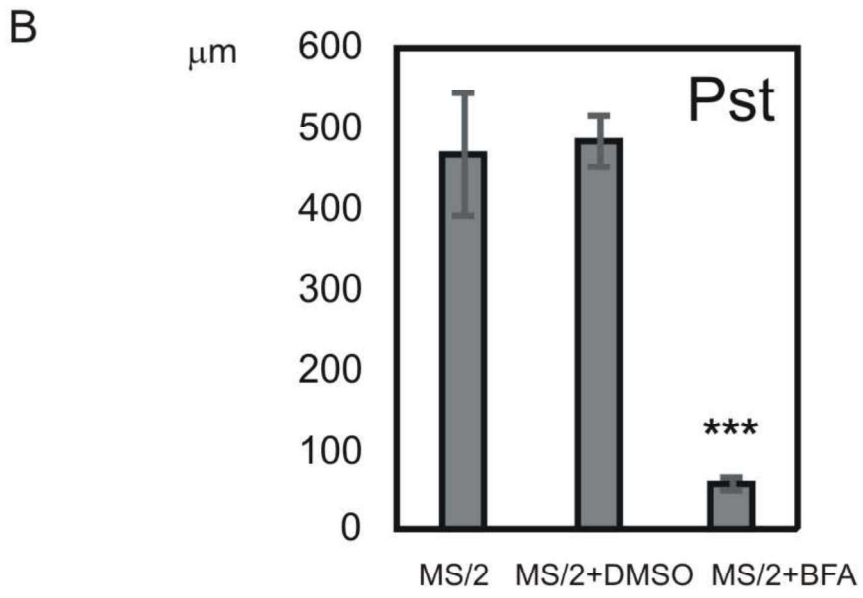

3. 3. PAPER No. 3

Title: EXO70B2-containing exocyst complex mediates fungal penetration resistance in Arabidopsis

Authors: Jitka Ortmannová, Tamara Pečenková, Juraj Sekereš, Ivan Kulich and Viktor Žárský

Summary:
Biotrophic fungal pathogens disrupt plant surface in an attempt to draw nutrients via their haustoria. To prevent the attack, plant cell builds cell wall reinforcement papilla or subsequently seal developing haustorium in encasement. We examined the role of the vesicle tethering complex exocyst in penetration resistance.

We tested penetration resistance in several *Arabidopsis* mutant lines of exocyst subunits upon the infection with non-adapted fungal pathogens *Blumeria graminis (Bgh)* and *Erysiphe pisi (Ep)* over time. We compared obtained phenotype of exocyst mutants with *syp121* mutant and examined possible interaction between exocyst and SYP121 in plant immunity.

We observed a diminished pre-invasive immunity but unaffected cell death response of exocyst mutants. Several exocyst core subunits along with the EXO70B2 isoform localized around the papillae and the encasements. We documented strong co-localization between the SYP121 and EXO70B2 profound especially during the papillae formation and direct SYP121 and EXO70B2 interaction.

Consistent with the importance of secretory pathway for the penetration resistance, we proved the substantial role of the exocyst complex in papilla and encasement formation. The EXO70B2 exocyst complex version in this process executed in cooperation with SYP121 – the double mutant *exo70B2/syp121* had significantly reduced defence efficiency against *Bgh* as compared to *syp121* single mutant.

My contribution: I performed or participated in all the experiments. I analyzed and discussed the obtained data. I wrote the manuscript with the help of other authors.

EXO70B2-containing exocyst complex mediates fungal penetration resistance in Arabidopsis

Jitka Ortmannová[1,2], Tamara Pečenková[1,2], Juraj Sekereš[1,2], Ivan Kulich[2], Viktor Žárský[1,2*]

1 Laboratory of Cell Biology, Institute of Experimental Botany, Academy of Sciences of the Czech Republic, Rozvojova 263, 165 02, Prague 6, Czech Republic

2 Laboratory of Cell Morphogenesis, Department of Experimental Plant Biology, Charles University in Prague, Faculty of Science, 128 44 Vinicna 5, Prague 2, Czech Republic

* Corresponding author

Laboratory of Cell Biology

Institute of Experimental Botany, Academy of Science, Czech Republic

Rozvojova 263

16502, Praha 6

The Czech Republic

zarsky@ueb.cas.cz; +420225106459

Manuscript:

Total word count of the main body: 6195

Introduction: 1181

Materials and Methods: 1196

Results: 2318

Discussion: 1404

Acknowledgements: 90

Number of figures: 7 (all in colour)

Supplementary data:9

Number of tables: 1

Number of figures: 7

Running title: EXO70B2-containing exocyst complex mediates fungal penetration resistance in Arabidopsis

Highlight: This study gives insight into a role of the exocyst complex in basal immunity and connects its functioning with the secretory pathway of SYP121-containing SNARE complex.

Summary

Biotrophic fungal pathogens disrupt plant surface in an attempt to draw nutrients via their haustoria. To prevent the attack, plant cell builds cell wall reinforcement papilla or subsequently seal developing haustorium in encasement. We examined the role of the vesicle tethering complex exocyst in penetration resistance.

We tested penetration resistance in several *Arabidopsis* mutant lines of exocyst subunits upon the infection with non-adapted fungal pathogens *Blumeria graminis (Bgh)* and *Erysiphe pisi (Ep)* over time. We compared obtained phenotype of exocyst mutants with *syp121* mutant and examined possible interaction between exocyst and SYP121 in plant immunity.

We observed a diminished pre-invasive immunity but unaffected cell death response of exocyst mutants. Several exocyst core subunits along with the EXO70B2 isoform localized around the papillae and the encasements. We documented strong co-localization between the SYP121 and EXO70B2 profound especially during the papillae formation and direct SYP121 and EXO70B2 interaction.

Consistent with the importance of secretory pathway for the penetration resistance, we proved the substantial role of the exocyst complex in papilla and encasement formation. The EXO70B2 exocyst complex version in this process executed in cooperation with SYP121 – the double mutant *exo70B2/syp121* had significantly reduced defence efficiency against *Bgh* as compared to *syp121* single mutant.

Keywords: complex exocyst, encasement, papilla, penetration resistance, plant immunity, secretory pathway, SNARE, SYP121

Introduction

In a struggle between a fungus and a plant, plant surface is the place where the battle starts. In the moment of detection of a pathogen/damage associated molecular patterns (PAMPs/DAMPs) and pressure, which a fungal pathogen exerts on the cell surface, plant cells start to react and re-polarize their secretory pathways to that point as a one of non-host resistance mechanisms (Schmelzer, 2002; Lee *et al.*, 2017). Through the massive secretion, plant cell forms a focal cell wall reinforcement called papilla (Bestwick *et al.*, 1995). The papilla is composed of a mixture of the cell wall and antimicrobial components, such as callose (beta-1,3-glucan), pectins, lignins, reactive oxygen species (ROS), phytoalexins and thionins (Schmelzer, 2002). If a fungus penetrates this barrier, it creates a feeding structure called haustorium surrounded by a specialized extrahaustorial membrane (EHM; Micali *et al.*, 2011). In return, plant cell may sequestrate the haustorium by secretion of an encasement, the defensive structure made of similar components as the papilla (Heath & Heath, 1971; Zeyen *et al.*, 2002, Meyer *et al*., 2009). The evolutionary non-adapted fungi to *Arabidopsis thaliana* host (further *Arabidopsis*) such as *Bgh* or *Ep*, in contrast to adapted once as *Golovinomyces cichoracearum*, cannot even effectively penetrate Arabidopsis cells or finish their live cycle using *Arabidopsis* as a host (Vogel & Somerville, 2000; Consonni *et al.*, 2006; Lipka *et al.*, 2008).

In *Arabidopsis*, three genes have been described as crucial for non-host penetration resistance against biotrophic fungi: t-SNARE *PENETRATION1* (*PEN1/SYP121*), myrosinase *PEN2* and ABC transporter *PEN3* (Collins *et al.*, 2003; Lipka *et al.*, 2005; Stein *et al.*, 2006). These three proteins operate in two separate pathways - while the SYP121 works as a part of the secretory pathway, the PEN2-PEN3 cooperate in secondary metabolite production and transport (Hückelhoven & Panstruga, 2011). Nevertheless, even the triple mutant *pen1pen2pen3*, which is dwarfish, displays complete resistance against *Bgh*, i.e. the fungus cannot complete its life cycle, thus other regulators of basal resistance must exist in *Arabidopsis* (Johansson *et al.*, 2014).

SYP121 is a transmembrane Qa-SNARE protein, which forms ternary SNARE complex with Qbc-SNARE SNAP33 (soluble N-ethylmaleimide-sensitive factor adaptor protein 33) and R-SNARE VAMP721/722 (vesicle-associated membrane protein 721/722) (Kwon *et al.*, 2008). This complex promotes exocytosis of secretory vesicles carrying so far unknown defence-related cargo to the plasma membrane PM/fungus contact sites (Assaad *et al.*, 2004; Kwon *et al.*, 2008; Meyer *et al.*, 2009). The GFP-SYP121 marks papillae and encasements. Besides that, it associates with exosomes in the extracellular matrix, the paramural space, of

those structures (Rutter & Innes, 2017). However, no functional impact of extracellular SYP121 on papilla or encasement function has been shown (Nielsen & Thordal-Christensen, 2013). Thus, the actual role of SYP121 takes place possibly on the membrane surrounding papilla and encasement after its transcytosis from its pool at the PM (Meyer *et. al.*, 2009; Nielsen *et al.*, 2012; Nielsen *et al.*, 2017). Only a few other regulators of the SYP121 defence secretory pathway have been described: the BFA sensitive ARF GTP exchange factor GNOM, as well as a component of the actin-myosin machinery MyosinIX (Nielsen *et al.*, 2012; Yang *et al.*, 2014). The SYP121 operates also in a complex with the specific MVB (multivesicular body) R-SNARE VAMP727, which may play the crucial role in the Rab-GTPase ARA6 dependent exosome secretion into the papillary matrix, thus rapidly delivering recycled pre-synthesized material to papilla (Ebine *et al.*, 2011; Nielsen *et al.*, 2012). Intriguingly, the ARA7 not ARA6 mediates the SYP121 transcytosis into the encasement, therefore two distinct MVB dependent secretory pathways may exist to distinguish between papilla and encasement formation (Nielsen *et al.*, 2017; Hansen and Nielsen *et al.*, 2018).

In yeasts and mammals, SNARE proteins execute their function in cooperation with other proteins and protein complexes, one of them being the exocyst complex (Hsu *et al.*, 1996; Sivaram *et al.*, 2005; Dubuke *et al.*, 2015; Yue *et al.*, 2017). In order for exocytosis to proceed through vesicle docking and fusion to the PM, vesicle first has to be properly tethered to it and this step is mediated by the exocyst (Munson & Novick, 2006; He *et al.*, 2007; Wu & Guo, 2015).

Exocyst is an octameric tethering complex, assembled from subunits SEC3, SEC5, SEC6, SEC8, SEC10, SEC15, EXO70 and EXO84 (TerBush *et al.*, 1996; Guo *et al.*, 1997). In plants, the exocyst complex has been found first by *in silico* analysis that showed the extensive multiplication of exocyst subunits genes, and later on its function was confirmed by genetic, biochemical and microscopic analyzes (Eliáš *et al.*, 2003; Cole *et al.*, 2005; Synek *et al.*, 2006; Hála *et al.*, 2008; Fendrych *et al.*, 2010, 2013). The phenomenon of evolutionary multiplication of exocyst subunit genes, particularly of *EXO70* gene family giving rise e. g. in *Arabidopsis* to 23 genes, could be related the necessity to specify and redirect secretory pathway to distinct cortical PM domains of an immobile plant cell (Žárský *et al.*, 2009; Vukašinović & Žárský, 2016). Recently, the comparative study of tobacco EXO70 family members has shown a diversity of behaviour of EXO70 isoforms and their ability to bind different domains within a pollen tube (Sekereš *et al.*, 2017). Current data indicate the possibility of an existence of more than one variant of the exocyst complex in a single plant cell, dependent on an EXO70 isoform bound to the core of the complex (Žárský *et al.*, 2013). Since the loss of EXO70A1 causes

dramatic developmental phenotype, the EXO70A1 may be the major isoform crucial for canonical secretion towards PM, whereas other isoforms may take its function in directing exocyst to other more specific cortical destinations.

In *Arabidopsis*, EXO70B clade represents two isoforms EXO70B1 and EXO70B2 (Cvrčková *et al.*, 2012). The EXO70B1, which mediates autophagy-related transport to the vacuole, is supposed to interfere with the effector-triggered immunity (Kulich *et al.*, 2013; Cui *et al.*, 2015; Zhao *et al.*, 2015). The connection with basal pathogen-associated molecular patterns triggered immunity (PTI) driven by SYP121 pathway has been excluded for EXO70B1, although it directly interacts with SYP121 and SNAP33 (Zhao *et al.*, 2015). On the contrary, EXO70B2, which also interacts with SNAP33, has been described as a positive regulator of PTI, the first layer of defence involved in penetration resistance (Pečenková *et al.*, 2011; Stegmann *et al.*, 2012) and so far no work has addressed the possible connection of EXO70B2 and SYP121 pathway in penetration resistance.

Based on our previous observation of EXO70B2 mutant impairment in the proper formation of papillae (Pečenková *et al.*, 2011), we studied the penetration resistance of several exocyst mutants toward two different non-adapted powdery mildew fungi *Bgh* and *Ep*. We detected defects in papillae formation and overall decreased penetration resistance in tested mutants. We showed an accumulation of a signal of the exocyst subunits tagged with GFP near papillae and in haustorial encasements. Genetic analysis indicated the synergic action of EXO70B2-containing exocyst and SYP121 t-SNARE, which also directly interacted and co-localized at the domain of papillae biogenesis. We conclude that the proper functioning of the exocyst complex involving isoform EXO70B2 is important for the penetration resistance, likely as a part of the previously characterised SYP121-dependent secretory pathway.

Material and Methods

Plant material

The seeds of *Arabidopsis thaliana* were sterilised and plated on 1/2 MS, 1% sucrose medium. The plants were grown in vitro for 10 days, and used for qRT-PCR, confocal imaging, or transferred into Jiffy tablets and grown in growth chamber under short day conditions (21°C, 10/14 light/dark h, 80% humidity and a light intensity of 125 μmol m^{-2} s^{-1} in a 400 - 700 nm range).

Pathogen inoculation and cytology

For pathogen inoculation experiments, plants were cultivated under short day conditions (21°C, 10/14 h, 75% humidity with a light intensity of 125 µmol m^{-2} s^{-1}). *Bgh* was cultivated continuously on fresh barley (Golden promise) grown under short day conditions (19°C, 10/14 h, 50% humidity, and a light intensity of 70 µmol m^{-2} s^{-1}). *Ep* was cultivated continuously on fresh pea (*Pisum sativum* variety petit provencal) cultivated under short day conditions (19°C, 10/14 h, 60% humidity and a light intensity of 70 µmol m^{-2} s^{-1}). The *Bgh* isolate A6 on barely genotype P01 was kindly provided by Laboratory of Pathological Plant Physiology. Max Planck Institute for Plant Breeding Research in Cologne Institute kindly provided the Ep isolate.

Plants, approximately 4 weeks old were inoculated by spreading of spores from infected barley or pea on the adaxial site of their leaves (from leaf to leaf). The 5th - 6th leaves were cut off at selected hpi and cleared with 96% ethanol or chloral hydrate. For callose visualisation cleared leaves were stained with an alkali solution of aniline blue (Eschrich & Currier, 1964). For penetration rate visualisation fungal structures were stained with 250 mg/ml trypan blue in lactophenol/ethanol solution (Vogel & Somerville, 2000). The additional protocol has been performed for the intense fungal structures staining as described by (Rate *et al.*, 1999). Stained leaves were observed with classical epifluorescence microscopy or optical microscopy by Nikon Eclipse TE 2000-E inverted microscope.

Transcript detection and semiquantitative RT-PCR

RNA was isolated from 100-120 mg of 14 days old plants using the RNeasy kit (Qiagen). RT-PCR was performed using Transcriptor High Fidelity cDNA synthesis kit (Roche) on 1 µg RNA. For PCR amplification, 2.5 µL of 20 × diluted cDNA was used and the gene-specific pairs of primers were used for semiquantitative PCR (Supplementary Table S8). The EXO70A1 was amplified as a cDNA quality control. Quantitative real-time PCR was carried out on a Light-Cycler 480, (Roche Applied Science, Mannheim, Germany) using GoTaq® qPCR Master Mix (Promega). Real-time PCR data were collected with following conditions: 5 min of initial denaturation at 95°C, then 45 cycles of 10 s at 95°C, 10 s at 58°C, and 15 s at 72°C. Cp values were normalized with the reference gene pUb, the plant ubiquitin (Czechowski et al., 2005). The expression level of each gene of interest (GOI) is presented as to http://www.plantphysiol.org/content/139/1/5.long (Janda et al., 2015).

Plasmid construction and generation of transgenic lines

All constructs were prepared by Phusion PC (NEB, USA) reaction using as a template either genomic DNA for intronless genes and promoters or cDNA obtained from RNA as described in the previous passage. List of used primers is presented in table (S8), as well as lengths of amplified fragments, restriction sites used for cloning procedure and destination vectors.

The sequenced vectors were transformed into *Agrobacterium tumefaciens* GV3101 strain. *Arabidopsis* WT or respective mutants were transformed by *Agrobacterium*-mediated floral dip method (Clough & Bent, 1998).

Microscopy

Microscopic observation of Arabidopsis plantlets attacked with pathogens was done by an inverted spinning disk confocal microscope with a high-resolution camera (Yokogawa CSU-X1 on Nikon Ti-E platform, laser box Agilent MLC400, with sCMOS camera Andor Zyla CSU-X1). The dynamic study was done with a high-speed camera (with sCMOS Andor iXon DU-897), using filter stringent cubes for GFP and RFP. Nikon Plan Apochromat x60 WI (NA = 1.2) and Plan Apochromat x100 OI (NA = 1.45) objective lenses were used for imaging, using 488- and 561-nm laser lines. Exposure time was 700 ms, 488 nm laser power of 75%. Fluorescence profiles and acquired images were exported from NIS ELEMENTS 4.1 software (Nikon, Tokyo, Japan) – identical settings were used for each image. Figures were then analyzed in ImageJ Fiji software (http://rsbweb.nih.gov/ij/). Microscopic analysis of tissue staining with aniline or trypan blue was performed using an Olympus BX51 microscope with attached DP50 camera x100 OI (NA = 1.35) objective (Olympus; Trypan blue) or Zeiss AxioImager ApoTome2 microscope 20x objective (Aniline blue). For fungal structure visualisation in vivo the propidium iodide PI 1:500 or FM4-64 dye 1:1000 diluted in water was used. To perform lambda scan the Zeiss LSM 880 confocal scanning microscope with a Zeiss C-Apochromat 40x (NA = 1.2) W Korr FCS M27 or C-Apochromat x63 OI (NA = 1.45) objective was used. Excitation wavelengths used were 488 nm for GFP and 561 nm for mRuby2, PI and FM4-64. The linear unmixing was performed with the ZEISS BLACK software.

Yeast Two-Hybrid Assay

The SYP121 DNA (obtained from Riken) was amplified from cDNA with primers excluding the transmembrane domain and cloned into pGADT7 vector (Clontech Laboratories,

Inc.). All the other exocyst constructs used in the study have already been described (Hála *et al.*, 2008; Pečenková *et al.*, 2011; Žárský *et al.*, 2013; Vukašinović *et al.*, 2014). Different pGBKTs with pGAD with an inserted non-coding piece of vector pENTR3C were used as negative controls. At least 10 positive colonies from –Leu/–Trp plates were resuspended in 150µl of sterile water, diluted 30x and 900x, and subsequently plated onto –Leu/–Trp/–His/-Ade plate.

Protein extraction, SDS Gel Electrophoresis and Western Blot

Total protein extracts were isolated from 2-4 weeks old plants transformed with EXO70B2-GFP in different time points 0-24 hpi *Bgh* or water (mock) inoculation. The protein extraction Sec6/8 buffer adjusted for the exocyst extraction was used (20 mM HEPES, pH 6.8, 150 mM NaCl, 1 mM EDTA, 1 mM DTT, and 0.5% Tween, supplemented with 13 protease inhibitor cocktail (Sigma-Aldrich). After one hour of lysis, the extracts were spun down and the supernatants were boiled with 6x SDS loading buffer.

The proteins were loaded on 10% SDS-PAGE, blotted to a nitrocellulose membrane and blocked overnight with 5% non-fat dry milk in PBS (137 mM NaCl, 2.7 mM KCl, 10 mM Na2HPO4, and 2 mM KH2PO4, pH 7.4, 0.25% Tween 20). Primary antibody dilutions in PBS were as follows: polyclonal mouse anti-GFP, 1:1000; polyclonal rabbit antibodies anti-AtEXO70A, 1:1500; anti-AtSEC3, 1:5000; anti-AtSEC5, 1:5000; anti-AtSEC6 (Agrisera Sweeden), 1:10000; anti-AtSEC8 (Agrisera Sweeden), 1:8000; anti-AtSEC10, 1:10000; anti-AtSEC15a, 1:1000 and anti-AtEXO84b, 1:1000. Appropriate secondary horseradish peroxidase–conjugated antibodies (Promega, Madison, WI, USA) were applied and followed by chemiluminescent ECL detection (Amersham, GE Healthcare, Chicago, IL, USA).

Co-immunoprecipitation

*Arabi*dopsis seedlings (1 g of 10-day-old) were used for the co-immunoprecipitation of proteins. Protein complexes with GFP-SYP121-GFP, PEN3-GFP and free GFP as a control, were isolated using the µMACS GFP-tagged protein isolation kit (Miltenyi Biotec), according to the manufacturer's instructions. The only exception was a utilisation of the Sec6/8 buffer (Hála *et al.*, 2008) as a wash buffer, two times and lysis buffer provided in the kit as a third more stringent wash. Bound proteins were eluted with 100 µL of the preheated elution buffer. In order to analyze bound proteins in an eluted fraction, SDS-PAGE and western blot were performed.

Results

Characterisation of non-host fungus/plant cell interaction phenotypes in exocyst mutants

To investigate a role of the exocyst complex in penetration resistance, we observed the interaction between germinated spores of *Bgh* or *Ep* and *Arabidopsis* lines with mutated genes of selected exocyst subunits. Although *Bgh* and *Ep* are not adapted to *Arabidopsis*, they evoke a range of defence reactions and are even able to accomplish the penetration (Takemoto *et al.*, 2006). We examined interaction sites on infected leaves of 4 weeks old plants using trypan blue staining for fungal structures and aniline blue staining for callose accumulation visualisation (Fig.1). Along with previously characterised stages or types of fungal propagation and defence reactions as known from *Arabidopsis* wild-type (WT) leaves (Takemoto *et al.*, 2006), we repeatedly observed also other deviations from a normal papillae deposition in exocyst mutant lines. We categorized observed fungus/plant cell interactions into 4 major types: A) regular papilla (properly developed papilla, circular from the top view); B) deviated papilla (papilla with vesicular clump described by (Pečenková *et al.*, 2011) or enlarged papilla with the diameter more than twice as compared to regular papilla); C) haustoria (completely unencased, partially or fully encased haustoria) and finally type D) cell death (cells undergoing programmed cell death, PCD) including dead cells with haustorium (Fig. 1). In the case of deviated papillae in mutant lines (type B), we identified two distinct patterns of callose deposition defect. The vesicular clump category exhibited a reduction of callose and stacking of faint callose spots around the appressorium (Fig. 1B). In contrast, the enlarged papillae showed over accumulation of callose as well as bigger papillae body observed in the bright field (Fig. 1B). Even though the observed stages and cellular phenotypes were the same for *Bgh* and *Ep*, generally the *Ep* inoculation caused slower but more successful penetration than *Bgh* and was less often associated with PCD.

The exocyst mutant lines display impaired penetration resistance

We quantified occurrence of A-D types of defence reactions (see Fig. 1) at 24 and 48 hours post inoculation (hpi) in three lines mutated in the exocyst core subunit genes: knockout line (KO) *sec15b-1* (salk_130663, Fig. S1D,E), KO *sec5a-1* (GABI_731C01, Fig. S1A-C), the knock-down *sec8-m4* (Cole *et al.*, 2005) and KO *exo70B2-2* mutant (further on *exo70B2)* representing *EXO70* gene known to be involved in the plant immunity (Pečenková *et al.*, 2011). We tested also KO mutant *exo70B1-1* (Kulich *et al.*, 2013) and KO mutant *exo70A1-2* (Synek *et al.*, 2006) - a mutant line of another *EXO70* clade for the comparison. As a positive control,

we used the KO mutant line *syp121-1* (Collins *et al.*, 2003). As a negative control, we used two independent outcrossed homozygous WT lines from *exo70B2*/Col-3 and *syp121*/Col-0 heterozygous mutant backgrounds. There was no significant difference between both WT lines. Since *Ep* spores germinated more slowly than *Bgh,* we used 48h longer treatment for *Ep* penetration evaluation. For quantification purposes, we considered epidermal cells attacked by a single germinated spore. During the staining procedure spores not forming appressorium were washed out, thus the "No interaction" category comprises germinated attached spores without visible plant cell reaction. All mutant lines in exocyst core subunit genes were more sensitive to fungal attack than WT (Fig. 1E and S2C, D). In accordance with published data (Pečenková *et al.*, 2011), *exo70B2* demonstrated a higher occurrence of deviated papillae and a slight increase of *Bgh* haustoria development (Fig. 1E, F). This trend was more prominent upon *Ep* infection, which is more successful also in penetration of WT (Fig. S2A, B). The most prominent feature of exocyst lines analyzed here was the formation of deviated papillae (Fig. 1E) and increased successful penetration of *Bgh* and *Ep* (Fig. 1F and S2C, D). This indicates a clear impairment of pre-invasive immunity in the exocyst mutants. Interestingly, a strong deviation from proper papillae formation in the *sec5a-1* mutant at 24 hpi with *Bgh* (Fig. 1E) disappeared one day later at 48 hpi (Fig. 1F). Strongly dwarfed *exo70A1-2* plants (Synek *et al.*, 2006) showed, in contrast to other exocyst mutants tested, lower number of interaction events to *Bgh* at 48 hpi (Fig. 1F) but sported the higher incidence of deviated papillae (Fig. 1F). On the other side, the *exo70B1-1* mutant was more prone to interact with *Bgh* and showed a higher occurrence of regular papillae than WT at 48 hpi (Fig. 1F). Thus among the three EXO70 isoform mutants tested, only the *exo70B2* showed the stable loss of penetration resistance.

The exocyst complex and SYP121 disruption similarly modulate the progression of fungal infection

Since the exocyst complex operates in the secretory pathway, we inspected if its role in the penetration defence could be similar to the previously reported role of SYP121, which is crucial for proper timing of papillae development and related callose deposition upon infection with *Bgh* (Assaad *et al.*, 2004; Nielsen *et al.*, 2012). We analyzed the development of haustoria (Fig. 2A), as an obvious penetration marker, in leaves together with the activation of PCD (Fig. 2B) in *sec8-m4* core subunit mutant and in *exo70B2,* in comparison with control lines WT and *syp121* mutant. The knock-down mutant *sec8-m4* plants exhibited normal growth under standard cultivation conditions (Cole *et al.*, 2005). The same applies to the KO mutant *syp121*, under the optimal growth conditions (Collins *et al.*, 2003; Eisenach *et al.*, 2012). In our

experiment the mutant *sec8-m4* allowed faster penetration of *Bgh* than the WT, but slower than *syp121* (Fig. 2A). The *exo70B2* penetration was slightly higher than WT (Fig. 2A), thus its major defect upon the *Bgh* infection are papillae with the vesicular clump formation. Both *sec8-m4* and *syp121* mutants exhibited the same trend in the PCD rate - the PCD gradually increased until bursting at 72 hpi. This burst occurred also in WT and *exo70B2,* but with less intensity (Fig. 2B). In this time point, most of the previously attacked cells underwent the PCD, therefore the number of observed haustoria dropped down. This tendency showed that in both mutants the activation of PCD occurred normally as in WT. Since the higher penetration success of *Bgh* in *syp121* has been associated with the delay in callose deposition in early defensive papillae development, we verified the amount of papillary callose in our mutant lines (Fig. 2C). We observed the comparable delay in callose deposition for *sec8-m4* and *syp121* mutants, while *exo70B2* mutant exhibited the strongest inhibition. These results were in contrast with the relative weak penetration defect of *exo70B2* and *sec8-m4* mutants that reflects incidence of created haustoria and dead cells (Fig. 2A, C).

Exocyst subunits localize to the defensive papillae formation domain

Using spinning disc confocal microscopy, we observed localization and dynamics of several GFP-tagged exocyst subunits in adult leaves at 20-24 hpi with *Bgh* (Fig. 3A). The FM4-64 dye was used to stain PM and fungal structures. The localization of exocyst subunits was imaged in parallel with positive control GFP-SYP121 (Kato *et al.*, 2010), which hyper-accumulates at the membrane domain of papilla (incidence of accumulation 58%±10 of 50 spores) and encasement as well as in their paramural space (Assaad *et al.*, 2004; Nielsen *et al.*, 2012). The signal of exocyst complex core subunits tested – Ub:SEC5a-GFP (52%±5) and with natural promoters GFP-SEC3a (50%±5; Bloch *et al.*, 2016), SEC6-GFP (60%±8), GFP-SEC8 (42%±9; Fendrych *et al.*, 2013), SEC10a-GFP (48%±3; Vukašinović *et al.*, 2017) and EXO70B2-GFP (38%±12) was enriched at the contact site with the fungus, the papillary membrane cortical domains (Fig. 3A, B). To avoid false positive exocyst localization signals, we always compared the GFP signal maxima of papillae with the autofluorescence of non-transformed plants (Fig. 3B). On the other side, the GFP-EXO70B1 (5%±2) under natural promoter appeared at the penetration site exceptionally and not with a higher abundance (Fig. S4B). We compared dynamics of the EXO70B2-GFP and the SEC6-GFP localization with the SYP121-GFP in the papilla cortical membrane domain. The kymographs generated from time series showed that the localization of exocyst within the papilla is stationary (Fig. S3). Therefore, we compare this stable exocyst domain to previously described exocyst PM

localization in secondary cell wall deposition in tracheary elements (Vukašinović *et al.*, 2017) in contrast to dynamic exocyst at the lateral PM domains of rhizodermal cells (Fendrych *et al.*, 2013).

Out of tested exocyst subunits, the EXO70B2-GFP signal was hardly detectable in leaves without a pathogen treatment (see further). Using the lambda scan mode, we confirmed that the faint signal observed in infected cells of EXO70B2-GFP plants was true GFP signal and not the autofluorescence (Fig. S4A). We concluded that the EXO70B2-containing exocyst complex is enriched at the cortical membrane domain of papilla. To investigate a mutual relationship between exocyst and SYP121 in a papilla development, we coexpressed the EXO70B2-mRuby2 with the GFP-SYP121, both under their natural promotors (Fig. 3C). The EXO70B2 co-localized with the SYP121 exclusively in the papilla cortical PM domain (Fig. 3C). Thus, contrary to transmembrane Qa-SNARE SYP121, the peripheral membrane EXO70B2 exocyst subunit did not accumulate in the paramural space of papilla, as confirmed using a plasmolysis and subsequent co-localization analysis (Fig. 3C).

Exocyst co-localizes with the growing structure of haustorial encasement

Bgh and *Ep* are both able to occasionally successfully penetrate non-host plant cell and develop haustoria, which become later encased. Using optical sectioning confocal microscopy, we observed GFP-fused exocyst subunits in haustorial encasements and their collars (for the description see Fig.1). We inspected the surface of haustorium and showed the three different stages of the encasement formation for EXO70B2-GFP (Fig. 4A, C, E) and SEC6-GFP (Fig. 4B, D, F). We observed that the EXO70B2-GFP signal outlined not only the papilla body (Fig. 4A) but also the collar of haustoria (Fig. 4C, E, yellow arrowheads) and the encasement itself (Fig. 4A, C). However, the signal was excluded from the part of haustoria lacking the encasement, i.e. it was not present at the extrahaustorial membrane (EHM, Fig. 4C, pink arrowheads). The very tips of haustoria were marked by EXO70B2-GFP only if they were in the stage of encasement closing. The same was true for SEC6-GFP representing the exocyst core subunit (Fig. 4F, pink arrowhead). The maximum intensity of signals showed the difference between EXO70B2-GFP and the SEC6-GFP signal. The SEC6 displayed higher signal in papilla (Fig. 4B) or the neck (Fig. 4D, yellow arrowhead) than EXO70B2-GFP, and stayed excluded from the EHM (pink arrowhead in Fig. 4D; this observation was verified by lambda scan analysis - Fig. S5). We observed the same localization pattern for GFP-SEC8 (Fig. S6). These observations indicated that a version of EXO70B2-containing exocyst complex may also have a specific role in encasement biogenesis.

EXO70B2 expression level increases after the fungal attack

EXO70B2 mRNA level was shown to be upregulated after various elicitor treatments in *Arabidopsis* (Pečenková *et al.*, 2011). To verify observation that the EXO70B2-GFP signal rises after the *Bgh* attack, we analyzed its mRNA and protein level upon fungus attack. For the understanding of complex behaviour, we compared EXO70B2 expression responsiveness to the biotic stress with the core exocyst subunit SEC8. We showed the striking difference between the upregulation of the EXO70B2 mRNA level compared to unaltered expression of SEC8 8 hpi with *Bgh* (Fig. 5A). We used several stable lines expressing the EXO70B2-GFP driven by the native promoter in the *exo70B2* mutant background, which complemented its phenotype in penetration resistance (Fig. S7). In those plants, we examined a protein level of SEC8, EXO70A1 and EXO70B2-GFP with or without the *Bgh* treatment. The level of the EXO70B2 protein grew significantly up at 4 hpi and stayed unchanged even at 24 hpi *Bgh*. The level of the EXO70A1 slightly decreased, while the level of the SEC8 stayed unchanged (Fig. 5B). This suggests a putative replacement of EXO70 isoforms in exocyst complex under specific conditions as proposed before (Žárský *et al.*, 2013).

In order to detect the earliest point of the EXO70B2 recruitment to the *Arabidopsis/Bgh* interaction PM cortical domain, we acquired images of a contact site with *Bgh* every two hours starting from the point of inoculation. We observed the very first signal of the EXO70B2 accumulated at the fungal attack site at 8±1 hpi (Fig. 5C). The GFP-SEC3 and SEC6-GFP presented mostly in the cytoplasm of the epidermal cells, were recruited to the papillae at the similar time point (Fig. S8).

The EXO70B2-containing exocyst complex interacts with SYP121

To address the possible direct association between the exocyst and SNARE SYP121 complexes, we performed co-immunoprecipitation with the total protein extracts of seedlings expressing GFP-SYP121 as a bait, both under normal and *Bgh* treatment conditions. The eluted fractions were tested for the presence of the exocyst by the set of available antibodies, mainly raised against the exocyst core subunits SEC3, SEC5, SEC6, SEC8, SEC10, SEC15b and EXO84b, as well as against the predominant EXO70 isoform EXO70A1. In the eluted GFP-SYP121 positive fraction, we identified the EXO70A1, SEC6 and SEC3 (Fig. 6A). We tested the possible direct interaction of SYP121ΔC, free from transmembrane domain, and exocyst in the yeast-two-hybrid system. As the positive control, we used known SEC3a/EXO70A1 interaction pair (Hála *et al.*, 2008). Unexpectedly, out of many pairs tested (AD-

SYP121ΔC/BD-EXO70A1, EXO70B1, EXO70B2, EXO70H1, SEC3a, SEC5a, SEC6, SEC8, SEC10a, SEC15b, EXO84b), we detected only weak interaction for EXO70B1-SYP121ΔC and EXO70B2-SYP121ΔC pairs (Fig. 6B). In order to show the possible biological relevance of the interactions, we created two double mutants *exo70B1/syp121* and *exo70B2/syp121*. We challenged these mutants with *Bgh* for 48 hours and then analyzed the fungal penetration success. We noticed that, although there was not a significant difference in a total number of interactions (Fig. 6C), both *exo70B1/syp121* and *exo70B2/syp121* double mutants had significantly increased number of unencased haustoria (Fig. 6D) when compared to *syp121* single mutant. Only *exo70B2/syp121* double mutant, however, had decreased number of encased haustoria when compared to *syp121* single mutant (Fig. 6C). The pronounced double mutant phenotype of *exo70B2/syp121* was even more apparent with respect to the reduction of callose deposition signal in leaves (callose from haustoria and papillae; Fig. 6E). Thus, double mutant *exo70B2/syp121* had significantly reduced defence efficiency against *Bgh*, unlike the *exo70B1/syp121*, which did not differ from *syp121*. We expected the recruitment of the rest of the exocyst complex might be damaged or slowed down, therefore, we expressed SEC6-GFP in the double mutant *exo70B2/syp121* and followed its localization after *Bgh* treatment. The SEC6-GFP signal surrounded the fungal attack site at the same time in both WT and *exo70B2/syp121* mutant background even when the penetration of a fungal germ tube occurred already (Fig. S8).

Discussion

The model system of interactions between non-host pathogens *Bgh* or *Ep* and *Arabidopsis* has been successfully used in studies of the role of the secretory pathway in the plant immunity before. In this report, we analyzed the cell immunity phenotypes of several *Arabidopsis* lines mutated in exocyst subunit genes in defence response against *Bgh* and *Ep*. We showed that the exocyst complex involving EXO70B2 is required for full penetration resistance against non-adapted biotrophic fungi.

The exocyst is the major regulator of plant cell secretion and polarity, so disruption of the complex leads to severe growth phenotypes (Synek *et al.*, 2006; Hála *et al.*, 2008; Fendrych *et al.*, 2010). In order to avoid pleiotropic mutation effects and to study the specific role of plant exocyst in reaction to fungal penetration, we worked with weak allele lines of core exocyst subunits *sec8-m4*, *sec5a-1* and *sec15b-1* that do not have severe growth phenotype. For these mutants, we were able to describe new interaction phenotypes resulting from a defence reaction of plant cells with impaired secretory machinery, apart from the previously described stages of *Bgh* progression in WT (Takemoto *et al.*, 2006). Along with the vesicular

clump, which has been previously characterised as a vesicular halo in the *exo70B2* mutants (Pečenková *et al.*, 2011), we newly described the presence of enlarged papillae. Using aniline blue staining, we showed that in the papillae with the clump, the aniline blue positive signal was present in vesicular compartment surrounding the attack sites (Underwood, 2012; Chowdhury *et al.*, 2014). In contrast to faint aniline blue signal of papillae with the vesicular clump, the enlarged papillae reflected probably the ectopic callose deposition behind the regular papillae body (Fig. 1B). Such papillae resembled the phenotype of the overexpressing line PMR4 (Blümke *et al.*, 2013). Although we categorized these papillae as deviated, we cannot exclude that they might be partly functional or transform into regular papillae or PCD as might be the case of *sec5a* mutant line (Fig. 1E, F). We also cannot exclude, that the enlarged callose deposition is the result of an impaired callose degradation. Even though all the exocyst mutants tested had diminished penetration resistance, they differed in some response categories. Therefore, we focused on mutant lines providing the most reproducible phenotype - the *exo70B2* and *sec8-m4*. We found that both have a distinct delay in penetration defence (Fig. 2), as well as the higher occurrence of successfully penetrated cells by haustoria (Fig. 1E, F). This phenotype resembles the more severe phenotype of *syp121*, in which major defect in penetration resistance is the delay of secretion marked by callose deposition in papillae (Assaad *et al.*, 2004; Nielsen *et al.*, 2012). The occurrence of deviated papillae, the lower penetration resistance, and the delayed callose deposition in the exocyst mutants reflected defects in the normal exocytotic machinery and importance of functional secretion pathway in defence over time. Recently, the exocyst and especially SEC5 role in callose secretion in PTI has been shown in tobacco (Du *et al.*, 2015; Du *et al.*, 2018). Here we showed that *exo70B2* and *sec8-m4* mutants have the delay in early callose deposition comparable to *syp121*, but their penetration resistance did not compromise so drastically. This result pointed to the importance of secretion timing in penetration resistance but indicated callose as a possibly less important component in it.

The exocyst subunits have been demonstrated to work within the stable protein complex in yeast cells (Heider *et al.*, 2015; Yue *et al.*, 2017; Picco *et al.*, 2017). The *EXO70* gene has many paralogs in plant genomes (Eliáš *et al.*, 2003) and several EXO70 protein isoforms (ie EXO70B2) are targets of rapid proteolytic degradation (Stegmann *et al.*, 2012; Seo *et al.*, 2016). Therefore we hypothesized, that the exocyst complex in plant cells is capable of exchanging EXO70 isoforms in order to target secretion to particular membrane domains as previously proposed (Žárský *et al.*, 2009, 2013; Pečenková *et al*., 2017). In this report, we focused on the EXO70B2, because it is the only exocyst subunit previously confirmed to be

involved in the papillae formation and penetration resistance against non-adapted fungi. Its localization has been analyzed only transiently in *Nicotiana benthamiana* or *Arabidopsis* protoplast and never in papilla structure (Pečenková *et al.*, 2011; Stegmann *et al.*, 2012). We compared the behaviour of EXO70B2, the closest paralog of EXO70B1 and the EXO70A1 (possibly major exocytotic EXO70 in Arabidopsis – Synek *et al.*, 2006), during the reaction to fungal penetration and confirmed the EXO70B2 is the isoform specifically involved in this particular process. We found only a faint cytoplasmic signal of the EXO70B2-GFP and the GFP-EXO70B1 at the edge of detection limit in non-treated seedlings or mature leaves. We spotted early protein upregulation and focal accumulation of the EXO70B2-GFP beneath the contact sites with *Bgh*. This was not a case of the GFP-EXO70B1 signal. Intriguingly, we showed that this increase in the EXO70B2-GFP protein level correlated with the EXO70A1 depletion, while the SEC8 stayed unchanged (Fig. 5). The level of EXO70B2 is thus tightly regulated in the context of a pathogen attack, as proposed before (Pečenková *et al.*, 2011). This notion is in concert with previous discovery of both the EXO70A1 and the EXO70B2 being the target of regulated proteasomal degradation (Samuel *et al.*, 2009; Stegmann *et al.*, 2012). After the recently reported different localization of EXO70 isoforms in spatially different membrane domains of pollen tubes (Sekereš *et al.*, 2017), we thus indicate the possible replacement of one EXO70 isoform by another one in time in response to a specific stimulus.

We demonstrated that both Arabidopsis EXO70Bs directly interact with soluble SYP121. We also showed that in defence against non-adapted powdery mildew, the simultaneous loss of EXO70B2 and SYP121 disturbed the penetration resistance and reduced the immunity response. Unlike the *exo70B1/syp121* double mutant, the *exo70B2/syp121* showed an additive phenotype in the penetration defence. This support a common role of SNARE and exocyst complexes in PTI. Nevertheless, the association between SYP121 and exocyst may found biological relevance in the canonical SNARE driven secretion, where different EXO70 may participate. The cooperation of EXO70B2 and SYP121 in non-host resistance has been proposed also based on their co-expression together with SNAP33 and VAMP722 (Humphry *et al.*, 2010). However, the cooperation dynamics of the two proteins might differ in the papillae and the encasement formation, since we found the additive phenotype of *exo70B2/syp121* double mutant only for the encasement formation and not the papilla. It has been shown before, that the SYP121 transcytosis plays possibly an important role in the formation of both the defensive structures by two independent pathways. The formation of the encasement, but not the formation of papillae, relied on the function of ARA7, the GTPase closely related to ARA6 (Nielsen *et al.*, 2017). The study has suggested a model

in which the influence of the SYP121 on the papillae formation might be stronger than in the case of encasement formation, where another Qa-SNARE may take the main function (Hansen and Nielsen *et al.*, 2018). This would be in agreement with our results showing the *syp121* mutation epistasis over *exo70B2* mutation in papillae formation and the increased importance of the EXO70B2 function in the encasement formation (see model Fig. 7). Based on the localization studies, our model introduces the membrane-localized EXO70B2-containing complex as a member of the secretory pathway, which drives a structural material towards papillae and encasements (Fig. 7). It remains to be further elucidated whether this reflects SYP121-dependent (cooperation on the level of the encasement formation) or - independent (SYP121 function in the papillae formation with subsequent EXO70B2 function in the encasement formation) process. A more detailed study is needed in order to assess these hypotheses.

The model situation of papillae development used in our study allowed us to demonstrate the functional relationship between SNARE and EXOCYST complexes. We conclude that our data on exocyst localization and behaviour resembles dynamics of SYP121 SNARE complex. Moreover, our genetic analyzes clearly indicate that the exocyst complex containing EXO70B2 is involved along with SYP121 in secretion process supporting the defence against non-adapted powdery mildew. It is possible, that the EXO70B2-containing exocyst complex recognizes the attack sites to target exocytosis and to regulate SYP121-mediated vesicle fusion there. Thus exocyst mediates the time-dependent focal secretion of papillae and encasements materials, including callose as one of the components. SYP121 localization to the paramural space vs. exocyst absence in it indicates that additional mechanistic details and time sequence of exocyst vs. SNARE action will need further studies.

Acknowledgement

This work was supported by Czech Science Foundation (CSF/GACR) project GA15-14886S and by NPUILO1417 of MEYS CR. It was founded by terminated student project GAUK-1102214 by Grant Agency of Charles University. The Institute of Experimental Botany (IEB) Imaging Facility is supported by the Operational Programme Prague Competitiveness (OPPC) CZ.2.16/3.1.00/21519 and Czech-BioImaging large RI project (LM2015062 funded by MEYS CR).

Authors would like to thank Peter Sabol for help with text editing and cloning assistance, Martin Potocký for fruitful discussion and image software guidance and Jana Šťovíčková for reliable technical support.

Author Contributions

Conceived and designed the experiments: JO, TP, VZ. Performed the experiments: JO, TP. Analyzed the data: JO. Contributed reagents/materials/analysis tools: JO, TP, JS, IK. Wrote the paper: JO, TP, JS, VZ.

References

Assaad FF, Qiu J-L, Youngs H, Ehrhardt D, Zimmerli L, Kalde M, Wanner G, Peck SC, Edwards H, Ramonell K, *et al.* 2004. The PEN1 syntaxin defines a novel cellular compartment upon fungal attack and is required for the timely assembly of papillae. *Molecular biology of the cell* **15**: 5118–5129.

Bestwick CS, Bennett MH, Mansfield JW. **1995**. Hrp Mutant of Pseudomonas syringae pv phaseolicola Induces Cell Wall Alterations but Not Membrane Damage Leading to the Hypersensitive Reaction in Lettuce. *Plant physiology* **108**: 503–516.

Bloch D, Pleskot R, Pejchar P, Potocký M, Trpkošová P, Cwiklik L, Vukašinović N, Sternberg H, Yalovsky S, Žárský V. **2016**. Exocyst SEC3 and Phosphoinositides Define Sites of Exocytosis in Pollen Tube Initiation and Growth. *Plant physiology* **172**: 980–1002.

Blümke A, Somerville SC, Voigt CA. **2013**. Transient expression of the *Arabidopsis thaliana* callose synthase PMR4 increases penetration resistance to powdery mildew in barley. *Advances in bioscience and biotechnology* **04**: 810–813.

Chowdhury J, Henderson M, Schweizer P, Burton RA, Fincher GB, Little A. **2014**. Differential accumulation of callose, arabinoxylan and cellulose in nonpenetrated versus penetrated papillae on leaves of barley infected with Blumeria graminis f. sp. hordei. *The New phytologist* **204**: 650–660.

Clough SJ, Bent AF. **1998**. Floral dip: a simplified method forAgrobacterium-mediated transformation ofArabidopsis thaliana. *The Plant journal: for cell and molecular biology* **16**: 735–743.

Cole RA, Synek L, Žárský V, Fowler JE. **2005**. SEC8, a subunit of the putative Arabidopsis exocyst complex, facilitates pollen germination and competitive pollen tube growth. *Plant physiology* **138**: 2005–2018.

Collins NC, Thordal-Christensen H, Lipka V, Bau S, Kombrink E, Qiu J-L, Hückelhoven R, Stein M, Freialdenhoven A, Somerville SC, *et al.* 2003. SNARE-protein-mediated disease resistance at the plant cell wall. *Nature* **425**: 973–977.

Consonni C, Humphry ME, Hartmann HA, Livaja M, Durner J, Westphal L, Vogel J, Lipka V, Kemmerling B, Schulze-Lefert P, *et al.* 2006. Conserved requirement for a plant host cell protein in powdery mildew pathogenesis. *Nature genetics* **38**: 716–720.

Cui H, Tsuda K, Parker JE. **2015**. Effector-Triggered Immunity: From Pathogen Perception to Robust Defense. *Annual review of plant biology* **66**: 487–511.

Cvrčková F, Grunt M, Bezvoda R, Hála M, Kulich I, Rawat A, Žárský V. **2012**. Evolution of the land plant exocyst complexes. *Frontiers in plant science* **3**: 159.

Czechowski T, Stitt M, Altmann T, Udvardi MK, Scheible W-R. **2005**. Genome-wide identification and testing of superior reference genes for transcript normalization in Arabidopsis. *Plant physiology* **139**: 5–17.

Dubuke ML, Maniatis S, Shaffer SA, Munson M. **2015**. The Exocyst Subunit Sec6 Interacts with Assembled Exocytic SNARE Complexes. *The Journal of biological chemistry* **290**: 28245–28256.

Ebine K, Fujimoto M, Okatani Y, Nishiyama T, Goh T, Ito E, Dainobu T, Nishitani A, Uemura T, Sato MH, *et al.* 2011. A membrane trafficking pathway regulated by the plant-specific RAB GTPase ARA6. *Nature cell biology* **13**: 853–859.

Eisenach C, Chen Z-H, Grefen C, Blatt MR. **2012**. The trafficking protein SYP121 of Arabidopsis connects programmed stomatal closure and K^+ channel activity with vegetative growth. *The Plant journal: for cell and molecular biology* **69**: 241–251.

Eliáš M, Drdová E, Ziak D, Bavlnka B, Hála M, Cvrčková F, Soukupová H, Žárský V. **2003**. The exocyst complex in plants. *Cell biology international* **27**: 199–201.

Eschrich W, Currier HB. **1964**. Identification of Cauose by its Diachrome and Fluorochrome Reactions. *Stain technology* **39**: 303–307.

Fendrych M, Synek L, Pečenková T, Drdová EJ, Sekereš J, de Rycke R, Nowack MK, Žárský V. **2013**. Visualization of the exocyst complex dynamics at the plasma membrane of Arabidopsis thaliana. *Molecular biology of the cell* **24**: 510–520.

Fendrych M, Synek L, Pečenková T, Toupalová H, Cole R, Drdová E, Nebesárová J, Sedinová M, Hála M, Fowler JE, *et al.* 2010. The Arabidopsis exocyst complex is involved

in cytokinesis and cell plate maturation. *The Plant cell* **22**: 3053–3065.

Guo W, Roth D, Gatti E, De Camilli P, Novick P. **1997**. Identification and characterization of homologues of the Exocyst component Sec10p. *FEBS letters* **404**: 135–139.

Hála M, Cole R, Synek L, Drdová E, Kulich I, Pečenková T, Hochholdinger F, Cvrčková F, Fowler J, Žárský V. **2008**. Exocyst complex functions in plant development. *Comparative biochemistry and physiology. Part A, Molecular & integrative physiology* **150**: S189.

Hansen LL and Nielsen ME. 2018. Plant exosomes: using an unconventional exit to prevent pathogen entry? *Journal of Experimental Botany* **1**: 59–68.

Heath MC, Heath IB. **1971**. Ultrastructure of an immune and a susceptible reaction of cowpea leaves to rust infection. *Physiological Plant Pathology* **1**: 277–287.

Heider MR, Gu M, Duffy CM, Mirza AM, Marcotte LL, Walls AC, Farrall N, Hakhverdyan Z, Field MC, Rout MP, *et al.* 2015. Subunit connectivity, assembly determinants and architecture of the yeast exocyst complex. *Nature structural & molecular biology* **23**: 59–66.

He B, Xi F, Zhang X, Zhang J, Guo W. **2007**. Exo70 interacts with phospholipids and mediates the targeting of the exocyst to the plasma membrane. *The EMBO journal* **26**: 4053–4065.

Hsu SC, Ting AE, Hazuka CD, Davanger S, Kenny JW, Kee Y, Scheller RH. **1996**. The mammalian brain rsec6/8 complex. *Neuron* **17**: 1209–1219.

Hückelhoven R, Panstruga R. **2011**. Cell biology of the plant–powdery mildew interaction. *Current opinion in plant biology* **14**: 738–746.

Humphry M, Bednarek P, Kemmerling B, Koh S, Stein M, Göbel U, Stüber K, Pislewska-Bednarek M, Loraine A, Schulze-Lefert P, *et al.* 2010. A regulon conserved in monocot and dicot plants defines a functional module in antifungal plant immunity. *Proceedings of the National Academy of Sciences of the United States of America* **107**: 21896–21901.

Janda M, Šašek V, Chmelařová H, Andrejch J, Nováková M, Hajšlová J, Burketová L, Valentová O. **2015**. Phospholipase D affects translocation of NPR1 to the nucleus in Arabidopsis thaliana. *Frontiers in plant science* **6**: 59.

Johansson ON, Fantozzi E, Fahlberg P, Nilsson AK, Buhot N, Tör M, Andersson MX. **2014**. Role of the penetration-resistance genes PEN1, PEN2 and PEN3 in the hypersensitive response and race-specific resistance in Arabidopsis thaliana. *The Plant journal: for cell and molecular biology* **79**: 466–476.

Kato N, Fujikawa Y, Fuselier T, Adamou-Dodo R, Nishitani A, Sato MH. **2010**. Luminescence detection of SNARE-SNARE interaction in Arabidopsis protoplasts. *Plant molecular biology* **72**: 433–444.

Kulich I, Pečenková T, Sekereš J, Smetana O, Fendrych M, Foissner I, Höftberger M, Zárský V. **2013**. Arabidopsis exocyst subcomplex containing subunit EXO70B1 is involved in autophagy-related transport to the vacuole. *Traffic* **14**: 1155–1165.

Kwon C, Neu C, Pajonk S, Yun HS, Lipka U, Humphry M, Bau S, Straus M, Kwaaitaal M, Rampelt H, *et al.* 2008. Co-option of a default secretory pathway for plant immune responses. *Nature* **451**: 835–840.

Lee H-A, Lee H-Y, Seo E, Lee J, Kim S-B, Oh S, Choi E, Choi E, Lee SE, Choi D. **2017**. Current Understandings of Plant Nonhost Resistance. *Molecular plant-microbe interactions: MPMI* **30**: 5–15.

Lipka V, Dittgen J, Bednarek P, Bhat R, Wiermer M, Stein M, Landtag J, Brandt W, Rosahl S, Scheel D, *et al.* 2005. Pre- and postinvasion defenses both contribute to nonhost resistance in Arabidopsis. *Science* **310**: 1180–1183.

Lipka U, Fuchs R, Lipka V. **2008**. Arabidopsis non-host resistance to powdery mildews. *Current opinion in plant biology* **11**: 404–411.

Meyer D, Pajonk S, Micali C, O'Connell R, Schulze-Lefert P. **2009**. Extracellular transport and integration of plant secretory proteins into pathogen-induced cell wall compartments. *The Plant journal: for cell and molecular biology* **57**: 986–999.

Micali CO, Neumann U, Grunewald D, Panstruga R, O'Connell R. **2011**. Biogenesis of a specialized plant-fungal interface during host cell internalization of Golovinomyces orontii haustoria. *Cellular microbiology* **13**: 210–226.

Munson M, Novick P. **2006**. The exocyst defrocked, a framework of rods revealed. *Nature*

structural & molecular biology **13**: 577–581.

Nielsen ME, Feechan A, Böhlenius H, Ueda T, Thordal-Christensen H. **2012**. Arabidopsis ARF-GTP exchange factor, GNOM, mediates transport required for innate immunity and focal accumulation of syntaxin PEN1. *Proceedings of the National Academy of Sciences of the United States of America* **109**: 11443–11448.

Nielsen ME, Jürgens G, Thordal-Christensen H. **2017**. VPS9a Activates the Rab5 GTPase ARA7 to Confer Distinct Pre- and Postinvasive Plant Innate Immunity. *The Plant cell* **29**: 1927–1937.

Nielsen ME, Thordal-Christensen H. **2013**. Transcytosis shuts the door for an unwanted guest. *Trends in plant science* **18**: 611–616.

Pečenková T, Hála M, Kulich I, Kocourková D, Drdová E, Fendrych M, Toupalová H, Žárský V. **2011**. The role for the exocyst complex subunits Exo70B2 and Exo70H1 in the plant-pathogen interaction. *Journal of experimental botany* **62**: 2107–2116.

Pečenková T, Marković V, Sabol P, Kulich I, Žárský V. **2017**. Exocyst and autophagy-related membrane trafficking in plants. *Journal of experimental botany* **69**: 47–57.

Picco A, Irastorza-Azcarate I, Specht T, Böke D, Pazos I, Rivier-Cordey A-S, Devos DP, Kaksonen M, Gallego O. **2017**. The In Vivo Architecture of the Exocyst Provides Structural Basis for Exocytosis. *Cell* **168**: 400–412.e18.

Rate DN, Cuenca JV, Bowman GR, Guttman DS, Greenberg JT. **1999**. The gain-of-function Arabidopsis acd6 mutant reveals novel regulation and function of the salicylic acid signaling pathway in controlling cell death, defenses, and cell growth. *The Plant cell* **11**: 1695–1708.

Rutter BD, Innes RW. **2017**. Extracellular Vesicles Isolated from the Leaf Apoplast Carry Stress-Response Proteins. *Plant physiology* **173**: 728–741.

Samuel MA, Chong YT, Haasen KE, Aldea-Brydges MG, Stone SL, Goring DR. **2009**. Cellular pathways regulating responses to compatible and self-incompatible pollen in Brassica and Arabidopsis stigmas intersect at Exo70A1, a putative component of the exocyst complex. *The Plant cell* **21**: 2655–2671.

Schmelzer E. **2002**. Cell polarization, a crucial process in fungal defence. *Trends in plant science* **7**: 411–415.

Sekereš J, Pejchar P, Šantrůček J, Vukašinović N, Žárský V, Potocký M. **2017**. Analysis of Exocyst Subunit EXO70 Family Reveals Distinct Membrane Polar Domains in Tobacco Pollen Tubes. *Plant physiology* **173**: 1659–1675.

Seo DH, Ahn MY, Park KY, Kim EY, Kim WT. **2016**. The N-Terminal UND Motif of the Arabidopsis U-Box E3 Ligase PUB18 Is Critical for the Negative Regulation of ABA-Mediated Stomatal Movement and Determines Its Ubiquitination Specificity for Exocyst Subunit Exo70B1. *The Plant cell* **28**: 2952–2973.

Sivaram MVS, Saporita JA, Furgason MLM, Boettcher AJ, Munson M. **2005**. Dimerization of the exocyst protein Sec6p and its interaction with the t-SNARE Sec9p. *Biochemistry* **44**: 6302–6311.

Stegmann M, Anderson RG, Ichimura K, Pečenková T, Reuter P, Žársky V, McDowell JM, Shirasu K, Trujillo M. **2012**. The ubiquitin ligase PUB22 targets a subunit of the exocyst complex required for PAMP-triggered responses in Arabidopsis. *The Plant cell* **24**: 4703–4716.

Stein M, Dittgen J, Sánchez-Rodríguez C, Hou B-H, Molina A, Schulze-Lefert P, Lipka V, Somerville S. **2006**. Arabidopsis PEN3/PDR8, an ATP binding cassette transporter, contributes to nonhost resistance to inappropriate pathogens that enter by direct penetration. *The Plant cell* **18**: 731–746.

Synek L, Schlager N, Eliás M, Quentin M, Hauser M-T, Zárský V. **2006**. AtEXO70A1, a member of a family of putative exocyst subunits specifically expanded in land plants, is important for polar growth and plant development. *The Plant journal: for cell and molecular biology* **48**: 54–72.

Takemoto D, Jones DA, Hardham AR. **2006**. Re-organization of the cytoskeleton and endoplasmic reticulum in the Arabidopsis pen1-1 mutant inoculated with the non-adapted powdery mildew pathogen, Blumeria graminis f. sp. hordei. *Molecular plant pathology* **7**: 553–563.

TerBush DR, Maurice T, Roth D, Novick P. **1996**. The Exocyst is a multiprotein complex required for exocytosis in Saccharomyces cerevisiae. *The EMBO journal* **15**: 6483–6494.

Underwood W. **2012**. The plant cell wall: a dynamic barrier against pathogen invasion. *Frontiers in plant science* **3**: 85.

Vogel J, Somerville S. **2000a**. Isolation and characterization of powdery mildew-resistant Arabidopsis mutants. *Proceedings of the National Academy of Sciences of the United States of America* **97**: 1897–1902.

Vukašinović N, Cvrčková F, Eliáš M, Cole R, Fowler JE, Žárský V, Synek L. **2014**. Dissecting a Hidden Gene Duplication: The Arabidopsis thaliana SEC10 Locus. *PloS one* **9**: e94077.

Vukašinović N, Oda Y, Pejchar P, Synek L, Pečenková T, Rawat A, Sekereš J, Potocký M, Žárský V. **2017**. Microtubule-dependent targeting of the exocyst complex is necessary for xylem development in Arabidopsis. *The New phytologist* **213**: 1052–1067.

Vukašinović N, Žárský V. **2016**. Tethering Complexes in the Arabidopsis Endomembrane System. *Frontiers in cell and developmental biology* **4**: 46.

Wu B, Guo W. **2015**. The Exocyst at a Glance. *Journal of cell science* **128**: 2957–2964.

Du Y, Overdijk EJR, Berg JA, Govers F, Bouwmeester K. 2018. Solanaceous exocyst subunits are involved in immunity to diverse plant pathogens. *Journal of experimental botany.* **69:** 655-666

Yang L, Qin L, Liu G, Peremyslov VV, Dolja VV, Wei Y. **2014**. Myosins XI modulate host cellular responses and penetration resistance to fungal pathogens. *Proceedings of the National Academy of Sciences of the United States of America* **111**: 13996–14001.

Yue P, Zhang Y, Mei K, Wang S, Lesigang J, Zhu Y, Dong G, Guo W. **2017**. Sec3 promotes the initial binary t-SNARE complex assembly and membrane fusion. *Nature communications* **8**: 14236.

Žárský V, Cvrčková F, Potocký M, Hála M. **2009**. Exocytosis and cell polarity in plants - exocyst and recycling domains. *The New phytologist* **183**: 255–272.

Žárský V, Kulich I, Fendrych M, Pečenková T. **2013**. Exocyst complexes multiple functions in plant cells secretory pathways. *Current opinion in plant biology* **16**: 726–733.

Zeyen RJ, Kruger WM, Lyngkjær MF, Carver TLW. **2002**. Differential effects of D -mannose and 2-deoxy- D -glucose on attempted powdery mildew fungal infection of inappropriate and appropriate G ramineae. *Physiological and molecular plant pathology* **61**: 315–323.

Zhao T, Rui L, Li J, Nishimura MT, Vogel JP, Liu N, Liu S, Zhao Y, Dangl JL, Tang D. **2015**. A truncated NLR protein, TIR-NBS2, is required for activated defense responses in the exo70B1 mutant. *PLoS genetics* **11**: e1004945.

Fig. 1

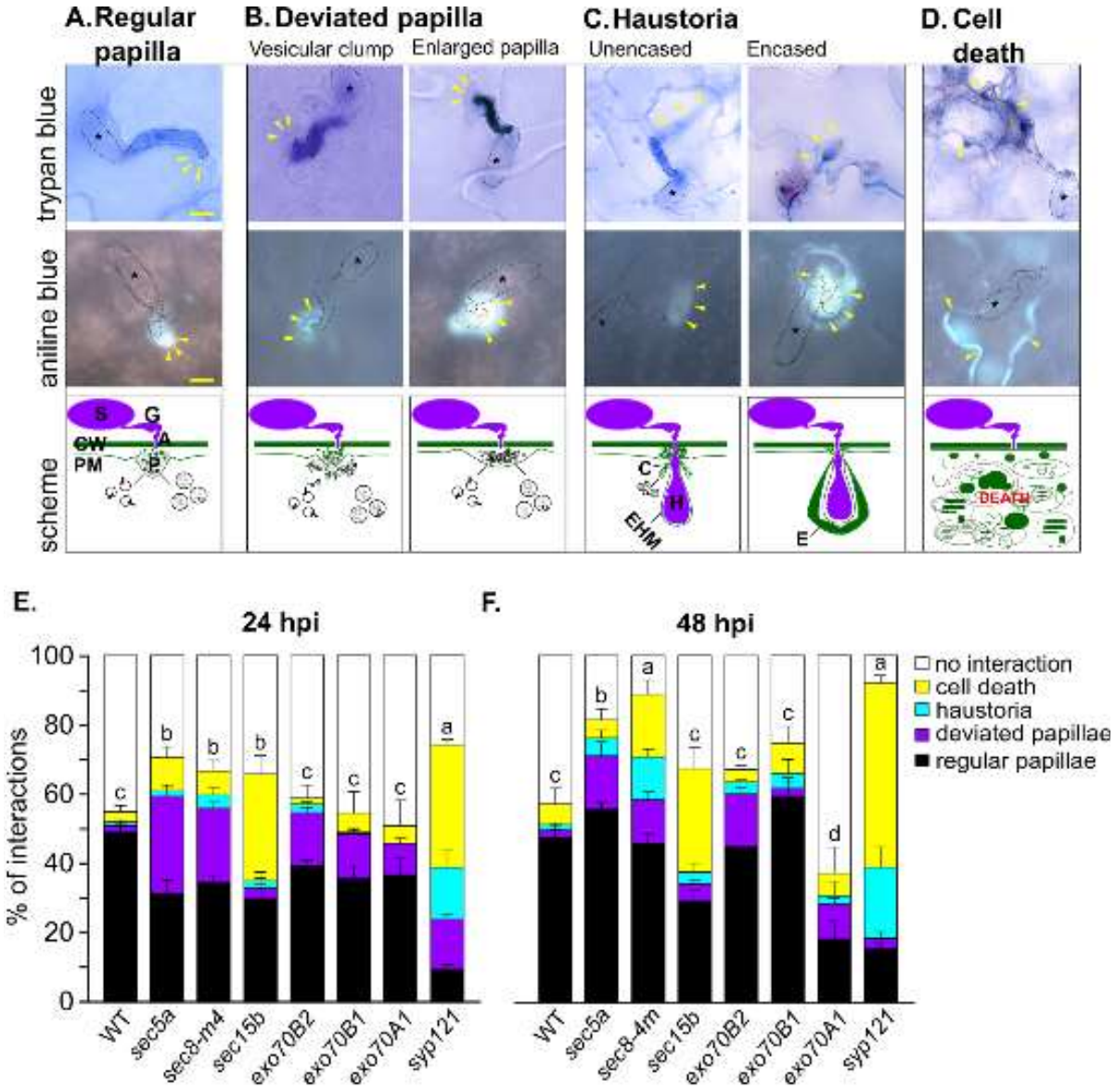
A. Regular papilla
B. Deviated papilla
Vesicular clump
Enlarged papilla
C. Haustoria
Unencased
Encased
D. Cell death
trypan blue
aniline blue
scheme
S
G
CW
PM
A
P
C
H
EHM
E
DEATH
E.
24 hpi
F.
48 hpi
% of interactions
100
80
60
40
20
0
no interaction
cell death
haustoria
deviated papillae
regular papillae
WT
sec5a
sec8-m4
sec15b
exo70B2
exo70B1
exo70A1
syp121
sec8-4m

Figure 1 Category of interactions between exocyst mutants and non-host pathogens.
Bgh and *Ep* evoked the same types of reactions - in the columns: (A) Regular papillae; (B) Deviated papillae (either smaller than regular papilla but with vesicular clump or enlarged papilla); (C) Haustoria (completely unencased and partially or fully encased haustoria); (D) Cell death/isolated programmed cell death. From the top: the first row shows independent interactions visualized by hot-phenol trypan blue staining (blue colour visualizes fungal structures or dead cells); second row, aniline blue staining visualisation of the callose (different experiment); third row, schematic model of reactions to fungi (inspired by Meyer *et al.*, 2009). The phenotypic deviation in penetration resistance according to described interaction types is shown (E) 24 hpi or (F) 48 hpi with *Bgh*. The elevated total amount of interactions (A+B+C+D) highlights defects in plant immunity of exocyst core subunit mutants (E, F). The increased portion of deviated papillae indicates imbalanced secretion in pre-invasive basal resistance in exocyst mutants. A number of haustoria and cell death show the weakening in penetration resistance. The dataset for each genotype was counted from 100 germinated spores on defined leaf area, two leaves from each of five plants were analyzed. For each column in the graph, the area complementary to 100 % presents the proportion of spores that did not provoke any reaction of the plant (empty bars). The experiment was repeated 4 times with similar results. The small letters indicate the significant difference calculated with one-way ANOVA (ANalysis Of VAriance) with post-hoc Tukey-Kramer HSD (Honestly Significant Difference), Z-score $p<0.01$. A appressorium; G germ tube; S spore; CW cell wall; PM plasma membrane; P papilla; C collar; EHM extrahaustorial membrane; H haustorium; E encasement. Yellow arrows mark outer borders of plant cell defensive structures. The black dashed line outlines fungal structures and the star marks a spore. Scale bars 5 µm.

Fig. 2

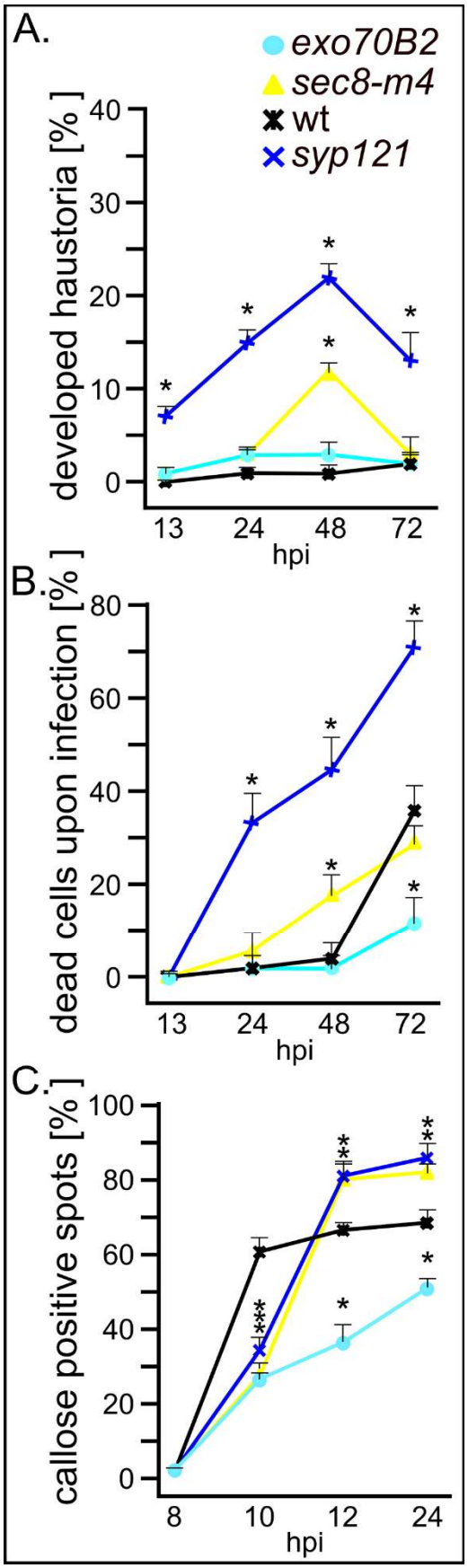

Figure 2 Timescale analysis of penetration success of *Bgh*.

(A) cells with developed haustoria and (B) cells undergoing PCD in WT and *sec8-m4*, *exo70B2*, *syp121* mutant lines were counted on a defined leaf area. The data were taken at 13, 24, 48 and 72 hpi with *Bgh*. (C) the frequency of callose deposition counted on a defined leaf area at the sites of *Bgh* attack was followed at 8, 10, 12, 24 hpi. The experiment was repeated 3 times with similar trend. The asterisks indicate significant difference from WT in each time point. One asterisk belongs to one mean of one genotype if there are two or three asterisks the more genotypes were different at this time point. The statistical difference was calculated with one way ANOVA with post-hoc Tukey-Kramer HSD with $p<0.01$. Error bar represent standard error.

Fig. 3

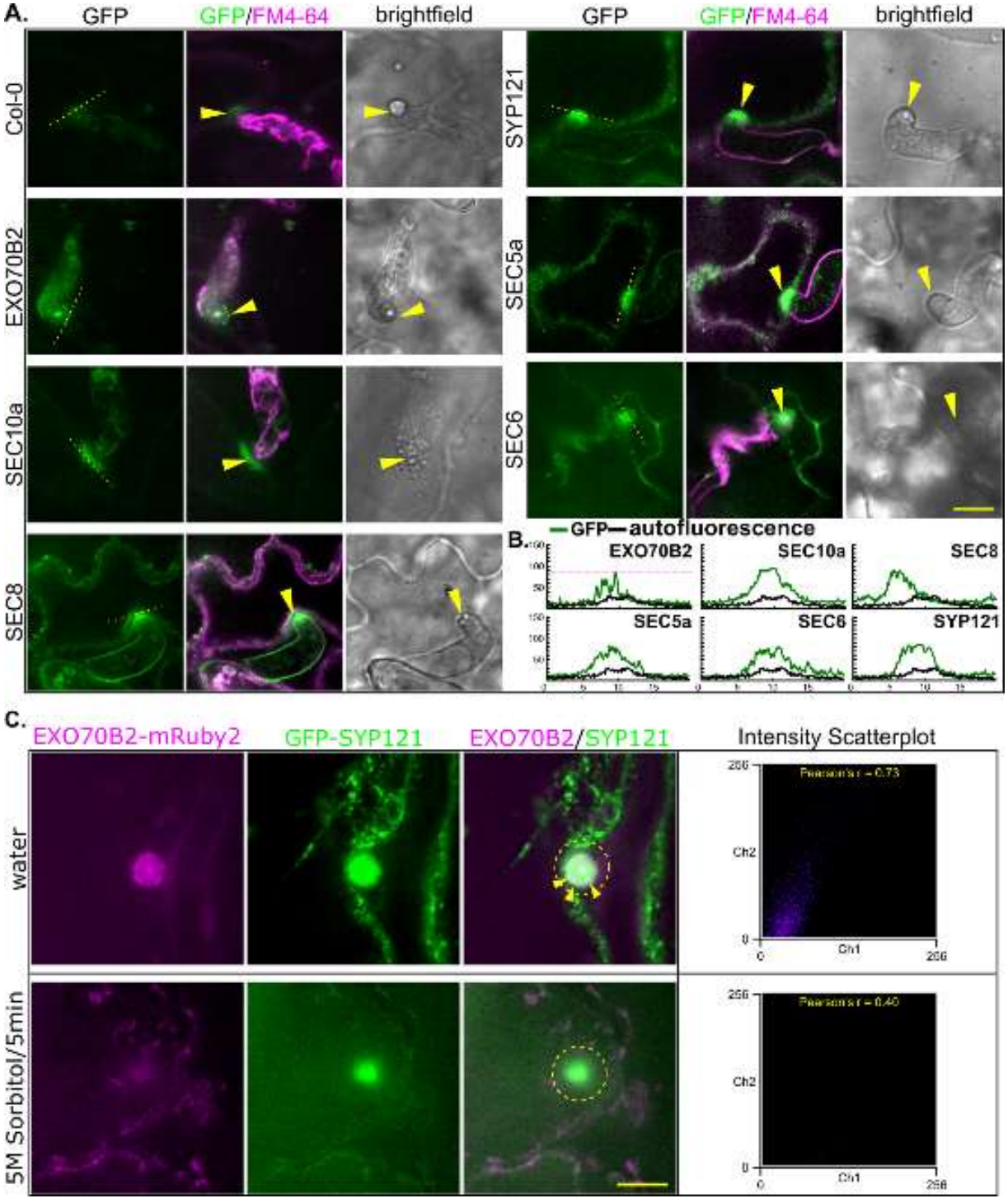
A.
GFP
GFP/FM4-64
brightfield
GFP
GFP/FM4-64
brightfield
Col-0
EXO70B2
SEC10a
SEC8
SYP121
SEC5a
SEC6
B.
GFP—autofluorescence
EXO70B2
SEC10a
SEC8
SEC5a
SEC6
SYP121
C.
EXO70B2-mRuby2
GFP-SYP121
EXO70B2/SYP121
Intensity Scatterplot
water
5M Sorbitol/5min
Pearson's r = 0.73
Pearson's r = 0.40
Ch2
Ch1
256
0

Figure 3 Exocyst subunits localised into defensive papilla.

(A) Signal accumulation of GFP-tagged exocyst subunits in papilla, for comparison the autofluorescence of fungal and plant cell structures are presented in the picture. The FM4-64 was used for visualisation of PM and fungal structures. For each line, the green channel (GFP/autofluorescence; left column), merged green and red channel (GFP with FM4-64 signal; middle) and brightfield channel (right) are shown. The Y-axis represents an intensity of a signal, the X-axis represents the length of the section. Yellow arrowheads point to the appressorium. Scale bar 10 μm. (B) The graphs represent an example of the difference between the GFP signal and the autofluorescence of papilla. (C) The co-localization of EXO70B2-mRuby2 and GFP-SYP121 in a papilla. The transgenic plants with the EXO70B2-mRuby2 and GFP-SYP121 were observed at 16 hpi with *Bgh* in a normal water or hyperosmotic condition. Pictures represent one out of 15 papillae observed through the one experiment. Approximately 2/3 of observed spores appeared to have the similar effect on protein localization after plasmolysis. Pearson's correlation graph of EXO70B2-mRuby2 (Ch1) and GFP-SYP121 (Ch2) for non-plasmolysed and plasmolysed cells. Scale bar 5μm.

The yellow dashed line marks the cross-section used for analysis.

Fig. 4

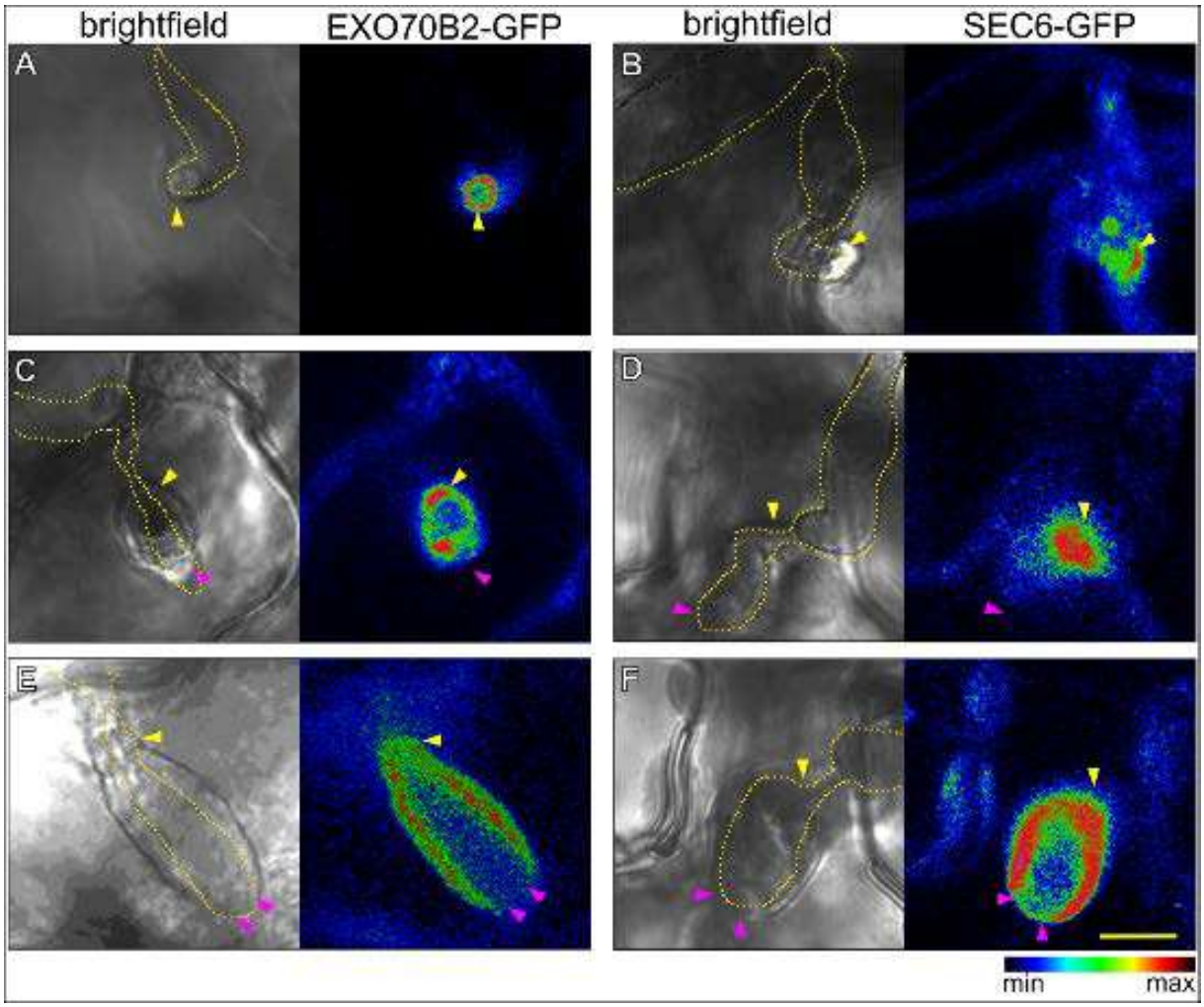

Figure 4 Exocyst localized into the encasement of haustoria.

The panels represent a bright field and a signal intensity analysis of the three stages of defensive structures growth: the papilla (A, B), the partially encased haustorium (C, D) and the enclosing encasement (E, F). The signal of EXO70B2 surrounds the papilla (A), the collar (C, E, yellow arrowheads) and the encasement (C, E). The signal of SEC6-GFP marks strongly papilla (B), the collar or initiations of the encasement (D, F yellow arrowheads) and the encasement (F). Pink arrowheads are pointing where the haustoria end and where the signal of the Exocyst subunits is disappearing. Scale bar 10 µm; scale bar of signal intensities on the left. The yellow dashed line outlines fungal structures.

Fig. 5

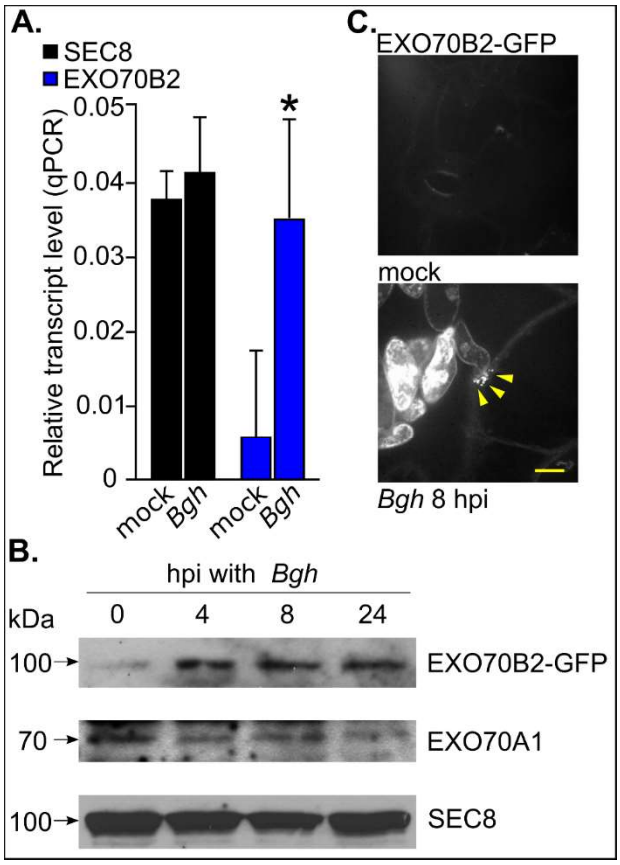

Figure 5 EXO70B2 was specifically induced on mRNA and protein level after *Bgh* inoculation.

(A) The relative transcript level, normalised to ubiquitin gene, of *EXO70B2* gene was elevated at 8 hpi with *Bgh*, in comparison to *SEC8*. (B) The protein level of EXO70B2-GFP in *exo70B2* mutant increased at 4 hpi with *Bgh* and stayed elevated during the time of interaction with the fungus, whereas the level of EXO70A1 dropped and the level of SEC8 stayed unchanged.The anti-GFP, anti-EXO70A1 and anti-SEC8 antibodies were used. (C) The early accumulation of EXO70B2-GFP signal in the cytoplasm in vesicle-like dots. The GFP signal labelled the papilla structure already at 8 hpi with *Bgh* in 3 weeks old plants. The asterisks indicate statistically significant differences calculated with nonparametric Tukey-Kramer HSD test at $p<0.01$. (n = 3 biological replicates). The error bars show standard deviation. The yellow arrowheads highlight signal maxima. The scale bar 5 μm.

Fig. 6

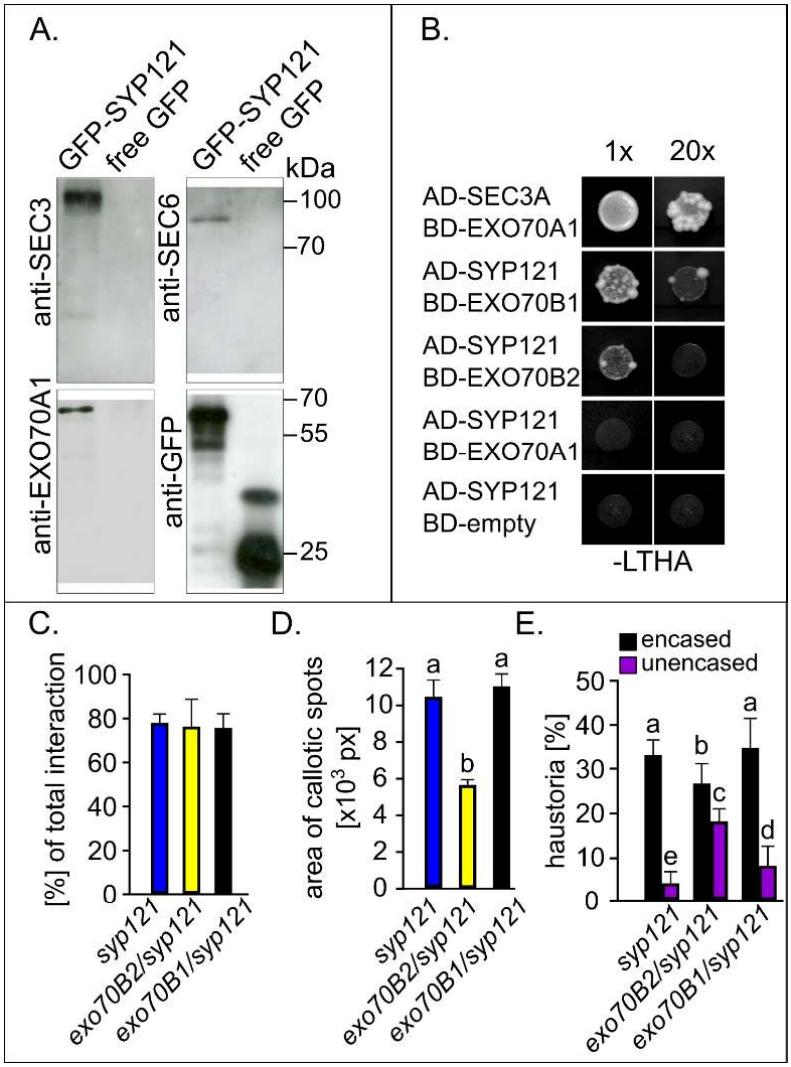
A.
GFP-SYP121
free GFP
GFP-SYP121
free GFP
kDa
anti-SEC3
anti-SEC6
anti-EXO70A1
anti-GFP
100
70
70
55
25
B.
1x
20x
AD-SEC3A
BD-EXO70A1
AD-SYP121
BD-EXO70B1
AD-SYP121
BD-EXO70B2
AD-SYP121
BD-EXO70A1
AD-SYP121
BD-empty
-LTHA
C.
[%] of total interaction
syp121
exo70B2/syp121
exo70B1/syp121
D.
area of callotic spots
[x10³ px]
a
b
a
E.
encased
unencased
haustoria [%]
a
e
b
c
a
d

Figure 6 SYP121 interacted with the EXO70B2-containing exocyst complex

Biochemical and genetic verification of SYP121 and EXO70B2 interaction. (A) The GFP-SYP121 seedlings were used for co-immunoprecipitation and the eluted fraction was tested for the exocyst subunits presence. For each gel, the arrangement of samples was always the same - on the left eluate of the GFP-SYP121 expressing seedlings, and the eluate of the free GFP expressing seedlings as a control. (B) The direct interaction between the exocyst and SYP121 was examined in a yeast two-hybrid assay. Yeasts containing both the binding and activation domain were spotted on the selection SD-His, Trp, Ade, Leu plates in two dilutions, and left to grow for 5 days. (C) Four weeks old plants of *syp121*, e*xo70B2/syp121*, *exo70B1/syp121* mutant lines were inoculated with the spores of *Bgh*. The leaves were collected at 48 hpi and stained with trypan or aniline blue. The sum of all evoked interactions by pathogen described graph. (D) The graph shows the mean area of callose spots created after the interaction counted on the predefined leaf area. (E) The mean percentage of developed encased (fully or partially) or unencased haustoria. Error bars indicate SE (n = 3 biological replicates). Comparisons between multiple groups were performed by ANOVA followed by the Tukey-Kramer test. The same letter indicates that there are no significant differences ($P<0.01$).

Fig. 7

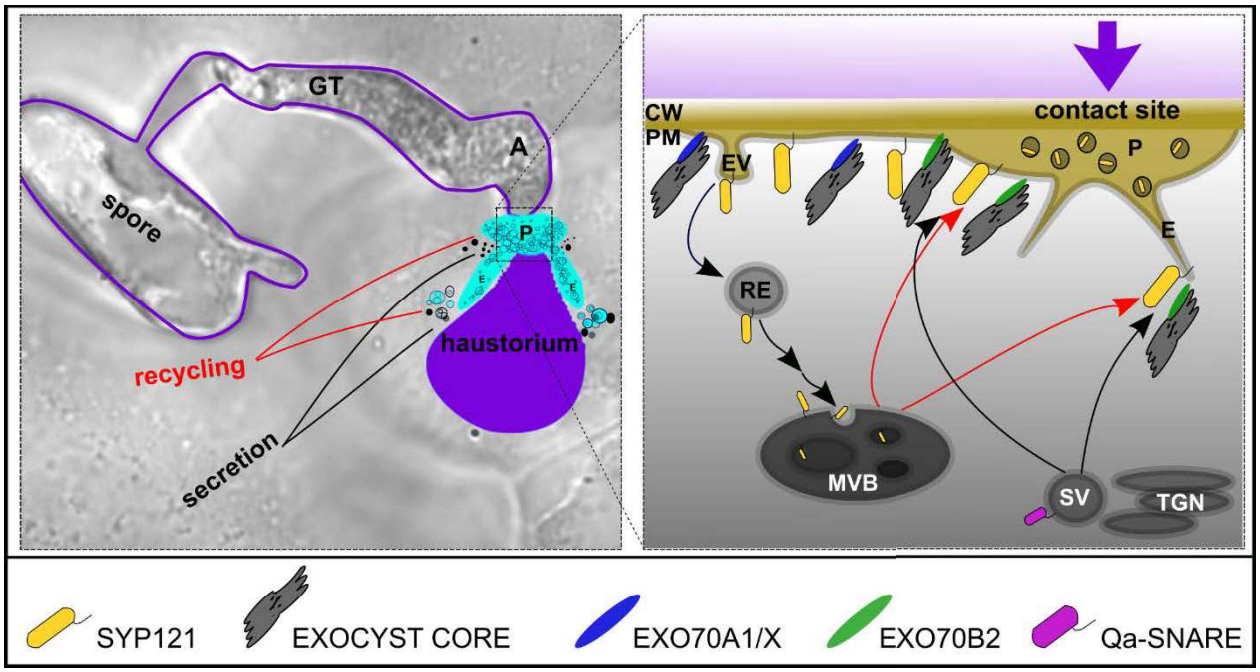

Figure 7 The interaction scheme

The model describing our working hypothesis of two pathways involved in the basal resistance to the fungal non-adapted pathogen. The left scheme shows germinated spore which successfully penetrated a plant cell and created haustorium before the cell started the programmed cell death. The cell uses two major secretory pathway to develop defensive papilla and encasement, the secretion and recycling. In detail, we hypothesise that according to EXO70 comprised in the complex, exocyst helps to distinguish the defensive structures from PM. EXO70B2-containing complex may help to establish the papilla membrane domain for SYP121 and similarly work for other Qa-SNARE in the encasement formation. The model also supports a variability of exocyst complex according to the bound EXO70X subunit. CW cell wall, PM plasma membrane, MVB multivesicular body, SE secretory vesicle, RV recycling vesicle, TGN trans-Golgi network, EV endocytosed vesicle, E encasement, P papilla, GT germ tube, A appressorium.

SFig. 1

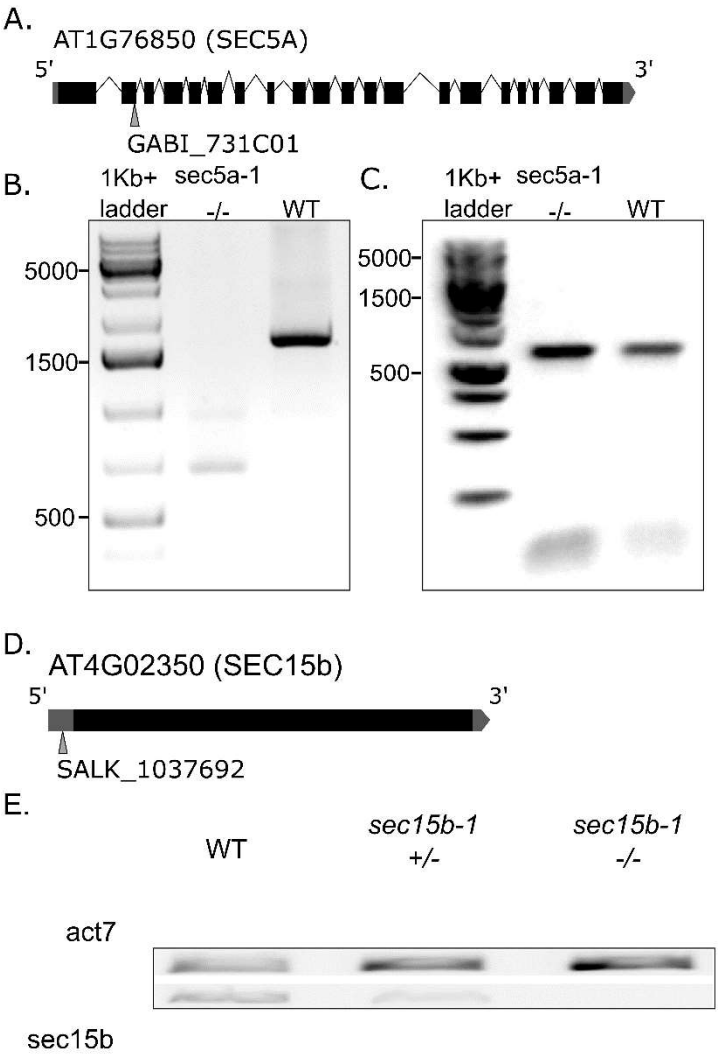

Supplementary Figure 1

Verification of the KO *sec5a-1* and KO *sec15b-1* mutants. The graphical illustration represents the genomic sequence of *Arabidopsis SEC5A* gene (A) and *SEC15B* (D) with the arrow point the place of insertion. The 1800 bp long segment of *SEC5A* was amplified from cDNA of 14 days old *sec5-1* mutant and WT seedlings (B). From the same cDNA samples, the 600 bp long fragment of control gene *EXO70B2* was amplified as the DNA quality control (C). The 1200 bp long segment of *SEC15B* was amplified as described above and the actin gene was used as a control. Primers used for the PCR were designed to cover the part with the insertion and to distinguish *SEC5A* from *SEC5B* or *SEC15B* from *SEC15A* (STable 1).

SFig. 2

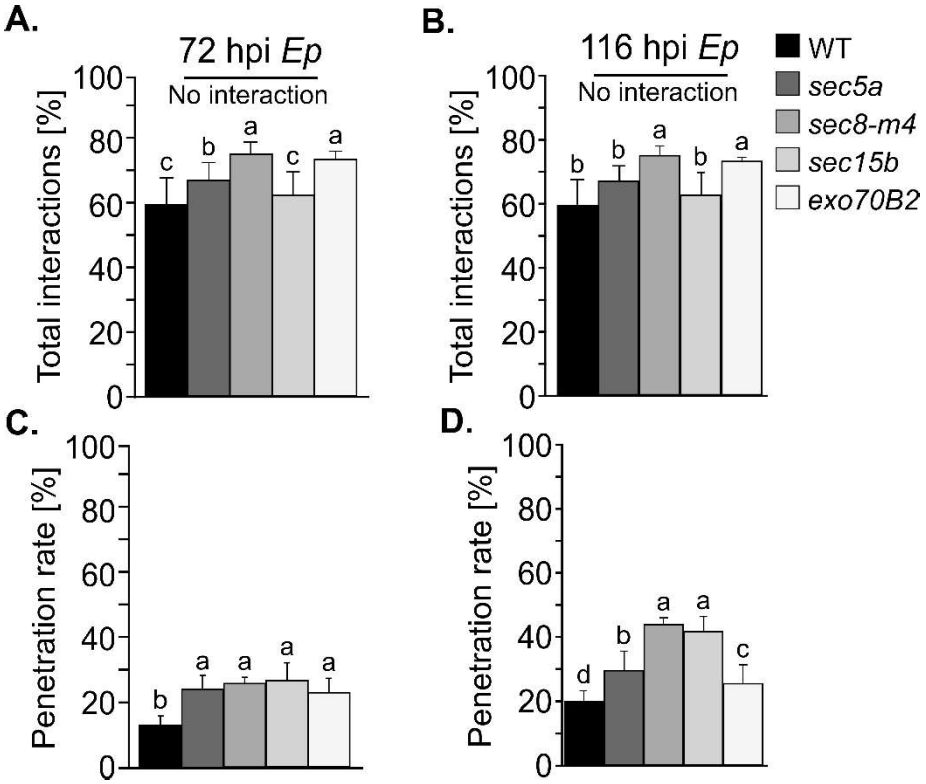

Supplementary Figure 2

Quantification of penetration resistance against *Ep* in exocyst mutants. The penetration resistance was analyzed at 72 (A, C) and 116 hpi (B, D) with *Ep* in comparison to WT. The percentage of total interactions indicates changes in responsiveness to fungal attack (A, B). In detail, the penetration rate showed the changes in penetration resistance of exocyst mutants (C, D). The letters indicate the statistically significant difference performed by ANOVA followed by the post-hoc Tukey-Kramer test, Z-score calculations $p<0.01$, n = 3 biological replicates.

SFig. 3

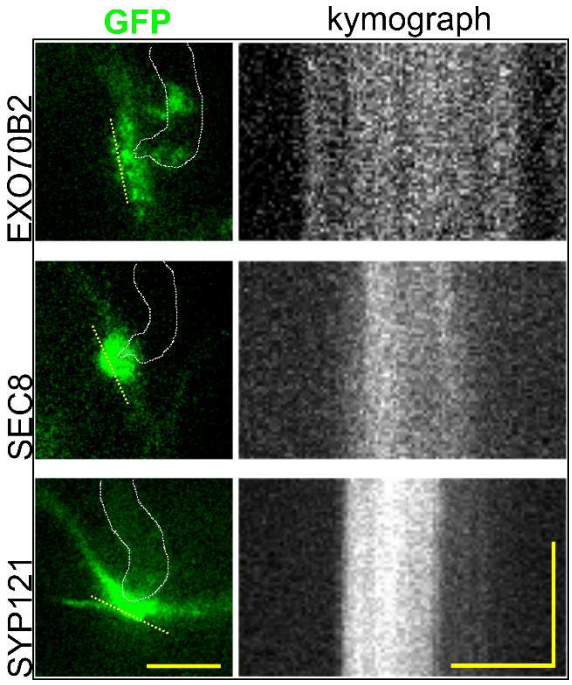

Supplementary Figure 3

The dynamics of exocyst subunits in papilla cross-section. Pictures on the left show the start section of time series used for kymographs (on the right); scale bar represents 10 μm. The yellow dash line defines the X-axis of the kymographs. Presented kymographs show the dynamics of GFP-tagged EXO70B2, SEC6 and SYP121. All proteins were expressed under their natural promoters. In kymograph, the vertical scale bar represents the 30s and the horizontal scale bar 3 μm. The white dashed line outlines fungal structures.

SFig. 4

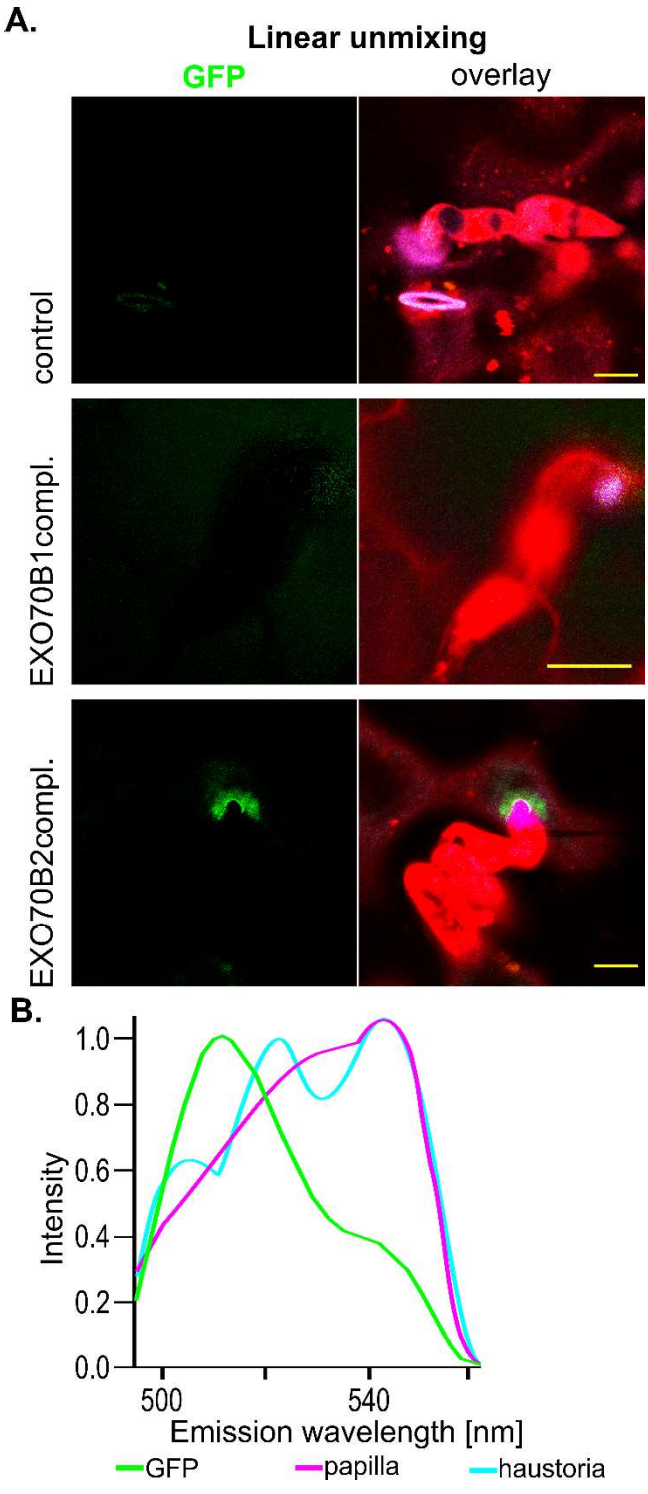

Supplementary Figure 4

(A) The accumulation of GFP signal and the overlay of GFP, autofluorescence of haustoria and papillae after the linear unmixing after lambda scan. The red colour shows the FM4-64 dye in an overlay picture. The non-transformed plants were used as the control to EXO70B2-GFP and SEC6-GFP expressing plants. (B) The unmixed channels represent the specific range of wavelengths described in the graph. Lambda scan was done to visualize GFP only with 488 nm argon laser with a range of 489-600 nm.

SFig.5

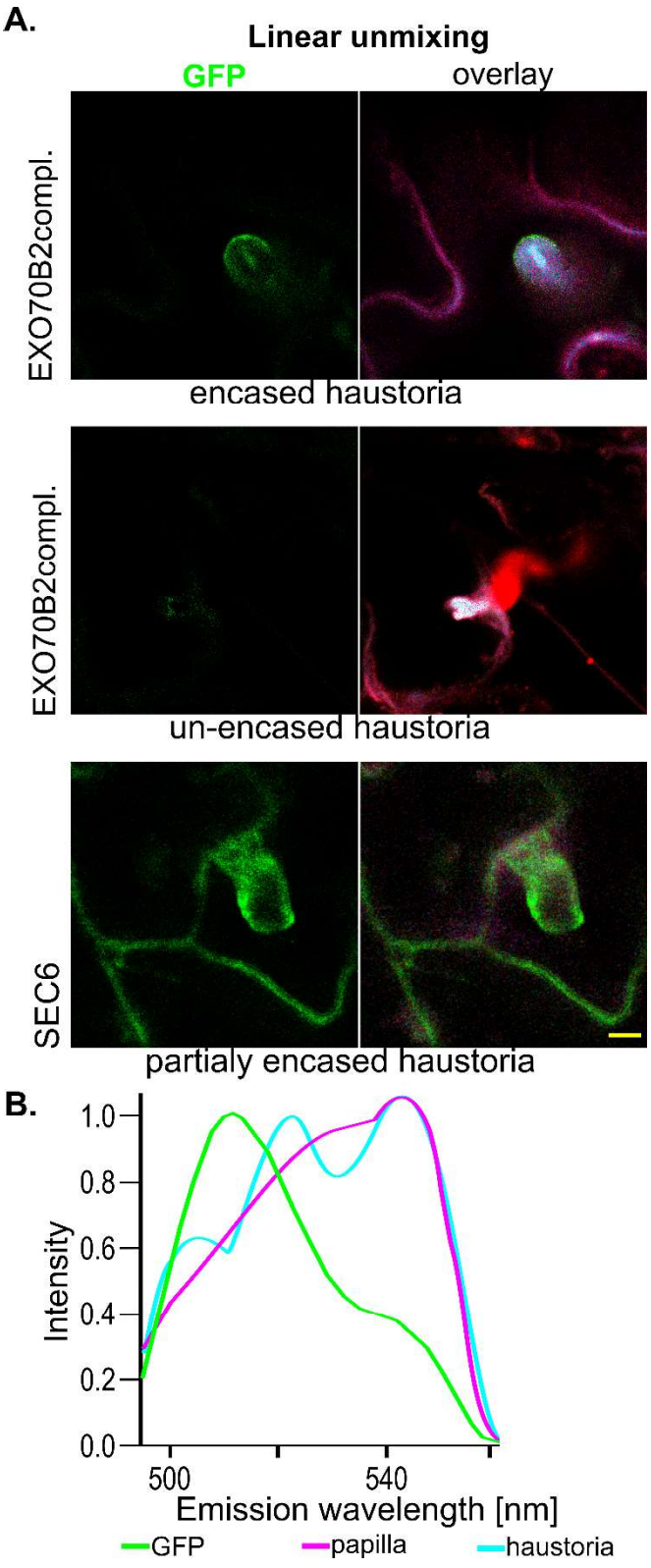

Supplementary Figure 5

(A) The localization of EXO70B2-GFP/*exo70B2* and SEC6-GFP in the haustoria was done by linear unmixing of characterised spectra. Scale bar 10µm. The lambda scan was done to visualize GFP only with 488 nm argon laser with a range of 489-600 nm. (B) The graphical illustration of used spectra for GFP and fungal structures obtained from the control plants for linear unmixing picture processing.

SFig. 6

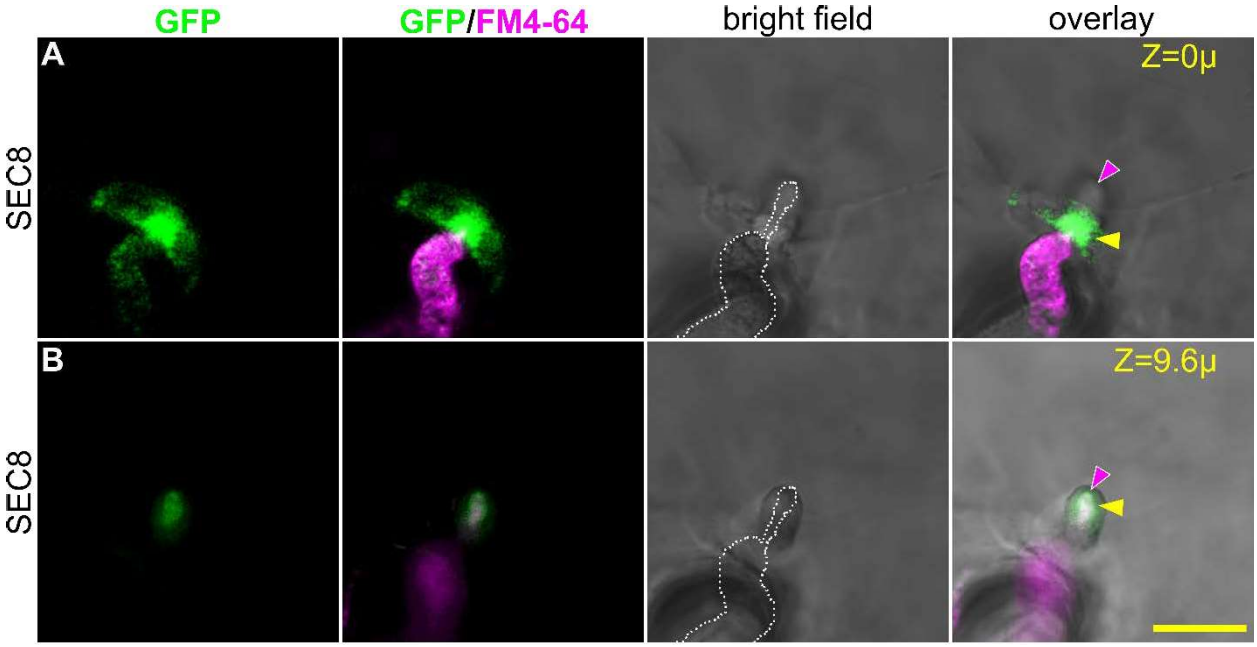

Supplementary Figure 6

The isolated stacks from the Z-stack scanning showing localization of GFP-SEC8 to the defensive structures papillae/collar or neck (A) and the growing encasement (B). The PI 1000x was used to visualise the fungal structure. The depth of a scan is indicated by yellow numbers, top right. Yellow arrowheads indicate the GFP maximum presence. Pink arrowhead shows the tip of haustoria. Scale bar 10µm.

SFig.7

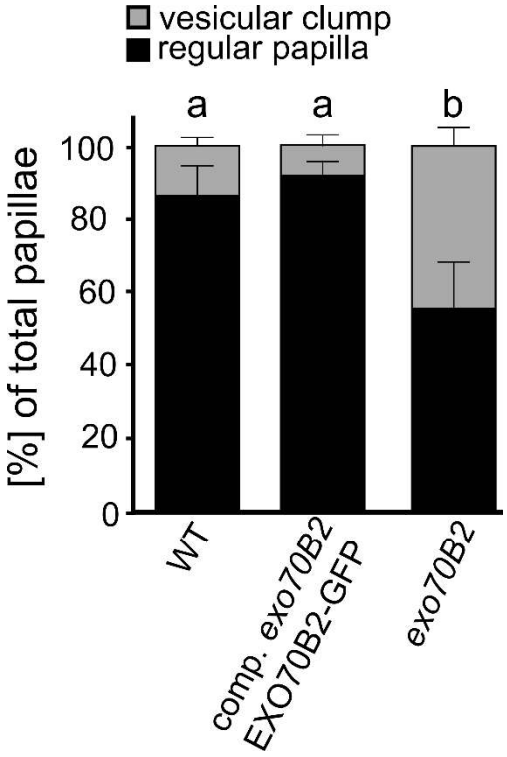

Supplementary Figure 7

The graph shows the ability of EXO70B2-GFP to fully complement the defect of *exo70B2* mutant in papilla development. Leaves were stained with the trypan blue method. From the total number of created papillae on a leaf, the two categories (vesicular clump and regular papilla) were counted. Error bars represent SE. The small letters indicate statistically significant difference calculated with ANOVA test at $p<0.01$.

SFig. 8

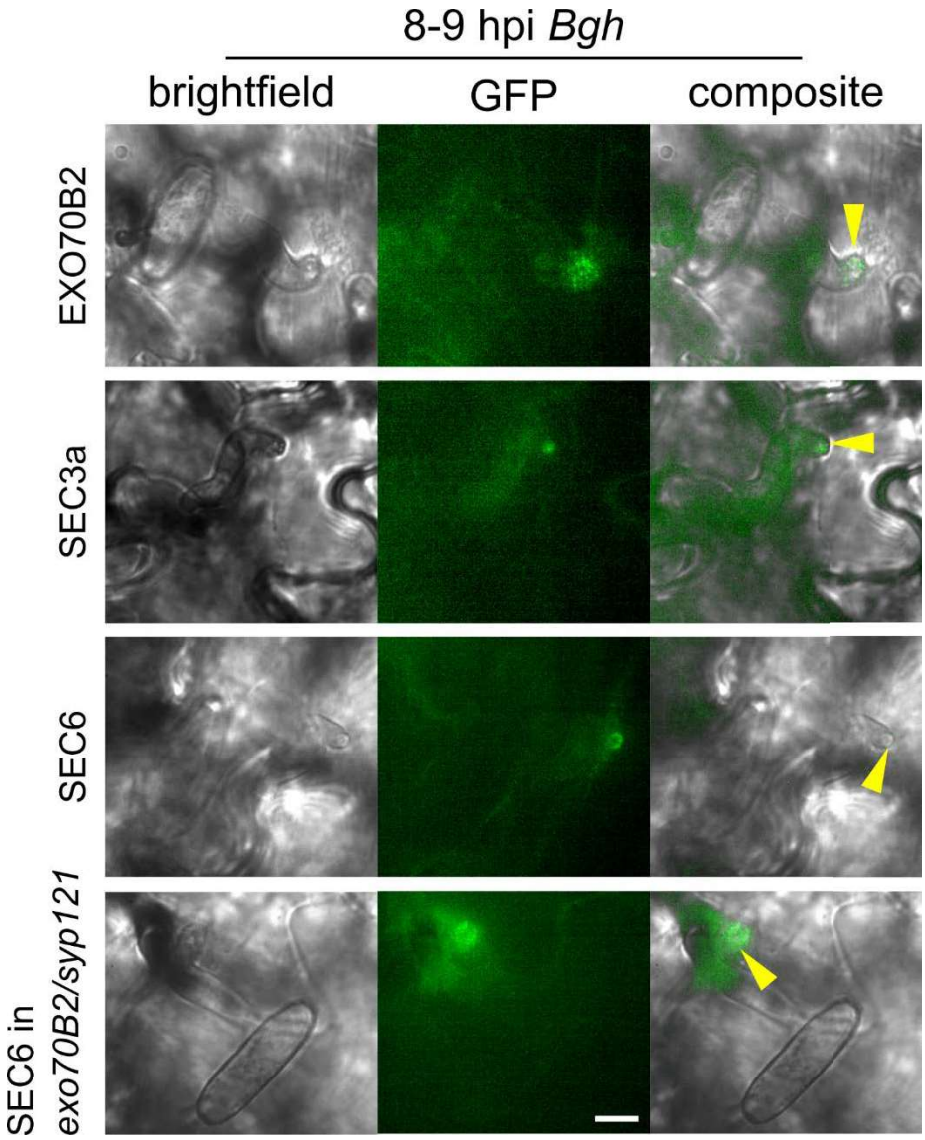

Supplementary Figure 8

Representative pictures of EXO70B2-GFP, GFP-SEC3a, SEC6-GFP expressed in WT and SEC6-GFP expressed in *exo70B2/syp121* mutant taken between 8-9 hpi *Bgh* by spinning disc confocal microscope, Andor Zyla CSU-X1. The intensities of the signal are normalized to treated non-transformed WT. Yellow arrows point to the appressorium of the fungus. Scale bar represent 10µm.

STable 1 **Supplementary Table 1** Primers used in this study.

Primers used for qPCR and semiqPCR		**Gene**
qUBQ10 F	GGCCTTGTATAATCCCTGATGAATAAG	AtUbiquitin
qUBQ10 R	AAAGAGATAACAGGAACGGAAACATAGT	
qSEC8F	GGGAATGGCGCCTTTCATCTCTGG	AtSEC8
qSEC8R	GCTGCCATGGCCTGTTCCACTGC	
qEXO70B2F	GAAGCACGCAGCGAAACTGAGGC	AtEXO70B2
qEXO70B2R	GCACCTTACACACCTCATCGAACTGTG	
sqSEC5F	TACAATCAGTGGAATTCCCCAGC	AtSEC5a
sqSEC5R	GTTGACTCTAATGGGGCTGA	
sqSEC15bF	GCAATCGTCGAAAGGACGGC	AtSEC15b
sqSEC15bR	AGCCATACCTGCGTAGAC	
qACT7F	GCCGATGGTGAGGATATTCAGC	AtACT7
sqACT7R	CAAACTCACCACCACGAACCAG	
sqEXO70BF	GGCGGTGGGATTCACCCG	AtEXO70B2
sqEXO70B2R	ACGCCTCCCATTAATCTCCG	
Primers used for genotyping		**size**
SEC5aF	CCTGTGGCTGCGGCTG	1000
SEC5aR	CCTCCTCGAGTACACGCTTG	
GABI_08474	ATAATAACGCTGCGGACATCTACATTTT	500
SYP121CapsF	CAACGAAACACTCTCTTCATGTCACGC	500
SYP121CapsR	CATCAATTTCTTCCTGAGAC	
digestion with MLU-1	100bp shift on gel	400
EXO70B2F	CGTGATCCGTCTTTGTGTTTC	1000
EXO70B2R	ACGCCTCCCATTAATCTCCG	
LB3	CATCTGAATTTCATAACCAATCTCG	600
EXO70B1F	TTCGTTTATGGAGGTTTGTCG	1100
EXO70B1R	TGGTCATTTAGCAGGTGGTTC	
GABI_08474	ATAATAACGCTGCGGACATCTACATTTT	700
SEC8R (Cole et al. 2005)	CCT GCT TCT CCT TTA TGA TTT CAC C	1200
SEC8F (Cole et al. 2005)	CAC GTA GGG AGG AGG GAA TGG	
LBB sec8-4	ATTTTGCCGATTTCGGAAC	600
SEC15bF	TTCACCAATAGCCAACTGACC	1000
SEC15bR	ACTAAGGACATTTATACCTACCAACTG	
LBB	ATTTTGCCGATTTCGGAAC	500
EXO70A1F	CTAGACGTTTGCAGCATCCTAT	1200
EXO70A1R	ATATGTGTAATGCATTGGAGAAGC	
LBB	ATTTTGCCGATTTCGGAAC	700

Primers used for cloning					
Name	**Sequence**	**Gene of interest**	**Vector**	**Destination vector**	**Source fo used vectors**
B2 prom EcoRI for	AAGAATTCGAGCTCCGACGGACGAG	AtEXO70B2	pENTR3C (Gateway)	pGWB4	Nakagawa et al., 2007
B2 nostopXhoI rev	AAACTCGAGAAACTTGAGCTTTCCTTGAAC				
B2prom	GGGGACAACTTTGTATAGAAAAGTTGCTGCCATTGGTATTGGTGG	AtEXO70B2	pDONR P4-P1R (Gateway)	pB7m34GW	Karimi et al. 2005
B2prom rev	GGGGACTGCTTTTTTGTACAAACTTGCATGATTGGATGGGAATTAATAATGT				
EXO70B2 CDS for	GGGGACAAGTTTGTACAAAAAAGCAGGCTTAATGGCTGAAGCCGG	AtEXO70B2	pDONR P2R-P3 (Gateway)	pB7m34GW	Karimi et al. 2005
EXO70B2 CDS rev	GGGGACCACTTTGTACAAGAAAGCTGGGTAACTTGAGCTTTCCTTGAACA				
B1 prom for	ATAGAAAAGTTGAATGCGGTAGAAGAGAGGATA	AtEXO70B1	pDONR P4-P1R (Gateway)	pB7m34GW	Karimi et al. 2005
B1 prom rev	TTGTACAAACTTGAGATTGAAACAGATGTGGAACC				
B1 CDS for	CTTGTACAAAGTGGCTATGGCGGAGAATGGT	AtEXO70B1	pDONR P2R-P3 (Gateway)	pB7m34GW	Karimi et al. 2005
B1 CDS rev	GTATAATAAAGTTGTCATTTTCTTCCCGTGGTA				
B2 mRuby2 F	AGTGAATTCTTCTCTGTTTATCCTCTCTATGC	AtEXO70B2	TaqRFP-AS-N (Evrogen)	pBGWT	Karimi et al., 2002 modified by Sabol et al. 2017
B2 mRuby N rev	TAACTCGAGCAACTTGAGCTTTCCTTGA				
EcoRVSec 5a rev	CTATAGTCTTCGTCTGGGTCGGG	AtSEC5a	pENTR3A (Gateway)	pUBvector	Grefen
KpnISec5a for	GGTACCgATGTCGAGCGATAGCAATG				
SYPdeltaC 1Eco	AAAGAATTCATGAACGATTTGTTTTC	AtSYP121	pGADT7 (Clontech)	pGADT7	Takara EU bio / http://www.clontech.com/US/Products/Protein_Interactions_and_Profiling/Yeast_Two-Hybrid/Vectors#
SYPdeltaC 1Sal	AGTCGACTCATTTTCGCGTGTTCT				
GFP_For	ATGGTGAGCAAGGGCG	eGFP	pDONR 221 (Gateway)	pB7m34GW	Karimi et al. 2005
GFP_Rev	CTTGTAGTTGCCGTCGTCC				
mRUBY2For	ACCGGTAATGGTGTCTAAGGGCGAAGAG	mRUBY2	TagRFP-AS-N (Evrogen)	pBGWT	Karimi et al., 2002 modified by Sabol et al. 2017
mRuby2Rev	TTTGCGGCCGCTTACTTGTACAGCTCGTCCATCC				

3. 4. Addition to the PAPER No. 3

Results

The phytohormonal analysis of exocyst mutants involved in plant immunity

The perturbations of plant hormone SA play the major role in plant biotic stress reaction. The elevated level of SA has been shown in *exo70B1* KO plants, this effect was attributed to the damage of autophagy pathway and auto-activation of hypersensitive cell death (Kulich et al. 2013). In the context of pathogen attack, the *exo70B1* is more resistant to adapted pathogens, but the resistance is not connected with SA accumulation more with PAD4 signalling pathway (Zhao et al. 2015). The SA disbalance was identified in untreated *syp121* mutant lines, where the higher SA level correlates with the elevated cell death after pathogen treatment (Zhang et al. 2007). The mutant *exo70B2* exhibits the decreased level of PR1 transcript level, the marker gene of SA pathway activation (Stegmann et al. 2012). The *exo70B2* also shows reduced activation of genes involved in PTI signalling, such as MAPK3, WRKY11, 22, 29 or RbohD. Due to this attenuated signalling machinery, the *exo70B2* may be less responsive to flg22, elf18, chitin or other PAMPs (Stegmann et al. 2012). The *exo70B2* mild phenotype does not correspond to such a theory. Moreover, it has been shown that the double mutant *exo70B1/exo70B2* did not show any increased effect, thus the possibility that EXO70B1 shares its function with EXO70B2 was excluded.

In contrast with previous data, we showed that the EXO70B2-GFP in *Arabidopsis* is stabilized after a pathogen treatment and its mRNA and protein level arises (see PAPER No. 3). We observed the lower incidence of the PCD in the *exo70B2* after pathogen treatment, but also in the case of the double mutant *syp121/exo70B2*. On the other hand, *exo70B1*, as observed before, in the stage prior to spontaneous lesions development, has only slightly higher incidence of PCD; similar is the situation with the double mutant *syp121/exo70B1*. We found the positive correlation between the amount of PCD in the single and double mutants and the total amount of free SA in plants before inoculation (Fig. A). Based on those results we conclude, that EXO70B2 positive function in SA pathway activation precede the negative role of SYP121. The *sec15b* mutants had also elevated incidence of PCD after pathogen treatment, this again correlates with increased SA level, although the ABA, the hormone deployed in abiotic stress, was elevated as well. In fact, the ABA level was increased in *exo70B1*, *exo70B2* and its double mutants with *syp121*. As a signalling pathway, ABA mediates the ROS detoxification, ion channels activity and thus osmotic adaptation of plant cell (Grant & Jones

2009). ABA play the important role in guard cell movements, generally, it inhibits stomata opening and promotes its closing.

We observed the significant difference between the SA/JA/ABA levels in plant growth either in short day or long day conditions for *exo70B1*. This result points to the specialized function of EXO70B1 in autophagy because the autophagy runs at most during the night and thus the effect of prolonged dark may have the significant effect on the experiments with *exo70B1*.

The mRNA level analysis of the exocyst subunit in the WT or mutant background

In contrast with previous data, we showed the EXO70B2-GFP in *Arabidopsis* is stabilized after a pathogen treatment and its mRNA and protein level arises (see PAPER No. 3). We observed the lower incidence of the PCD in the *exo70B2* after pathogen treatment, but also in the double mutant's *syp121/exo70B2*. On the other hand, *exo70B1*, observed before the stage of spontaneous lesion phenotype, only slightly higher incidence of PCD and similarly the double mutant *syp121/exo70B1*. We found the positive correlation between the amount of PCD in the single and double mutants and the total amount of free SA in plants before inoculation (Fig. B). Based on those results we conclude, that EXO70B2 positive function in SA pathway activation precedence the negative role of SYP121. The *sec15b* mutants had also elevated incidence of PCD after pathogen treatment, this again correlates with increased SA level, although the ABA, the hormone deployed in abiotic stress was elevated as well. In fact, the ABA level was increased in *exo70B1*, *exo70B2* and its double mutants with *syp121* (Fig B). As a signalling pathway, ABA mediates the ROS detoxification, ion channels activity and thus osmotic adaptation of the plant cell. ABA play the important role in guard cell movements, generally, it inhibits stomata opening and promotes its closing.

We observed the significant difference between the SA/JA/ABA levels in plant growing either in short day or long day conditions for *exo70B1*. This result points to the specialized function of EXO70B1 in autophagy because the autophagy runs at most during the night and thus the effect of prolonged dark may have the significant effect on the experiments with *exo70B1*.

The proteomic analysis of bound fraction to GFP tagged exocyst

We performed the LC-MS/MS analysis of a bound fraction of GFP Co-IP. As the bait, we used at least one paralog of each exocyst subunit. As the control protein fraction, we used the extracts from the free GFP protein expressing plants. We summarized the three MS analysis of the GFP

and used it as the reference sample, as well the samples from treated free GFP plants with *Bgh* or *Psm*. First, we analyzed the exocyst-exocyst interactions and compared them with the yeast model (Dubbuke et al., 2016). Surprisingly, we got almost the similar situation as in yeast, where the exocyst assembles from two highly stable halves the SEC6-SEC8-SEC5-SEC3 and EXO70-EXO84-SEC10-SEC15 (Table 1). Nevertheless, in the Co-IP fraction, the SEC5a was relatively weak bait and bounded only one subunit, in contrast to the EX070A1 which bounded almost full complex. Both EXO70B1 and EXO70B2 (treated with *Psm* in order to get higher expression level for Co-IP) were able to bind several interactors with the other exocyst subunits, as CDC48 or VAMP721 (Table 2), but didn't bind any of the exocyst subunits. This might reflect the relative strong EXO70A1 association with the rest of the complex and a weaker affinity of EXO70Bs with the exocyst.

The proteins designated as the exocyst associated never appeared in the free GFP fraction and are unique for the binding to the exocyst fraction (Table 2). According to their localization in the plant cell, we sorted the exocyst bound proteins to the several categories according to their function or localization in plant cell (Table 2).

Similarly, we analyzed the fractions from Co-IP of GFP-SYP121 and GFP-VAMP721. In both fraction, we got an overlap with the previously identified proteins in exocyst bait experiments, such as ABCG36, CALS9, CDC48A, ACA8/10 and more (Table 3). Intriguingly, we found only one subunit, the SEC8, present in the SYP121 bait fraction (Table 3).

Figures

Figure A Analysis of plant hormone level

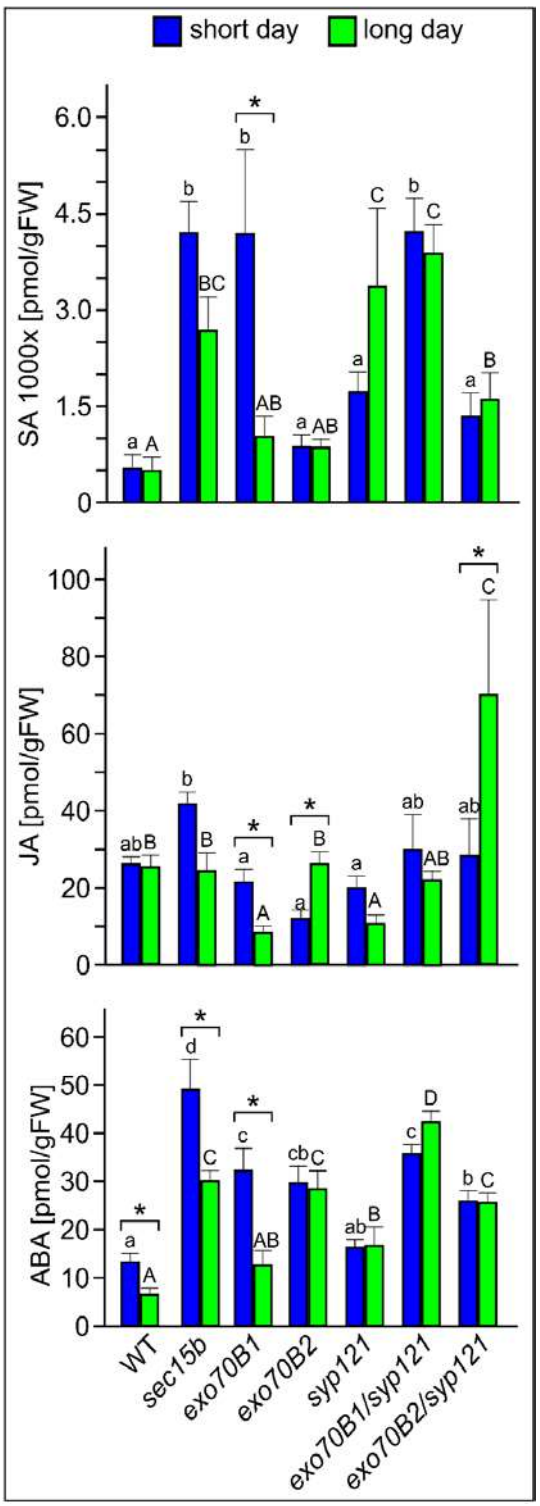

Graphs represent the results of acidic hormones SA, JA, ABA level in the short day (8/16h; light/dark) and long day (16/8h; light/dark) cultivated 4-week old plants. The statistic was performed with ANOVA $p<0.01$, in between the group of used genotypes grown under either short or long day conditions. The non-parametric Kruscal-Wallis H-test was performed between the short/long conditions in each genotype $p<0.01$. Error bars represent SE.

Figure B

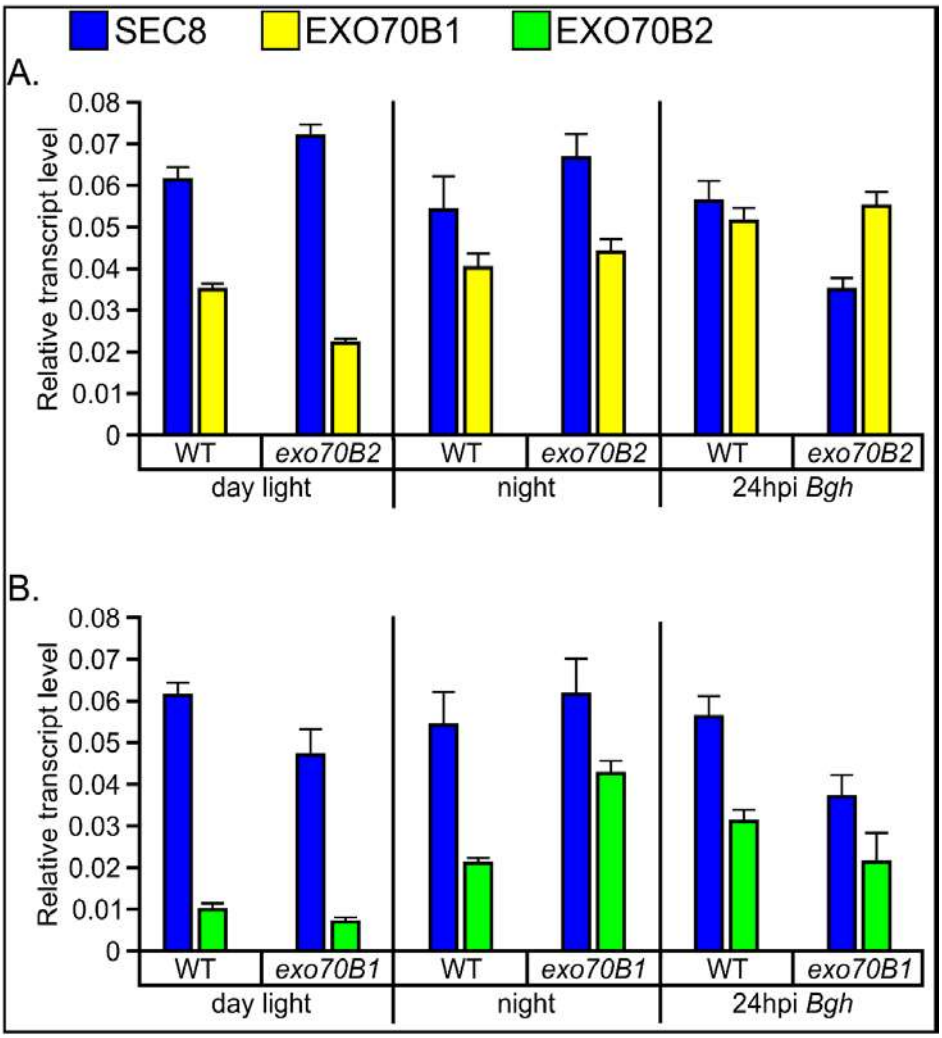

Analysis of exocyst subunits transcript level in different conditions

The blue colour indicates the relative transcript level of *SEC8* gene, yellow indicates *EXO70B1* and green indicates *EXO70B2*. Each column represents mean of three samples and the experiment was done in three biological replicas within three months. Error bars represent SE.

Table 1

	SEC3a	SEC5a	SEC6	SEC8	SEC10 a/b	SEC15 b	EXO84b	EXO70A1
SEC3a	**SI**	+	+	+		+		+
SEC5a	+	**SI**						
SEC6		+	**SI**	+				+
SEC8	+	+	+	**SI**				+
SEC10a/b	+				**SI**	+	+	+
SEC15b					+	**SI**	+	+
EXO84b					+	+	**SI**	+
EXO70A1					+	+		**SI**

Confirmed interactors between the exocyst complex bound in Co-IP.

(First row) One paralog of each subunit of the exocyst has been used as the GFP tagged bait to obtain the bound proteins in its co-sediment fraction (left line). The presence of the GFP tagged protein was confirmed with the western blot prior to the LC-MS-MS analysis always. The three different controls from the free GFP expressing plants were done as the negative control, none of the exocyst subunits was found in the GFP bound fraction. (SI) Self-Identified bait proteins. (+) Positive interaction.

Table 2

Group	AGI code	short name	Bait
Secretory Regulators	**AT3G56190**	ASNAP2	SEC3a, EXO70B1
	AT3G09840	CDC48A	SEC3a, EXO70A1/G1/B1/B2
	AT2G21390	COPI/Coatomer, alpha subunit	SEC3a, EXO70B1/B2
	AT3G15980	COPI/Coatomer, beta subunit	SEC3a
	AT5G42080	DL1	SEC3a, EXO70B1
	AT2G01470	STL2P/SEC12 like	SEC3a, EXO70B1
	AT3G11820	SYP121/PEN1	SEC6, SEC8, EXO84b
	AT1G28490	SYP61	EXO70B1/B2
	AT3G09740	SYP71	SEC3a, EXO70B1, EXO70B2
	AT4G32150	VAMP711	SEC3a
	AT1G04750	VAMP721	SEC3a, SEC8, EXO70B1, EXO70B2
	AT5G39510	VTI11/12	SEC3a, EXO70B1
Rab GTPases	**AT1G07410**	RABA2b/Ras-related protein	SEC15b, EXO70G1/B1/B2
	AT1G09630	RABA2a	SEC3a
	AT3G46830	RABA2c	SEC3a
	AT3G16100	RABG3c/RAB7d	SEC3a, EXO70B2
	AT3G18820	RABG3f	EXO70B1
Secreted Cargoes	**AT3G52500**	Aspartyl protease	SEC6, EXO84b, EXO70B2
	AT3G54400	aspartyl protease family protein	SEC6, EXO70G1/B1/B2
	AT5G20950	Beta-D-glucan exohydrolase-like protein	SEC6, EXO84b, EXO70B1
	AT1G09310	Protein with DUF538	SEC5a, EXO70B1/G1
	AT5G11420	Protein with DUF642/Cell Wall	EXO84b, EXO70B1, EXO70G1
PM proteins	**AT3G28860**	ABCB19/MDR1, MDR11, PGP19	SEC3a
	AT4G25960	ABCB2/MDR2, PGP2	SEC3a, EXO70B1
	AT4G25450	ABCB28	EXO70B1/B2
	AT1G59870	ABCG36/PEN3	SEC3a, EXO70B1/B2
	AT4G29900	ACA10	SEC3a, EXO70B2
	AT3G61050	CaLB protein	SEC3a, EXO70B1
	AT3G07160	CALS9/GSL10	SEC3a, EXO70B1/B2
	AT2G38480	CASP-like	SEC3a
	AT5G41790	COP1-interactive protein 1	SEC5, SEC8, SEC15b, EXO84b, EXO70B1/B2
	AT5G16590	LRR kinase receptor	SEC3a, EXO70B1

Vacuole	**AT1G30400**	ABCC1	SEC3a
	AT2G44640	Expressed protein	SEC3a, EXO70B1/B2/G1
	AT4G38350	Patched family protein	SEC3a/EXO70B1
ER	**AT1G48440**	B-cell receptor-associated 31-like protein	SEC3a, EXO70B1
	AT3G19820	DIM/Delta(24)-sterol reductase	SEC3a, SEC15b, EXO70B2
Golgi	**AT3G49720**	CGR2	SEC3a
	AT3G22845	p24beta2	SEC3a, EXO70B2
Cytoplasm	**AT3G11930**	Adenine nucleotide alpha hydrolase/membrane domain	EXO70B1/B2/G1
	AT3G48140	B12D-like protein	SEC10a, EXO70B1/B2
	AT3G16400	NSP1/Nitrile specifier protein 1	SEC5a, EXO70B2
	AT3G16390	NSP3/Nitrile-specifier protein 3	SEC5/8/15b, EXO84b, EXO70B1
	AT5G48180	NSP5	SEC5a
	AT1G64520	RPN12A/26S proteasome subunit	EXO70B1/B2
	AT3G03250	UDP2/UTP--glucose-1-phosphate uridylyltransferase 2	EXO84b, EXO70B1/2

Identified proteins in an exocyst bound fraction from Co-IP.

The table shows the most abundant proteins identified as unique in exocyst bound fraction after Co-IP, (they were not found in any of free GFP Co-IP fractions). From the left, the table describes Group of sorted proteins according to their either function or localization, the ATG code of each protein from TAIR.org the database, the Short name of protein and the Bait subunit used for Co-IP.

Table 3

Prey		Bait	
AGI code	**short name**	**SYP121**	**VAMP721**
AT3G28860	ABCB19	x	x
AT1G59870	ABCG36/PEN3	x	x
AT4G29900	ACA10		x
AT5G57110	ACA8		x
AT3G11930	Adenine nucleotide alpha hydrolases-like protein	x	
AT3G56190	ASNAP2	x	
AT3G43300	BIG5		x
AT3G07160	CALS9	x	x
AT4G15610	CASP1-like	x	
AT2G28790	CBP1		x
AT1G30450	CCC1	x	
AT3G09840	CDC48A		x
AT3G49720	CGR2		x
AT5G41790	COP1 interacting protein	x	
AT2G21390	COPI coatomer alpha		x
AT3G15980	COPI coatomer beta		x
AT5G25460	DGR2	x	
AT1G59610	DRP2B		x
AT1G07810	ECA1	x	
AT2G44640	Expressed protein	x	
AT5G16590	LRR kinase receptor		x
AT3G14840	LRR-RLK	x	
AT4G20260	PCAP1	x	
AT3G15060	RABA1g	x	
AT1G09630	RABA2A	x	
AT5G65270	RABA4A	x	
AT3G10380	SEC8	x	
AT3G11820	SYP121	x	x
AT3G52400	SYP122		x
AT5G08080	SYP132		x
AT1G28490	SYP61		x
AT3G09740	SYP71	x	x
AT1G04750	VAMP721	x	x
AT4G15780	VAMP724	x	
AT3G54300	VAMP727	x	
AT5G39510	VTI11/12		x

Identified proteins in SNARE proteins bound fraction from Co-IP.

The table summarizes proteins identified as unique in the SNARE SYP121 and VAMP721 bound fraction after Co-IP, (they were not found in any of free GFP Co-IP fractions). The table describes the ATG code of each protein according to TAIR (https://www.arabidopsis.org/) database, the Short name of protein from UniProt (http://www.uniprot.org/) database and the Bait subunit used for Co-IP.

Methods

Plant hormone isolation

We adopted previously published a method for acidic hormone isolation and purification (Dobrev & Kamínek 2002). The 4-week old plants grown directly in the soil in climate chambers in either long day or short day conditions were used for current experiments. The plants of several genotypes were used for analysis: Col-0 (WT), *syp121-1*(Collins et al. 2003), *exo70B2-2* (Pečenková et al. 2011), *exo70B1-1* (Kulich et al. 2013), *sec15b-1*, *exo70B2/syp121*, *exo70B1/syp121* (all three used in PAPER No. 3). Plants were grown in individual pots, the genotypes were mixed on the plate to prevent a position influence. The fresh 6^{th} and 7^{th} leaf was cut from each plant, 6 plants in total were used for each genotype. The cut leaves were weighed, homogenized with liquid nitrogen and used for the acidic hormone extraction (Dobrev & Kamínek 2002). The hormones were analyzed by HPLC (Ultimate 3000, Dionex) coupled to hybrid triple quadrupole/linear ion trap MS (3200 Q Trap, Applied Biosystems). The experiment was done in duplicate.

mRNA isolation and qPCR analysis

The 10 days old plantlets grown in sterile long day conditions on 1/2MS 2%sucrose media were isolated for the RNA isolation at 4 hours post light induction (the daylight), 2 hours prior the light induction (night) and 24 hours post inoculation with *Bgh* (at the same time interval as the daylight). The mRNA analysis and qPCR were done same as in PAPER No 3.

Co-IP and LC-MS-MS analysis

The 10 days old plantlets were grown in sterile long day conditions on 1/2MS 2% sucrose media and for each reaction 1g of plant tissue was used. The day before the experiments the expression of GFP in plantlets was confirmed by epifluorescence microscopy, without a disruption of sterile conditions. Plantlets inoculated with the *Bgh* of *Psm* were transferred to the short day conditions for 12 hours before isolation. The EXO70B1 and EXO70B2 plantlets were treated with *Psm* before the analysis. The SYP121 and VAMP721 were treated with *Bgh*. The treated plants provided more robust results than the untreated. As the control plants were used free GFP expressing plantlets treated in the same way as the experimental one. For Co-IP, we used plantlets expressing GFP tagged protein: free GFP (Fendrych et al. 2010), SYP121::GFP:SYP121, VAMP721::GFP:VAMP721 (Fendrych et al. 2013), SEC3a::GFP:SEC3a (Bloch et al. 2016), Ub::SEC5a:GFP (PAPER No. 3), SEC6::SEC6:GFP, SEC8::GFP:SEC8 (Fendrych et al. 2013), SEC10a::SEC10a:GFP (Vukasinovic et al. 2017), SEC15b::GFP:SEC15b (Aldorfova in prep.), EXO84b::GFP:EXO84b (Fendrych et al, 2010), 35S::EXO70A1:GFP (Fendrych et al. 2010), EXO70H4::GFP:EXO70B1 (Kulich in prep.), EXO70B2::EXO70B2:GFP (PAPER No. 3), 35S:EXO70G1:GFP (Jankova Drdova in prep.). The plant tissue was homogenized with liquid nitrogen, the inhibitor of proteases (Sigma Aldrich) was added together with lysis buffer Sec6/8 (Hála et al. 2008). Next, the protocol from anti-GFP Miltenyi Biotec Company kit was followed. The bound fractions were blotted via western blot and tested with anti-GFP antibody to confirm the presence of desired proteins. The bound fractions were sent to the LC-MS-MS analysis. The data sets were compared in excel, the presence of unique proteins was noted.

Statistical Evaluation

We tested the distribution of data with the Shapiro-Wilk Test Calculator. We used the one-way ANOVA analysis either with or without the post-hoc Tukey HSD (Honestly Significant Difference) nonparametric test to identify a statistical difference, between the groups. The T-test or non-parametric Kruscal-Wallis H-test was used to compare pair-wise interactions; p-value < 0.01.

3. 5. PAPER No. 4

Title: Interaction between exocyst complex and SNAREs are required for vesicle transport to the plasma membrane in Arabidopsis

Authors: Emily R Larson, Jitka Ortmannová, Naomi A Donald, Jiří Šantrůček, Viktor Žárský, and Michael R Blatt

Summary: Exocytosis mediates transport of membrane lipid vesicles that carry various cargo to the plasma membrane (PM). The exocyst and the **SNA**P (Soluble NSF Attachment Protein) **RE**ceptor (SNARE) complexes orchestrate vesicular fusion; the exocyst protein complex tethers vesicles to the PM, while the SNARE complex promotes vesicle docking and fusion. There is no current evidence of direct cooperation between these complexes in plants. Here we confirm the role of the direct interaction between exocyst and SNARE complexes in plant development. We show the double mutant *exo70A1/vamp721* plants are strongly inhibited in cell expansion resulting in dwarf phenotype, additive to the single *exo70A1*. For the first time, we report that exocyst subunits directly interact with a subset of SNAREs at the PM. Our results provide an updated mechanism of plant exocytosis that includes direct interactions between exocyst and SNARE complexes. We suggest that the individual functions of these complexes could be coordinated through their interactions to support vesicle trafficking patterns required for plant cell function and development.

My contribution: I performed or participated in all the experiments. I analyzed and discussed the obtained data. I wrote the manuscript with the help of other authors.

The interaction between EXOA1-containing exocyst complex and SNAREs are required for vesicle transport to the plasma membrane in Arabidopsis

Emily R Larson[1,5], Jitka Ortmannová[2,5], Naomi A Donald[1], Jiří Šantrůček[4], Viktor Žárský[2,3*], and Michael R Blatt[1*]

[1] Laboratory of Plant Physiology and Biophysics, University of Glasgow, Glasgow G12 8QQ, United Kingdom

[2] Institute of Experimental Botany, Academy of Sciences of the Czech Republic, 165 02 Prague 6, Czech Republic

[3] Department of Experimental Plant Biology, Faculty of Science, Charles University, 128 44 Prague 2, Czech Republic

[4] Department of Biochemistry and Microbiology, University of Chemistry and Technology, Prague, Czech Republic

[5] These author made equal contributions to the project

[*]Corresponding author:

Abstract

Exocytosis mediates transport of membrane lipid vesicles that carry various cargo to the plasma membrane (PM). The exocyst and the **SNA**P (Soluble SNF Attachment Protein) **RE**ceptor (SNARE) complexes orchestrate vesicular fusion; the exocyst protein complex tethers vesicles to the PM, while the SNARE complex promotes vesicle docking and fusion. There is no current evidence of direct cooperation between these complexes in plants. Here we confirm the role of the direct interaction between exocyst and SNARE complexes in plant development. We show the double mutant *exo70A1/vamp721* plants are strongly inhibited in cell expansion resulting in dwarf phenotype, additive to the single *exo70A1*. For the first time, we report that exocyst subunits directly interact with a subset of SNAREs at the PM. Our results provide an updated mechanism of plant exocytosis that includes direct interactions between exocyst and SNARE complexes. We suggest that the individual functions of these complexes could be coordinated through their interactions to support vesicle trafficking patterns required for plant cell function and development.

Introduction

Exocytosis in eukaryotes is required for the delivery and fusion of membrane containers with transporting diverse types of cargo to the PM. Exocytotic vesicles are trafficked along the cytoskeleton to specific membrane regions where they are tethered, docked and fused for cargo delivery (Varlamov et al. 2004; Bassham & Blatt 2008; Südhof & Rothman 2009; Žárský et al. 2009). The families of highly conserved proteins assist in vesicle fusion regulation; SNARE proteins mediate fusion events between vesicle and target membranes in conjunction with tethering complexes as effectors of Rab and Rho/Rop GTPases (Cai et al. 2007; Žárský et al. 2009; Dey et al. 2016). SNARE proteins are classified as either Qa-, b-, c-, or R-SNARES that are located on the vesicle and target membranes, respectively. This classification is dependent on amino acid residues found in conserved domains of the SNARE proteins that contribute to the core complex upon assembly (Fasshauer et al. 1998; Kato et al. 2010; Uemura et al. 2004). While there is much conservation of SNARE proteins between plants and animals, the gene families have significantly expanded in plants, suggesting that vesicle trafficking pathways are more diverse or specialized in plant cells compared to animal cells (Sanderfoot et al. 2000; Jahn & Scheller 2006). Well characterised evolutionary derived Qa-SNARE syntaxin of plants SYP111/KNOLLE regulates cell plate biogenesis in angiosperms (Lukowitz et al. 1996), while the ancient PM-localized SYP132 function in cytokinesis only in the early embryogenesis (Enami et al. 2009; Park et al. 2018). The PM-localized SYP121 and SYP122, which two major Qa-SNAREs expressed in plants; have overlapping but not entirely redundant functions (Zhang et al. 2015; Sanderfoot 2007; Grefen & Blatt 2008; Enami et al. 2009). Along with the Qbc-SNARE SNAP33 and vesicle-associated membrane protein (VAMP) R-SNAREs, these proteins form complexes that drive vesicle fusion at the PM (Uemura et al. 2004). All plants R-SNARE have the N-terminal conserved longin domain (Lipka et al. 2007). There are eight VAMP72 proteins in plants that primarily participate in vesicle fusion at the PM. The homologous VAMP721 and VAMP722 directly interact with SYP111, SYP132, SYP121 and SYP122 to form a complex during membrane fusion (Kwon et al. 2008a; El Kasmi et al. 2013; Enami et al. 2009). Thus the VAMP721/722 are involved in the various secretory pathways towards PM/cell plate and it's disruption cause severe growth defect and seedling lethality (Zhang et al. 2011; Kwon et al. 2008).

The exocyst is a conserved octameric tethering complex involved in binding of secretory vesicles to the PM (Wu & Guo 2015). The exocyst assembles from eight subunits, SEC3, SEC5, SEC6, SEC8, SEC10, SEC15, EXO70 and EXO84 (Guo et al. 1999; TerBush et al. 1996; TerBush & Novick 1995), which structural modelling suggests are composed of

highly conserved helical bundles typical of the CATCHR (complexes associated with tethering containing helical rod) family of tethering complexes subunits (Moore & Xu 2007; Sivaram & Munson 2006; Chen et al. 2017). In yeast, all members of the CATCHR protein family directly interact with specific SNARE partners, although evidence for direct cooperation between exocyst and SNARE complexes at the PM is still fragmentary (Vukašinović & Žárský 2016; Ravikumar et al. 2017). The functional direct interaction in yeast was revealed between the exocyst SEC6 subunit and Qbc-SNARE Sec9 as a binary Sec9-Sso1 and ternary Sec9-Sso1-Snc2/1 complex. Lately, the direct interaction between SEC3 subunit and Qa-SNARE Sso2 that facilitates exocytosis was shown (Dubuke et al. 2015; Yue et al. 2017; Morgera et al. 2012). This evidence suggests that the interaction between a SNARE protein and a subunit of exocyst want be a unique and may be found in other organisms.

Similar to the SNAREs associated with the PM, exocyst subunits also underwent gene multiplication in land plants, especially the EXO70 subunit, which has 23 paralogues in Arabidopsis and 47 in rice (Eliáš 2003; Cvrčková et al. 2012). However, the core subunits SEC6 and SEC8 are present as single copy genes in Arabidopsis and they are essential for the male gametophyte transmission (Cole et al. 2005; Hála et al. 2008), but also sporophyte growth and development (Žárský et al. 2013). The multiplication of the EXO70 subunit may be a result of the need for an immobile plant cell to specifically target exocytotic cargos to PM domains or maintain those domains. The exocyst landmarks parts of the PM as destinations for vesicles and mediates vesicle tethering to the target membrane before the fusion; specific membrane targeting/landmarking may be the main function of the membrane interacting subunit EXO70 in plants (Pleskot et al. 2015; Kulich et al. 2015; Žárský et al. 2009). Thus, the cooperation between specific exocyst and SNARE partners may determine secretory pathways and exocyst might enhance the efficiency of SNARE complexes formation where very efficient exocytosis is required (Heider & Munson 2012a; Wu & Guo 2015).

In plants, there is little experimental evidence of direct interactions between these protein complexes. A direct interaction between the SNAP33 and the EXO70B2 and EXO70B1 has been described, but function was not tested (Pečenková et al. 2011; Zhao et al. 2015). The localization of VAMP721 is shifted to the cytoplasm in *exo70a1* dwarf mutant root cells because of the disturbed exocytosis (Fendrych et al. 2013). As vesicle tethering and docking happen before the SNARE complex formation, it is supposed that both functional SNARE and exocyst complexes are close enough to interact with each other or influence each other's functions such that they contribute to the cellular process resulting in vesicle PM fusion (Heider & Munson 2012).

Here, we identify a seedling lethal phenotype in the *exo70A1/vamp721* double mutant, which is an additive phenotype in comparison to single mutant *exo70A1*. To understand the molecular basis of this defect, we analyzed the ability of several exocyst and SNARE subunits to interact in a mating based split-ubiquitin system – mbSUS (Grefen et al. 2009). We found that EXO70A1 and some other exocyst subunits interact with the SNARE proteins associated with vesicle fusion at the PM, including SYP121, VAMP721, VAMP722 and SNAP33. However, we did not observe any positive interaction with the endomembrane associated R-SNARE VAMP723. We identified the longin domain of VAMP721 as a motif required for its interaction with EXO70A1; furthermore, not only is VAMP721, VAMP722 and SYP121 localization defective in the *exo70A1* single mutant, but secretion monitored by sec-YFP is impaired in this mutant as well. Therefore, the synthetic phenotype in the *exo70A1/vamp72*1 double mutant is a result of a synergic loss of exocytotic functions of these interacting exocyst and SNARE proteins. Our results provide new evidence for the direct interactions between the exocyst with R- and Q-SNAREs involved in vesicle fusion at the PM, as well as the genetic support of the cooperative functions these complexes that facilitates endomembrane organization, protein localization, and plant development.

Methods

Plant growth conditions and crosses

Plants in soil

Seeds from wild-type WT (Col-0) and mutant *Arabidopsis* lines were sown onto compost soil mix and stratified at 4°C in the dark for 48 h. The seeds were then germinated in long-day conditions in growth chambers set at 60% relative humidity and 22°C. Seedlings were allowed to grow for 10-15 days until they were transplanted to single pots or 15-holder trays for further growth and observation.

Plants on solid medium

Arabidopsis seed was surface sterilized with a 20% sodium hyperchlorite solution for 20 min at room temperature and then washed multiple times with sterile water. Sterilized was suspended in sterile distilled water and stratified at 4°C for 48 h in the dark before being plated onto the surface of 0.5 X MS medium solidified with 7% agar. Plates were sealed with surgical tape (3M) and placed in long-day light conditions for 10-15 d before seedlings were evaluated for mutant phenotypes and collected for genotyping.

Mutant crosses

To generate an *exo70A1/vamp721* double mutant, the heterozygous *exo70A1*$^{+/-}$ (Synek et al. 2006; SALK_135462) mutant was used as a maternal parent in a cross with the homozygous *vamp721* mutant (SALK_037273) as the paternal parent. The F_1 generation was allowed to self-fertilize and the F_2 seed was collected for further analysis.

Genotyping

Leaf tissue from mature plants or whole seedlings were individually harvested from the F_1 and F_2 lines from the initial *ex70A1*$^{+/-}$ x *vamp721* cross. Gene-specific primers were used to amplify the WT gene products and the mutant product was amplified using one of the gene-specific primers with the T-DNA left border primer. Standard PCR conditions were used in conjunction with appropriate annealing temperatures for each primer set. In the F_1 generation, double heterozygous mutants were identified and allowed to set seed. Since the *exo70A1* single mutant is infertile, a segregating population of *exo70A1*$^{+/-}$*vamp721*$^{-/-}$ was maintained for isolating double mutants.

mbSUS

Two haploid yeast lines were used to express pMetYOst-Dest or pNX35-Dest constructs of exocyst subunits or SNARE proteins, respectively. These lines were mated and protein-protein interactions were analyzed as previously described (Grefen et al. 2009).

Protein isolation and western blot

Yeast was grown overnight in 5 ml selective medium and harvested by centrifugation at 5,000 rcf. Pelleted yeast was dissolved in diluted lysis buffer (1/1 V/V, 10% SDS, 4 mM EDTA, 0.2% Triton-X 100, 0.01% bromophenol blue, 20 mM DTT, 20% Glycerol and 100 mM Tris, pH 6.8.), sonicated 2x for 30 s and boiled 5 min at 100 °C. Prepared protein samples were loaded on the 10% polyacrylamide gel and blotted onto the nitrocellulose membrane. The membrane was blocked in the buffer (1x PBS, 0.25% Tween, 5% low-fat milk) overnight and incubated with primary α-HA or α-VP16 antibodies. Proteins were detected using the secondary α-mouse or α-rabbit (Promega) antibodies.

The protein isolation for Co-Immunoprecipitation was done from 10 days old seedlings grown on 1/2MS 1% Sucrose, horizontal plates, long-day conditions. Seedlings were homogenized in liquid nitrogen using mortar and pestle and sec6/8 lysis buffer (Hála et al. 2008) was applied with protease inhibitor cocktail (Sigma Aldrich). Then we followed the Miltenyi Biotec kit protocol for Co-IP. Bound proteins were separated by 10% SDS-PAGE, and the lane was cut

into three bands. After in-gel digestion with trypsin, eluted peptides were identified using UHPLC Dionex Ultimate3000 RSLC nano (Dionex) connected with the mass spectrometer ESI-Q-TOF Maxis Impact (Bruker). Measurements were carried out in positive ion mode with precursor ion selection in the range of 400 to 1,400 mass-to-charge ratio; up to 10 precursor ions were selected for fragmentation from each mass spectrometry spectrum. Peak lists were extracted from raw data by Data Analysis version 4.1 (Bruker Daltonics) and uploaded to the data management system Proteinscape (Bruker Daltonics). For protein identification, the Mascot server (version 2.4.1; Matrix Science) was used with a SwissProt proteins.

Yeast and plant vector construction

All plasmids were constructed using the Gateway cloning system (Thermo Fisher Scientific, UK). The used primers for gene amplification and cloning are summarised in the table (Supplementary Table 1). Yeast and plant expression vectors can be found at www.prg.org.uk.

Tobacco transformation for FRET analysis

Tobacco plants (*Nicotiana benthamiana*) with fully expanded true leaves were used for transient transformation with *Agrobacterium tumefaciens* strain GV3101 carrying bicistronic vectors (Hecker et al. 2015) that enabled simultaneous expression of GFP tagged and mCherry tagged protein fusions. Overnight cultures of GV3101 expressing these constructs were diluted in infiltration buffer (10 mM MgCL2, 100 μM acetosyringone) until OD 0.07 and infiltrated by syringe into the abaxial surface of *N. benthamiana* leaves. Two days after inoculation, transformed leaves were used for microscopic FRET and FRET/FLIM analysis.

Ratiometric secretion assay

Arabidopsis seed was sterilized and sown into 0.05X MS liquid medium and allowed to germinate in long-day light conditions. Once the root and cotyledons emerged from the seed coat (approx. 2-3 d), they were co-cultured with *Agrobacterium* carrying the bicistronic constructs for an additional 3-4 d as previously described (Karnik et al). Seedling roots were then imaged near the root-shoot junction using a confocal scanning laser microscope (Leica/Zeiss) with a 20x objective. The 488-nm and 415-nm laser lines were used in sequence to excite the GFP and YFP protein fusions, respectively, which were then collected between 521 and 565 nm. The fluorescence measurements for both GFP and YFP were offset by subtracting autofluorescence captured in untransformed seedlings; the normalized YFP

measurements were divided by the normalized GFP values to calculate the ratio of YFP fluorescence relative to the GFP expression control. A total of at least six seedlings were used in each condition for analysis; 6-12 measurements were taken from each seedling. The experiments were repeated at least three times to provide biological replicates.

Microscopy and protein localization

A ZEISS LSM 880 microscope with x40 water immersion objective was used for image acquisition of transformed *N. benthamiana* leaves. For FRET, the GFP constructs were excited at 488 nm and detected at 505–530 nm, mCherry constructs were excited at 488 nm and detected at 600–620 nm to collect the FRET signal. The FRET image analysis was performed with the PixFRET tool as previously described (Feige et al. 2005).

The dynamic study of the lateral membranes of root epidermal cells of the elongation zone was performed on a Nikon TE200e with a Yokogawa Andor spinning disc unit an x40 and x63 oil immersion objectives. The images were processed by Fiji/ImageJ software and the membrane/cytoplasm ratio was calculated as previously described (Fendrych et al. 2013).

Results

The exo70A1/vamp721 double mutant in Arabidopsis is plantlet lethal

The exocyst *exo70A1* single mutant has several severe phenotypes in multiple tissue types suggesting its ubiquitous requirement throughout the development, including cytokinesis, cell expansion, root and hypocotyl elongation, pollen tube growth and plant branching (Synek et al. 2006; Fendrych et al. 2010). Likewise, many mutants in SNARE subunits can also have pleiotropic defects but due to the partial redundancies and multiple isoforms, more severe mutant phenotypes are often seen in double mutants (Hála et al. 2008; Kulich et al. 2013). Previously, a localization defect of GFP-VAMP721, but not GFP-SYP121 was shown in *exo70A1* (Fendrych et al. 2013). Therefore, we hypothesized that if the exocyst and SNARE functions were in the consecutive steps of the same secretory pathway, the double mutants would have more severe phenotypes than the single mutant parents. We crossed the *exo70A1*$^{+/-}$ heterozygote with the *vamp721*$^{-/-}$ homozygote, selected the double heterozygote individuals from the F_1 generation, and then looked for segregation in the F_2 generation. There was a distinct phenotypic segregation within the F_2 population, including extremely underdeveloped and stunted seedlings (Fig. S1), which were collected for genotyping and identified as double *exo70A1/vamp721* mutants (Fig 1C). When seedlings were grown for 7

days on 1/2MS plates, the *exo70A1/vamp721* double mutants appeared the impaired growth phenotype in comparison to *exo70A* (Fig. 1B). After transfer to soil, the *exo70A1/vamp721* seedlings progressed past the first true leaf stage in the soil and often died shortly thereafter in the long day cultivation condition (Fig. S1). In the short day conditions, the double mutants were able to sustain growth till the age of 10 weeks but displayed the additive growth defect still (Fig. 1A). Therefore EXO70A1 and VAMP721 either function in the same secretory pathway or require one another for their functions. Further analysis of seed development and seed set will be necessary to evaluate where these defects are first appearing in early plant development.

Exocyst is required for secretion in Arabidopsis

The exocyst has been linked to secretion in plants and the mutants of several subunits have phenotypes that are consistent with defects in pectin secretion, cell expansion and membrane protein regulation or localization (Rybak et al. 2014; Pečenková et al. 2011; Kulich et al. 2010; Fendrych et al. 2010; Hála et al. 2008; Drdová et al. 2013). Previously, the transient expression of multicistronic vectors in Arabidopsis seedling roots has been used to visualize changes in bulk secretion at the PM (Karnik et al. 2013; Grefen et al. 2015). These vectors express multiple cassettes on the same vector backbone, including sec-YFP, GFP-HDEL and an additional cassette for a gene of interest. The GFP-HDEL can serve as an expression control as well as a way to ratiometrically quantify changes in secretion. It has been shown that the expression of a cytoplasmic fragment of SYP121 (SYP121$^{\Delta C}$) severely block a secretion (Karnik et al. 2013). Using the SYP121$^{\Delta C}$ expression as a positive control for the secretory block, we measured sec-YFP fluorescence in WT, *exo70A1* knock out mutant and *sec8-m4* knock-down mutant (Cole et al. 2005) seedlings by confocal scanning electron microscopy (LSCM). Compared to the secretion of sec-YFP in WT seedling roots, secretion was blocked in the *exo70A1* and *sec8-m4* mutants (Fig. 2) seedlings with and without the additional expression of SYP121$^{\Delta C}$. Thus similarly to the SNARE complex, these results indicating that entire exocyst complex function is required for secretion in *Arabidopsis* as expected.

Exocyst and SNAREs interactions in yeast

We used the yeast mbSUS (Grefen et al. 2009) to ask if the *EXO70A1* and *VAMP721* genetic association was relevant on the protein interaction level and if this association was unique for both partners. The mbSUS assay allows for candidate proteins to be expressed in or

at the PM, providing a native-like environment for testing interactions between the transmembrane SNAREs and PM-associated exocyst subunits. We interrogated the interactions between the EXO70A1 and the several SNAREs involved in secretion at the PM, along with non-PM SNAREs for comparison. Before the actual assay, we first evaluated the expression of VP16 tagged exocyst baits (Fig. S3) and HA-tagged SNARE prays (Fig. S4). From evaluated proteins expressed in yeasts, two exocyst subunits SEC6 and SEC3 provided critically low level of expression (Fig. S3), therefore we assumed the level of protein wasn't sufficient to provide a positive interaction (data not shown). We observed interactions between the SYP121 and SYP122 Qa-SNAREs; we also observed interactions between the VAMP721, VAMP722, VAMP724, VAMP727 R-SNAREs, but not the VAMP723 R-SNAREs and EXO70A1 (Fig. 3). We wanted to resolve if these interactions were specific for EXO70A1 subunit or could also occur between the other EXO70 isoforms or core exocyst subunits. We performed the same mbSUS test with the EXO70B1, EXO70B2, EXO70H1, SEC8, SEC10a and EXO84b subunits and got almost the identical results (Fig. S2A, B). None of tested exocyst subunits interacted with the VAMP723. The Qbc-SNARE SNAP33, which is an adaptor protein involved in SNARE complex formation, interacted with the EXO70B1, EXO70B2 as have been reported (Pečenková et al. 2011; Zhao et al. 2015), but not EXO70H1 and only weakly with EXO70A1 (Fig. S2A). The exocyst core subunit SEC8 also interacted with the SNAREs but had weaker interactions with SNAP33 and did not interact with VAMP723 (Fig. S2B). These results suggest that there are multiple interactions that can occur directly between the exocyst and SNARE complexes at the PM in yeasts.

We stayed focus on EXO70A1, probably the main isoform involved in canonical exocytosis, for our initial investigation of the exocyst-SNARE relationship in *Arabidopsis*. Furthermore, we chose the contrasting interactions between EXO70A1 and the VAMP721 and VAMP723 SNAREs as a study model to better understand the requirements for these interactions. Chimaera constructs that combine the protein domains of VAMP721 and VAMP723 have been used before to identify the protein domains required for the interaction between the VAMPs and other PM proteins (Zhang et al. 2016). We asked if specific VAMP721 domains were required for its interaction with exocyst subunits and found that the longin domain was necessary for the EXO70A1-VAMP interaction to occur in yeast (Fig. 4), indicating that the longin domain is the key component for protein-protein interactions between the R-SNARE and other proteins involved in secretion at the PM now including also exocyst.

The exocyst interacts with SNARE in plants

The mbSUS results provided an indication that EXO70A1 could directly interact with VAMP721 at the PM but not VAMP723 potentially due to its ER localization in plants (Uemura et al. 2004). We wanted to confirm the interactions observed in yeasts in the more natural system and also without the transmembrane domain added to exocyst subunits. Therefore we transiently expressed multi-cassette FRET constructs containing both the mCherry-EXO70A1 and GFP-SNARE under the 35S promoter in *N. benthamiana* (Fig. S5). We used the known interaction between mCherry-SYP121 and GFP-VAMP721 (Kwon et al. 2008) as a positive control and mCherry-EXO70 and free-2xGFP as a negative control for the Pix-FRET analysis processing, which allowed us to visualize FRET efficiency minima and maxima in the grey scale value (Feige et al. 2005b). We observed significant FRET signals between mCherry-EXO70A1 and GFP-VAMP721, but not GFP-VAMP723 (Fig. 5). GFP-VAMP721 also interacted with the core subunit GFP-SEC8 (Fig. 5). These results indicate that the direct interaction between the EXO70A1-containing exocyst and VAMP721 R-SNARE occurs *in vivo*.

We used the stable transformants of Col-0 with GFP-SYP121, GFP-VAMP721, GFP-SEC8, SEC6-GFP, GFP-SEC3a, EXO70A1-GFP to search for their interactors in *Arabidopsis* with the Co-IP and subsequent LC-MS/MS analysis. We identified SNAREs in the exocyst fractions and the SEC8 in the SNARE fraction (Table 1). Surprisingly, no peptides belonging to SNAREs were found in the EXO70A1 fraction and *vice versa*. This supports the hypothesis that both complexes meet *in vivo* only for a limited time at the place of actual secretion and their association is rather transient.

Localization of VAMP721 and SYP121 is disrupted in exo70A1 mutants

EXO70A1 as an exocyst subunit should play a role in vesicle tethering before the SNARE orchestrated docking at the PM. We hypothesised if both complexes interact, the loss of single partner would cause the disbalance of another one. We asked if the localization of GFP-EXO70A1 is altered in SNARE mutants and *vice versa* if the SNARE localization is affected in the *exo70A1* mutant. We quantified the PM GFP tagged SNARE proteins signal as a ratio between the fluorescence present at the PM and cytoplasm. We observed a shift of the GFP-VAMP721 localization from PM towards cytoplasm in the lateral root cells (transient zone) in *exo70A1*, as previously reported (Fendrych et al. 2013), and also in *sec8-m4* mutants (Fig. 6A, C). The same effect, we could observed for GFP-SYP121, although we have to stress

the GFP:SYP121 in *exo70A1* pictures were taken from T1 line, just after the *Agrobacterium* transformation because the construct was from unknown reason silenced in the T2 generation (Fig. 6A, C). The GFP-VAMP722 PM signal was also reduced but significantly only in the *exo70A1* mutant background (Fig. 6A, C - stronger cytoplasm signal of GFP-VAMP722 in WT than GFP-VAMP721 is also visible). The strength of SNARE proteins internalization thus correlates with actual growth phenotype of *sec8-m4* and *exo70A1* mutant lines. The GFP-VAMP723 expression naturally present in the endoplasmic reticulum (ER) did not show any obvious changes (Fig. S6).

The EXO70A1-GFP fusion protein localized on the lateral membrane of the *syp121*, *vamp721* and *vamp722* mutant similar to its localization in WT seedlings, but there was an obvious reduction of the PM signal (Fig. 6B, C). These results indicate that both the exocyst and SNARE subunits that associate with the PM can alter each other's localization in respective Arabidopsis LOF mutants, presumably through affecting final steps of exocytotic machinery and direct interactions during vesicle docking and fusion events.

Discussion

Current models of exocytosis include three distinct stages: vesicle tethering, docking, and fusion. These stages are expected to be linked, either through sequential pathways or through interactions between the protein complexes that regulate each step. Here, we present new findings of a direct interaction between the exocyst complex, which mediates vesicle tethering and recruitment to the PM, and the Q- and R-SNAREs that are required for membrane fusion in plants. We also provide the genetic evidence that indicates that these interactions are important at several stages of development in the plant model *Arabidopsis*.

The pleiotropic phenotypes of the *exo70A1* single mutant imply the importance of this subunit for general exocyst function (Fendrych et al. 2013; Synek et al. 2006). Indeed, a growing number of cargos have been identified that require EXO70A1 and are mislocalized in the mutant (Fendrych et al. 2013; Kalmbach et al. 2017; Vukašinović et al. 2017; Kulich et al. 2010). The internalization of the VAMP721 protein in the *exo70A1* mutant we show here (Fig. 6) is consistent with previous work (Fendrych et al. 2013). However, other members of the complex VAMP722 and SYP121 are also internalized in *exo70A1* mutants (Fig. 6). As membrane-bound proteins thus SNAREs could be assumed as another cargo for the exocyst regulated vesicles. However, we provide additional evidence that this mislocalization is concomitant with defects in secretion in *exo70A1* and *sec8-m4* mutants monitored by sec-YFP secretion (Fig 2), as well as escalated growth and developmental defect observed in the *exo70A1/vamp721* double mutant (Fig. 1). In the double mutant, two major component of the common secretory pathway EXO70A1 and VAMP721 are disrupted. Both proteins belong to heteromeric complexes, which might remain partially functional, therefore the seedlings survive. The double mutant *exo70A1/vamp721* resemble the double mutant within the exocyst, such as *exo70A1/sec5a* (Hála et al. 2008), this phenomenon points to the potential direct interaction between exocyst and VAMP721. The secretory defect and SNAREs internalization in *exo70A1* and *sec8-m4* suggest the complex exocyst facilitate the SNARE driven PM secretion. However, the EXO70A1 signal internalization in *vamp721*, *vamp722* and *syp121* mutants implicates the cooperation between SNARE and exocyst at the PM is reciprocal. In yeast model, the individual exocyst and SNARE subunits along with the SM protein Sec1 may compete with each other and thus either block or facilitate the assembly of the intrinsic or tangential complex (Heider & Munson 2012; Dubuke et al. 2015).

To reveal the mechanistic details of those interactions, we used mbSUS assay at PM in yeasts. Surprisingly, the PM localization provides almost identical binding between tested exocyst subunits and PM SNAREs and denied binding with ER-specific VAMP723. Thus our

data show the potential for many exocyst subunits, including EXO70A1, to interact with multiple PM-localized SNARE proteins. Moreover, the protein structure does not necessarily provide the specificity between those partners. If some of the interactions between exocyst and SNARE proteins are biologically relevant, they are dependent on the spatial and temporal conditions, as well as other interactors such as RAB GTPases (Hutagalung & Novick 2011). The internalization of GFP tagged interaction partner (Fig. 6) caused by mutation also suggests the direct binding between both proteins is connected to PM. We admit the interactions observed in yeast and *N. bentahmiana* provide the mechanistic view and are still far from the native situation in *Arabidopsis*. Therefore the week interactions obtained in the Co-IP and LC-MS/MS analysis may correspond to the native situation at most. From the data, the clear interaction between the SYP121/VAMP721 SNAREs and exocyst complex occurs in both directions, although the EXO70A1 does not show such a tendency (Table 1). Therefore we assume, the potential of exocyst/SNARE interaction wasn't fulfilled in our test or the interactions might be fast and transient in *Arabidopsis*.

The EXO70A1 was able to interact with SYP121, VAM721, and VAMP722, and all of them were affected in the *exo70A1* mutant, suggesting that the exocyst could provide a spatial landmark for SYP121/VAMP721/722 binary complex formation at the PM. SYP121 is relatively immobile, unlike the VAMP721/722 proteins, which localize to mobile intracellular compartments. This might explain why the exocyst subunit was found rather in the SYP121 bait Co-IP than in vesicle-associated VAMP721 fraction (Table 1). The PM/cytoplasm ratio of EXO70A1-GFP affected in the *syp121, vamp721/2* mutants also points to the necessity of interaction partners for EXO70A1 to prolong its PM working time (Fig. 6). Interestingly, the VAMP721 mislocalization seen in *exo70A1* mutants was also observed in a knockdown mutant *sec8-m4* of the core exocyst subunit SEC8, which also interacts with VAMP721 (Fig 2). These results prove the entire exocyst complex participate in the targeting of VAMP721/722 vesicles at the PM and further implicate a direct interaction between SNAREs and the exocyst in vesicle tethering or recruitment to specific regions of the PM for cargo delivery. This is in agreement with the result, that the SYP121 localization is altered in the *exo70A1* and *sec8-m4* mutants, indicating a potential exocyst function in the delivery or maintenance of SYP121 to the PM.

Efforts to isolate exocyst complex from yeast (Songer & Munson 2009) and recently mapping of exocyst connectivity (Heider et al. 2016; Picco 2017) resulted in a new model of exocyst function. In contrast to previous models proposing sequential assembly during the tethering (Novick et al. 2006) in yeast, a stable exocyst holocomplex consisting of all eight subunits is uncovered (Mei et al. 2018; Picco et al. 2017; Heider et al. 2016). This holocomplex

is however easily split into two subcomplexes consisting of Sec3-Sec5-Sec6-Sec8 and Sec10-Sec15-Exo70-Exo84 (Heider et al. 2016). Details uncovered by ingenious *in vivo* analysis of exocyst complex clearly indicate a topologically optimal space/cavity between the exocyst complex, PM and tethered vesicle membrane (there are more than 10 complexes tethering one vesicle). Like that intermembrane cavity may optimally accommodate more exocyst-SNARE interactions (Picco et al. 2017). Because both EXO70 isoforms and the core exocyst subunits interact with the same SNAREs, we speculate that the exocyst participates in these SNARE interactions prior to vesicle fusion as an assembled complex at the PM. Further analysis will be needed to determine the sequential or dynamic nature of these interactions. To understand basic mechanistic details of exocytosis in plants will also necessitate studying interactions between partners of other candidate exocytotic SNAREs and tethering factors not studied yet.

Acknowledgements

We thank Jana Šťovíčková, the technician of Laboratory of Cell Biology, for help with plants harvesting and Martin Potocký for the critical reading.

References

Bassham, D.C. & Blatt, M.R., 2008. SNAREs: cogs and coordinators in signaling and development. *Plant physiology*, 147(4), pp.1504–1515.

Cai, H., Reinisch, K. & Ferro-Novick, S., 2007. Coats, tethers, Rabs, and SNAREs work together to mediate the intracellular destination of a transport vesicle. *Developmental cell*, 12(5), pp.671–682.

Chen, J. et al., 2017. Crystal structure of Sec10, a subunit of the exocyst complex. *Scientific reports*, 7, p.40909.

Cole, R.A. et al., 2005. SEC8, a subunit of the putative Arabidopsis exocyst complex, facilitates pollen germination and competitive pollen tube growth. *Plant physiology*, 138(4), pp.2005–2018.

Cvrčková, F. et al., 2012. Evolution of the land plant exocyst complexes. *Frontiers in plant science*, 3, p.159.

Dey, G., Thattai, M. & Baum, B., 2016. On the Archaeal Origins of Eukaryotes and the Challenges of Inferring Phenotype from Genotype. *Trends in cell biology*, 26(7), pp.476–485.

Drdová, E.J. et al., 2013. The exocyst complex contributes to PIN auxin efflux carrier recycling and polar auxin transport in Arabidopsis. *The Plant journal: for cell and molecular biology*, 73(5), pp.709–719.

Dubuke, M.L. et al., 2015. The Exocyst Subunit Sec6 Interacts with Assembled Exocytic SNARE Complexes. *The Journal of biological chemistry*, 290(47), pp.28245–28256.

Eliáš, M., 2003. The exocyst complex in plants. *Cell biology international*, 27(3), pp.199–201.

El Kasmi, F. et al., 2013. SNARE complexes of different composition jointly mediate membrane fusion in Arabidopsis cytokinesis. *Molecular biology of the cell*, 24(10), pp.1593–1601.

Enami, K. et al., 2009. Differential expression control and polarized distribution of plasma membrane-resident SYP1 SNAREs in Arabidopsis thaliana. *Plant & cell physiology*, 50(2), pp.280–289.

Fasshauer, D. et al., 1998. Conserved structural features of the synaptic fusion complex: SNARE proteins reclassified as Q- and R-SNAREs. *Proceedings of the National Academy of Sciences of the United States of America*, 95(26), p.15781.

Feige, J.N. et al., 2005. PixFRET, an ImageJ plug-in for FRET calculation that can accommodate variations in spectral bleed-throughs. *Microscopy research and technique*, 68(1), pp.51–58.

Fendrych, M. et al., 2010. The Arabidopsis exocyst complex is involved in cytokinesis and cell plate maturation. *The Plant cell*, 22(9), pp.3053–3065.

Fendrych, M. et al., 2013. Visualization of the exocyst complex dynamics at the plasma membrane of Arabidopsis thaliana. *Molecular biology of the cell*, 24(4), pp.510–520.

Grefen, C. et al., 2015. Erratum: A vesicle-trafficking protein commandeers Kv channel voltage sensors for voltage-dependent secretion. *Nature Plants*, p.15166.

Grefen, C. & Blatt, M.R., 2008. SNAREs--molecular governors in signalling and development. *Current opinion in plant biology*, 11(6), pp.600–609.

Grefen, C., Obrdlik, P. & Harter, K., 2009. The determination of protein-protein interactions by the mating-based split-ubiquitin system (mbSUS). *Methods in molecular biology* , 479, pp.217–233.

Guo, W., Grant, A. & Novick, P., 1999. Exo84p Is an Exocyst Protein Essential for Secretion. *The Journal of biological chemistry*, 274(33), pp.23558–23564.

Hála, M. et al., 2008. An exocyst complex functions in plant cell growth in Arabidopsis and tobacco. *The Plant cell*, 20(5), pp.1330–1345.

Hecker, A. et al., 2015. Binary 2in1 Vectors Improve in Planta (Co)localization and Dynamic Protein Interaction Studies. *Plant physiology*, 168(3), pp.776–787.

Heider, M.R. et al., 2016. Subunit connectivity, assembly determinants and architecture of the yeast exocyst complex. *Nature structural & molecular biology*, 23(1), pp.59–66.

Heider, M.R. & Munson, M., 2012. Exorcising the exocyst complex. *Traffic* , 13(7), pp.898–907.

Hutagalung, A.H. & Novick, P.J., 2011. Role of Rab GTPases in Membrane Traffic and Cell Physiology. *Physiological reviews*, 91(1), pp.119–149.

Jahn, R. & Scheller, R.H., 2006. SNAREs--engines for membrane fusion. *Nature reviews. Molecular cell biology*, 7(9), pp.631–643.

Kalmbach, L. et al., 2017. Transient cell-specific EXO70A1 activity in the CASP domain and Casparian strip localization. *Nature plants*, 3, p.17058.

Karnik, R. et al., 2013. Arabidopsis Sec1/Munc18 Protein SEC11 Is a Competitive and Dynamic Modulator of SNARE Binding and SYP121-Dependent Vesicle Traffic. *The Plant cell*, 25(4), pp.1368–1382.

Kato, N. et al., 2010. Luminescence detection of SNARE-SNARE interaction in Arabidopsis protoplasts. *Plant molecular biology*, 72(4-5), pp.433–444.

Kulich, I. et al., 2013. Arabidopsis exocyst subcomplex containing subunit EXO70B1 is involved in autophagy-related transport to the vacuole. *Traffic* , 14(11), pp.1155–1165.

Kulich, I. et al., 2010. Arabidopsis exocyst subunits SEC8 and EXO70A1 and exocyst interactor ROH1 are involved in the localized deposition of seed coat pectin. *The New phytologist*, 188(2), pp.615–625.

Kulich, I. et al., 2015. Cell Wall Maturation of Arabidopsis Trichomes Is Dependent on Exocyst Subunit EXO70H4 and Involves Callose Deposition. *Plant physiology*, 168(1), pp.120–131.

Kwon, C. et al., 2008. Co-option of a default secretory pathway for plant immune responses. *Nature*, 451(7180), pp.835–840.

Lipka, V., Kwon, C. & Panstruga, R., 2007. SNARE-ware: the role of SNARE-domain proteins in plant biology. *Annual review of cell and developmental biology*, 23, pp.147–174.

Lukowitz, W., Mayer, U. & Jürgens, G., 1996. Cytokinesis in the Arabidopsis embryo involves the syntaxin-related KNOLLE gene product. *Cell*, 84(1), pp.61–71.

Mei, K. et al., 2018. Cryo-EM structure of the exocyst complex. *Nature structural & molecular biology*, 25(2), pp.139–146.

Moore, B.A. & Xu, Z., 2007. The Crystal Structure of Mouse Exo70 Reveals Unique Features of the Mammalian Exocyst. Available at: http://dx.doi.org/10.2210/pdb2pft/pdb.

Morgera, F. et al., 2012. Regulation of exocytosis by the exocyst subunit Sec6 and the SM protein Sec1. *Molecular biology of the cell*, 23(2), pp.337–346.

Novick, P. et al., 2006. Interactions between Rabs, tethers, SNAREs and their regulators in exocytosis. *Biochemical Society transactions*, 34(Pt 5), pp.683–686.

Park, M. et al., 2018. Concerted Action of Evolutionarily Ancient and Novel SNARE Complexes in Flowering-Plant Cytokinesis. *Developmental cell*. Available at: http://dx.doi.org/10.1016/j.devcel.2017.12.027.

Pečenková, T. et al., 2011. The role for the exocyst complex subunits Exo70B2 and Exo70H1 in the plant-pathogen interaction. *Journal of experimental botany*, 62(6), pp.2107–2116.

Picco, A. et al., 2017. The In Vivo Architecture of the Exocyst Provides Structural Basis for Exocytosis. *Cell*, 168(3), pp.400–412.e18.

Picco, G., 2017. *Cap in Hand: How Charities Are Failing the People of Canada and the World*, Hilborn Civil Sector Press.

Pleskot, R. et al., 2015. Membrane targeting of the yeast exocyst complex. *Biochimica et biophysica acta*, 1848(7), pp.1481–1489.

Ravikumar, R., Steiner, A. & Assaad, F.F., 2017. Multisubunit tethering complexes in higher plants. *Current opinion in plant biology*, 40, pp.97–105.

Rybak, K. et al., 2014. Plant cytokinesis is orchestrated by the sequential action of the TRAPPII and exocyst tethering complexes. *Developmental cell*, 29(5), pp.607–620.

Sanderfoot, A., 2007. Increases in the number of SNARE genes parallels the rise of multicellularity among the green plants. *Plant physiology*, 144(1), pp.6–17.

Sanderfoot, A.A., Assaad, F.F. & Raikhel, N.V., 2000. The Arabidopsis genome. An abundance of soluble N-ethylmaleimide-sensitive factor adaptor protein receptors. *Plant physiology*, 124(4), pp.1558–1569.

Sivaram, M.V. & Munson, M., 2006. Crystal structure of the C-terminal domain of the exocyst subunit Sec6p. Available at: http://dx.doi.org/10.2210/pdb2fji/pdb.

Songer, J.A. & Munson, M., 2009. Sec6p anchors the assembled exocyst complex at sites of secretion. *Molecular biology of the cell*, 20(3), pp.973–982.

Südhof, T.C. & Rothman, J.E., January 23 , 2009. Membrane Fusion: Grappling with SNARE and SM Proteins. *Science*, 323(5913), pp.474–477.

Synek, L. et al., 2006. AtEXO70A1, a member of a family of putative exocyst subunits specifically expanded in land plants, is important for polar growth and plant development. *The Plant journal: for cell and molecular biology*, 48(1), pp.54–72.

TerBush, D.R. et al., 1996. The Exocyst is a multiprotein complex required for exocytosis in Saccharomyces cerevisiae. *The EMBO journal*, 15(23), pp.6483–6494.

TerBush, D.R. & Novick, P., 1995. Sec6, Sec8, and Sec15 are components of a multisubunit complex which localizes to small bud tips in Saccharomyces cerevisiae. *The Journal of cell biology*, 130(2), pp.299–312.

Uemura, T. et al., 2004. Systematic analysis of SNARE molecules in Arabidopsis: dissection of the post-Golgi network in plant cells. *Cell structure and function*, 29(2), pp.49–65.

Varlamov, O. et al., 2004. i-SNAREs: inhibitory SNAREs that fine-tune the specificity of membrane fusion. *The Journal of cell biology*, 164(1), pp.79–88.

Vukašinović, N. et al., 2017. Microtubule-dependent targeting of the exocyst complex is necessary for xylem development in Arabidopsis. *The New phytologist*, 213(3), pp.1052–1067.

Vukašinović, N. & Žárský, V., 2016. Tethering Complexes in the Arabidopsis Endomembrane System. *Frontiers in cell and developmental biology*, 4, p.46.

Wu, B. & Guo, W., 2015. The Exocyst at a Glance. *Journal of cell science*, 128(16), pp.2957–2964.

Yue, P. et al., 2017. Sec3 promotes the initial binary t-SNARE complex assembly and membrane fusion. *Nature communications*, 8, p.14236.

Zhang B, Karnik R, Waghmare S, Donald NA, Blatt MR, 2016. VAMP721 conformations unmask an extended motif for K+ channel binding and gating control | Plant Physiology. Available at: http://www.plantphysiol.org/content/early/2016/11/07/pp.16.01549?utm_source=TrendMD&utm_medium=cpc&utm_campaign=Plant_Physiol_TrendMD_0 [Accessed October 2, 2017].

Zhang, B. et al., 2015. The Arabidopsis R-SNARE VAMP721 Interacts with KAT1 and KC1 K+ Channels to Moderate K+ Current at the Plasma Membrane. *The Plant cell*, 27(6), pp.1697–1717.

Zhang, L. et al., 2011. Arabidopsis R-SNARE proteins VAMP721 and VAMP722 are required for cell plate formation. *PloS one*, 6(10), p.e26129.

Zhao, T. et al., 2015. A truncated NLR protein, TIR-NBS2, is required for activated defense responses in the exo70B1 mutant. *PLoS genetics*, 11(1), p.e1004945.

Žárský, V. et al., 2009. Exocytosis and cell polarity in plants - exocyst and recycling domains. *The New phytologist*, 183(2), pp.255–272.

Žárský, V. et al., 2013. Exocyst complexes multiple functions in plant cells secretory pathways. *Current opinion in plant biology*, 16(6), pp.726–733.

Fig. 1

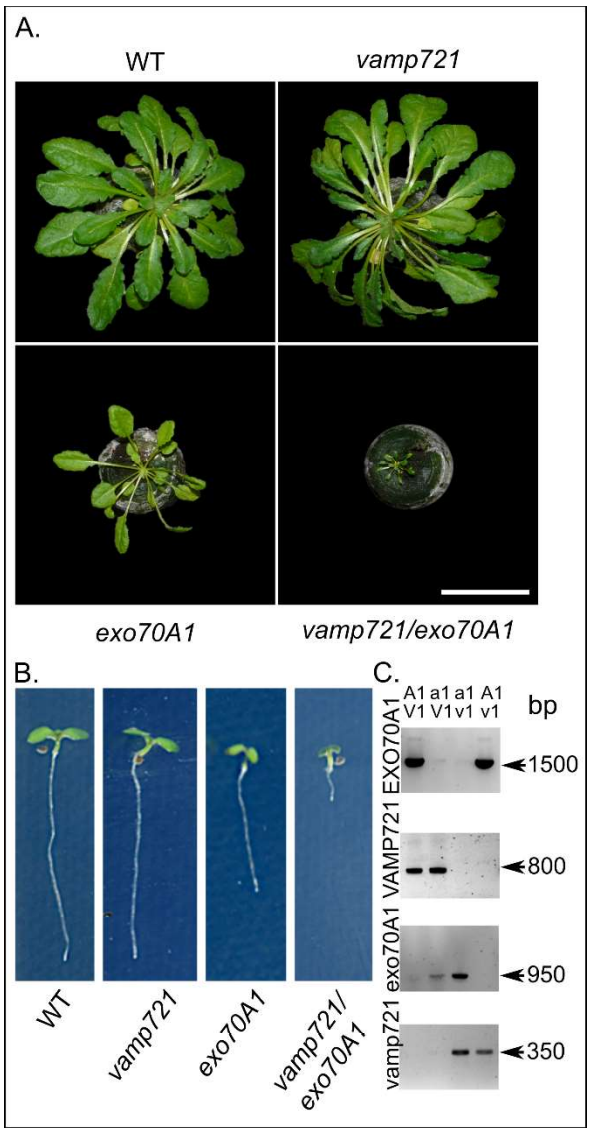

Figure 1 The *exo70A1/vamp721* double mutant exhibits an additive growth defect compared to the single mutant *exo70A1*

(A) Representative images of WT, *vamp721*, *exo70A1*, and the *exo70A1/vamp721* double mutants 10 weeks after germination. (B) Seedling and root development of WT, single, and double mutants sown on 1/2 MS plates. The *vamp721* has no phenotype; *exo70A1* has a short, slanted root and small cotyledons; *vamp721/exo70A1* double mutant seedlings are stunted with short roots and small cotyledons. (C) The PCR confirming the genotype of the *vamp721/exo70A1* double mutant seedlings selected. The entire stunted plant was harvested for genotyping to confirm the double mutant. Scale bar represents 5cm.

Fig. 2

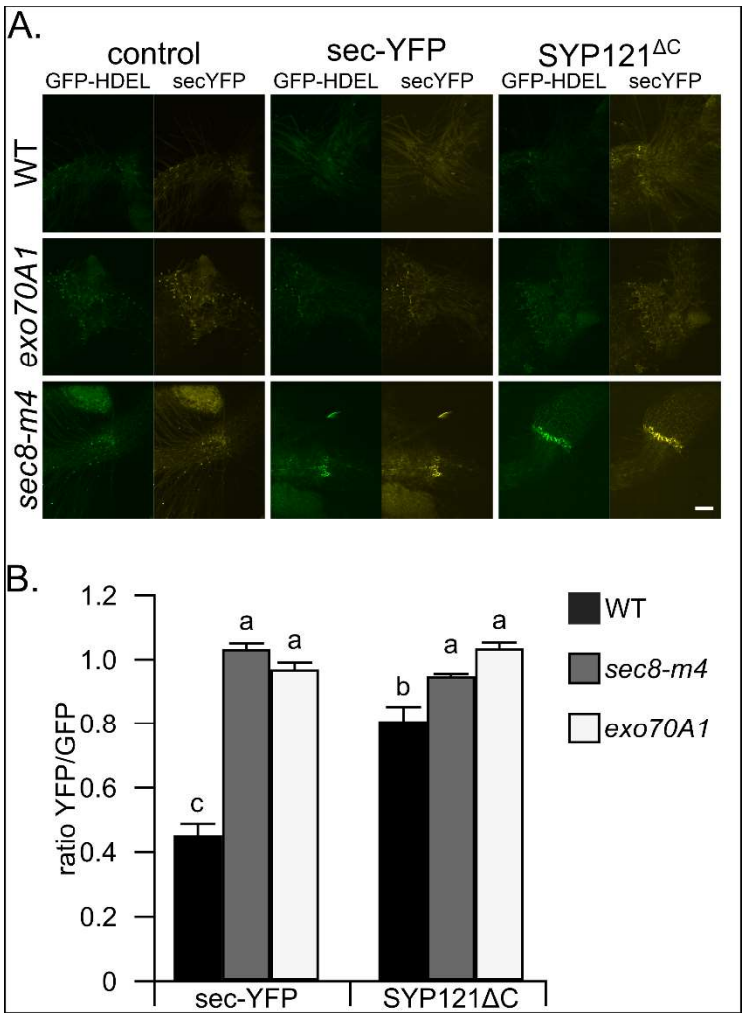

Figure 2 The *exo70A1* and *sec8-m4* mutants are impaired in secretion

(A) The transient expression analysis of secretory blockage in root and hypocotyl/root transition zone in WT, *exo70A1* and *sec8-m4* mutant *Arabidopsis* lines. Scale bar represents 100 μm (B) Graphical illustration of secretory assay done by a transient transformation in the root of 2-5 days old seedlings. From bicistronic vector plant expressed sec-YFP together with HDEL-GFP. We measured in the Root Collet area the ratio between YFP/GFP and normalized it by autofluorescence of non-transformed seedlings. The experiment was repeated three times with a similar trend. The letters indicate statistically significant difference calculated with one way ANOVA and nonparametric post-hoc Tukey HSD test at $p<0.01$.

Fig. 3

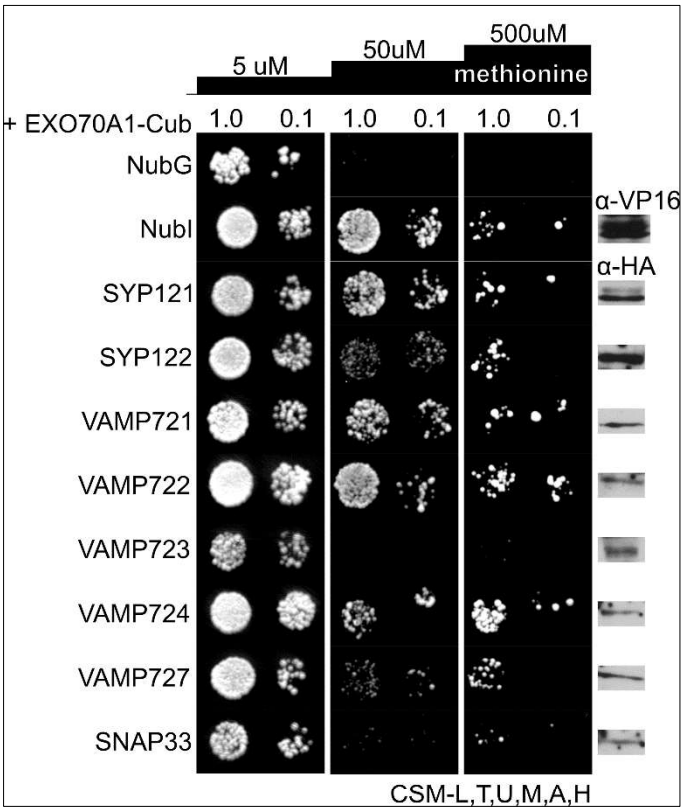

Figure 3 Q- and R- SNAREs interact with exocyst subunit EXO70A1

The AP.4 yeast strains expressing the EXO70A1 bait was mated with AP.5 strains expressing the SNAREs prey and serial plated at dilutions of 1.0 and 0.1 on selective media containing increasing concentrations of methionine. The EXO70A1 interacted with SYP121 and SYP122, as well as the VAMP family members except for VAMP723. The adaptor protein, SNAP33 interacted weakly with the EXO70A1. The expression of SNARE and EXO70A1 in mated yeast was identified with commercial α-HA and α-VP16, respectively.

Fig. 4

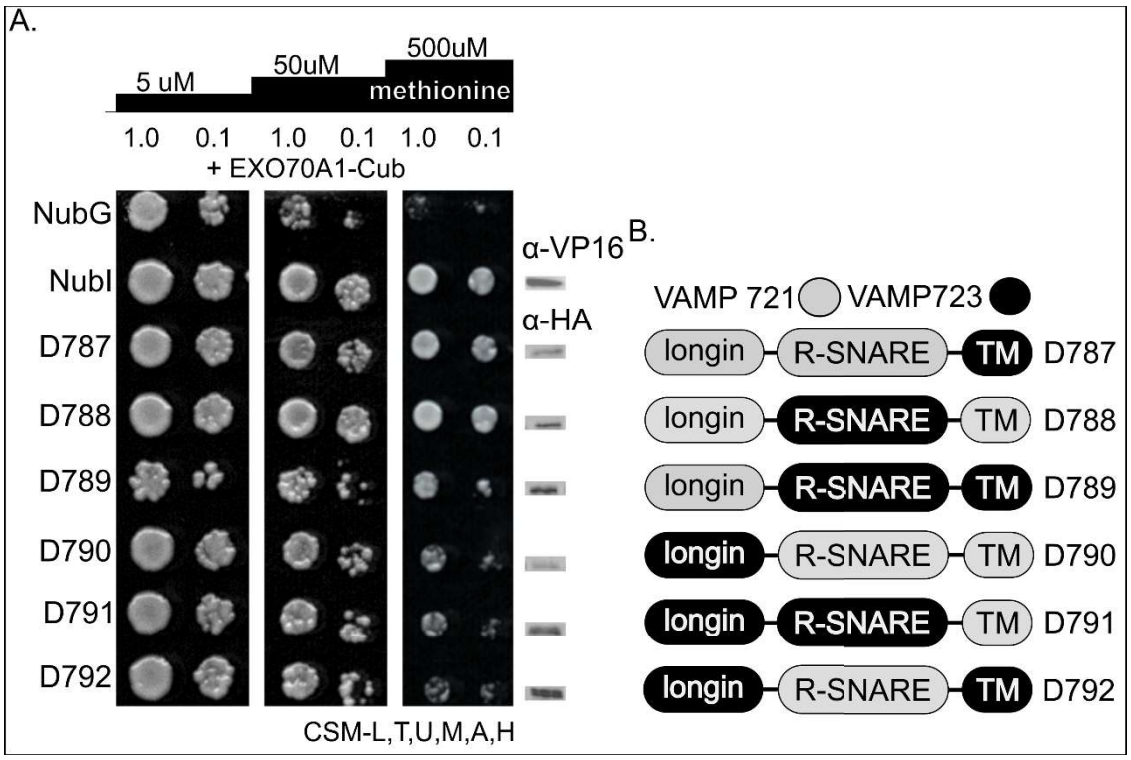

Figure 4 The interaction between EXO70A1 and VAMP721 requires the longin domain of the SNARE protein

Using chimaera constructs composed of different combinations of VAMP721 and VAMP723 SNARE domains allowed for the investigation of which domains are important for the mbSUS interactions between the EXO70A1 and SNARE proteins. (A) Mated yeast expressing EXO70A1 and the VAMP721/723 chimaera constructs were plated at 1.0 and 0.1 dilutions on SC+Methionine media to select for interactions between the two constructs. The lack of yeast growth at 500 μM Methionine in the D790-D792 rows reflects the need for the longin domain of VAMP721 for its interaction with EXO70A1. The expression SNARE and EXO70A1 proteins in mated yeast cultures were identified with α-HA and α-VP16 antibodies, respectively. (B) Schematic description of the VAMP721/723 chimaera constructs and their corresponding construct identifiers.

Fig. 5

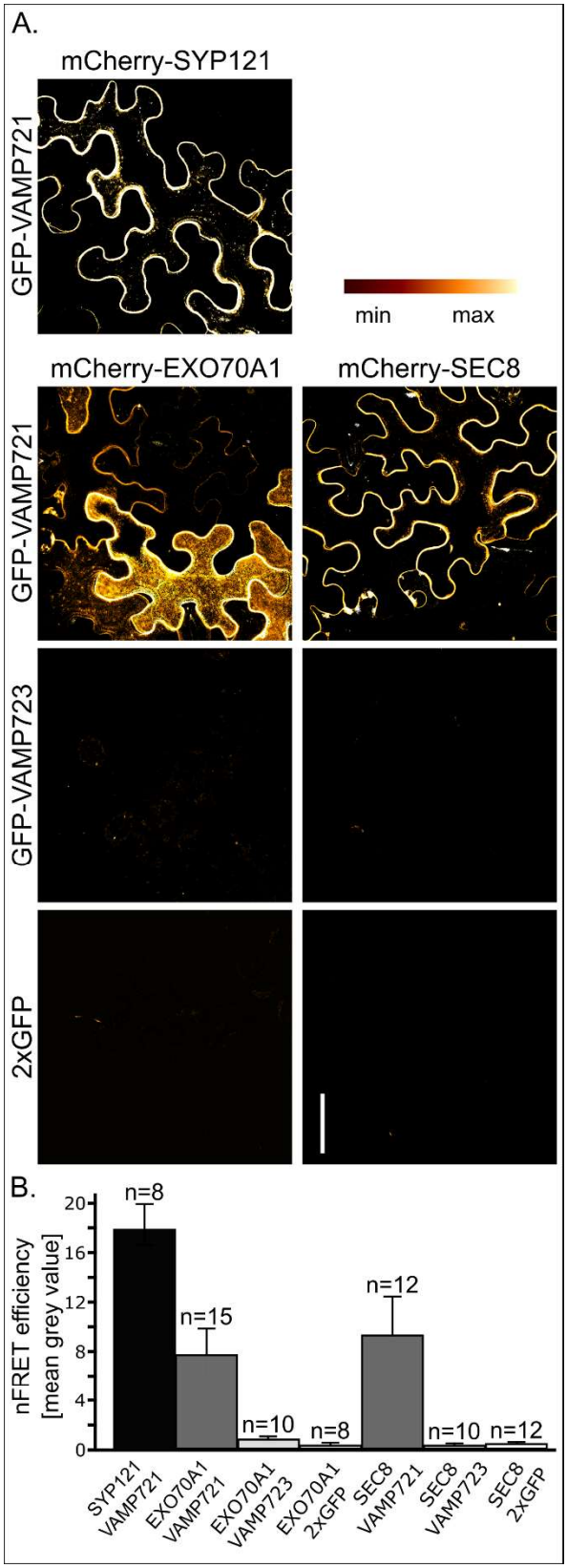

Figure 5 Interaction between VAMP721 and exocyst subunits in *N. benthamiana*

The interaction between VAMP721 and EXO70A1 was quantified using FRET analysis. (A) A multicistronic vector co-expressing mCherry-EXO70A1 in combination with GFP-VAMP721, GFP-VAMP723 or free-2xGFP were transiently expressed in *N. benthamiana* leaves. The known interaction between mCherry-SYP121 and GFP-VAMP721 was used as the positive control. A positive FRET signal was observed between two pairs EXO70A1-VAMP721 and SEC8-VAMP721. (B) Graphical representation of levels of FRET efficiency measured as a grey value obtained from the images above by PixFRET software. The n = number of scored pictures. Scale bar represents 50 μm.

Fig. 6

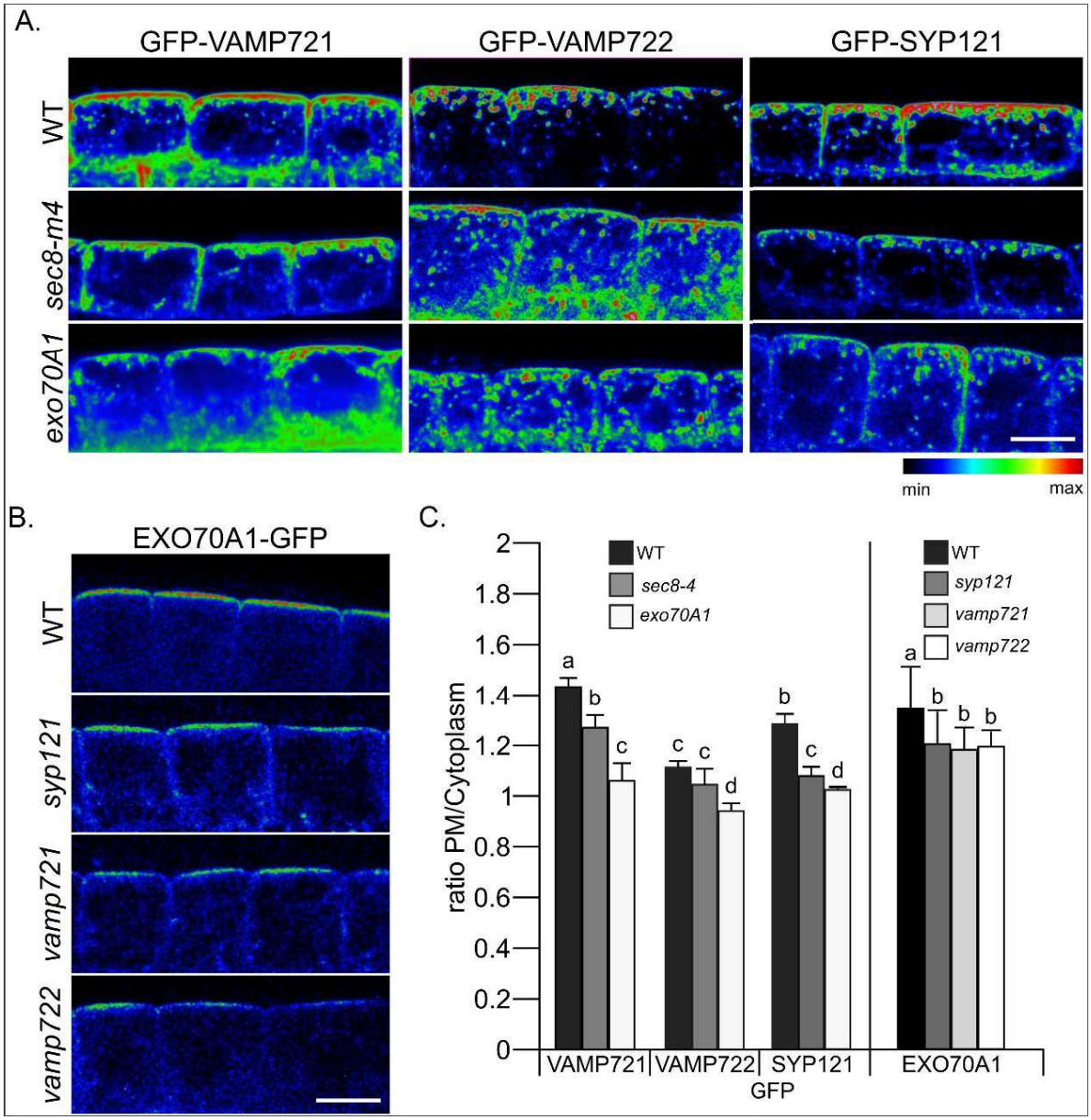
A.
GFP-VAMP721
GFP-VAMP722
GFP-SYP121
WT
sec8-m4
exo70A1
min
max
B.
EXO70A1-GFP
WT
syp121
vamp721
vamp722
C.
ratio PM/Cytoplasm
WT
sec8-4
exo70A1
WT
syp121
vamp721
vamp722
VAMP721
VAMP722
SYP121
EXO70A1
GFP

Figure 6 SNARE and EXOCYST internalization

(A) The representative image of GFP-VAMP721, GFP-VAMP722, GFP-VAMP723 and GFP-SYP121 localization in WT and *exo70A1*, *sec8-m4* mutant lines. (B) The EXO70A1-GFP localization in WT and *syp121, vamp721, vamp722* mutant lines. (C) The graphical illustration of the effect of mutated background for the GFP-VAMP721, GFP-VAMP722, GFP-SYP121 and EXO70A1-GFP localization, exhibiting the shift from PM towards cytoplasm (signal from entire cell was taken as the cytoplasm). The graph represents data from one experiment, 6 plants for each genotype were observed, a total number of scored cells for the PM/cytoplasm ratio n=36-54 in three independent replica. The letters indicate statistically significant difference calculated with one way ANOVA and nonparametric post-hoc Tukey HSD test at $p<0.01$. Scale bar represents 10 μm.

Table 1

AGI code	**short name**	SEC3a	SEC6	SEC8	Exo70B1	Exo70B2	VAMP721	SYP121
AT3G11820	SYP121	x	1	2	x	x	4	15
AT1G04750	VAMP721	1	x	x	2	1	14	8
AT3G09740	SYP71	3	x	x	1	4	5	6
AT5G39510	VTI 11/12	1	x	x	1	x	x	4
AT4G32150	VAMP711	1	x	x	x	x	x	x
AT1G28490	SYP61	x	x	x	2	1	2	2
AT3G10380	SEC8	31	4	7	x	x	x	1

Table 1 The identified proteins in exocyst and SNAREs Co-IP experiments
With the LC-MS/MS analysis, we measured a number of peptides of bound proteins to GFP-SEC3a, GFP-SEC8, SEC6-GFP, GFP-SYP121, GFP-VAMP721 baits. None of the proteins displayed in the table was found in the free-GFP bait control fraction. The bait and GFP were always identified in each fraction.

Supplementary Figure 1

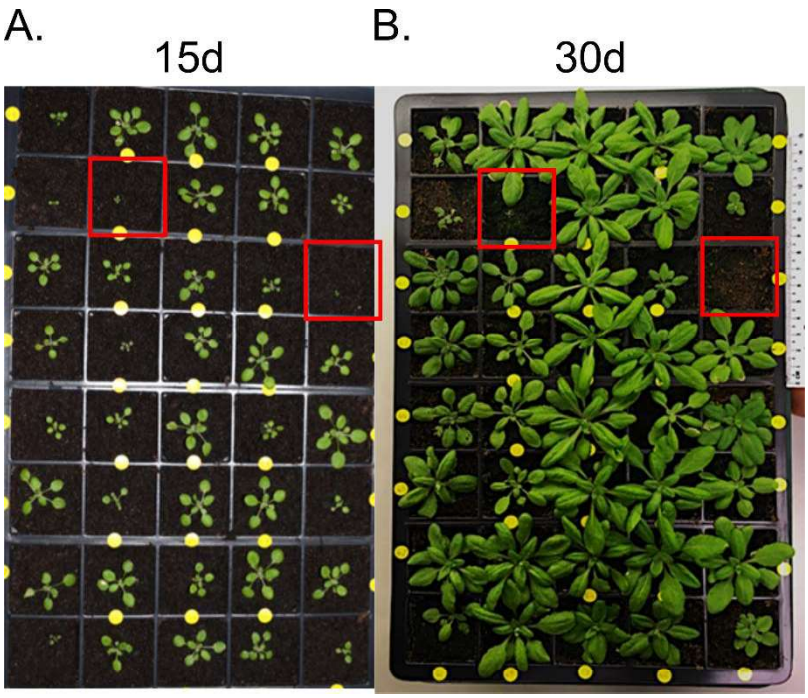

Figure S1 Segregation of the F_2 offspring from *exo70A1*$^{+/-}$ *vamp721*$^{+/-}$ F_1 plants

F_2 seed was germinated in soil and grown under long day conditions. Where possible, leaf samples or the entire plant was harvested for genotyping. A representative tray of F_2 seedlings at (A) 15 d and (B) 30 d after germination illustrating the segregation of phenotypes. Red boxes indicate confirmed *exo70A1/vamp721* double mutants.

Supplementary Figure 2A

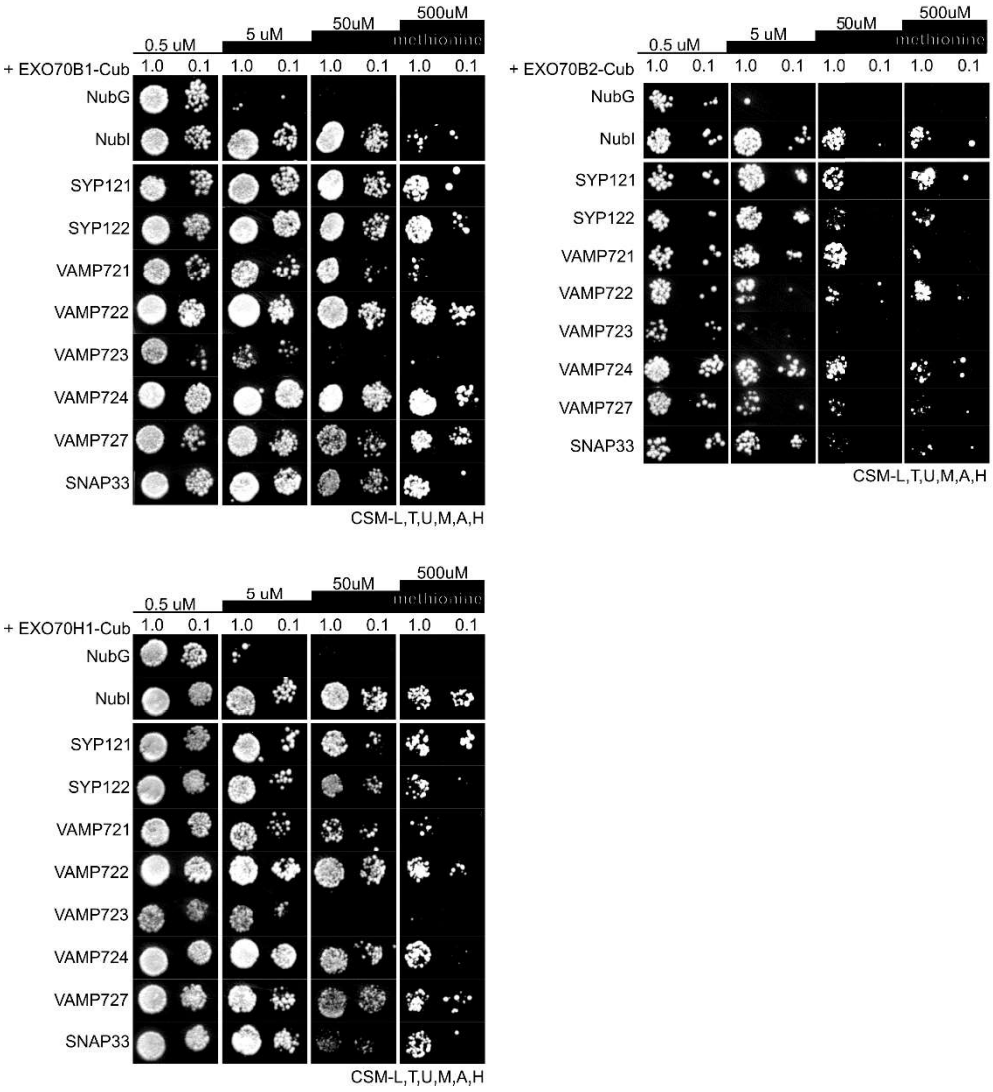

Supplementary Figure 2B

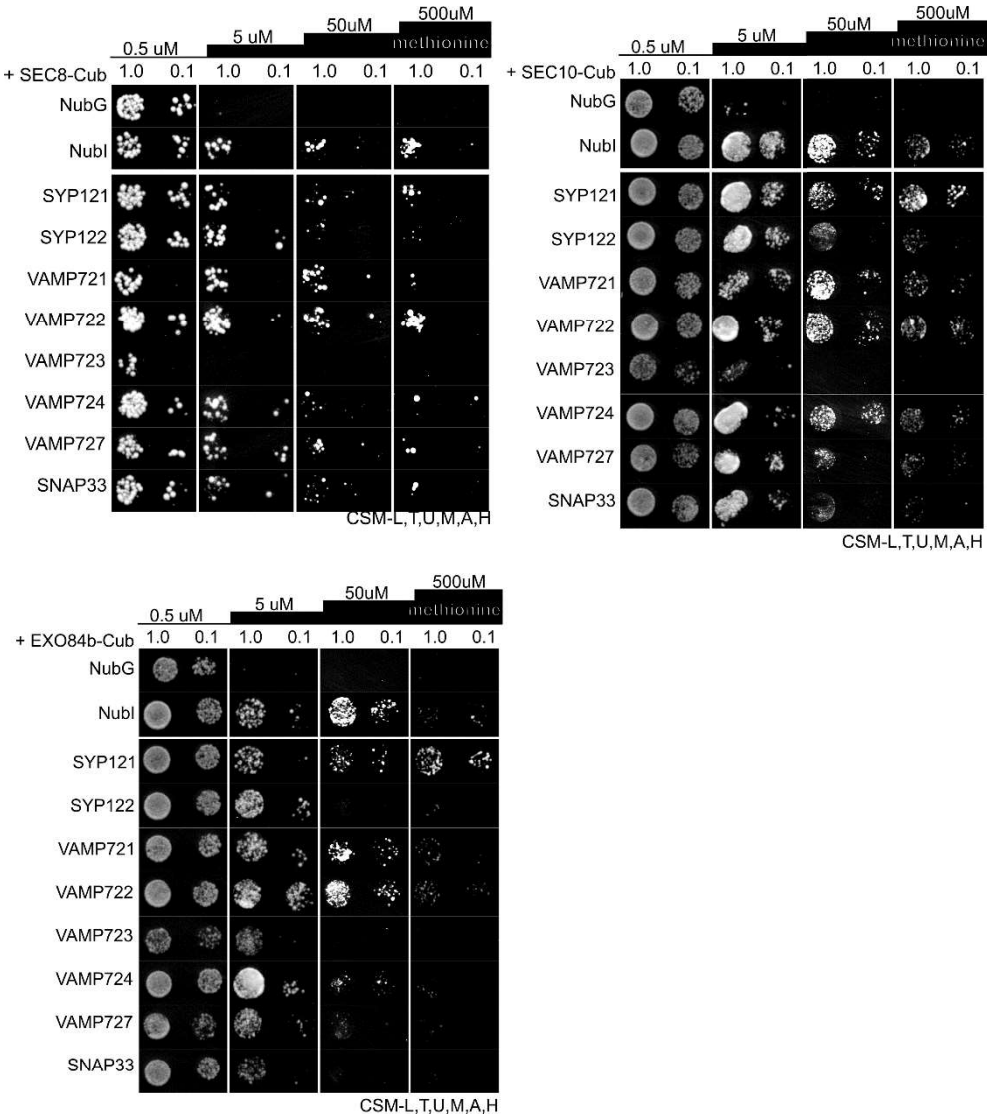

Figure S2 A, B mbSUS assay between SNAREs and exocyst subunits

(A) The additional Exo70 subunits interacted with SNAREs and the adaptor protein SNAP33 similar to EXO70A1. Interactions were evaluated using the yeast mbSUS. (B) Similarly, the core exocyst subunits SEC8, SEC10a and EXO84b interacted with SNAREs but avoid to interact with SNAP33 adaptor protein in mbSUS. Mated yeast was plated at dilutions of 1 and 0.1 on SC media that included increasing concentrations of Methionine to evaluate the protein-protein interactions.

Supplementary Figure 3

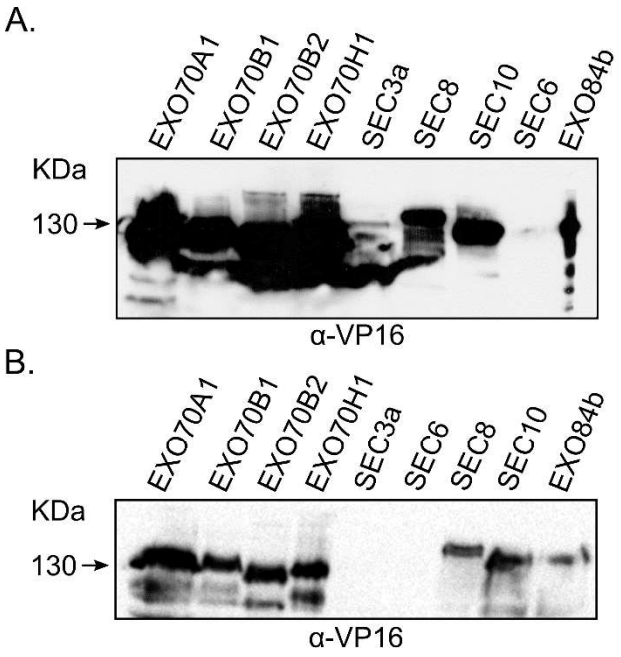

Figure S3. Western blots of constructs expressed in haploid yeast for mbSUS assay

The AP.4 strain expressing the exocyst subunits. The α-VP16 polyclonal antibody was used to identify the exocyst subunits in the AP.4, which were approximately 130 kDa (EXO70) or in 150 kDa (SEC3, SEC6, SEC8, SEC10, EXO84b) in size, including the additional protein tags. The 1µg of total proteins were loaded on the gel. (A) the 3 min UV exposition. (B) the 10 s UV exposition. This yeast expressing these constructs were mated to identify protein-protein interactions between SNARE (prey) and exocyst (bait) subunits.

Supplementary Figure 4

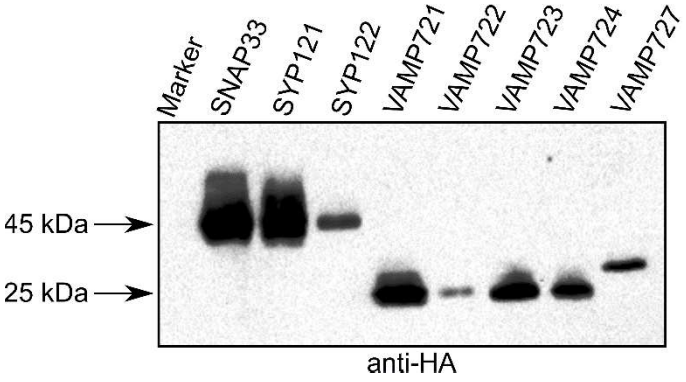

Figure S4. Western blot of constructs expressed in haploid yeast for mbSUS assay

The AP.5 strain of *S. cerevisiae* expressing the Qa-, Qbc- and R-SNARE. The construct expressing in AP.5 was identified by a 2x-HA tag and monoclonal antibody. The SYP and SNAP33 proteins were approximately 70-75 kDa big, and the VAMPs were 25-30 kDa. Of total proteins, 1µg sample was loaded on the gel. Yeast expressing these constructs were mated to identify protein-protein interactions between SNARE (prey) and exocyst (bait) subunits.

Supplementary Figure 5

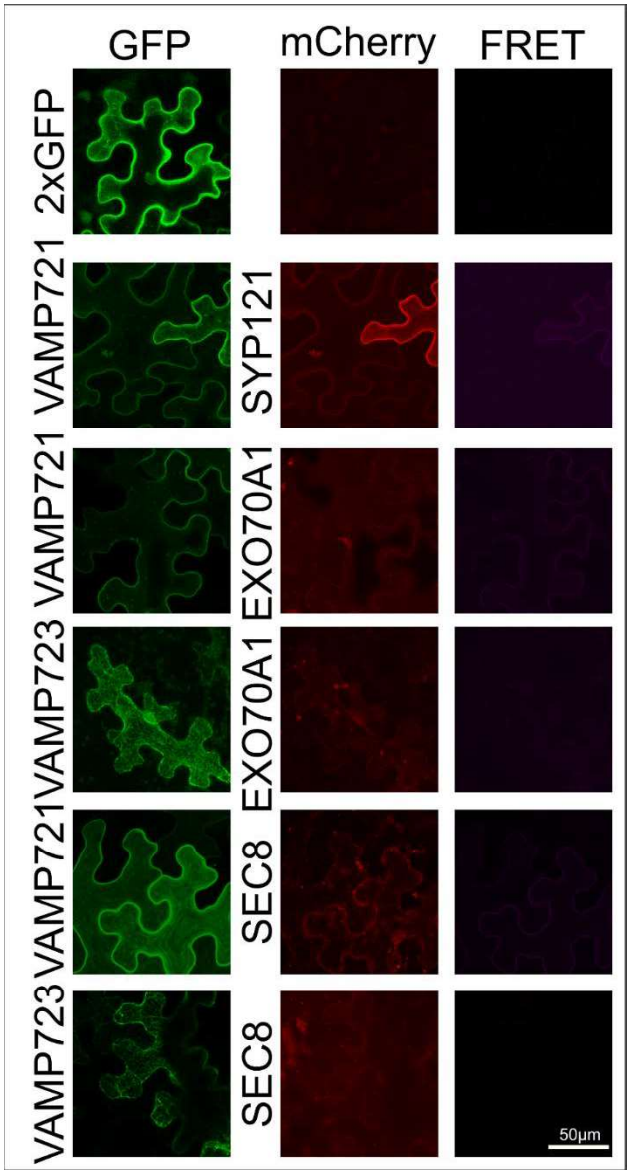

Figure S5 The input data for pixFRET analysis

The experimental setting for the FRET analysis. The GFP channel and FRET channel was excited by λ=488nm laser. The mCherry channel was excited with λ=561nm laser. All proteins were expressed according to their localization but with different efficiency. Scale bar represents 50µm.

Supplementary Figure 6

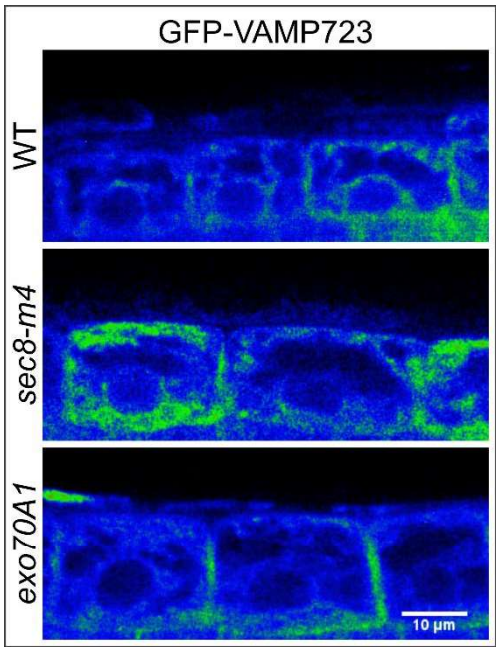

Figure S6 The GFP-VAMP723 localization

The localization of GFP-VAMP723 in endoplasmic reticulum of WT, *exo70A1* and *sec8-m4* background did not show a difference. Scale bar represents 10µm.

Supplementary Table 1 **Table S1** List of primers used in the study.

Cloning			
name	sequence 5'-> 3'	gene	Tn=°C
AttB1	GGGGACAAGTTTGTACAAAAAAGCAGGCT NN	extension	72
AttB2	GGGGACCACTTTGTACAAGAAAGCTGGGT A	extension	72
AttB3	GGGGACAACTTTGTATAATAAAGTTG NN	extension	72
AttB4	GGGGACAACTTTGTATAGAAAAGTTGGGT G	extension	72
AttB1Sec10new	AAAAGCAGGCTCCATGACAGAACGAATCAGAGC	SEC10a	59
AttB2Sec10ns	CAAGAAAGCTGGGTA CTCAAGCTTGGCCACAAGG	Sec10ans	59
AttB1Sec8	AAAAAGCAGGCTCCATGGGGATTTTCAATGGTTTG	Sec8	62
AttB4Sec8	GAAAAGTTGGGTCTTAATGAGAAAGAATTTCCAAAAG	Sec8	62
AttB2Sec8ns	CAAGAAAGCTGGGTA ATGAGAAAGAATTTCC	Sec8ns	62
AttB3VAMP721	GTATAATAAAGTTG CC ATGGCGCAACAATCG	atVAMP721	60
AttB2Vamp721	CAAGAAAGCTGGGTA TTATTAACACTTAAACCCAT	atVAMP721	60
AttB3Vamp723	GTATAATAAAGTTGCCATGGCGCAACAATCGTTG	atVAMP723	60
AttB2Vamp723	CAAGAAAGCTGGGTATTATTTACCGCAGTTGAATC	atVAMP723	60
AttB3eGFP	GTATAATAAAGTTGCCATGGTGAGCAAGGGC	eGFP	60
AttB2eGFP	CAAGAAAGCTGGGTACTTGTAGTTGCCGTCG	eGFP	60
AttB1Syp121	AAAAGCAGGCTCCATGAACGATTTGTTTTCC	atSYP121	60
AttB4Syp121	GAAAAGTTGGGTCTCAACGCAATAGACGC	atSYP121	60
AttB1Exo70A1	AAAAGCAGGCTCCATGGCTGTTGATAGCAGAATG	atEXO70A1	60
AttB4Exo70A1	GAAAAGTTGGGTCTTACCGGCGTGGTTCATTC	atEXO70A1	60
AttB2Exo70A1ns	CAAGAAAGCTGGGTA CCGGCGTGGTTCATTC	atEXO70A1	60
AttB1Exo70B1	AAAAGCAGGCTCCATGGCGGAGAATGGTG	atEXO70B1	60
AttB2Exo70B1ns	CAAGAAAGCTGGGTA TTTTCTTCCCGTGG	atEXO70B1	60
AttB1Exo70B2	AAAAGCAGGCTCCATGGCTGAAGCCGGTG	atEXO70B2	60
AttB2Exo70B2ns	CAAGAAAGCTGGGTA ACTTGAGCTTTCCTTGA	atEXO70B2	60
AttB1Exo70H1	AAAAGCAGGCTCCATGGCGAAAATGGCG	atEXO70H1	60
AttB2Exo70H1ns	CAAGAAAGCTGGGTA GCCTGAAACACACCC	atEXO70H1	60
AttB1Sec3a	AA AAA GCA GGC TAA ATGGCGAAATCAAGCG	atSEC3a	60
AttB2Sec3ans	A GAA AGC TGG GTC CATGGAAGCCAGAAGTCC	atSEC3aCfusion	60
AttB1Sec6	AAAAGCAGGCT CC ATGATGGTCGAAGATCTTGG	atSEC6	64
AttB2Sec6ns	A GAA AGC TGG GTN AGTGAGTTTTCGCCACATAG	atSEC6Cfusion	64
AttB1Exo84b	AA AAA GCA GGC TAA ATGGCGGCGAAGACG	atEXO84b	68
AttB2Exo84bns	A GAA AGC TGG GTC ATAGCTGCCATGAGATCTCGC	atEXO84bCfusion	68
Genotyping			
gene	sequence	gene	Tn=°C
LP"exo70A1e	CTAGACGTTTGCAGCATCCTAT	AtEXOA1	62
RP"exo70A1e	ATATGTGTAATGCATTGGAGAAGC		62
Lbb1 (*exo70A1-2* – SALK_135462)	GAACAACACTCAACCCTATCTCGGGC		62
LP"vamp721	CCCATGTCCACTTTAGTCCTCG	AtVAMP721	62
RP"vamp721	CTCCTTGTCTTCCCTTACGGGAT		62
Lbb1 (*vamp721* SALK_037237)	GAACAACACTCAACCCTATCTCGGGC		62

4. Discussion

Results and main hypothesis presented in this thesis have been already discussed separately in published papers in case of PAPER No. 1 and 2 or in papers submitted for a publication in case of PAPER No. 3 and 4. Therefore the discussion is shortened and addresses topics which have not been discussed in papers because of space limitations or which deserves to be put in context with the latest research.

4. 1. Early root growth response to living bacteria treatment

In the soil environment, plants have to face bacteria, which are either beneficial, pathogenic or neutral in their relationships. In PAPER No.2, we have described the early root hair growth stimulation and main root growth inhibition response after a direct contact with living plant pathogenic bacteria *Psm* and *Pst*. This phenomenon resembles the previously described response to plant growth promoting bacteria (PGPB) from *Pseudomonas* strain (Zamioudis et al. 2013). However, we identified that the early plant growth reaction relies neither on the auxin signalling pathway nor on the bacteria strategy. In our work (PAPER No. 2), the fast growth reaction is dependent on the proper functioning of the ET signalling and secretory pathway. Both the living PGPB and pathogenic bacteria are able to promote this early growth response. Intriguingly, we failed to identify the factor triggering the growth response, but we have discovered that only living plant-associated bacteria can induce it. It is possible that this phenomenon is related to the capability of plant-associated bacteria to interact directly with the root surface by creating biofilms which contain cues interpreted by plants as growth signals (Beauregard et al. 2013). Another candidate factor which could cause this growth stimulation and also serve as the marker of bacterial viability is bacterial mRNA. The prokaryotic mRNA differs from the eukaryotic one and it is a highly sensitive molecule which is quickly degraded if the cell dies, therefore can be identified as the viability associated PAMPs (vita-PAMPs) (Sander et al. 2011). Indeed, the prokaryotic mRNA coming from both pathogenic and neutral bacteria triggers the innate immunity response in animals (Sander et al. 2011). Thus, host cells can recognize in advance not only the presence but also a viability status of a potential danger and mobilize the immunity before the actual attack. Other vita-PAMPs candidates may be the second messengers such as c-di-AMP or cGMP (Woodward et al. 2010; Sander et al. 2011). Nevertheless, the mechanism of growth stimulation remains elusive in plants and the theory of vita-PAMPs involvement requests further investigation.

4. 2. Role of exocyst complex in defensive structures formation

Even though the plant-pathogen interaction studies have made immense progress during last few years, some aspects still remain unknown, such as the origin of the EHM. There are two major hypothesis on the possible source of the EHM, according to the one the EHM was supposed to be formed as an invagination of the PM, while the other one says it is directly formed from the ER membrane. The invagination theory was supported by a remarkable growth rate of EHM and the alleged continuity with the PM. Nevertheless, the increasing evidence of the distinct EHM composition from PM strongly argues against it (Koh et al. 2005; Micali et al. 2011; Kwaaitaal et al. 2017). The usual PM proteins, such as ATPase ACA8 or various aquaporins are absent in the EHM. The TGN secretion-blocking drug BFA does not influence the EHM formation, neither does the mutation in the exocytotic SNARE SYP121 or the exocyst complex subunits disruption (Assaad et al. 2004; Nielsen et al. 2012; PAPER No3). Therefore the canonical exocytotic pathway is not involved in EHM biogenesis upon powdery mildew attack. Furthermore, the PM/endocytic pathway tracer FM4-64 dye does not stain the EHM (Lu et al. 2012). The haustorium grows through the papilla or the collar structure, which may create the physical constriction between the PM and the luminal EHM. EHM continuity with PM is therefore unlikely, yet several PM proteins were found to localize at EHM upon oomycetes attack. The peripheral PM-localized protein SYT1 has been found to associate with EHM surrounding oomycetes haustoria (Lu et al. 2012). Further on, the detergent insensitive domain localized remorin REM1.3 protein is present in patchy domains at EHM (Bozkurt et al. 2014). Also, the PRR protein and receptor kinases FLS2, BRI1 and SERK3 mark the EHM in tobacco/oomycetes interaction (Bozkurt et al. 2015). Interestingly, the MVB associated Rab GTPases ARA6, RABG3c and ARA7 localize at the EHM, supporting the theory that the unconventional secretion pathway may exist towards the EHM. However, this secretion also probably does not influence the EHM formation, but may have the impact on protein and material delivery towards it. Similarly, the R-SNARE protein VAMP721 mediates the secretion of EHM specific R protein RPW8.2 in defence to adapted powdery mildew fungi *Gvo* (H. Kim et al. 2014). The RPW8.2 proteins is necessary for the plant cell to recognize a fungus and activate immunity, therefore its delivery has the major impact on its function. Intriguingly, the same R-SNARE participates in the SYP121 secretory pathway in papillae biogenesis, cell division and post-invasive immunity, such results demonstrate the versatile capacity of VAMP721. The future research has to elucidate the partners and regulators of VAMP721 driven secretion towards EHM and the possible secretory pathways involved in it. We may

speculate, that exocyst can participate in the VAMP721 regulated RPW8.2 secretory pathway, since the exocyst is one of VAMP721 interacting partners, however, this theory has to be tested.

The striking difference is between the EHM surrounding oomycetes or powdery mildew fungi haustoria. The most investigated filamentous pathogens belong to either oomycetes, such as *Phytophtora* and *Hpa*, or ascomycetes such as *Gvo* and *Bgh*. Indeed, SYP121 localizes at the EHM upon *Hpa* attack (Lu et al. 2012) but is not present the EHM upon *Gvo* attack (Meyer et al. 2009). Importantly, the collar or neckband found in reaction to ascomycetes is missing in reaction to oomycetes haustorium (Heath 1976; Celio et al. 2004; Mims et al. 2004). Therefore, it remains to be elucidated if the biogenesis of the EHM is a conserved process in defence to fungal pathogens/oomycetes and the described differences are result of distinct morphology of the invasive structure. Since we confirmed the physical interaction between SYP121 and exocyst, we cannot exclude that exocyst may associate with the EHM upon *Phytophtora* attack. Moreover, the SEC5 exocyst subunit was identified as a member of plant defence and regulator of callose deposition in defence response against *Phytophtora* in tobacco (Du et al. 2015).

Although close physical association between ER and EHM has been observed and the ER membrane lipophilic tracer stains the EHM, ER-resident proteins have not been found in EHM (Harder et al. 1978; Leckie et al. 1995; Kwaaitaal et al. 2017). Instead, the small GTPases Sar1, which is involved in COPII coated vesicle assembly and RabD2a, essential for membrane transport from ER to Golgi, both localize to EHM (Kwaaitaal et al. 2017). However, the loss of RabD2a or Sar1 function did not influence the EHM formation. Thus the EHM shares only the ER structural properties and its origin can be mediated by an unconventional transport pathway originated at ER, similarly to originating of the autophagosomes and peroxisomes (Dimitrov et al. 2013; Kuhn et al. 2016; Kwaaitaal et al. 2017).

The papillae and haustorial encasements are on the other hand surrounded by the membrane which exhibits PM properties and is filled with CW components and exosomes. Remarkable, almost all tested proteins accumulate in the encasement, such as ACA8, SYP121, PEN3, PIP1.4, VAMP721/722 also RPW8.2 (Meyer et al. 2009; Lu et al. 2012). Moreover, the GFP-SYP121 positive exosomes were identified there, thus MVB fusion with papillae and encasements occurs. The loading of encasements has been compared with the vesicular cloud prior the cell division. Thus the localization of the encasement for many proteins may be a consequent of the cell effort to concentrate material in the focal point. The study of plant-specific ARA6 and ARA7 showed two independent MVB/late endosome secretory pathways mediate the secretion of papillae and encasements (Inada et al. 2016; Nielsen et al. 2017). The

localization of plasmodesmata-like protein (PDLP1) protein, which associates with the EHM prior to encasement formation and disappears after the encasement closing, brought the new insights into the encasement biogenesis. PDLP1 drives the encasement formation and its loss resulted in the encasement disruption, but not the EHM (Caillaud et al. 2014; H. Kim et al. 2014). For the future study of the EHM and the encasement formation, will be necessary to follow their development in time. VAMP721 has been precipitated with PDLP1, thus PDLP1 may share same secretory pathway on the EHM with RPW8.2 (Caillaud et al. 2014). In our study, we revealed that the exocyst tethering complex has the ability to associate with the membrane of both defensive structures - papillae and encasement (PAPER No. 3). Indeed, in exocyst mutants, their arrangement and structure are disrupted (Pečenková et al. 2011; PEPER No. 3). The role of the exocyst in papillae development required SYP121. Nevertheless, the encasement defect was independent of the loss of SYP121. Therefore, we expect the exocyst might cooperate with another SNAREs on the encasement biogenesis. Thus exocyst is one of few proteins identified to have the impact on the encasement biogenesis. Nevertheless, exocyst was found in ARA6- and ARA7-bound fractions (Heard et al. 2015). Surprisingly, we identified neither ARA6 nor ARA7 in the EXO70B1- or EXO70B2-bound fraction after *Bgh* attack, instead, we found RabG3f to associate with EXO70B1 and RabG3c to bind EXO70B2 (Addition to PAPER No. 3). This result supports the role of EXO70Bs in Golgi derived degradation pathway to the vacuole. While the RabG3f recruits late endosomes or PVC to the vacuole (Zelazny et al. 2013; Cui et al. 2014), RabG3c localizes at the EHM upon *Phytophtora* attack and its signal overlaps with ARA7 (Bozkurt et al. 2015). Intriguingly, RabG3f positively regulates sequestration of viral mRNA into the Golgi derived vesicles and thus negatively regulates ETI in tobacco (Huang et al. 2015). This pathway may be the link between TN2 R protein regulation in *Arabidopsis* and EXO70B1, although the viral strategy differs from biotrophs (Zhao et al. 2015). Future research has to be done to resolve if the closely related proteins EXO70B1 and EXO70B2 deploy in post-Golgi degradation pathway towards vacuole and differ in Rab GTPase partners/cargo pool.

4. 3. Exocyst complex and callose deposition

Callose is a polymer composed from glucose residues in β-1,3-linkage, what actually allows this molecule to get an amorphous gel-like structure which may fill the tiny niches between the cellulose and hemicellulose fibrils of the CW (Eggert et al. 2014). In *Arabidopsis,* 12 genes encode callose synthases, *CalS,* and this diversity corresponds to the functional and transcriptional variability of them. Indeed, callose is involved in many developmental

processes, such as cell plate biogenesis, where callose forms the middle lamella, or in plasmodesmata enclosure and thus in regulation of cell-to-cell movement. In plant immunity, callose deposited by CalS12/PMR4 plays important role, since its overexpression causes compleat resistance to powdery mildew in *Arabidopsis* (Ellinger at al. 2013). Nevertheless, it remains elusive, how are CalSs deposited towards the point of threat, since not only pathogen, but also chemical, mechanical, or ultrasonic treatments cause the callose accumulation within minutes (Stone & Clarke 1992). The CalSs are usually transmembrane proteins and therefore might be delivered through the exocyst dependent secretory pathway. Indeed, CalS12 has been shown as the cargo protein for EXO70H4-containing exocyst variant which regulates the secretory pathway in *Arabidopsis* trichome (Kulich et al. 2018). Furthermore, the disruption of callose deposition has been found in *N. benthamiana plants* with silenced SEC5a subunit, resulting in the higher incidence of *Phytophtora* infection. In our work, we manifested the diminished penetration resistance of exocyst mutants upon attack of non-adapted fungus, however, we observed imbalanced callose deposition in the contact sites rather than its loss. In addition, we followed callose deposition upon the fungal attack in time, observing the significant delay in callose deposition in *sec8-m4* and *exo70B2* mutant lines, app. 2h if compared with WT (PAPER No. 3). Also, the mutant in the SYP121 exhibits the delay in callose deposition, app. 2h, corresponding to the higher incidence of fungal penetration, app. 50%. Although the exocyst mutants show similar delay in callose deposition as *syp121* mutant, they are not massively penetrated, app. 10-20% (PAPER No. 3). The results may have two possible explanation. First, the loss of SYP121 reflects non-efficient membrane fusion of vesicles recycled and secreted, while the loss of exocyst reflects the non-efficient membrane fusion of secreted vesicles only. This secretion is in minority in comparison to recycling (Nielsen et al. 2012). Second, the exocyst mutants tested are mild, and its impact is more visible in cell rapid response, such as callose deposition, but the other cargoes might be delivered without damage.

Importantly, the free SA level and SA pathways influence the callose deposition upon the attack of an adapted pathogen (Ellinger et al. 2013). This was shown on the *calS12/pmr4* mutant lines, which contrary to its total lack of stress-induced callose showed resistance against the adapted fungal pathogens but increased penetration incidence of non-adapted fungal pathogens (Jacobs et al. 2003). It has been lately revealed taht this resistance is dependent on elevated SA level (Nishimura et al. 2003). In our analyzes, the free SA level was increased in non-treated mutant lines of *sec15b*, *exo70B1*, *exo70B1/syp121* but not in *exo70B2*, *exo70B2/syp121* (Addition to PAPER No.3). The elevated level of SA corresponded with the

higher incidence of PCD upon fungal attack for *sec15b*, *exo70B1, exo70B1/syp121*, accompanying penetrated cells. However, the *exo70B1* mutant SA level does not correspond with the mild increase in PCD compare to *syp121* mutant. The *exo70B2* and *exo70B2/syp121* also exhibited higher penetration incidence (increase in haustoria and unencased haustoria formation), but not PCD activation, and also the callose deposition was reduced in these mutants (PAPER No. 3). These results show that EXO70B2, as described before (Stegmann et al. 2012), works as either the positive regulator of SA dependent PTI or it regulates the deposition of callose in plant defensive structures. In conclusion, the SA activation did not influence penetration success of non-adapted powdery mildew in exocyst mutants in a higher extent, similarly with loss of *cals12/pmr4*.

4. 4. Exocyst complex structure and SNARE complex interactions

Our comprehensive mass spectrometry analysis of fractions bound to all exocyst core subunits and several EXO70s allowed us to compare the stability of the entire exocyst complex in *Arabidopsis* seedlings, as well to identified novel potential interactors or cargoes. We showed the ability of individual subunits to bind other exocyst partners in plants (Addition to PAPER No. 3). The obtained results reflect situation previously described in yeasts. Thus, also in *Arabidopsis,* the exocyst might form a stable octameric complex, which assembles from two halves EXO70A1-SEC15-SEC10-EXO84b or SEC3-SEC5-SEC6-SEC8. The ability of EXO70A1 to bind almost entire complex in plants, may reflect its importance in canonical exocytosis (Synek et al. 2006; Drdová et al. 2013; Zhao et al. 2015) or the structural distinction from the yeast Exo70p (Pleskot et al. 2015), which would allow the stronger binding to the rest of complex. Interestingly, although previously EXO70B2 isoform demonstrated the capability to bind several exocyst subunits in Y2H assay, the Co-IP data showed that the weak association with the rest of subunits is more probable (Addition to PAPER No. 3). This is supported also by the data from localization study, where under the pathogen attack, SEC6, SEC8 and EXO70B2 occur simultaneously at the contact site with the fungus (PAPER No. 3). Moreover, both EXO70B1 and B2 share common interactors with the other subunits (Addition to PAPER No. 3).

The prominent interactor of exocyst complex is SYP121 along with other SNAREs such as SYP71, VAMP721, VAMP711, VTI11/12. We confirmed the obvious exocyst willingness to interact with SNAREs in the split-Ub system (PAPER No. 4). We realize that the developmental and environmental status will play a huge role in the experiments with plants

since the EXO70Bs displayed striking differences between pathogen treated and untreated Co-IP data (data not shown). Moreover, from the Efp Browser expression database (http://bar.utoronto.ca/efp/cgi-bin/efpWeb.cgi), it is obvious that EXO70Bs are more abundant in the later ontogenetic stages. EXO70 isoforms also undergoes posttranslational modifications, which may influence their accessibility to the interactors and rest of the complex. Therefore, we expect that the pool of interacting proteins will change over time. The Co-IP data also show that the SEC3 can work as the landmark regardless of what EXO70 is bound to it (Addition to PAPER No. 3). This theory supports our data, that loss of EXO70A1 disrupts the SYP121, VAMP721/722 PM enrichment, but does not affect the ER-bound VAMP723 (PAPER No. 4). Therefore, we believe that EXO70A1-containing complex mediates the canonical exocytosis towards PM or cell division plane, while another EXO70x-containing complexes regulate e.g. vesicular transport to the vacuole, CASP domain, defensive papillae or autophagosomes.

The Co-IP screen revealed other potential interactors, which deserves to be discussed closer. First of all, the previously described cargoes/interactor, the CASPs and CASP-like proteins were identified as the cargo of exocyst complex in Casparian boundary formation (Kalmbach et al. 2017). Intriguingly, we found callose synthase CALS9/GSL10 as the novel interactor. Previously, we described the callose synthase CALS12/GSL5/PMR4 has been confirmed as the cargo for trichome specific EXO70H4-containing exocyst complex (Kulich et al. 2018). Here we show the CALS9 it is the common cargo or interactor of SYP121 and VAMP721 (Addition to PAPER No. 3), thus it remains to be elucidated if this pathway cooperates in callose secretion in trichome as well. Except for callose synthases, other CW-associated cargoes have been found, such as xyloglucanase. This protein may play an important role also in the papillae or encasements structure. The ABCG36/PEN3 transporter involved in glucosinolate synthesis in plant immunity has been identified before as the cargo for EXO84b (Mao et al. 2016). Thus exocyst may participate in the glucosinolate secretion in defence through the ABC transporter secretion or the NSP3 protein. Similarly, the ACA8/10 or CALSP point to CA^{2+} signalling and transport regulation may be connected with the CW, osmotic stress and signalling regulation. The exocyst has been described as the effector of Rab GTPases, surprisingly we identified several groups of *Arabidopsis* Rab GTPase family, supporting that the exocyst complex has a role in multiple secretory pathways.

5. Conclusion

The main aim of this study was to confirm the positive role of the exocyst complex in plant immunity and to identify novel immunity implicated exocyst interactors.

In cooperation with my colleagues, I provided the evidence that secretory pathways driven by exocyst along with signalling pathway of ethylene execute the fast root growth reaction upon living *Psm* and *Pst* bacteria treatment. We showed that the rapid inhibition of the main root and root hairs stimulation of *Arabidopsis* seedlings upon pathogenic bacteria is comparable to PGPB. Thus, our data confirmed that a plant does not distinguish between PGPB and pathogens at the first point of contact. Another study of ours proved the necessity of the exocyst complex in penetration resistance against non-adapted powdery mildew fungi. The exocyst plays the crucial role in the regulation of secretory pathway mediated by the defensive papillae or encasement structures formation. Both those structures contain callose and we identified that exocyst dependent secretory pathways is involved in the defensive callose secretion. However, we show that exocyst mutants display much weaker penetration phenotype than *syp121* against non-adapted powdery mildew fungi. Therefore we claim that the callose deposition is the marker of functional defensive secretory pathway rather than its crucial component. Moreover, exocyst interacts with Qa-SNARE SYP121 through the EXO70Bs. We described the common role for EXO70B2 and SYP121 in papillae formation and the EXO70B2 role in haustorial encasement formation. On the other hand, the exocyst is not involved in the secretory pathway, which mediates EHM formation. We identified several interactor partners for the whole complex, including the SYP121/PEN1 and VAMP721 SNARE proteins previously described as the regulator of the secretory pathway in penetration resistance.

Although the Co-IP analyzes suggest that the exocyst forms the stable holocomplex in plant cells, our results point to the spatiotemporal posttranslational regulation and possible exchange between the EXO70 isoforms, which otherwise may compete for the rest of complex. Exocyst subunits are willing to interact with many SNARE proteins, especially PM associated SNAREs in yeasts and also in plants. Thus, all the versions of the exocyst complex may have the same affinity for the SNARE complex. The specificity of a membrane fusion can actually be regulated by a set of interactors and membrane composition. Nevertheless, we described an additive phenotype for the *exo70A1/vamp721* double mutant in comparison to single *exo70A1* mutant. Since we demonstrated that both proteins are able to interact in yeast and plants and they influence each other function, we suggested the EXO70A1-containing exocyst complex facilitate membrane fusion driven by R-SNARE VAMP721-containing SNARE complex.

With the comprehensive Co-IP screen of interactors, I selected several exocyst unique proteins, which I sorted into secretory pathway associated proteins, PM and membrane proteins, potentially secreted cargoes and Rab GTPases, therefore this work provides a solid background for a future research.

6. Závěr

Hlavním cílem mé práce bylo prověřit funkci proteinového komplexu exocyst v rostlinné obranně, dále najít a popsat jeho interakční partnery spojené s obranou a prokázat jejich vzájemnou spolupráci v rostlinné buňce.

Růst kořene je jednou z reakcí rostliny jak se vyhnout nepříznivým podmínkám. Podařilo se nám popsat fenomén rychlé růstové odpovědi kořene v reakci na přítomnost bakterií. Dle našich výsledků rostlinné patogenní bakterie *Psm* a *Pst* vyvolávají shodnou růstovou reakci kořene jako dříve popsané bakterie podporující růst. Tato růstová odpověď je závislá na funkční sekretorické dráze závislé na exocystu, signální dráze etylénu a přítomnosti živých rostlinně specifických bakterií. Rostlina tedy nerozlišuje v časné odpovědi mezi mikroby podporujícími růst či patogeny. V další studii jsme prokázali nezbytnost komplexu exocyst v rostlinné obraně a to především před průnikem houbových patogenů způsobujících rostlinnou chorobu padlí. Ukazujeme, že exocyst je zapojen do sekreční dráhy, která se podílí na včasné tvorbě obranných struktur, papil a obalů obklopujících houbová haustoria. Jednou z hlavních komponent buněčné stěny těchto obranných struktur je polymer kalóza, která je syntetizována pomocí enzymu kalózasyntázy. Přítomnost kalózy se tak běžně používá jako marker fungující sekreční dráhy závislé na Qa-SNARE SYP121 proteinu. Naše data ukazují, že tato sekreční dráha je řízená také exocystem, ale samotná kalóza není podle nás tou nejzásadnější obrannou složkou papil či haustoriálních obalů, jelikož její nepřítomnost či zpoždění u mutantů exocystu nepůsobí takový defekt rostlinné obrany jako u *syp121*. Z našich dat vyplývá, že exocystem řízená sekrece nepřispívá ke vzniku specializované extrahaustoriální membrány, jejíž původ je spojován s membránou endoplasmatického retikula. Nicméně nemůžeme vyloučit, že se exocystem řízená sekrece podílí na dopravě komponent do extrahaustoriální membrány po jejím vzniku jako je tomu u SNARE proteinů VAMP721/VAMP722.

Tento objev nás vedl k bližšímu prozkoumání možné interakce mezi podjednotkami SNARE a exocyst komplexů. Pomocí ko-imunoprecipitační analýzy jsme identifikovali několik interaktorů komplexu exocyst a mezi nimi i SYP121/VAMP721 SNARE proteiny. Přestože tato analýza také naznačila existenci exocystu jako stabilního komplexu v rostlinných buňkách, naše předcházející pozorování napovídá možnost aktivní výměny mezi izoformami podjednotky EXO70, které mohou soutěžit o zbytek komplexu. Všechny námi testované podjednotky exocystu ochotně interagovaly se SNARE proteiny v kvasinkovém i rostlinném modelu, proto si myslíme, že všechny varianty komplexu exocyst mohou mít stejnou afinitu ke

SNARE komplexu. Specifičnost membránové fúze bude tak určena souhrou SNARE, exocystu, membránovým složením a dalšími interakčními partnery. Pozitivní vliv interakce mezi komplexy SNARE a exocyst jsme pak popsali na příkladu dvojitého mutanta *exo70A1/vamp721*, který vykazoval značně zpomalený růst oproti jednoduchému mutantu *exo70A1*. Pprokázali jsme, že oba proteiny jsou schopny interagovat a ovlivňují vzájemnou funkci, proto jsme navrhli, že komplex exocyst obsahující EXO70A1 může usnadnit membránovou fúzi řízenou SNARE komplexem obsahujícím VAMP721.

Na závěr chci vyzdvihnout seznam potencionálních interaktorů, které se během práce podařilo identifikovat a mohou posloužit pro budoucí výzkum.

7. List of Abbreviations

Abbreviation	Explanation
ABA	abscisic acid
ANOVA	analysis of variance
ARA	Arabidopsis Rab GTPase
Arabidopsis	*Arabidopis thaliana*
ARF	ADP ribosylation factor of Ras superfamily of GTPases
Avr	protein of avirulence
BFA	brefeldin A
Bgh	*Blumeria graminis f. sp. hordei*
CATCHR	complexes associated with tethering containing helical rods
Co-IP	coimmunopreciptitation
Col-0	Columbia 0
CW	cell wall
DAMPs	damage associated molecular patterns
EHM	extrahaustorial membrane
Ep	*Erysiphe f. sp. pisi*
ER	endoplasmic reticulum
ET	ethylen
ETI	effector triggered immunity
GFP	green fluorescent protein
Gvo	*Golovinomyces orontii*
Hpa	*Hyalonoperenospora arabidopsis*
JA	Jasmonic acid
LC-MS-MS	Liquid chromatography with tandem Mass Spectrometry
LOF	loss of function
LRR	leucin rich repeat (protein motiv)
MAMPs	microbe associated molecular patterns
mCherry	red fluorescent protein from DsRED
MTC	multisubunit tethering complex
MVB	multivesicular body
PAD4	Phytoalexin deficient 4
PAMPs	pathogen associated molecular patterns
PAS	phagophore assembly site
PCD	programmed cell death
PEN1/3	penetration 1/3
PGPB	plant growth promoting bacteria
PM	plasma membrane
PRR	pathogenesis-related receptor protein
Psm	*Pseudomonas syringae* pv. *maculicola*
Pst	*Pseudomonas syringae* pv. *tomato*
PTI	pattern triggered immunity
R	resistance protein

ROS	reactive oxygen specious
SA	salycilic acid
SD	standard deviation
SE	standard error
SNAP	soluble NSF adaptor protein
SNARE	Soluble NSF Attachment REceptor Protein
SNF	N-ethylmaleimide-sensitive factor
SYP	syntaxin of plants
TGN	trans Golgi network
VAMP	vesicle-associated membrane protein
WT	wild type
YFP	yellow fluorescent protein

References

Aist, J.R., 1977. Papilla Formation: Timing and Significance during Penetration of Barley Coleoptiles by Erysiphe graminis hordei. *Phytopathology*, 77(4), p.455.

Assaad, F.F., 2004a. The PEN1 Syntaxin Defines a Novel Cellular Compartment upon Fungal Attack and Is Required for the Timely Assembly of Papillae. *Molecular biology of the cell*, 15(11), pp.5118–5129.

Axe, E.L. et al., 2008. Autophagosome formation from membrane compartments enriched in phosphatidylinositol 3-phosphate and dynamically connected to the endoplasmic reticulum. *The Journal of cell biology*, 182(4), pp.685–701.

Bacete, L. et al., 2018. Plant cell wall-mediated immunity: cell wall changes trigger disease resistance responses. *The Plant journal: for cell and molecular biology*, 93(4), pp.614–636.

Barlowe, C. & Schekman, R., 1993. SEC12 encodes a guanine-nucleotide-exchange factor essential for transport vesicle budding from the ER. *Nature*, 365(6444), pp.347–349.

Bartetzko, V. et al., 2009. The Xanthomonas campestris pv. vesicatoria type III effector protein XopJ inhibits protein secretion: evidence for interference with cell wall-associated defense responses. *Molecular plant-microbe interactions: MPMI*, 22(6), pp.655–664.

Beauregard, P.B. et al., 2013. Bacillus subtilis biofilm induction by plant polysaccharides. *Proceedings of the National Academy of Sciences of the United States of America*, 110(17), pp.E1621–30.

Beck, M. et al., 2012. Spatio-Temporal Cellular Dynamics of theArabidopsisFlagellin Receptor Reveal Activation Status-Dependent Endosomal Sorting. *The Plant cell*, 24(10), pp.4205–4219.

Bednarek, P. & Osbourn, A., 2009. Plant-Microbe Interactions: Chemical Diversity in Plant Defense. *Science*, 324(5928), pp.746–748.

Berkey, R. et al., 2017. Homologues of the RPW8 Resistance Protein Are Localized to the Extrahaustorial Membrane that Is Likely Synthesized De Novo. *Plant physiology*, 173(1), pp.600–613.

Bloch, D. et al., 2016. Exocyst SEC3 and Phosphoinositides Define Sites of Exocytosis in Pollen Tube Initiation and Growth. *Plant physiology*, 172(2), pp.980–1002.

Bodemann, B.O. et al., 2011. RalB and the exocyst mediate the cellular starvation response by direct activation of autophagosome assembly. *Cell*, 144(2), pp.253–267.

Böhlenius, H. et al., 2010. The multivesicular body-localized GTPase ARFA1b/1c is important for callose deposition and ROR2 syntaxin-dependent preinvasive basal defense in barley. *The Plant cell*, 22(11), pp.3831–3844.

Bonifacino, J.S. & Glick, B.S., 2004. The Mechanisms of Vesicle Budding and Fusion. *Cell*, 116(2), pp.153–166.

Bozkurt, T.O. et al., 2015. Rerouting of Plant Late Endocytic Trafficking Toward a Pathogen Interface. *Traffic* , 16(2), pp.204–226.

Bracker, C.E. & Littlefield, L.J., 1973. Structural Concepts of Host–Pathogen Interfaces**A table of contents appears after this paper, on p. 318. In *Fungal Pathogenicity and the Plant's Response*. pp. 159–317.

Bremser, M. et al., 1999. Coupling of coat assembly and vesicle budding to packaging of putative cargo receptors. *Cell*, 96(4), pp.495–506.

Bücherl, C.A. et al., 2017. Plant immune and growth receptors share common signalling components but localise to distinct plasma membrane nanodomains. *eLife*, 6. Available at: http://dx.doi.org/10.7554/eLife.25114.

Caillaud, M.-C. et al., 2014. The plasmodesmal protein PDLP1 localises to haustoria-associated membranes during downy mildew infection and regulates callose deposition. *PLoS pathogens*, 10(10), p.e1004496.

Celio, G.J., Mims., C.W. & Richardson, E.A., 2004. Ultrastructure and immunocytochemistry of the host–pathogen interface in poinsettia leaves infected with powdery mildew. *Canadian journal of botany. Journal canadien de botanique*, 82(4), pp.421–429.

Chaparro-Garcia, A. et al., 2015. Phytophthora infestans RXLR-WY Effector AVR3a Associates with Dynamin-Related Protein 2 Required for Endocytosis of the Plant Pattern Recognition Receptor FLS2. *PloS one*, 10(9), p.e0137071.

Chisholm, S.T. et al., 2006. Host-microbe interactions: shaping the evolution of the plant immune response. *Cell*, 124(4), pp.803–814.

Chowdhury, J. et al., 2014. Differential accumulation of callose, arabinoxylan and cellulose in nonpenetrated versus penetrated papillae on leaves of barley infected with Blumeria graminis f. sp. hordei. *The New phytologist*, 204(3), pp.650–660.

Chowdhury, J. et al., 2016. Down-regulation of the glucan synthase-like 6 gene (HvGsl6) in barley leads to decreased callose accumulation and increased cell wall penetration by Blumeria graminis f. sp. hordei. *The New phytologist*, 212(2), pp.434–443.

Chowdhury, S., Basu, A. & Kundu, S., 2017. Biotrophy-necrotrophy switch in pathogen evoke differential response in resistant and susceptible sesame involving multiple signaling pathways at different phases. *Scientific reports*, 7(1), p.17251.

Cole, R.A. et al., 2005. SEC8, a subunit of the putative Arabidopsis exocyst complex, facilitates pollen germination and competitive pollen tube growth. *Plant physiology*, 138(4), pp.2005–2018.

Collins, N.C. et al., 2003. SNARE-protein-mediated disease resistance at the plant cell wall. *Nature*, 425(6961), pp.973–977.

Cui, Y. et al., 2014. Activation of the Rab7 GTPase by the MON1-CCZ1 Complex Is Essential for PVC-to-Vacuole Trafficking and Plant Growth in Arabidopsis. *The Plant cell*, 26(5), pp.2080–2097.

Cui, Y. et al., 2016. Biogenesis of Plant Prevacuolar Multivesicular Bodies. *Molecular plant*, 9(6), pp.774–786.

Cvrčková, F. et al., 2012. Evolution of the land plant exocyst complexes. *Frontiers in plant science*, 3, p.159.

Cvrčková, F. & Zárský, V., 2013. Old AIMs of the exocyst: evidence for an ancestral association of exocyst subunits with autophagy-associated Atg8 proteins. *Plant signaling & behavior*, 8(11), p.e27099.

Dacks, JB. & Robinson, M. 2017. Outerwear through the ages: evolutionary cell biology of vesicle coats. *Current Opinion in Cell Biology*. Aug;47:108-116.

Demircioglu, F.E., Burkhardt, P. & Fasshauer, D., 2014. The SM protein Sly1 accelerates assembly of the ER-Golgi SNARE complex. *Proceedings of the National Academy of Sciences*, 111(38), pp.13828–13833.

Dimitrov, L., Lam, S.K. & Schekman, R., 2013. The role of the endoplasmic reticulum in peroxisome biogenesis. *Cold Spring Harbor perspectives in biology*, 5(5), p.a013243.

Dobrev, P.I. & Kamínek, M., 2002. Fast and efficient separation of cytokinins from auxin and abscisic acid and their purification using mixed-mode solid-phase extraction. *Journal of chromatography. A*, 950(1-2), pp.21–29.

Drdová, E.J. et al., 2013. The exocyst complex contributes to PIN auxin efflux carrier recycling and polar auxin transport in Arabidopsis. *The Plant journal: for cell and molecular biology*, 73(5), pp.709–719.

Dubuke, M.L. et al., 2015. The Exocyst Subunit Sec6 Interacts with Assembled Exocytic SNARE Complexes. *The Journal of biological chemistry*, 290(47), pp.28245–28256.

Du, Y. et al., 2015. Phytophthora infestans RXLR Effector AVR1 Interacts with Exocyst Component Sec5 to Manipulate Plant Immunity. *Plant physiology*, 169(3), pp.1975–1990.

Du, Y. et al., 2018. Solanaceous exocyst subunits are involved in immunity to diverse plant pathogens. *Journal of experimental botany*, 69(3), pp.655–666.

Eliáš, M. et al., 2003. The exocyst complex in plants. *Cell biology international*, 27(3), pp.199–201.

Eggert, D. et al., 2014. Nanoscale glucan polymer network causes pathogen resistance. *Scientific Reports*. volume4, Article number: 4159

Ellinger, D. et al., 2013. Elevated early callose deposition results in complete penetration resistance to powdery mildew in Arabidopsis. *Plant physiology*, 161(3), pp.1433–1444.

Enrique Gomez, R. et al., 2018. Lipids in membrane dynamics during autophagy in plants.

Journal of experimental botany, 69(6), pp.1287–1299.

Fasshauer, D. et al., 1998. Conserved structural features of the synaptic fusion complex: SNARE proteins reclassified as Q- and R-SNAREs. *Proceedings of the National Academy of Sciences of the United States of America*, 95(26), pp.15781–15786.

Fendrych, M. et al., 2010. The Arabidopsis exocyst complex is involved in cytokinesis and cell plate maturation. *The Plant cell*, 22(9), pp.3053–3065.

Fendrych, M. et al., 2013. Visualization of the exocyst complex dynamics at the plasma membrane of Arabidopsis thaliana. *Molecular biology of the cell*, 24(4), pp.510–520.

Fernandez, I. et al., 1998. Three-dimensional structure of an evolutionarily conserved N-terminal domain of syntaxin 1A. *Cell*, 94(6), pp.841–849.

Friedrich, G.A., Hildebrand, J.D. & Soriano, P., 1997. The secretory protein Sec8 is required for paraxial mesoderm formation in the mouse. *Developmental biology*, 192(2), pp.364–374.

Fujiwara, M. et al., 2014. Interactomics of Qa-SNARE in Arabidopsis thaliana. *Plant & cell physiology*, 55(4), pp.781–789.

Gao, C. et al., 2015. Dual roles of an Arabidopsis ESCRT component FREE1 in regulating vacuolar protein transport and autophagic degradation. *Proceedings of the National Academy of Sciences of the United States of America*, 112(6), pp.1886–1891.

Geldner, N. & Robatzek, S., 2008. Plant receptors go endosomal: a moving view on signal transduction. *Plant physiology*, 147(4), pp.1565–1574.

Gil, F. & Gay, J.L., 1977. Ultrastructural and physiological properties of the host interfacial components of haustoria of Erysiphe pisi in vivo and in vitro. *Physiological Plant Pathology*, 10(1), pp.1–12.

Göhre, V. et al., 2008. Plant pattern-recognition receptor FLS2 is directed for degradation by the bacterial ubiquitin ligase AvrPtoB. *Current biology: CB*, 18(23), pp.1824–1832.

Gordon, T.R., 2017. Fusarium oxysporum and the Fusarium Wilt Syndrome. *Annual review of phytopathology*, 55, pp.23–39.

Grant, M.R. & Jones, J.D.G., 2009. Hormone (dis)harmony moulds plant health and disease. *Science*, 324(5928), pp.750–752.

Green, J.R. et al., 1995. Analysis of differentiation and development of the specialized infection structures formed by biotrophic fungal plant pathogens using monoclonal antibodies. *Canadian journal of botany. Journal canadien de botanique*, 73(S1), pp.408–417.

Hackenberg, T. et al., 2013. Catalase and NO CATALASE ACTIVITY1 promote autophagy-dependent cell death in Arabidopsis. *The Plant cell*, 25(11), pp.4616–4626.

Hacquard, S. et al., 2017. Interplay Between Innate Immunity and the Plant Microbiota. *Annual review of phytopathology*, 55, pp.565–589.

Hafrén, A. et al., 2017. Selective autophagy limits cauliflower mosaic virus infection by NBR1-mediated targeting of viral capsid protein and particles. *Proceedings of the National Academy of Sciences of the United States of America*, 114(10), pp.E2026–E2035.

Hála, M. et al., 2008. An exocyst complex functions in plant cell growth in Arabidopsis and tobacco. *The Plant cell*, 20(5), pp.1330–1345.

Hansen, L.L. & Nielsen, M.E., 2017. Plant exosomes: using an unconventional exit to prevent pathogen entry? *Journal of experimental botany*, 69(1), pp.59–68.

Harder, D.E. et al., 1978. Electron microscopy of susceptible and resistant near-isogenic (sr6/Sr6) lines of wheat infected by Puccinia graminis tritici. I. The host–pathogen interface in the compatible (sr6/P6) interaction. *Canadian journal of botany. Journal canadien de botanique*, 56(23), pp.2955–2966.

Heard, W. et al., 2015. Identification of Regulatory and Cargo Proteins of Endosomal and Secretory Pathways in Arabidopsis thaliana by Proteomic Dissection. *Molecular & cellular proteomics: MCP*, 14(7), pp.1796–1813.

Heath, M.C., 1976. Ultrastructural and functional similarity of the haustorial neckband of rust fungi and the Casparian strip of vascular plants. *Canadian journal of botany. Journal canadien de botanique*, 54(21), pp.2484–2489.

Heider, M.R. et al., 2016. Subunit connectivity, assembly determinants and architecture of the yeast exocyst complex. *Nature structural & molecular biology*, 23(1), pp.59–66.

Hinrichsen, L. et al., 2006. Bending a membrane: how clathrin affects budding. *Proceedings of the National Academy of Sciences of the United States of America*, 103(23), pp.8715–8720.

Hofius, D. et al., 2009. Autophagic components contribute to hypersensitive cell death in Arabidopsis. *Cell*, 137(4), pp.773–783.

Honigmann, A. et al., 2013. Phosphatidylinositol 4,5-bisphosphate clusters act as molecular beacons for vesicle recruitment. *Nature structural & molecular biology*, 20(6), pp.679–686.

Huang, Y.-P. et al., 2015. NbRABG3f, a member of Rab GTPase, is involved inBamboo mosaic virusinfection inNicotiana benthamiana. *Molecular plant pathology*, 17(5), pp.714–726.

Humphry, M. et al., 2010. A regulon conserved in monocot and dicot plants defines a functional module in antifungal plant immunity. *Proceedings of the National Academy of Sciences of the United States of America*, 107(50), pp.21896–21901.

Hurley, J.H. & Hanson, P.I., 2010. Membrane budding and scission by the ESCRT machinery: it's all in the neck. *Nature reviews. Molecular cell biology*, 11(8), pp.556–566.

Imada, K. et al., 2014. Antifungal effect of 405-nm light on Botrytis cinerea. *Letters in applied microbiology*, 59(6), pp.670–676.

Inada, N. et al., 2016. Modulation of Plant RAB GTPase-Mediated Membrane Trafficking Pathway at the Interface Between Plants and Obligate Biotrophic Pathogens. *Plant & cell physiology*, 57(9), pp.1854–1864.

Inada, N. & Ueda, T., 2014. Membrane Trafficking Pathways and their Roles in Plant–Microbe Interactions. *Plant & cell physiology*, 55(4), pp.672–686.

Jahn, R. & Fasshauer, D., 2012. Molecular machines governing exocytosis of synaptic vesicles. *Nature*, 490(7419), pp.201–207.

Jacobs A. K., et al. (2003). An *Arabidopsis* callose synthase, GSL5, is required for wound and papillary callose formation. *Plant Cell* (15), pp. 2503–2513

Jirage D, Tootle TL, Reuber TL, et al. Arabidopsis thaliana PAD4 encodes a lipase-like gene that is important for salicylic acid signaling. *Proceedings of the National Academy of Sciences of the United States of America*. 1999;96(23):13583-13588.

Jones, J.D.G. & Dangl, J.L., 2006. The plant immune system. *Nature*, 444(7117), pp.323–329.

Kale, S.D. et al., 2010. External lipid PI3P mediates entry of eukaryotic pathogen effectors into plant and animal host cells. *Cell*, 142(2), pp.284–295.

Kale, S.D. & Tyler, B.M., 2011. Entry of oomycete and fungal effectors into plant and animal host cells. *Cellular microbiology*, 13(12), pp.1839–1848.

Kalmbach, L. et al., 2017. Transient cell-specific EXO70A1 activity in the CASP domain and Casparian strip localization. *Nature plants*, 3, p.17058.

Karnik, R. et al., 2017. Commandeering Channel Voltage Sensors for Secretion, Cell Turgor, and Volume Control. *Trends in plant science*, 22(1), pp.81–95.

Kershaw, M.J. & Talbot, N.J., 2009. Genome-wide functional analysis reveals that infection-associated fungal autophagy is necessary for rice blast disease. *Proceedings of the National Academy of Sciences of the United States of America*, 106(37), pp.15967–15972.

Kim, H. et al., 2014. The powdery mildew resistance protein RPW8.2 is carried on VAMP721/722 vesicles to the extrahaustorial membrane of haustorial complexes. *The Plant journal: for cell and molecular biology*, 79(5), pp.835–847.

Kim, Y. et al., 2014. Mechanisms underlying robustness and tunability in a plant immune signaling network. *Cell host & microbe*, 15(1), pp.84–94.

King, B.C. et al., 2011. Arsenal of plant cell wall degrading enzymes reflects host preference among plant pathogenic fungi. *Biotechnology for biofuels*, 4, p.4.

Kleemann, J. et al., 2012. Sequential delivery of host-induced virulence effectors by appressoria and intracellular hyphae of the phytopathogen Colletotrichum higginsianum. *PLoS pathogens*, 8(4), p.e1002643.

Koh, S. et al., 2005. Arabidopsis thaliana subcellular responses to compatible Erysiphe

cichoracearum infections. *The Plant journal: for cell and molecular biology*, 44(3), pp.516–529.

Kuhn, H. et al., 2016. Biotrophy at Its Best: Novel Findings and Unsolved Mysteries of the Arabidopsis-Powdery Mildew Pathosystem. *The Arabidopsis book / American Society of Plant Biologists*, 14, p.e0184.

Kulich, I. et al., 2010. Arabidopsis exocyst subunits SEC8 and EXO70A1 and exocyst interactor ROH1 are involved in the localized deposition of seed coat pectin. *The New phytologist*, 188(2), pp.615–625.

Kulich, I. et al., 2013. Arabidopsis exocyst subcomplex containing subunit EXO70B1 is involved in the autophagy-related transport to the vacuole. *Traffic* . Available at: http://dx.doi.org/10.1111/tra.12101.

Kulich, I. et al., 2015. Cell wall maturation of Arabidopsis trichomes is dependent on exocyst subunit EXO70H4 and involves callose deposition. *Plant physiology*, 168(1), pp.120–131.

Kulich, I. et al., 2018. Exocyst subunit EXO70H4 has a specific role in callose synthase secretion and silica accumulation. *Plant physiology*. Available at: http://dx.doi.org/10.1104/pp.17.01693.

Kwaaitaal, M. et al., 2017. The plant membrane surrounding powdery mildew haustoria shares properties with the endoplasmic reticulum membrane. *Journal of experimental botany*, 68(21-22), pp.5731–5743.

Kwon, C. et al., 2008. Co-option of a default secretory pathway for plant immune responses. *Nature*, 451(7180), pp.835–840.

Kwon, S.I. et al., 2013. The Rab GTPase RabG3b positively regulates autophagy and immunity-associated hypersensitive cell death in Arabidopsis. *Plant physiology*, 161(4), pp.1722–1736.

Laufman, O., Hong, W. & Lev, S., 2013. The COG complex interacts with multiple Golgi SNAREs and enhances fusogenic assembly of SNARE complexes. *Journal of cell science*, 126(6), pp.1506–1516.

Le Bars, R. et al., 2014. ATG5 defines a phagophore domain connected to the endoplasmic reticulum during autophagosome formation in plants. *Nature communications*, 5, p.4121.

Leckie, C.P., CALLOW and, J.A. & Green, J.R., 1995. Reorganization of the endoplasmic reticulum in pea leaf epidermal cells infected by the powdery mildew fungusErysiphe pisi. *The New phytologist*, 131(2), pp.211–221.

Li, F. et al., 2016. Kinetic barriers to SNAREpin assembly in the regulation of membrane docking/priming and fusion. *Proceedings of the National Academy of Sciences of the United States of America*, 113(38), pp.10536–10541.

Liu, D. et al., 2018. Two subunits of the exocyst, Sec3p and Exo70p, can function exclusively on the plasma membrane. *Molecular biology of the cell*. Available at:

http://dx.doi.org/10.1091/mbc.E17-08-0518.

Li, W. et al., 2011. The crystal structure of a Munc13 C-terminal module exhibits a remarkable similarity to vesicle tethering factors. *Structure* , 19(10), pp.1443–1455.

Li, Y. et al., 2017. Exocyst subunit SEC3A marks the germination site and is essential for pollen germination in Arabidopsis thaliana. *Scientific reports*, 7, p.40279.

Lundmark, R. et al., 2008. Arf family GTP loading is activated by, and generates, positive membrane curvature. *Biochemical Journal*, 414(2), pp.189–194.

Luo, G., Zhang, J. & Guo, W., 2014. The role of Sec3p in secretory vesicle targeting and exocyst complex assembly. *Molecular biology of the cell*, 25(23), pp.3813–3822.

Lu, S. et al., 2013. Intracellular and extracellular phosphatidylinositol 3-phosphate produced by Phytophthora species is important for infection. *Molecular plant*, 6(5), pp.1592–1604.

Lu, X. et al., 2015. Mutant Allele-Specific Uncoupling of PENETRATION3 Functions Reveals Engagement of the ATP-Binding Cassette Transporter in Distinct Tryptophan Metabolic Pathways. *Plant physiology*, 168(3), pp.814–827.

Lu, Y.-J. et al., 2012. Patterns of plant subcellular responses to successful oomycete infections reveal differences in host cell reprogramming and endocytic trafficking. *Cellular microbiology*, 14(5), pp.682–697.

Maekawa, T., Kufer, T.A. & Schulze-Lefert, P., 2011. NLR functions in plant and animal immune systems: so far and yet so close. *Nature immunology*, 12(9), pp.817–826.

Ma, J. et al., 2018. Corrigendum: Disruption of OsSEC3A increases the content of salicylic acid and induces plant defense responses in rice. *Journal of experimental botany*. Available at: http://dx.doi.org/10.1093/jxb/ery003.

Manners, J.M., 1989. The Host-Haustorium Interface in Powdery Mildews. *Australian journal of plant physiology*, 16(1), p.45.

Manning, V.A. et al., 2008. The Arg-Gly-Asp-containing, solvent-exposed loop of Ptr ToxA is required for internalization. *Molecular plant-microbe interactions: MPMI*, 21(3), pp.315–325.

Mansour, S.J. et al., 1999. p200 ARF-GEP1: a Golgi-localized guanine nucleotide exchange protein whose Sec7 domain is targeted by the drug brefeldin A. *Proceedings of the National Academy of Sciences of the United States of America*, 96(14), pp.7968–7973.

Mao, H. et al., 2016. A Framework for Lateral Membrane Trafficking and Polar Tethering of the PEN3 ATP-Binding Cassette Transporter. *Plant physiology*, 172(4), pp.2245–2260.

Matsuoka, K. et al., 1998. COPII-coated vesicle formation reconstituted with purified coat proteins and chemically defined liposomes. *Cell*, 93(2), pp.263–275.

Mbengue, M. et al., 2016. Clathrin-dependent endocytosis is required for immunity mediated by pattern recognition receptor kinases. *Proceedings of the National Academy of*

Sciences of the United States of America, 113(39), pp.11034–11039.

Mei, K. et al., 2018. Cryo-EM structure of the exocyst complex. *Nature structural & molecular biology*. Available at: http://dx.doi.org/10.1038/s41594-017-0016-2.

Meyer, D. et al., 2009. Extracellular transport and integration of plant secretory proteins into pathogen-induced cell wall compartments. *The Plant journal: for cell and molecular biology*, 57(6), pp.986–999.

Micali, C.O. et al., 2011. Biogenesis of a specialized plant-fungal interface during host cell internalization of Golovinomyces orontii haustoria. *Cellular microbiology*, 13(2), pp.210–226.

Mims, C.W. et al., 2004. Ultrastructure of the host–pathogen interface in Arabidopsis thaliana leaves infected by the downy mildew Hyaloperonospora parasitica. *Canadian journal of botany. Journal canadien de botanique*, 82(7), pp.1001–1008.

Munch, D. et al., 2015. Retromer contributes to immunity-associated cell death in Arabidopsis. *The Plant cell*, 27(2), pp.463–479.

Nielsen, M.E. et al., 2012. Arabidopsis ARF-GTP exchange factor, GNOM, mediates transport required for innate immunity and focal accumulation of syntaxin PEN1. *Proceedings of the National Academy of Sciences of the United States of America*, 109(28), pp.11443–11448.

Nielsen, M.E., Jürgens, G. & Thordal-Christensen, H., 2017. VPS9a Activates the Rab5 GTPase ARA7 to Confer Distinct Pre- and Postinvasive Plant Innate Immunity. *The Plant cell*, 29(8), pp.1927–1937.

Nielsen, M.E. & Thordal-Christensen, H., 2013. Transcytosis shuts the door for an unwanted guest. *Trends in plant science*, 18(11), pp.611–616.

Nishimura M. T.,et al. (2003). Loss of a callose synthase results in salicylic acid-dependent disease resistance. *Science* (301), pp. 969–972

Noack, L.C. & Jaillais, Y., 2017. Precision targeting by phosphoinositides: how PIs direct endomembrane trafficking in plants. *Current opinion in plant biology*, 40, pp.22–33.

Nomura, K. et al., 2006. A bacterial virulence protein suppresses host innate immunity to cause plant disease. *Science*, 313(5784), pp.220–223.

Nomura, K. et al., 2011. Effector-triggered immunity blocks pathogen degradation of an immunity-associated vesicle traffic regulator in Arabidopsis. *Proceedings of the National Academy of Sciences of the United States of America*, 108(26), pp.10774–10779.

Nossal, R., 2001. Energetics of clathrin basket assembly. *Traffic* , 2(2), pp.138–147.

Ortiz-Morea, F.A. et al., 2016. Danger-associated peptide signaling in Arabidopsis requires clathrin. *Proceedings of the National Academy of Sciences of the United States of America*, 113(39), pp.11028–11033.

Pečenková, T. et al., 2016. Constitutive Negative Regulation of R Proteins in Arabidopsis also via Autophagy Related Pathway? *Frontiers in plant science*, 7, p.260.

Pečenková, T. et al., 2011. The role for the exocyst complex subunits Exo70B2 and Exo70H1 in the plant-pathogen interaction. *Journal of experimental botany*, 62(6), pp.2107–2116.

Peer, R. van & van Peer, R., 1991. Induced Resistance and Phytoalexin Accumulation in Biological Control of Fusarium Wilt of Carnation byPseudomonassp. Strain WCS417r. *Phytopathology*, 81(7), p.728.

Penninckx, I.A. et al., 1998. Concomitant activation of jasmonate and ethylene response pathways is required for induction of a plant defensin gene in Arabidopsis. *The Plant cell*, 10(12), pp.2103–2113.

Picco, A. et al., 2017. The In Vivo Architecture of the Exocyst Provides Structural Basis for Exocytosis. *Cell*, 168(3), pp.400–412.e18.

Pleskot, R. et al., 2015. Membrane targeting of the yeast exocyst complex. *Biochimica et biophysica acta*, 1848(7), pp.1481–1489.

Postma, J. et al., 2016. Avr4 promotes Cf-4 receptor-like protein association with the BAK1/SERK3 receptor-like kinase to initiate receptor endocytosis and plant immunity. *The New phytologist*, 210(2), pp.627–642.

Regente, M. et al., 2017. Plant extracellular vesicles are incorporated by a fungal pathogen and inhibit its growth. *Journal of experimental botany*, 68(20), pp.5485–5495.

Reichardt, I. et al., 2011. Mechanisms of Functional Specificity Among Plasma-Membrane Syntaxins in Arabidopsis. *Traffic* , 12(9), pp.1269–1280.

Renault, L., Guibert, B. & Cherfils, J., 2003. Structural snapshots of the mechanism and inhibition of a guanine nucleotide exchange factor. *Nature*, 426(6966), pp.525–530.

Rutter, B.D. & Innes, R.W., 2017. Extracellular Vesicles Isolated from the Leaf Apoplast Carry Stress-Response Proteins. *Plant physiology*, 173(1), pp.728–741.

Rybak, K. et al., 2014. Plant cytokinesis is orchestrated by the sequential action of the TRAPPII and exocyst tethering complexes. *Developmental cell*, 29(5), pp.607–620.

Sabol, P., Kulich, I. & Žárský, V., 2017. RIN4 recruits the exocyst subunit EXO70B1 to the plasma membrane. *Journal of experimental botany*, 68(12), pp.3253–3265.

Sanderfoot, A.A. et al., 2001. Disruption of Individual Members of Arabidopsis Syntaxin Gene Families Indicates Each Has Essential Functions. *The Plant cell*, 13(3), p.659.

Sanderfoot, A.A., Assaad, F.F. & Raikhel, N.V., 2000. The Arabidopsis Genome. An Abundance of SolubleN-Ethylmaleimide-Sensitive Factor Adaptor Protein Receptors. *Plant physiology*, 124(4), pp.1558–1569.

Sander, L.E. et al., 2011. Detection of prokaryotic mRNA signifies microbial viability and promotes immunity. *Nature*, 474(7351), pp.385–389.

Sato, M. et al., 2010. Network modeling reveals prevalent negative regulatory relationships between signaling sectors in Arabidopsis immune signaling. *PLoS pathogens*, 6(7), p.e1001011.

Schouten, A., van Baarlen, P. & van Kan, J.A.L., 2008. Phytotoxic Nep1-like proteins from the necrotrophic fungus Botrytis cinerea associate with membranes and the nucleus of plant cells. *The New phytologist*, 177(2), pp.493–505.

Schwartz, M.L. et al., 2017. Sec17 (α-SNAP) And An SM-Tethering Complex Control The Outcome Of SNARE Zippering In Vitro And In Vivo. Available at: http://dx.doi.org/10.1101/123133.

Seaman, M.N.J., 2012. The retromer complex - endosomal protein recycling and beyond. *Journal of cell science*, 125(Pt 20), pp.4693–4702.

Sekereš, J. et al., 2015. The song of lipids and proteins: dynamic lipid protein interfaces in the regulation of plant cell polarity at different scales. *J Exp Bot.* Mar;66(6):1587-98.

Sekereš, J. et al., 2017. Analysis of Exocyst Subunit EXO70 Family Reveals Distinct Membrane Polar Domains in Tobacco Pollen Tubes. *Plant physiology*, 173(3), pp.1659–1675.

Seo, D.H. et al., 2016. The N-Terminal UND Motif of the Arabidopsis U-Box E3 Ligase PUB18 Is Critical for the Negative Regulation of ABA-Mediated Stomatal Movement and Determines Its Ubiquitination Specificity for Exocyst Subunit Exo70B1. *The Plant cell*, 28(12), pp.2952–2973.

Siddiqui, T.J. et al., 2007. Determinants of Synaptobrevin Regulation in Membranes. *Molecular biology of the cell*, 18(6), pp.2037–2046.

Silva, R., 2013. Regulation of Plant Cell Wall Degrading Enzymes Formation in Filamentous Fungi. In *Fungal Enzymes*.

Simon, M.L.A. et al., 2014. A multi-colour/multi-affinity marker set to visualize phosphoinositide dynamics in Arabidopsis. *The Plant journal: for cell and molecular biology*, 77(2), pp.322–337.

Smith, J.M. et al., 2014. Sensitivity to Flg22 is modulated by ligand-induced degradation and de novo synthesis of the endogenous flagellin-receptor FLAGELLIN-SENSING2. *Plant physiology*, 164(1), pp.440–454.

Söllner, T.H., 2002. Vesicle tethers promoting fusion machinery assembly. *Developmental cell*, 2(4), pp.377–378.

Spallek, T. et al., 2013. ESCRT-I Mediates FLS2 Endosomal Sorting and Plant Immunity. *PLoS genetics*, 9(12), p.e1004035.

Spitzer, C. et al., 2015. The endosomal protein CHARGED MULTIVESICULAR BODY PROTEIN1 regulates the autophagic turnover of plastids in Arabidopsis. *The Plant cell*, 27(2), pp.391–402.

Stegmann, M. et al., 2012. The ubiquitin ligase PUB22 targets a subunit of the exocyst

complex required for PAMP-triggered responses in Arabidopsis. *The Plant cell*, 24(11), pp.4703–4716.

Stegmann, M. et al., 2013. The exocyst subunitExo70B1is involved in the immune response ofArabidopsis thalianato different pathogens and cell death. *Plant signaling & behavior*, 8(12), p.e27421.

Stein, M., 2006. Arabidopsis PEN3/PDR8, an ATP Binding Cassette Transporter, Contributes to Nonhost Resistance to Inappropriate Pathogens That Enter by Direct Penetration. *THE PLANT CELL ONLINE*, 18(3), pp.731–746.

Stone BA & Clarke AE. 1992. Chemistry and Biology of (1-3)-β-D-Glucans. Victoria, Australia: *La Trobe University Press*. 23(2), pp. 35-42.

Surpin, M. et al., 2003. The VTI family of SNARE proteins is necessary for plant viability and mediates different protein transport pathways. *The Plant cell*, 15(12), pp.2885–2899.

Suttangkakul, A. et al., 2011. The ATG1/ATG13 protein kinase complex is both a regulator and a target of autophagic recycling in Arabidopsis. *The Plant cell*, 23(10), pp.3761–3779.

Sutton, R.B. et al., 1998. Crystal structure of a SNARE complex involved in synaptic exocytosis at 2.4 A resolution. *Nature*, 395(6700), pp.347–353.

Synek, L. et al., 2006. AtEXO70A1, a member of a family of putative exocyst subunits specifically expanded in land plants, is important for polar growth and plant development. *The Plant journal: for cell and molecular biology*, 48(1), pp.54–72.

Synek, L. et al., 2017. EXO70C2 Is a Key Regulatory Factor for Optimal Tip Growth of Pollen. *Plant physiology*, 174(1), pp.223–240.

Talley, S.M., Coley, P.D. & Kursar, T.A., 2002. The effects of weather on fungal abundance and richness among 25 communities in the Intermountain West. *BMC ecology*, 2, p.7.

TerBush, D.R., 1995. Sec6, Sec8, and Sec15 are components of a multisubunit complex which localizes to small bud tips in Saccharomyces cerevisiae. *The Journal of cell biology*, 130(2), pp.299–312.

TerBush, D.R. et al., 1996. The Exocyst is a multiprotein complex required for exocytosis in Saccharomyces cerevisiae. *The EMBO journal*, 15(23), pp.6483–6494.

Thomma, B.P. et al., 1999. Requirement of functional ethylene-insensitive 2 gene for efficient resistance of Arabidopsis to infection by Botrytis cinerea. *Plant physiology*, 121(4), pp.1093–1102.

Tsuda, K. et al., 2009. Network properties of robust immunity in plants. *PLoS genetics*, 5(12), p.e1000772.

Turgeman, T. et al., 2016. The Role of Aquaporins in pH-Dependent Germination of Rhizopus delemar Spores. *PloS one*, 11(3), p.e0150543.

Uemura, T. et al., 2012. Qa-SNAREs localized to the trans-Golgi network regulate multiple transport pathways and extracellular disease resistance in plants. *Proceedings of the National Academy of Sciences*, 109(5), pp.1784–1789.

Uemura, T. et al., 2004. Systematic Analysis of SNARE Molecules in *Arabidopsis*: Dissection of the post-Golgi Network in Plant Cells. *Cell structure and function*, 29(2), pp.49–65.

Üstün, S., Hafrén, A. & Hofius, D., 2017. Autophagy as a mediator of life and death in plants. *Current opinion in plant biology*, 40, pp.122–130.

Vargas, W.A. et al., 2012. Plant Defense Mechanisms Are Activated during Biotrophic and Necrotrophic Development of Colletotricum graminicola in Maize. *Plant physiology*, 158(3), pp.1342–1358.

Vukašinović, N. & Žárský, V., 2016. Tethering Complexes in the Arabidopsis Endomembrane System. *Frontiers in cell and developmental biology*, 4, p.46.

Vukašinović, N. et al., 2017. Microtubule-dependent targeting of the exocyst complex is necessary for xylem development in Arabidopsis. *The New phytologist*, 213(3), pp.1052–1067.

Wang, J. et al., 2010. EXPO, an Exocyst-Positive Organelle Distinct from Multivesicular Endosomes and Autophagosomes, Mediates Cytosol to Cell Wall Exocytosis inArabidopsisand Tobacco Cells. *The Plant cell*, 22(12), pp.4009–4030.

Wang, P., Mugume, Y. & Bassham, D.C., 2017. New advances in autophagy in plants: Regulation, selectivity and function. *Seminars in cell & developmental biology*. Available at: http://dx.doi.org/10.1016/j.semcdb.2017.07.018.

Wang, W. et al., 2007. Expression of the Membrane-Associated Resistance Protein RPW8 Enhances Basal Defense Against Biotrophic Pathogens. *Molecular plant-microbe interactions: MPMI*, 20(8), pp.966–976.

Wang, W. et al., 2009. Specific targeting of the Arabidopsis resistance protein RPW8.2 to the interfacial membrane encasing the fungal Haustorium renders broad-spectrum resistance to powdery mildew. *The Plant cell*, 21(9), pp.2898–2913.

Watanabe, S. et al., 2013. Pathogen infection trial increases the secretion of proteins localized in the endoplasmic reticulum body of Arabidopsis. *Plant physiology*, 163(2), pp.659–664.

Weber, T. et al., 1998. SNAREpins: minimal machinery for membrane fusion. *Cell*, 92(6), pp.759–772.

White, R.F., 1979. Acetylsalicylic acid (aspirin) induces resistance to tobacco mosaic virus in tobacco. *Virology*, 99(2), pp.410–412.

Winter, D. et al., 2007. An “Electronic Fluorescent Pictograph” browser for exploring and analyzing large-scale biological data sets. *PloS one*, 2(8), p.e718.

Woodward, J.J., Iavarone, A.T. & Portnoy, D.A., 2010. c-di-AMP secreted by intracellular

Listeria monocytogenes activates a host type I interferon response. *Science*, 328(5986), pp.1703–1705.

Xie, Z. & Klionsky, D.J., 2007. Autophagosome formation: core machinery and adaptations. *Nature cell biology*, 9(10), pp.1102–1109.

Xin, X.-F. et al., 2016. Bacteria establish an aqueous living space in plants crucial for virulence. *Nature*, 539(7630), pp.524–529.

Yue, P. et al., 2017. Sec3 promotes the initial binary t-SNARE complex assembly and membrane fusion. *Nature communications*, 8, p.14236.

Zamioudis, C. et al., 2013. Unraveling root developmental programs initiated by beneficial Pseudomonas spp. bacteria. *Plant physiology*, 162(1), pp.304–318.

Žárský, V. et al., 2013. Exocyst complexes multiple functions in plant cells secretory pathways. *Current opinion in plant biology*, 16(6), pp.726–733.

Žárský, V. et al., 2009. Exocytosis and cell polarity in plants - exocyst and recycling domains. *The New phytologist*, 183(2), pp.255–272.

Zelazny, E. et al., 2013. Mechanisms Governing the Endosomal Membrane Recruitment of the Core Retromer inArabidopsis. *The Journal of biological chemistry*, 288(13), pp.8815–8825.

Zhang, Z. et al., 2007. A SNARE-protein has opposing functions in penetration resistance and defence signalling pathways. *The Plant journal: for cell and molecular biology*, 49(2), pp.302–312.

Zhao, T. et al., 2015. A truncated NLR protein, TIR-NBS2, is required for activated defense responses in the exo70B1 mutant. *PLoS genetics*, 11(1), p.e1004945.

Zheng, X.-Y. et al., 2012. Coronatine promotes Pseudomonas syringae virulence in plants by activating a signaling cascade that inhibits salicylic acid accumulation. *Cell host & microbe*, 11(6), pp.587–596.

Zhuang, X. et al., 2013. A BAR-domain protein SH3P2, which binds to phosphatidylinositol 3-phosphate and ATG8, regulates autophagosome formation in Arabidopsis. *The Plant cell*, 25(11), pp.4596–4615.

Zhuang, X. et al., 2017. ATG9 regulates autophagosome progression from the endoplasmic reticulum in Arabidopsis. *Proceedings of the National Academy of Sciences of the United States of America*, 114(3), pp.E426–E435.